

UCH-L1 AS A SUSCEPTIBILITY FACTOR FOR NIGROSTRIATAL AND MESOLIMBIC
DOPAMINE NEURONS AFTER NEUROTOXICANT EXPOSURE AND AGING

By

Brittany Michele Winner

A DISSERTATION

Submitted to
Michigan State University
in partial fulfillment of the requirements
for the degree of

Pharmacology and Toxicology - Environmental Toxicology - Doctor of Philosophy

2017

ABSTRACT

UCH-L1 AS A SUSCEPTIBILITY FACTOR FOR NIGROSTRIATAL AND MESOLIMBIC DOPAMINE NEURONS AFTER NEUROTOXICANT EXPOSURE AND AGING

By

Brittany Michele Winner

Parkinson disease (PD), the second most prevalent neurodegenerative disorder, is most commonly diagnosed in elderly individuals and is characterized by manifestation of motor deficits such as bradykinesia, postural instability, resting tremor, and shuffling gait. The motor symptoms of PD arise when dopamine (DA) neurons in the nigrostriatal DA (NSDA) pathway degenerate, which are involved in regulating voluntary motor coordination via the basal ganglia pathway. NSDA neurons are progressively lost in the disease, which has no known cure. Other DA neuronal pathways in the central nervous system are less affected by neuronal death, however: mesolimbic DA (MLDA) neurons are less vulnerable to PD. Therefore, we seek to understand how MLDA neurons resist degeneration. Since Lewy bodies, which are proteinaceous deposits of misfolded and aggregated proteins, are the hallmark pathology of PD, we predict that major deficits in protein degradation are involved in development and progression of PD. A gene found mutated in a rare case of familial PD called ubiquitin carboxy-terminal hydrolase L1 (*UCHL1*) is involved in one of the major mechanisms of protein degradation, the ubiquitin proteasome system (UPS) and functions as a deubiquitinating enzyme to maintain pools of available monomeric ubiquitin. UCH-L1 is decreased in the SN of mice exposed to the neurotoxicant, MPTP. MPTP exposure in rodents recapitulates loss of DA and oxidative stress observed in patients with PD and can also be used to recapitulate the differential susceptibility of NSDA and MLDA neurons. The goal of this

dissertation research was to investigate the role of UCH-L1 in influencing susceptibility of NSDA and MLDA neurons to acute neurotoxic insult, and if aging plays a role in determining vulnerability of NSDA and MLDA neurons or expression and function of UCH-L1. UCH-L1 expression and function are maintained in non-susceptible MLDA neurons, which corresponds to the pattern of MLDA susceptibility to MPTP exposure. UCH-L1 expression is not affected by advanced age in either NSDA and MLDA neurons, but UPS function is impaired in both cell body regions with advanced age. These studies shed light on the potential contribution of the PD-linked neuronal deubiquitinating enzyme UCH-L1 to selective vulnerability in PD.

ACKNOWLEDGEMENTS

I have so many people to thank for helping me along this journey, which sometimes felt akin to Frodo's journey to Mount Doom with the One Ring. He needed a whole Fellowship to get there relatively unscathed, and then a crazy old wizard flying on eagles to get him back. Quotes are from the fantastic movie adaptations of J.R.R. Tolkien's Lord of the Rings trilogy.

Although sometimes my graduate school journey felt like I didn't know the sheer depth of what I had gotten myself into, I must thank my undergraduate mentor, Dr. Ilona Petrikovics, for suggesting the quest. She saw potential in me when I did undergraduate research in her lab, and she's the reason I decided to do a PhD in Toxicology in the first place. Thank you, Ilona!

Next, I must thank the wizards who outlined what I needed to do and where I needed to go to complete my journey: my mentors, Dr. Keith Lookingland and Dr. John Goudreau. Sometimes the voyage seemed too daunting and I often thought I wasn't cut out for the it, but these benevolent forces used their powers for good and helped me along the way—sometimes with good, sound advice, and other times with cryptic hints that I wasn't prepared at the time to understand. The quote by Gandalf is so appropriate than with you: "A wizard is never late, Frodo Baggins. He arrives precisely when he means to." Thank you, Keith and John, for not giving up on me when I wanted to flee, and by being patient with me when I lost patience with myself.

In addition, I would like to thank the other members of my guidance committee who were kind enough to help guide me along this journey: Dr. Michelle Mazei-Robison and Dr. James Galligan. Michelle and Jim, thank you so much for your advice, for sitting through all my committee meetings, for making sure I knew my stuff, and finally, for reading this document. My experience was richer having you on my thesis committee.

Now, the important lovely elves who sacrificed time for me: Dr. Anne Dorrance, our graduate program director, and Dr. Stephanie Watts, all around awesome unofficial science/life coach! Anne was always there for me in her office with her famous box of never-ending tissues, telling me not to give up and sympathizing with my various woes as well as sometimes helping to make sure I got paid. Stephanie read some of my writing to make sure it made sense, and graciously offered use of the equipment I dearly needed (not to mention the chocolate and fancy hand soap!). These fantastic ladies made the journey more bearable, and the gifts they gave me along the way reminded me of Galadriel's gift to Frodo: "May it be a light to you in dark places, when all other lights go out." Thank you, Anne and Stephanie, for being a light to me in the dark times of my journey.

Next, Frodo wouldn't have gotten out of Rivendell (let's be honest, Hobbiton!) without a great squad by his side. I would like to thank the previous members of the Goudreau/Lookingland laboratory: Dr. Bahareh Behrouz, Dr. Chelsea Tiernan, Dr. Matthew Benskey, Dr. Tyrell Simkins, Dr. Hae-young Hawong, Dr. Joseph Patterson, and Dr. Teri Lansdell. Each member of this unique and fun Fellowship gave scientific advice and helped me grow into the explorer/scientist I needed to be to complete this quest—and are still helpful today! Special thanks to Teri for putting up with me the

longest in the lab and enduring my shenanigans—from the misguided saltine cracker challenge to running circles around the lab holding the perforated ribbons of the dot matrix paper we use for our HPLC printer—and being a fantastic role model. Thank you all, most excellent Fellowship, for helping me on my quest.

There isn't a convenient Tolkien metaphor for who I'd like to thank next, but I do want to express my thanks to the entire Pharmacology and Toxicology Department. To Beverly, Wendy, Erica, Michelle, Rosie, Diane, Stephen, Brian, Brad, Rick, and everyone else who has helped me get things done (say, if Frodo needed to register for classes and he consistently forgot to do it every single semester...): thank you so much for making the Pharm/Tox department a functional and fun place for me to spend all of my time. To all of the Pharm/Tox graduate students I've gotten to know over the years: ya'll are fantastic, and keep being fantastic forever! So many of you became close friends, and our camaraderie truly lifted my spirits as I trudged toward my goal. Each of you inspired me with your fervor for your own quests.

Although family wasn't as big of a deal in Frodo's life (he was close to Bilbo, but his parents died when he was small), I wouldn't have gotten anywhere without mine. My mother, Billie Winner-Davis, has been my biggest enthusiast my whole life; she embarrassingly calls me her Firework (after that Katy Perry song) and is convinced that I can do anything astronomically difficult, like finish a PhD/throw a magical ring into a fiery mountain. Her encouragement kept me going when I was ready to quit, seriously. My father, the late Ronald Winner, also inspired me to be anything I wanted to be. He told me once, when I had come home in elementary school with a failing grade on a math test that everyone else in my class had failed, "don't judge your performance by

how everyone else is doing—only focus on yourself and what you can do.” These words served me well through this journey and my life. My stepfather, Gary Davis, is a cool character like Aragorn and selflessly made sure that I had everything I needed to be a functional person, which often included many, many keychain flashlights that came in handy during those hours I spent using various fluorescent microscopes in the dark. And then there’s my sister, Reality Winner, who is indescribable, but has always supported my endeavors. She tells everyone that her “sister is going to cure Parkinson’s,” which I wish were true, but it’s touching she believes in me that much. Thank you to all my family. I love you more than words. This Dissertation is dedicated to you.

Finally, Frodo would never have made it through the final stretches of the journey to Mordor, arguably the most difficult part of the journey, without his best pal Sam. The Sam in my life—my best friend—is also my husband, Christopher John. You know that part in the third movie where Sam carries Frodo up to Mount Doom (if you haven’t seen it yet, you really should!)? Chris has done that and more for me in my time in graduate school, which is amazing considering that his also has his own mountain to scale and quest to yet complete. I am so fortunate to have such a wonderful husband in Chris, and I know for sure I would never have been able to do any of this without him. I love you, C-Ro! <3

TABLE OF CONTENTS

LIST OF TABLES	xi
LIST OF FIGURES.....	xii
KEY TO ABBREVIATIONS	xviii
Chapter 1: General Introduction	1
History and motor symptoms of PD.....	1
Non-motor dysfunction in PD and Braak staging.....	2
Current therapies for PD	3
Mutations that cause PD	5
Genetic risk factors for PD	6
Environmental risk factors for PD.....	7
Selective vulnerability of central DA neurons to PD	7
Vulnerability of DA neuronal populations to models of neurodegeneration	11
Protein degradation pathways in PD	12
Deubiquitinating enzymes in the UPS and UCH-L1	14
UCH-L1 in PD	16
Gracile axonal dystrophy (gad) phenotype.....	20
nm3419 mouse phenotype.....	21
Regulation of UCH-L1 expression in neurons	22
UCH-L1 in AD	22
Goals of this Dissertation	23
Specific aims	26
REFERENCES.....	26
Chapter 2: Materials and Methods.....	37
Animals, drugs, and brain tissue collection	37
Preparation of crude synaptosomes.....	39
Bicinchoninic acid assay for protein concentrations	39
Neurochemical analyses via HPLC-ED	40
Immunoblot analyses	40
Immunohistochemistry	43
Confocal analysis of colocalization.....	43
DCF-DA assay	44
MN9D cell culture and drug treatment.....	44
Cytotoxicity assay.....	45
UCH-L1 hydrolase activity	45
Cayman total glutathione measurements	46
Abcam GSH/GSSG ratio measurements	46
HA-Ub-VME DUB labeling assay	46

Statistical analyses.....	47
REFERENCES.....	48
Chapter 3: Oxidative Stress, Dopaminergic Phenotypic Markers, and UCH-L1 Expression in NSDA and MLDA Neurons after Exposure to Acute MPTP ..	51
Introduction	51
Results	52
<i>Oxidative stress in brain regions containing NSDA vs. MLDA neurons.....</i>	<i>52</i>
<i>Differential susceptibility of NSDA and MLDA neurons to MPTP: DA, DOPAC, and TH.....</i>	<i>57</i>
<i>UCH-L1 and mono-Ub in MLDA neurons after MPTP exposure</i>	<i>64</i>
<i>Total glutathione concentrations in brain regions containing NSDA and MLDA neurons</i>	<i>66</i>
<i>Expression of UCH-L1 in NSDA and MLDA neurons</i>	<i>69</i>
Discussion.....	82
Summary and conclusions	84
REFERENCES.....	85
Chapter 4: Effects of Neurotoxicant and UCH-L1 Inhibitor in MN9D Cells and ST Synaptosomes, and a Potential Interaction between UCH-L1 and Parkin with Relevance to Autophagy	88
Introduction	88
Results	92
<i>MN9D expression of DA phenotypic markers and UCH-L1.....</i>	<i>92</i>
<i>Effects of MPTP on UCH-L3 and USP14 in NSDA neurons in vivo</i>	<i>104</i>
<i>Effects of MPTP on UCH-L1 expression in NSDA axon terminals</i>	<i>108</i>
<i>Relationship between UCH-L1 and parkin</i>	<i>116</i>
Discussion.....	126
Summary and conclusions	129
REFERENCES.....	130
Chapter 5: Effects of Inhibition of UCH-L1 on Susceptibility of NSDA and MLDA Neurons to Neurotoxicant Exposure	134
Introduction	134
Results	136
<i>Characterization of effects of LDN-57444 under basal conditions.....</i>	<i>136</i>
<i>Effects of LDN-57444 on susceptibility of NSDA and MLDA neurons to MPTP</i>	<i>148</i>
Discussion.....	168
Summary and conclusions	172
REFERENCES.....	174
Chapter 6: Effects of Aging on DA Metabolic Homeostasis in NSDA and MLDA Neurons and Susceptibility to MPTP Toxicity	177
Introduction	177
Results	179

<i>Aged mice have less stored DA in the NAc, but astroglial metabolism of DA remains intact</i>	179
<i>Acute MPTP exposure decreases DA, DOPAC, and astroglial DA metabolites in ST and NAc of both young and aged mice</i>	185
<i>Total and phosphorylated TH are decreased in the ST but not the NAc after MPTP in young and aged mice</i>	188
<i>DAT is decreased in the ST, but not the NAc, after MPTP while VMAT2 is unchanged in both young and aged mice treated with MPTP</i>	188
Discussion.....	191
Summary and conclusions	196
REFERENCES.....	198

Chapter 7: Effects of Aging on UCH-L1 Expression and Function in Brain Regions Containing NSDA and MLDA Neurons 203

Introduction	203
Results	205
<i>UPS and UCH-L1 function and expression in NSDA and MLDA neurons in aged mice exposed to MPTP</i>	205
<i>UPS function and UCH-L1 expression in ST synaptosomes from young and aged mice following acute MPTP exposure</i>	205
<i>UPS impairment, UCH-L1 expression and function in SN and VTA in aged mice</i>	210
<i>Effects of MPTP on UCH-L1 expression in the SN and VTA of young and aged mice</i>	210
Discussion.....	216
Summary and conclusions	218
REFERENCES.....	220

Chapter 8: General Discussion 223

<i>Differential regulation of UCH-L1 in regions containing NSDA and MLDA neurons</i>	223
<i>Possible contribution of UCH-L1 function in autophagy</i>	228
<i>Use of the UCH-L1 inhibitor LDN-57444 in vivo</i>	230
<i>Effects of aging on susceptibility of NSDA and MLDA neurons</i>	232
<i>Effects of aging on UPS and UCH-L1 function</i>	234
<i>Future directions</i>	237
Conclusions.....	237
REFERENCES.....	239

LIST OF TABLES

Table 2.1.	Primary and secondary antibodies used for Western blotting.	42
Table 5.1.	Mono-Ub and total Ub proteins in the ST	144
Table 5.2.	Mono-Ub and total Ub proteins in the NAc	145
Table 5.3.	Mono-Ub and total Ub proteins in the SN	146
Table 5.4.	Mono-Ub and total Ub proteins in the VTA	147
Table 5.5.	Injection paradigm for LDN + MPTP study	150
Table 5.6.	UCH-L1 protein expression in the ST	154
Table 5.7.	UCH-L1 protein expression in the NAc.....	155
Table 5.8.	UCH-L1 protein expression in the SN.....	156
Table 5.9.	UCH-L1 protein expression in the VTA.....	157
Table 5.10.	Mono-Ub and total Ub protein in the ST	158
Table 5.11.	Mono-Ub and total Ub protein in the NAc.....	159
Table 5.12.	Mono-Ub and total Ub protein in the SN.....	160
Table 5.13.	Mono-Ub and total Ub protein in the VTA.....	161

LIST OF FIGURES

Figure 1.1.	DA Metabolism and Common Pharmacological Therapeutics for PD	4
Figure 1.2.	Mouse brain diagrams highlighting NSDA (top, red) and MLDA (bottom, blue) neuronal pathways	8
Figure 1.3.	Importance of protein clearance mechanisms in PD	13
Figure 1.4.	Mechanisms of mono-Ub recycling by UCH-L1	15
Figure 2.1.	Images from the online Allen Brain Atlas (mouse.brain-map.org)	38
Figure 3.1.	<i>Ex vivo</i> ROS production in ST (white) and NAc (teal) lysates.	53
Figure 3.2.	In vivo ROS levels in the ST (white) and NAc (teal) 6 after MPTP exposure.....	54
Figure 3.3.	DA in the ST 6 h post MPTP exposure.....	56
Figure 3.4.	DA in the ST (white) and NAc (teal) 24 h after MPTP exposure.....	58
Figure 3.5	DOPAC in the ST (white) and NAc (teal) 24 h after MPTP exposure.....	60
Figure 3.6.	DOPAC/DA ratio in the ST (white) and NAc (teal) 24 h after MPTP exposure.....	61
Figure 3.7.	Total TH protein expression in the ST (white) and NAc (teal) 6 h after MPTP exposure.	62
Figure 3.8.	Total TH protein expression in the ST (white) and NAc (teal) 24 h after MPTP exposure.....	63
Figure 3.9.	UCH-L1 protein expression in the ST (white) and NAc (teal) 6 h after MPTP exposure	65
Figure 3.10.	UCH-L1 protein expression in the ST (white) and NAc (teal) 24 h after MPTP exposure	68

Figure 3.11.	UCH-L1 protein expression in the SN after MPTP exposure.....	70
Figure 3.12.	UCH-L1 protein expression in the VTA after MPTP exposure.....	71
Figure 3.13.	Mono-Ub protein expression in the ST (white) and NAc (teal) 24 h after MPTP exposure	72
Figure 3.14.	Mono-Ub protein expression in the SN 24 h after MPTP exposure.....	73
Figure 3.15.	Mono-Ub protein expression in the VTA 24 h after MPTP exposure.....	74
Figure 3.16.	Total GSH concentrations in the ST (white) and NAc (teal) ..	75
Figure 3.17.	Total GSH concentrations in the SN (white) and VTA (teal)..	76
Figure 3.18.	Immunohistochemical staining for UCH-L1 and TH in the SN (white dashed oval) and VTA (white dotted circle).....	77
Figure 3.19.	Percent of TH and UCH-L1 positive neurons in the SN 24 h after MPTP	78
Figure 3.20.	Percent of TH and UCH-L1 positive neurons in the VTA 24 h after MPTP	79
Figure 3.21.	Pearson's correlation coefficient values for co-localization of UCH-L1 and TH signal in the SN (white) and VTA (teal) ...	80
Figure 3.22.	Mander's overlap correlation values for co-localization of UCH-L1 and TH signal in the SN (white) and VTA (teal) ..	81
Figure 4.1.	Images of differentiated MN9D cells: phase contrast (top left), TH (top right), DAT (bottom left) and UCH-L1 (bottom right)	94
Figure 4.2.	DA content in MN9D cells exposed to various concentrations of MPP ⁺ at 2 and 8 h.....	95
Figure 4.3.	DA and DOPAC concentrations in MN9D cells exposed to 100 μ M MPP ⁺ for 2 h	96
Figure 4.4.	UCH-L1 expression in MN9D cells exposed to various concentrations of MPP ⁺ at 2 h (left) and 8 h (right).....	97

Figure 4.5.	UCH-L1 hydrolase activity in MN9D cells 2 h after 100 μ M MPP ⁺ exposure.....	98
Figure 4.6.	DA (left) and DOPAC (right) in MN9D cells treated with MPP ⁺ , LDN-57444, or a combination for 2 h	99
Figure 4.7.	DOPAC/DA ratio in MN9D cells treated with MPP ⁺ , LDN-57444, or a combination for 2 h.....	101
Figure 4.8.	DA concentration in MN9D cells exposed to various inhibitors for 2 h.....	102
Figure 4.9.	TH protein in MN9D cells exposed to various inhibitors for 2 h.....	103
Figure 4.10.	Cytotoxicity profile of MN9D cells exposed to various inhibitors for 2 h.....	106
Figure 4.11.	LC3B-II protein in MN9D cells exposed to various inhibitors for 2 h.....	107
Figure 4.12.	Diagram showing three relevant DUBs in the context of mono-Ub recycling: UCH-L1, UCH-L3, and USP14	109
Figure 4.13.	UCH-L3 staining in TH neurons in the SN of mice	110
Figure 4.14.	USP14 staining in TH neurons in the SN of mice.....	111
Figure 4.15.	UCH-L3 levels in the mouse SN 24 h after MPTP exposure.....	112
Figure 4.16.	USP14 levels in the mouse SN 24 h after MPTP exposure.....	113
Figure 4.17.	UCH-L1 (left) and mono-Ub (right) protein levels in ST synaptosomes various time points after acute MPTP exposure.....	114
Figure 4.18.	Pearson correlation analysis of UCH-L1 and mono-Ub levels after acute MPTP exposure.....	115
Figure 4.19.	UCH-L1 protein expression in the SN of WT (black) and Park2 ^{-/-} (red) mice various points after single injection of MPTP	117

Figure 4.20.	UCH-L1 protein expression in the SN of WT (white) and Park2 ^{-/-} (red) mice.....	118
Figure 4.21.	Mono-Ub protein expression in the SN of WT (white) and Park2 ^{-/-} (red) mice.....	119
Figure 4.22.	K48-linked ubiquitinated proteins in the SN of WT (white) and Park2 ^{-/-} (red) mice exposed to MPTP	120
Figure 4.23.	LC3B-II protein levels in ST synaptosomes between WT (black) and Park2 ^{-/-} (red) mice at various time points after MPTP injection	122
Figure 4.24.	p62 protein levels in the SN between WT (black) and Park2 ^{-/-} (red) mice 24 h after MPTP injection.....	123
Figure 4.25.	p62 protein levels in ST synaptosomes between WT (black) and Park2 ^{-/-} (red) mice at various time points after MPTP injection	124
Figure 4.26.	hsc70 protein levels in the SN between WT (black) and Park2 ^{-/-} (red) mice 24 h after MPTP injection.....	125
Figure 5.1.	The UCH-L1 inhibitor LDN-57444 is predicted to cross the blood brain barrier (BBB)	138
Figure 5.2.	Injection paradigm for LDN dose response study.....	139
Figure 5.3.	DA (left) and DOPAC (right) concentrations in the ST following saline VH, DMSO VH, 0.5 mg/kg LDN, or 5 mg/kg LDN	140
Figure 5.4.	DOPAC/DA ratio in the ST after saline VH, DMSO VH, and 0.5 and 5 mg/kg LDN.....	141
Figure 5.5.	DA (left) and DOPAC (right) concentrations in the NAc following saline VH, DMSO VH, 0.5 mg/kg LDN, or 5 mg/kg LDN	142
Figure 5.6.	DOPAC/DA ratio in the NAc after saline VH, DMSO VH, and 0.5 and 5 mg/kg LDN.....	143
Figure 5.7.	Proposed mechanism of action of the UCH-L1 inhibitor LDN in the context of UCH-L1 activity and the UPS	149

Figure 5.8.	DA concentrations in the ST of mice and various drug treatments	152
Figure 5.9.	DA concentrations in the NAc of mice and various drug treatments	153
Figure 5.10.	Gel image representing Ub-VME DUB labeling assay for the ST and NAc	162
Figure 5.11.	Gel image representing Ub-VME DUB labeling assay for the SN and VTA	163
Figure 5.12.	Reduced GSH concentration in the ST	164
Figure 5.13.	Reduced GSH concentration in the NAc	165
Figure 5.14.	Reduced GSH concentration in the SN	166
Figure 5.15.	Reduced GSH concentration in the VTA	167
Figure 6.1.	DA and DOPAC concentrations and DOPAC/DA ratio in ST (A, C, E) and NAc (B, D, F) in Young, Mature, Old, and Aged mice	180
Figure 6.2.	HVA and 3-MT concentrations after MPTP in Young and Aged ST (A, C) and NAc (B, D)	183
Figure 6.3.	DA and DOPAC concentrations after MPTP in Young and Aged ST (A, C) and NAc (B, D)	184
Figure 6.4.	Ser40 p-TH and total TH protein levels in ST (A, C) and NAc (B, D)	186
Figure 6.5.	DAT and VMAT2 protein levels in ST (A, C) and NAc (B, D)	187
Figure 6.6.	COMT protein levels in ST (A, C) and NAc (B, D).....	189
Figure 6.7.	Overview of neuronal synthesis of DA and astrocyte metabolism	190
Figure 7.1.	Total Ub protein in the ST	206
Figure 7.2.	Total Ub protein in the NAc	207

Figure 7.3.	Total Ub proteins in ST synaptosomes.....	208
Figure 7.4.	UCH-L1 protein in ST synaptosomes.....	209
Figure 7.5.	Total Ub protein in the SN and VTA in Young and Aged mice	211
Figure 7.6.	UCH-L1 protein in the SN and VTA in Young and Aged mice.....	212
Figure 7.7.	Mono-Ub protein in the SN and VTA in Young and Aged mice	213
Figure 7.8.	UCH-L1 protein in the SN Young and Aged mice treated with VH or MPTP	214
Figure 7.9.	UCH-L1 protein in the VTA Young and Aged mice treated with VH or MPTP	215
Figure 8.1.	Summary of major findings in this Dissertation	236

KEY TO ABBREVIATIONS

α -syn	Alpha synuclein
AAV	Adeno-associated virus
ALP	Autophagy lysosome pathway
AD	Alzheimer's disease
ANOVA	Analysis of variance
ARC	Arcuate nucleus
ATP13A2	ATPase type 13A2
BCA	Bicinchoninic acid
CMA	Chaperone mediated autophagy
CNS	Central nervous system
COMT	Catechol-O-methyl transferase
DA	Dopamine
DAergic	Dopaminergic
DAT	Dopamine transporter
DCF-DA	2'-7'-Dichlorofluorescein diacetate
DDC	DOPA decarboxylase
DJ-1	Protein deglycase DJ-1
DMSO	Dimethylsulfoxide
DOPA	Dihydroxyphenylalanine
DOPAC	3,4-dihydroxyphenylacetic acid
FBX07	F-box protein 7

GAPDH	Glyceraldehyde phosphate dehydrogenase
gad	Gracile axonal dystrophy
GLP-1	Glucagon-like peptide 1
GSH	Reduced glutathione
GSSG	Oxidized glutathione
Hsc70	Heat shock protein 70
HTRA2	High temperature requirement protein A2
HVA	Homovanillic acid
HPLC-ED	High pressure liquid chromatography-electrochemical detection
IHC	Immunohistochemistry
K	Lysine
Lamp-2A	Lysosomal associated membrane protein 2A
LC3	Microtubule associated protein 1A/1B-light chain 3
LDN-57444	5-Chloro-1-[(2,5-dichlorophenyl)methyl]-1H-indole-2,3-dione 3-(O-acetyloxime)
Levodopa	Levo-dihydroxyphenylalanine
LRRK2	Leucine-rich repeat kinase 2
MAO-B	Monoamine oxidase B
MAPT	Microtubule associated protein tau
ME	Median eminence
MLDA	Mesolimbic dopamine
MN9D	Mouse neuroblastoma cells clone 9D
MPP ⁺	1-methyl-4-phenylpyridinium

MPTP	1-methyl-4-phenyl-1,2,3,6-tetrahydropyridine
MSN	Medium spiny neuron
3-MT	3-methoxytyramine
NAc	Nucleus accumbens
NSDA	Nigrostriatal dopamine
Park2	Parkin
Park2 ^{-/-}	Parkin deficient
PD	Parkinson disease
p62	Sequestome-1
PINK1	PTEN-induced putative kinase 1
PLA2G6	Phospholipase A2 Group 6
ROS	Reactive oxygen species
SN	Substantia nigra
SNCA	Human alpha synuclein gene
ST	Striatum
STN	Subthalamic nucleus
TH	Tyrosine hydroxylase
TIDA	Tuberoinfundibular dopamine
UCH-L1	Ubiquitin carboxy-terminal hydrolase L1
UCH-L3	Ubiquitin carboxy-terminal hydrolase L3
Ub	Ubiquitin
UPS	Ubiquitin proteasome system
USP14	Ubiquitin specific protease 14

VMAT2	Vesicular monoamine transporter 2
VPS35	Vacuolar protein sorting 35
VTA	Ventral tegmental area

Chapter 1: General Introduction

History and motor symptoms of PD

Two hundred years before the completion of this Dissertation, the physician Dr. James Parkinson wrote the first comprehensive description of Parkinson disease (PD): his *Essay on the Shaking Palsy*. Dr. Parkinson observed his own patients and citizens of London exhibiting a host of distinctive motor disturbances (Parkinson, 1817) that physicians now use to diagnose PD. Dr. Parkinson termed the disease “paralysis agitans.” Later, Dr. Jean-Martin Charcot renamed the disorder “Parkinson’s disease” in honor of Dr. Parkinson and to recognize that Dr. Parkinson was the first to medically describe the disorder’s symptoms in detail. The progression of PD is characterized by motor dysfunction such as bradykinesia (slowness of movement), postural instability, resting tremor and shuffling gait, and is most commonly diagnosed in elderly patients (> 65 years old) (Gelb et al., 1999). Neurodegenerative diseases are expected to increase dramatically in the United States and worldwide as the population ages (Brown et al., 2005), and aging is the greatest risk factor for developing PD (Calne and William Langston, 1983). Accumulation of oxidative stress with aging is expected to play a large role in development and progression of the disease (Liu and Mori, 1999).

The motor symptoms associated with PD are caused by the specific degeneration of nigrostriatal (NS) dopamine (DA) neurons in the substantia nigra (SN) (Hornykiewicz, 1966), which regulate motor coordination in the basal ganglia pathway by releasing DA in the striatum (ST) to synapse on D1 and D2 DA receptors on medium spiny neurons (MSNs). DA functions in both the direct (mediated by D1 receptor activation) and indirect (mediated by D2 receptor activation) pathways and allows the motor cortex to

execute appropriate motor programs. However, when DA neurons in the SN degenerate, DA signaling in the ST is lost, and tonic activity of the globus pallidus internus prevents initiation of voluntary motor function, leading to the hallmark motor dysfunctions characteristic of PD.

Non-motor dysfunction in PD and Braak staging

In addition to motor dysfunction in PD, there are non-motor symptoms that often precede motor symptoms. These early non-motor disturbances include constipation, hyposmia (loss of smell), and sleep disturbances (Chaudhuri et al., 2006). There are DA neurons in the enteric nervous system (ENS), and as these neurons degenerate, complications in gastrointestinal motility become apparent (Singaram et al., 1995). One hypothesis is that PD originates in the ENS (Braak et al., 2006), since constipation is an early common non-motor manifestation of PD and deposition of alpha synuclein (α -syn) known as Lewy bodies has been observed in the ENS of PD patients (Wakabayashi et al., 1988). The vagus nerve is hypothesized to be the avenue through which pathological α -syn gains access to the central nervous system (CNS) (Ulusoy et al., 2013). In fact, due to the spread and propagation of α -syn aggregates throughout the brain, PD has been proposed to be a prion-like disorder (Brundin et al., 2010).

In Braak staging (Braak et al., 2003), pathology is first manifested in the lower brainstem, chiefly in the medulla oblongata and dorsal motor nucleus of the vagus nerve degeneration (Stage I), which strengthens the evidence for pathology arising first in the ENS and traveling through the vagus nerve to the CNS. In Stage II, the raphe nucleus (the major site of serotonin neuronal cell bodies in the CNS) and locus coeruleus (the

major site of norepinephrine neuronal cell bodies in the CNS) are affected.

Degeneration of the raphe nucleus and locus coeruleus contribute to development of depression and autonomic defects in PD patients (Alexander, 2004). The midbrain is affected in Stage III, particularly the SN, leading to the canonical motor symptoms and diagnostic criteria for PD. In Stages IV, V, and VI, pathology spreads to various areas of the cortex, resulting in cognitive impairment and dementia (Dubois and Pillon, 1996). These non-motor symptoms are considered to be just as devastating if not more to patients with PD (Chaudhuri et al., 2006) and present a significant burden on general well-being and family members of those afflicted.

Current therapies for PD

Current therapeutics for PD address the motor symptoms of the disease but do not halt or slow the progression of the disease, and are not disease-modifying. Levodopa or L-DOPA is the most commonly prescribed drug to treat parkinsonism and is employed as DA replacement therapy, often in combination with other drugs that prevent peripheral metabolism of L-DOPA (such as a catechol-O-methyl (COMT) inhibitor, entacapone and the DA decarboxylase (DDC) inhibitor, carbidopa). DA itself does not cross the blood-brain barrier, but L-DOPA crosses it easily. In addition, DA replacement with L-DOPA rather than tyrosine bypasses the rate-limiting enzyme for DA synthesis, tyrosine hydroxylase (TH) (**Fig. 1**). Another symptom-modifying approach to treating parkinsonism is deep brain stimulation (DBS). DBS involves implanting a pacemaker-like device with an electrode in the brain to stimulate various parts of the basal ganglia pathway, such as the subthalamic nucleus (STN) to compensate for the loss of DA and allow patients to move freely (Group, 2001). Finally, transplantation of human fetal DA

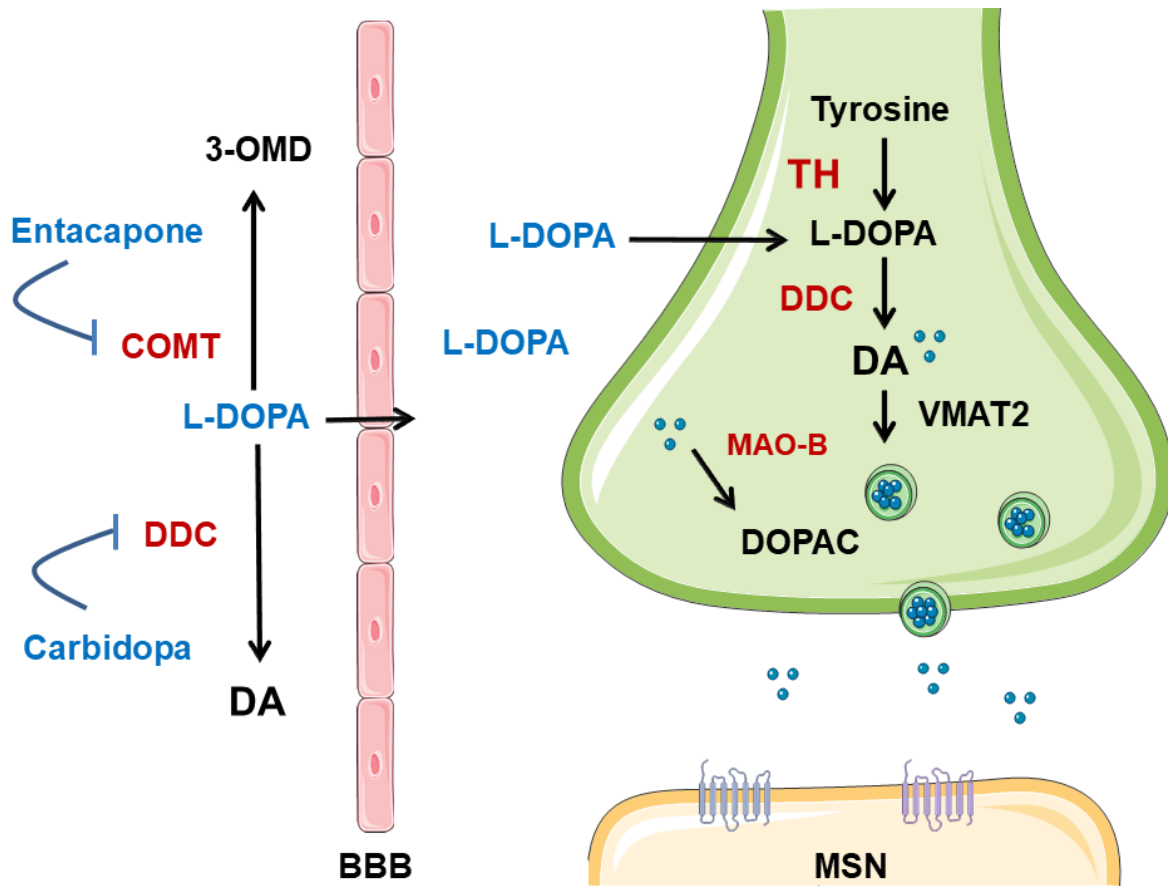


Figure 1.1. DA Metabolism and Common Pharmacological Therapeutics for PD. DA is synthesized within the axon terminal (green) from tyrosine to L-DOPA via TH. After synthesis, DA is packaged into vesicles by vesicular monoamine transporter 2 (VMAT2) and released into the synapse, where DA can bind to D1 or D2 receptors in MSNs. DA replacement with L-DOPA (blue) is often used in conjunction with COMT or DDC inhibitors (entacapone and carbidopa, respectively, in blue) to prevent peripheral metabolism of L-DOPA.

neurons has had some success (Li et al., 2016), but transplanted DA neurons often fall victim to the same disease mechanisms responsible for the destruction of original NSDA neurons (Li et al., 2008). In addition, DA grafts do not prevent degeneration of non-DA neuronal populations affected by the disease and do not alleviate non-motor symptoms (Politis et al., 2012). Perhaps the fetal graft option is not the most desirable disease-modifying therapeutic intervention. To date, no disease-modifying treatments for PD are available, which represents a major unmet need in patients affected worldwide. A clinical trial involving a promising type 2 diabetes drug, exenatide, has recently been highlighted as effective for reducing motor symptoms in PD patients during “off” periods (Athauda et al., 2017). Exenatide is capable of crossing the blood-brain barrier and acts as a glucagon-like peptide 1 (GLP-1) receptor agonist. Whether exenatide slows or halts progression of PD is yet to be determined.

Mutations that cause PD

The vast majority of PD cases are idiopathic, meaning that a specific cause cannot be attributed to development of the disease. However, several monogenic mutations that cause PD have been identified and given a “PARK” locus designation. Autosomal dominant point mutations in the gene for leucine-rich repeat kinase 2 (*LRRK2*, *PARK8*) (Zimprich et al., 2004) are the most common cause of familial late-onset PD. Autosomal dominant mutations in the gene for α -syn (*SNCA*, *PARK1-4*) (Polymeropoulos et al., 1997) also cause PD. The involvement of α -syn is impossible to ignore: triplication of the α -syn gene has also been shown to cause PD (Singleton et al., 2003). An autosomal dominant mutation in the gene for ubiquitin carboxy-terminal hydrolase L1 (*UCHL1*, *PARK5*) was identified in two members of a German family with PD (Leroy et

al., 1998). A rare cause of PD, an autosomal dominant mutation in vacuolar sorting-associated protein 35 (*VPS35*) has recently been identified (Zimprich et al., 2011).

There are many more recessively inherited mutations that cause PD, however.

Mutations in the E3 ligase parkin (*PARK2*) are the most common cause for autosomal recessive juvenile parkinsonism (Kitada et al., 1998). The gene for PTEN-induced putative kinase 1 (*PINK1*, *PARK6*) has also been found to be mutated in PD (Valente et al., 2004). A mutation in the gene for protein deglycase DJ-1 (*DJ-1*, *PARK7*) caused autosomal recessive PD (Bonifati et al., 2003). A lysosomal type 5 P-type ATPase (*ATP13A2*, *PARK9*) is mutated in PD (Ramirez et al., 2006). A serine protease called Omi/HTRA2 (*PARK13*) is also mutated in PD (Strauss, 2005). A phospholipase A2 (*PLA2G6*, *PARK14*) mutation causes young onset PD (Lu et al., 2012). F-box protein 7 (*FBX07*, *PARK15*) was found to be mutated in familial PD (Di Fonzo et al., 2009). By investigating pathways affected by these relatively rare mutations that cause PD, we can understand which mechanisms are especially vital in protecting DA neurons from degeneration.

Genetic risk factors for PD

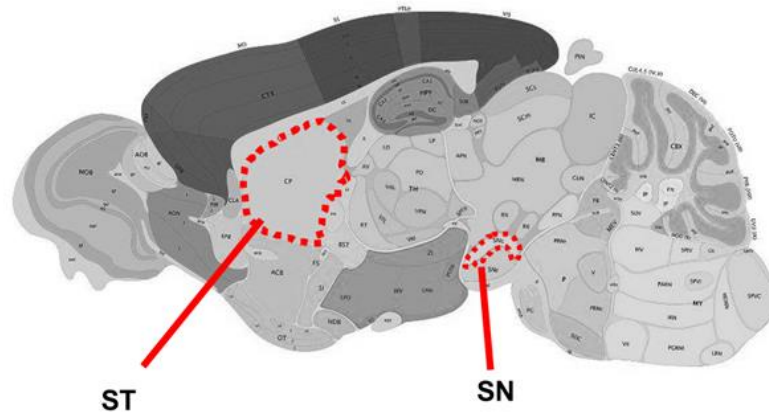
Although monogenic forms of PD are rare, genetic risk factors that contribute to incidence of idiopathic PD have been identified through genome-wide association studies. One such genetic risk factor is a mutation in β -glucocerebrosidase A (*GBA*) which increases the risk of developing PD (Goker-Alpan et al., 2004). Mutation in *GBA* causes Gaucher's disease in which lysosomal storage is compromised by accumulation of mutated *GBA* protein (Hruska et al., 2008). Single nucleotide polymorphisms and

variants in *SNCA* and mutations in the *MAPT* gene (coding for microtubule associated protein tau) were detected in a genome-wide association study in patients with PD (Davis et al., 2016). Interestingly, the genetic testing company 23andMe has recently been approved by the FDA to test customer's DNA and disclose two risk factors for developing PD: the G2019S variant in *LRRK2* and the N370S variant in *GBA*. In addition, there are genetic factors that are also associated with the age-at-onset of familial PD (Hill-Burns et al., 2016).

Environmental risk factors for PD

In addition to genetic risk factors for development of PD, environmental risk factors have also been identified that affect incidence of PD (Klingelhoefer and Reichmann, 2015). Since the GI tract and olfactory bulb, both sites affected by PD, are avenues through which exposure to potentially harmful chemicals can take place, environmental exposure is predicted to play a role in PD. These environmental factors include exposure to herbicides and pesticides, as well as drinking well water (Gorell et al., 1998). Most notoriously, lipophilic pesticides such as the organochloride dieldrin (Fleming et al., 1994) and herbicides rotenone and paraquat (Tanner et al., 2011) are thought to be especially toxic because they inhibit Complex I of the mitochondria and cause oxidative stress. Air pollution is also implicated in a host of human diseases, and increased oxidative stress is caused by certain volatile chemicals (Kampa and Castanas, 2008). While no conclusive studies have definitively linked development to PD to air pollution, exposure to toxic chemicals in the air could plausibly contribute to development of PD. In addition, a role for the gut microbiome has been proposed and

NSDA



MLDA

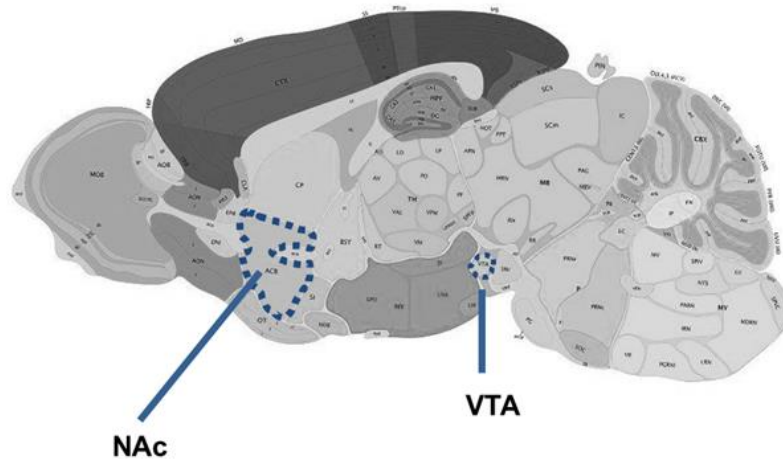


Figure 1.2. Mouse brain diagrams highlighting the NSDA (top, red) and MLDA (bottom, blue) neuronal pathways. Images were modified from the Allen brain atlas (mouse.brain-map.org). In the NSDA pathway, DA neurons from the SN in the midbrain project to the ST. In the MLDA pathway, DA neurons from the VTA in the midbrain project to the NAc.

differences in gut bacteria were associated with severity of motor dysfunction in PD patients (Scheperjans et al., 2015).

Selective vulnerability of central DA neurons to PD

Although NSDA neurons are lost over time as PD progresses, other DA neurons in the brain are spared: tuberoinfundibular (TI) DA neurons and mesolimbic (ML) DA neurons resist degeneration (Braak and Braak, 2000). TIDA neurons have cell bodies located in the arcuate nucleus (ARC) and axon terminals in the median eminence (ME) and are involved in DA-mediated regulation of prolactin secretion (Lookingland and Moore, 2005). MLDA neurons have cell bodies in the ventral tegmental area (VTA) of the midbrain and axon terminals in the nucleus accumbens (NAc) ventral to the ST (**Fig. 1.2**) and function in the reward pathway to stimuli such as food and drugs. MLDA neurons are also implicated in addiction.

MLDA neurons are often compared to NSDA neurons since they are phenotypically and anatomically similar, and are regulated by DA receptor-mediated mechanisms (Demarest and Moore, 1979). There is evidence that a link between the two DA systems in limbic control of motor activation exists (Mogenson et al., 1980), highlighting a potential interaction between NSDA and MLDA function. Additionally, neuronal pathways that are physically or functionally linked are predicted to be affected similarly by Lewy pathology in PD (Braak et al., 2003). One main physiological difference between NSDA and MLDA neurons that is predicted to affect susceptibility to neurodegeneration involves calcium spiking and the fact that NSDA neurons express more L-type (Cav1) Ca^{2+} channels than MLDA neurons, which can drastically affect how

much Ca^{2+} enters the cell (Philippart et al., 2016). This difference also highlights the importance of calbindin, a key Ca^{2+} binding protein that confers the ability of MLDA neurons to buffer intracellular Ca^{2+} . Since NSDA neurons do not express high levels of calbindin (Foehring et al., 2009), unrelenting influx of Ca^{2+} into the cytoplasm can initiate the apoptotic cascade (Nagley et al., 2010) and promote production of reactive oxygen species (ROS). One promising drug trial for the calcium channel blocker isradipine is underway to determine efficacy in PD patients.

In PD, DA loss is more pronounced in the putamen of PD patients versus other regions in the ST (Kish et al., 1988). In a study aimed at comparing regional differences in neurotransmitter uptake systems, [^3H] mazindol uptake was found to be decreased in both the ST and NAc of PD patients, with slightly more loss of [^3H] mazindol uptake in the ST (-75%) compared to the NAc (-65%) (Chinaglia et al., 1992). DA transport insufficiency in the NAc may partially explain why elderly patients with PD display deficits in reward processing (Schott et al., 2007), but does not explain why MLDA neurons do not degenerate. Physiologically, both NSDA and MLDA neurons use DA as the key neurotransmitter, which has been linked to production of toxic DA adducts (Caudle et al., 2007; Hastings et al., 1996) and ROS. Previous studies have examined differences between NSDA and MLDA neurons and how their dissimilarities translate into differential susceptibility between the two DA neuron populations (Surmeier et al., 2017). How MLDA neurons resist degeneration is an important question that, if answered, could lead to new therapeutics to slow or halt the progression of PD.

Vulnerability of DA neuronal populations to models of neurodegeneration

The molecule 1-methyl-4-phenyl-1,2,3,6-tetrahydropyridine (MPTP) has been used extensively in PD research to model oxidative stress-mediated specific degeneration of DA neurons. Discovered as a contaminant in the synthesis of illicit substances, MPTP caused parkinsonian symptoms in people who consumed the contaminated drugs (Langston et al., 1983). Dr. J. William Langston, a physician treating the afflicted patients, identified MPTP as the cause of toxicity (Langston et al., 1984) and developed the first *in vivo* MPTP model using squirrel monkeys (Langston et al., 1984). MPTP is highly lipophilic and easily crosses the blood-brain barrier. Once in the brain, it is metabolized in glial cells by monoamine oxidase B (MAO-B) to its active metabolite, 1-methyl-4-phenylpyridinium (MPP⁺), which has high affinity for the DA transporter (DAT). Since MPP⁺ selectively enters DAT expressing neurons, it is considered a specific DA neuron toxicant. Specific central DA neuronal degeneration could be replicated in mice (Sonsalla and Heikkila, 1986), and an MPTP mouse model was born.

MPP⁺ was discovered to inhibit Complex I of the mitochondria (Mizuno et al., 1986), preventing ATP production and leading to apoptotic cell death. Mitochondrial dysfunction is hypothesized to play a major role in development of PD (Schapira et al., 1990). Additionally, MPP⁺ causes oxidative stress (Johannessen et al., 1986), which can damage organelles and cytosolic proteins, leading to widespread dysfunction and can trigger cell death. Oxidative stress is thought to be a major factor in many neurodegenerative diseases and is heavily implicated in PD (Blesa et al., 2015). While neurotoxicant treated mice have limitations in modeling every aspect of PD, the MPTP

model of DA depletion and oxidative stress can recapitulate differential susceptibility between NSDA and MLDA neurons (Behrouz et al., 2007; Hung and Lee, 1998).

The differential susceptibility of MLDA and NSDA neurons observed in toxicant models has also been demonstrated in transgenic rodent models of PD-like pathology (Maingay et al., 2006). In addition, studies in nonhuman primates have also recapitulated the resistance of VTA DA neurons to MPTP (Dopeso-Reyes et al., 2014). MLDA neurons are not susceptible to damage in rats after rAAV-mediated overexpression of α -syn in the ventral midbrain (Maingay et al., 2006), which indicates MLDA neurons are resistant to neurodegeneration elicited by distinct, but likely convergent etiologies of PD. Since we have a model that recapitulates oxidative stress and selective DA loss, we can use MPTP to recapitulate the differential susceptibilities of NSDA and MLDA neurons in mice and examine pathways involved in determining vulnerability or resistance.

Protein degradation pathways in PD

A hallmark pathology of PD is the presence of Lewy bodies in NSDA neurons, which are proteinaceous deposits of α -syn (Baba et al., 1998; Spillantini et al., 1997), ubiquitin (Kuzuhara et al., 1988), and components of the ubiquitin proteasome system (UPS), suggesting that PD pathology is profoundly linked to disruption in protein homeostasis (**Fig. 1.3**). Within the family of human genes with the PARK denotation, two code for proteins involved in the UPS such as UCH-L1 (PARK5) and parkin (PARK2). Although diverse mechanisms of cellular dysfunction are implicated in development and progression of PD, deficits in the ability of neurons to maintain protein homeostasis are especially evident.

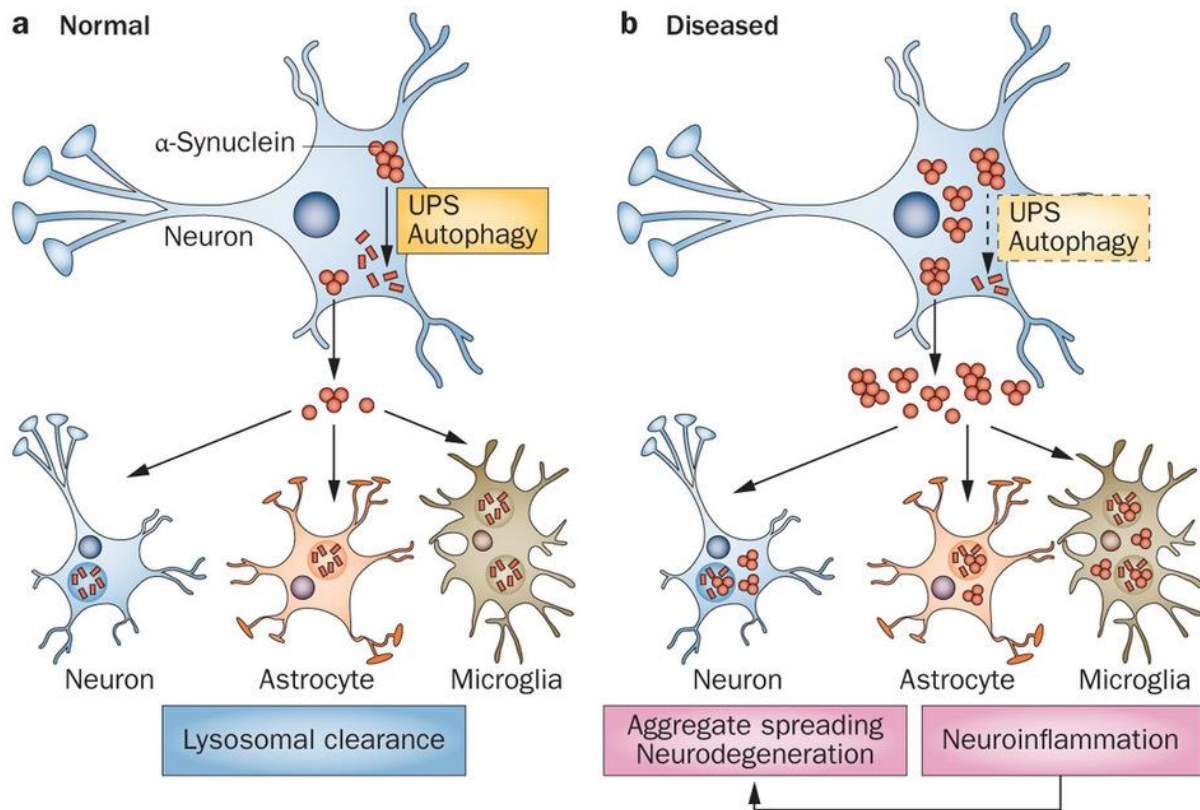


Figure 1.3. Importance of protein clearance mechanisms in PD. In the left panel, **A**, a neuron is shown with functional UPS and autophagy pathways and can degrade excess α -syn. Also shown is the secretion of α -syn from neurons to other neurons, astrocytes, or microglia, which also must control the amount of α -syn. In the right panel, **B**, a neuron with impaired UPS and autophagy shows abnormal accumulation of α -syn which can spread to other cell types, causing neuroinflammation and eventually neurodegeneration. From Lee *et al.*, 2014 (Lee *et al.*, 2014).

The UPS is one of the major pathways of protein degradation in the cell that clears damaged and misfolded proteins in a selective manner. In the UPS, substrates are tagged with polyubiquitin (poly-Ub) chains by successive actions of E1 activating and E2 conjugating enzymes passing activated ubiquitin to E3 ubiquitin ligases, which form K48-linked Ub chains attached to a substrate one monomer at a time. The poly-Ub substrate can be degraded by the 26S proteasome. The other major protein degradation pathway is autophagy or the autophagy lysosome pathway (ALP) that is also implicated in PD. Rather than requiring the use of a poly-Ub tag to target substrates to the ALP, a form of the ALP called macroautophagy can occur without substrate specificity, which is in contrast to the UPS. In chaperone mediated autophagy (CMA), another type of autophagic degradation, proteins must contain a specific amino acid motif (KFERQ) to be substrates (Bandyopadhyay et al., 2008). The PD-related protein α -syn is linked to dysfunction of CMA in that it is routinely degraded by CMA, but can impair CMA-mediated degradation of other substrates in its mutant form (Cuervo et al., 2004). Emerging evidence suggests that the UPS and ALP could be functionally linked: if one pathway is impaired, the other may be upregulated in a compensatory attempt to maintain proteostasis (Ross and Pickart, 2004).

Deubiquitinating enzymes in the UPS and UCH-L1

Fine-tuning the specificity of UPS activity are de-ubiquitinating (DUB) enzymes, which are diverse in structure and remove either polymeric Ub (poly-Ub) or monomeric Ub (mono-Ub) as well as perform other functions to modify or mature Ub itself (Todi and Paulson, 2011). In humans, there are five known families of DUBs which are also conserved in mice: UCH (ubiquitin carboxy-terminal hydrolases), USP (ubiquitin-specific

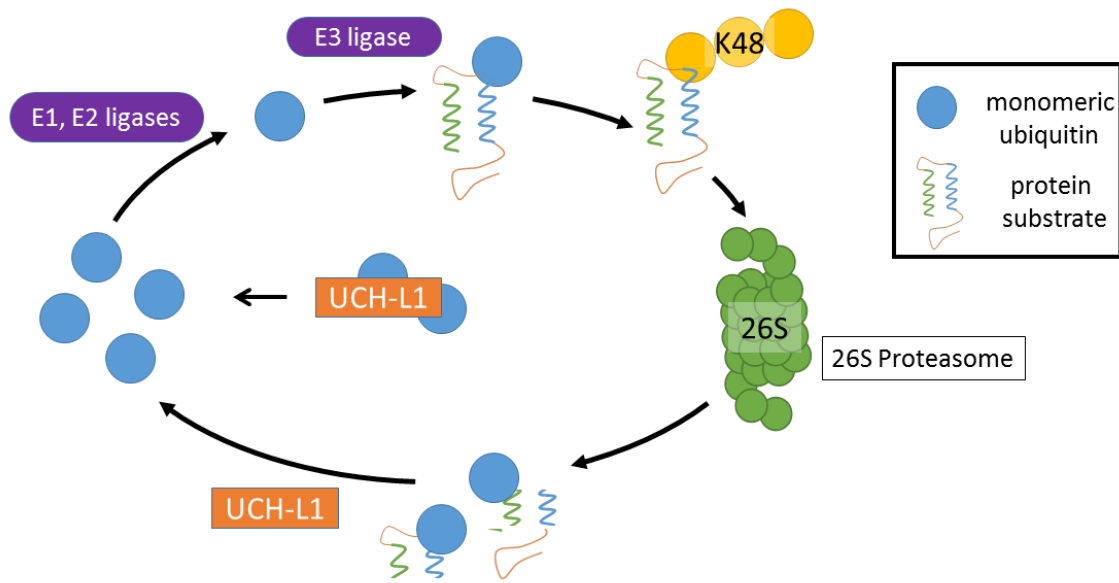


Figure 1.4. Mechanisms of mono-Ub recycling by UCH-L1. The pool of available mono-Ub can be activated and passed along by E1 and E2 ligases and attached onto a protein substrate for degradation by an E3 ligase. The Ub chain is elongated (a chain of K48-linked Ub destined the protein for destruction) and the protein is degraded by the 26S proteasome. If the Ub chain is not removed before degradation of the substrate by a different DUB, UCH-L1 can recover mono-Ub attached to peptide fragments to replenish the pool of mono-Ub. Additionally, UCH-L1 has high affinity for mono-Ub and can bind and stabilize mono-Ub to prevent it from degradation.

proteases), OTU (ovarian tumor proteases), Josephins, and JAMM/MPN+. UCH, USP, OTU and Josephin enzymes are cysteine proteases while JAMM/MPN+ DUBs are zinc metalloproteases (Eletr and Wilkinson, 2014). Of the three known UCH enzymes, UCH-L1 is the most studied in the context of neurodegenerative diseases (notably PD and Alzheimer disease (AD)) because in the brain it is expressed selectively in neurons. With an extremely knotted structure thought to provide protection against proteasomal degradation (Virnau et al., 2006), UCH-L1 hydrolyzes the bond between the C-terminus of small peptide substrates and the Ub monomer (Wilkinson et al., 1989). The main function of the enzyme is to replenish pools of free mono-Ub to be recycled in the UPS, which it can accomplish via its hydrolase activity and its ability to bind and sequester mono-Ub to protect it from degradation (Osaka et al., 2003) (**Fig. 1.4**). A role for UCH-L1 in cancer has been well-reviewed (Hurst-Kennedy et al., 2012) and will not be further discussed here.

UCH-L1 in PD

UCH-L1, also known as protein gene product (PGP) 9.5, was first described in 1989 as a neuron specific DUB (Chen et al., 2010) enzyme that comprises 1-2% of total soluble brain protein (Wilkinson et al., 1989). Due to its abundance in the nervous system, staining for UCH-L1 is used as a pan-neuronal marker (Thompson et al., 1983). UCH-L1 contains a catalytic triad composed of a cysteine at position 90, an aspartate at position 176, and a histidine at position 161 responsible for the cysteine protease hydrolytic activity of the enzyme (Das et al., 2006). The first indication that UCH-L1 plays a role in the pathogenesis of PD came almost ten years later in 1998 when an autosomal dominant mutation was found in two members of a German family diagnosed

with PD (Leroy et al., 1998). The affected siblings had an isoleucine to methionine substitution in position 93 (I93M) in UCH-L1 which later was found to decrease the hydrolase activity of the enzyme by 50% (Setsuie et al., 2007). Accordingly, loss of UCH-L1 hydrolase function was predicted to result in the parkinsonian phenotype of the original patients. The I93M mutation also increased the incidence of aggregation of UCH-L1 and caused the protein exhibit characteristics of being oxidatively modified (Kabuta et al., 2008). Although mutations causing PD are rare and represent a minority of clinical cases, immunohistochemical (IHC) staining for UCH-L1 is observed in Lewy bodies of idiopathic PD patients (Lowe et al., 1990). This relationship between loss of UCH-L1 expression and incidence of PD led to the designation of the UCHL1 human gene as PARK5.

A mutation within the domain that binds ubiquitin in UCH-L1 which resulted in a substitution from glutamine to alanine in position 7 (GLU7ALA) caused early onset neurodegeneration in three siblings of a consanguineous union, resulting in optical nerve atrophy and blindness (Bilguvar et al., 2013). This mutation renders UCH-L1 less able to bind to ubiquitin and results in a dramatic decrease in hydrolase activity (reported to be greater than 100-fold reduction) (Bilguvar et al., 2013). Taken together, mutations in the UCHL1 gene in humans are linked to PD (I93M) and are causative in an early-onset neurodegenerative disease (GLU7ALA) suggest that UCH-L1 protein function (UPS related or otherwise) is extremely important in the nervous system. It is interesting to note, however, that two mutations in the Uchl1 gene cause two very different neurodegenerative phenotypes in human patients.

A common polymorphism found in humans, S18Y (Zhang et al., 2000), is linked to decreased incidence of PD. Further studies showed that the S18Y mutation confers antioxidant activity (Xilouri et al., 2012) to the protein, but the association between the polymorphism and the incidence of PD is controversial (Mellick and Silburn, 2000). Nevertheless, multiple forms of UCH-L1 have distinct hydrolase activities and diverse reported functions, especially in transgenic mouse models engineered to explore the possibilities of isoforms and splice variants. While the possibility of a protective polymorphism of UCH-L1 being associated with lower risk for PD is intriguing, it has not been explored much further in published literature.

These findings lead to the hypothesis that loss of UCH-L1 hydrolase activity could contribute to the pathogenesis and progression of PD. After acute MPTP in mice, UCH-L1 was discovered to be decreased in the SN but was maintained in the ARC (Benskey et al., 2012), which was the first inkling that maintenance of UCH-L1 could confer protection in resilient DA neurons while loss of UCH-L1 could be a factor that promotes susceptibility. However, expression of UCH-L1 in MLDA neurons was not yet known. In transgenic mice expressing the I93M mutation of UCH-L1, neurodegeneration is prominent in the NSDA system (Setsuie et al., 2007), illustrating the effects of the mutation on the ability of UCH-L1 to function as a DUB. However, in a neuronal cell line where UCH-L1 is mutated with a substitution of cysteine to serine in position 90 which prevents hydrolase activity, mono-Ub levels remain intact, which is evidence that the ability of UCH-L1 to bind and stabilize mono-Ub may be more important than its hydrolase activity to maintain mono-Ub within the cell (Osaka et al., 2003).

Another important DUB contributor to mono-Ub levels within neurons is USP14, a ubiquitin specific protease that is associated with the proteasome which is also responsible for recycling mono-Ub (B J Walters et al., 2008). Although both UCH-L1 and USP14 contribute to recycling of mono-Ub, they do so in different ways and have been hypothesized to therefore regulate separate pools of mono-Ub (B J Walters et al., 2008). Nevertheless, there is much literature linking UCH-L1 to the free available pool of mono-Ub and measuring mono-Ub is considered an important index of UCH-L1 function.

In addition to its ubiquitin hydrolase activity, UCH-L1 possesses ligase activity requiring dimerization of the protein (Liu et al., 2002). This novel activity of UCH-L1 has been described as a “toxic gain of function” because UCH-L1 ubiquitinates α -syn via K63-linked chains which prevents proteasomal degradation of α -syn (and may target α -syn for other pathways or protein trafficking). Additional potential substrates of UCH-L1 ligase activity have not yet been identified. Although UCH-L1 ligase activity was demonstrated *in vitro*, it remains unconfirmed *in vivo*.

The E3 ubiquitin ligase parkin was demonstrated to regulate UCH-L1, ubiquitinating it via K63-linked chains to signal degradation by autophagy (McKeon et al., 2014). In the study, UCH-L1 levels were elevated in parkin deficient mice (McKeon et al., 2014). The consequences of parkin regulating UCH-L1 have not been fully explored *in vivo*, but perhaps in certain conditions such as during oxidative stress it is beneficial for the E3 ligase function of parkin to predominate over the DUB function of UCH-L1. In this scenario, UCH-L1 directly opposes parkin by removing mono-Ub from parkin substrates and therefore preventing subsequent addition of poly-Ub chains. UCH-L1 would rescue

both the substrate and mono-Ub, thereby preventing degradation of the substrate and increasing the mono-Ub pool simultaneously. Although this relationship and its consequences on UPS activity have yet to be fully explored *in vivo*, the possible interplay between two PD-related gene loci could represent an interesting new angle connecting two important players in the UPS to progression of PD.

Gracile axonal dystrophy (gad) phenotype

A spontaneous (and rather fortuitous) mutation in a mouse colony at the Jackson Laboratory occurred in a mouse termed *gad* for gracile axonal dystrophy (Saigoh et al., 1999). These mice displayed hind limb atrophy preceded by loss of sensory input and a “dying back” phenotype in the gracile tract occurring late in development until the animals die after 5-6 months of age. A mutation in the *Uchl1* gene where two exons (7 and 8) are deleted was discovered which appeared to primarily affect the gracile nucleus located in the medulla oblongata (Saigoh et al., 1999). This deletion results in a truncated non-functional version of UCH-L1, as the mutation affects a central histidine in the catalytic triad (His161).

One hypothesis for the reason why deletion of UCH-L1 causes degeneration specifically in the gracile tract leading to degeneration in the gracile nucleus (as opposed to a parkinsonian phenotype, for example) is that loss of UCH-L1 function preferentially affects the longest axons in the central nervous system (Oda et al., 1992) due to its apparent effects on axonal transport (Ichihara et al., 1995) and that the mice do not live long enough for other neurons to be affected. In the case of PD where NSDA neurons

degenerate, it is plausible that these neurons could also suffer from a lack or decrease in UCH-L1 protein as a product of aging, though this hypothesis has yet to be tested.

Although the molecular cause of neurodegeneration due to loss of functional UCH-L1 in the *gad* mice has not been fully explored, mice with the mutation exhibit increased oxidative stress (Goto et al., 2009). One clue about the function of UCH-L1 revealed by the *gad* mice was that mice lacking UCH-L1 displayed reduced amount of mono-Ub in brain lysates, emphasizing the role of UCH-L1 in maintaining the mono-Ub pool (Osaka et al., 2003).

nm3419 mouse phenotype

The nm3419 mouse, a relatively new example of a mammal in which the *Uchl1* gene is altered, possesses a mutation that causes loss of 78 amino acids in the C-terminus resulting in a non-functional version of UCH-L1 protein (Walters et al., 2008). Recently, the loss of UCH-L1 hydrolase function in the nm3419 mouse has been shown to cause selective motor neuron degeneration (with no loss in sensory function) (Jara et al., 2016). Although much of the mouse's phenotype with regard to UPS function has not been characterized, it is considered to be a UCH-L1 null model and future studies should distinguish the consequences of loss of UCH-L1 function by mutation.

Interestingly, the nm3419 mice and *gad* mice do not have identical phenotypes, which would be expected if the degenerative phenotype was caused by a simple loss of UCH-L1 function. Additional characterization (and perhaps targeting of specific neuronal populations) of loss of UCH-L1 function is needed to fully understand the degenerative phenotype differences between nm3419 and *gad* mice.

Regulation of UCH-L1 expression in neurons

Not much has been published about how UCH-L1 gene expression is regulated. At the time of this publication, there is one report that demonstrated that a long noncoding RNA antisense to UCH-L1 promotes expression of UCH-L1 (Carrieri et al., 2015). In the study, an antisense UCH-L1 lncRNA increased UCH-L1 transcription (Carrieri et al., 2015). Importantly, a novel transcription factor for UCH-L1 was identified: Nurr 1 (Carrieri et al., 2015). Nurr1 is heavily involved in differentiation of dopaminergic neurons and required for developing the DA neuronal phenotype (Saucedo-Cardenas et al., 1998). The fact that a DA neuron specific transcription factor binds to the UCH-L1 promoter suggests potentially differential regulation of UCH-L1 depending on neuronal type, which has previously not been discovered. Future studies into UCH-L1 regulation should further examine this interesting possibility.

UCH-L1 in AD

The role of UCH-L1 in AD is less well-studied compared to PD. At the time of writing this dissertation, there was no published evidence that mutations in UCH-L1 can cause or contribute to development or progression of AD in humans. Since UCH-L1 is highly expressed in neuron cell bodies but considerably more abundant in axons and synapses, UCH-L1 is likely highly important in synaptic transmission. Indeed, UCH-L1 had been shown to be necessary to maintain the neuromuscular junction (Chen et al., 2010) especially synaptic structure (Cartier et al., 2009). One of the first indications that UCH-L1 could contribute to AD was the finding of downregulation and oxidative modification of UCH-L1 in brains of patients diagnosed with AD (Choi et al., 2004).

Furthermore, the amount of soluble UCH-L1 negatively correlated with the number of neurofibrillary tangles: a decrease in soluble UCH-L1 was associated with an increased number of neurofibrillary tangles (Choi et al., 2004). It is unclear whether this relationship between UCH-L1 and neurofibrillary tangles relates to UCH-L1's involvement in proteasomal degradation of tau, but it is a possibility.

A major protective role for UCH-L1 against β -amyloid toxicity was discovered when UCH-L1 was overexpressed in a mouse model of AD, which restored synaptic function in brain slices from AD mice and from mice treated with β -amyloid oligomers (Gong et al., 2006). In addition, UCH-L1 overexpression improved the ability of the AD mice to retain contextual learning (Gong et al., 2006). In fact, overexpression of UCH-L1 *in vivo* rescued AD-like deficits in mice (Zhang et al., 2014). These findings were the first to describe a role for UCH-L1 in preserving cognition in AD but also suggest a broader role in synaptic structure and plasticity, which has potentially widespread relevance in the nervous system. Future studies will shed brighter light on the emerging role of UCH-L1 and other DUBs in pathogenesis and prognosis of AD.

Goals of this Dissertation

As a highly abundant DUB in neurons UCH-L1 clearly has important functions within the nervous system with respect to proteolytic pathways, synaptic structure, and structure of the neuromuscular junction. However, the role of UCH-L1 in neuronal susceptibility to PD is less clear. The following specific aims were proposed to better understand the role of UCH-L1 as a potential susceptibility factor in NSDA and MLDA neurons in mice exposed to MPTP.

Central Hypothesis: Maintenance of UCH-L1 expression and function is an important factor that decreases the susceptibility of MLDA neurons and the decrease in UCH-L1 expression contributes to the susceptibility of NSDA neurons to acute MPTP. UCH-L1 expression and activity promotes UPS homeostasis by maintaining pools of free mono-Ub.

AIM 1: Oxidative Stress, Dopaminergic Phenotypic Markers, and UCH-L1 Expression in NSDA and MLDA neurons after Exposure to Acute MPTP

Hypothesis: NSDA neurons are more susceptible to acute MPTP treatment than MLDA neurons and are predicted to have increased markers of oxidative stress. DA and TH are decreased to a greater extent in the NSDA neurons compared to MLDA neurons in mice exposed to acute MPTP. UCH-L1 expression is predicted to be maintained in MLDA neurons but decreased in NSDA neurons after acute MPTP.

AIM 2: Effects of Neurotoxicant and UCH-L1 Inhibitor in MN9D Cells and ST Synaptosomes, and a Potential Interaction between UCH-L1 and Parkin with Relevance to Autophagy

Hypothesis: Neurotoxicant treatment in MN9D cells is predicted to cause a decrease in intracellular DA and UCH-L1 expression and function. The UCH-L1 inhibitor is predicted to cause a decrease in DA phenotype in MN9D cells. UCH-L1 is predicted to decrease in ST synaptosomes, as they are the axon terminals of the vulnerable NSDA neurons. UCH-L1 is predicted to be elevated in parkin deficient mice, since parkin has been previously demonstrated to downregulate UCH-L1 expression. The upregulation of UCH-L1 in parkin deficient mice is predicted to increase autophagy.

AIM 3: Effects of Inhibition of UCH-L1 on Susceptibility of NSDA and MLDA Neurons to Neurotoxicant Exposure

Hypothesis: UCH-L1 inhibition in NSDA and MLDA neurons is expected to increase the sensitivity of these neurons to acute MPTP exposure with respect to a decrease in DA and TH. With UCH-L1 inhibition, MLDA neurons will be rendered susceptible to acute MPTP exposure.

AIM 4: Effects of Aging on DA Metabolic Homeostasis in NSDA and MLDA Neurons and Susceptibility to MPTP Toxicity

Hypothesis: DA phenotype in NSDA and MLDA neurons is predicted to be decreased with normal aging, and aged mice are predicted to be more susceptible to acute MPTP in both NSDA and MLDA neurons.

AIM 5: Effects of Aging on UCH-L1 Expression and Function in Brain Regions Containing NSDA and MLDA Neurons

Hypothesis: UCH-L1 expression is predicted to decrease with normal aging in regions containing NSDA and MLDA neurons. Aged MLDA neurons are expected to become susceptible to a decrease in UCH-L1 expression after acute MPTP.

REFERENCES

REFERENCES

- Alexander, G.E., 2004. Biology of Parkinson's disease: pathogenesis and pathophysiology of a multisystem neurodegenerative disorder. *Dialogues Clin. Neurosci.* 6, 259–80.
- Athauda, D., Maclagan, K., Skene, S.S., Bajwa-Joseph, M., Letchford, D., Chowdhury, K., Hibbert, S., Budnik, N., Zampedri, L., Dickson, J., Li, Y., Aviles-Olmos, I., Warner, T.T., Limousin, P., Lees, A.J., Greig, N.H., Tebbs, S., Foltynie, T., 2017. Exenatide once weekly versus placebo in Parkinson's disease: a randomised, double-blind, placebo-controlled trial. *Lancet*. doi:10.1016/S0140-6736(17)31585-4
- Baba, M., Nakajo, S., Tu, P.H., Tomita, T., Nakaya, K., Lee, V.M., Trojanowski, J.Q., Iwatsubo, T., 1998. Aggregation of alpha-synuclein in Lewy bodies of sporadic Parkinson's disease and dementia with Lewy bodies. *Am. J. Pathol.* 152, 879–84.
- Bandyopadhyay, U., Kaushik, S., Varticovski, L., Cuervo, A.M., 2008. The chaperone-mediated autophagy receptor organizes in dynamic protein complexes at the lysosomal membrane. *Mol. Cell. Biol.* 28, 5747–63. doi:10.1128/MCB.02070-07
- Behrouz, B., Drolet, R.E., Sayed, Z. a., Lookingland, K.J., Goudreau, J.L., 2007. Unique responses to mitochondrial complex I inhibition in tuberoinfundibular dopamine neurons may impart resistance to toxic insult. *Neuroscience* 147, 592–598. doi:10.1016/j.neuroscience.2007.05.007
- Benskey, M., Behrouz, B., Sunryd, J., Pappas, S.S., Baek, S.-H.H., Huebner, M., Lookingland, K.J., Goudreau, J.L., 2012. Recovery of hypothalamic tuberoinfundibular dopamine neurons from acute toxicant exposure is dependent upon protein synthesis and associated with an increase in parkin and ubiquitin carboxy-terminal hydrolase-L1 expression. *Neurotoxicology* 33, 321–31. doi:10.1016/j.neuro.2012.02.001
- Bilguvar, K., Tyagi, N.K., Ozkara, C., Tuysuz, B., Bakircioglu, M., Choi, M., Delil, S., Caglayan, A.O., Baranoski, J.F., Erturk, O., Yalcinkaya, C., Karacorlu, M., Dincer, A., Johnson, M.H., Mane, S., Chandra, S.S., Louvi, A., Boggon, T.J., Lifton, R.P., Horwich, A.L., Gunel, M., 2013. Recessive loss of function of the neuronal ubiquitin hydrolase UCHL1 leads to early-onset progressive neurodegeneration. *Proc. Natl. Acad. Sci. U. S. A.* 110, 3489–94. doi:10.1073/pnas.1222732110
- Blesa, J., Trigo-Damas, I., Quiroga-Varela, A., Jackson-Lewis, V.R., 2015. Oxidative stress and Parkinson's disease. *Front. Neuroanat.* 9, 91. doi:10.3389/fnana.2015.00091
- Bonifati, V., Rizzu, P., van Baren, M.J., Schaap, O., Breedveld, G.J., Krieger, E., Dekker, M.C.J., Squitieri, F., Ibanez, P., Joosse, M., van Dongen, J.W., Vanacore, N., van Swieten, J.C., Brice, A., Meco, G., van Duijn, C.M., Oostra, B.A., Heutink, P., 2003. Mutations in the DJ-1 Gene Associated with Autosomal Recessive Early-

- Onset Parkinsonism. *Science* (80-.). 299, 256–259. doi:10.1126/science.1077209
- Braak, H., Braak, E., 2000. Pathoanatomy of Parkinson's disease. *J. Neurol.* 247 Suppl, I13-10. doi:10.1007/PL00007758
- Braak, H., de Vos, R.A.I., Bohl, J., Del Tredici, K., 2006. Gastric α -synuclein immunoreactive inclusions in Meissner's and Auerbach's plexuses in cases staged for Parkinson's disease-related brain pathology. *Neurosci. Lett.* 396, 67–72. doi:10.1016/j.neulet.2005.11.012
- Braak, H., Del Tredici, K., Rüb, U., De Vos, R.A.I., Jansen Steur, E.N.H., Braak, E., 2003. Staging of brain pathology related to sporadic Parkinson's disease. *Neurobiol. Aging* 24, 197–211. doi:10.1016/S0197-4580(02)00065-9
- Brown, R.C., Lockwood, A.H., Sonawane, B.R., 2005. Neurodegenerative Diseases: An Overview of Environmental Risk Factors. *Environ. Health Perspect.* 113, 1250–1256. doi:10.1289/ehp.7567
- Brundin, P., Melki, R., Kopito, R., 2010. Prion-like transmission of protein aggregates in neurodegenerative diseases. *Nat. Rev. Mol. Cell Biol.* 11, 301–7. doi:10.1038/nrm2873
- Calne, D., William Langston, J., 1983. AETIOLOGY OF PARKINSON'S DISEASE. *Lancet* 322, 1457–1459. doi:10.1016/S0140-6736(83)90802-4
- Carrieri, C., Forrest, A.R.R., Santoro, C., Persichetti, F., Carninci, P., Zucchelli, S., Gustincich, S., 2015. Expression analysis of the long non-coding RNA antisense to Uchl1 (AS Uchl1) during dopaminergic cells' differentiation in vitro and in neurochemical models of Parkinson's disease. *Front. Cell. Neurosci.* 9, 114. doi:10.3389/fncel.2015.00114
- Cartier, A.E., Djakovic, S.N., Salehi, A., Wilson, S.M., Masliah, E., Patrick, G.N., 2009. Regulation of synaptic structure by ubiquitin C-terminal hydrolase L1. *J. Neurosci.* 29, 7857–68. doi:10.1523/JNEUROSCI.1817-09.2009
- Caudle, W.M., Richardson, J.R., Wang, M.Z., Taylor, T.N., Guillot, T.S., McCormack, A.L., Colebrooke, R.E., Di Monte, D.A., Emson, P.C., Miller, G.W., 2007. Reduced Vesicular Storage of Dopamine Causes Progressive Nigrostriatal Neurodegeneration. *J. Neurosci.* 27, 8138 LP-8148.
- Chaudhuri, K.R., Healy, D.G., Schapira, A.H., 2006. Non-motor symptoms of Parkinson's disease: diagnosis and management. *Lancet Neurol.* 5, 235–245. doi:10.1016/S1474-4422(06)70373-8
- Chen, F., Sugiura, Y., Myers, K.G., Liu, Y., Lin, W., 2010. Ubiquitin carboxyl-terminal hydrolase L1 is required for maintaining the structure and function of the neuromuscular junction. *Proc. Natl. Acad. Sci.* 107, 1636–1641. doi:10.1073/pnas.0911516107
- Chinaglia, G., Alvarez, F.J., Probst, A., Palacios~ li, J.M., 1992. Mesostriatal and

- Mesolimbic Dopamine Uptake Binding Sites Are Reduced in Parkinson's Disease and Progressive Supranuclear Palsy: a Quantitative Autoradiographic Study Using [3H]Mazindol. *Neuroscience* 49, 317–327. doi:10.1016/0306-4522(92)90099-N
- Choi, J., Levey, A.I., Weintraub, S.T., Rees, H.D., Gearing, M., Chin, L.-S., Li, L., 2004. Oxidative modifications and down-regulation of ubiquitin carboxyl-terminal hydrolase L1 associated with idiopathic Parkinson's and Alzheimer's diseases. *J. Biol. Chem.* 279, 13256–64. doi:10.1074/jbc.M314124200
- Cuervo, A.M., Stefanis, L., Fredenburg, R., Lansbury, P.T., Sulzer, D., 2004. Impaired degradation of mutant alpha-synuclein by chaperone-mediated autophagy. *Science* 305, 1292–5. doi:10.1126/science.1101738
- Das, C., Hoang, Q.Q., Kreinbring, C. a, Luchansky, S.J., Meray, R.K., Ray, S.S., Lansbury, P.T., Ringe, D., Petsko, G. a, 2006. Structural basis for conformational plasticity of the Parkinson's disease-associated ubiquitin hydrolase UCH-L1. *Proc. Natl. Acad. Sci. U. S. A.* 103, 4675–80. doi:10.1073/pnas.0510403103
- Davis, A.A., Andruska, K.M., Benitez, B.A., Racette, B.A., Perlmutter, J.S., Cruchaga, C., 2016. Variants in GBA , SNCA , and MAPT influence Parkinson disease risk, age at onset, and progression. *Neurobiol. Aging* 37, 209.e1-209.e7. doi:10.1016/j.neurobiolaging.2015.09.014
- Demarest, K.T., Moore, K.E., 1979. Comparison of dopamine synthesis regulation in the terminals of nigrostriatal, mesolimbic, tuberoinfundibular and tuberohypophyseal neurons. *J. Neural Transm.* 46, 263–277. doi:10.1007/BF01259333
- Di Fonzo, A., Dekker, M.C.J., Montagna, P., Baruzzi, A., Yonova, E.H., Correia Guedes, L., Szczerbinska, A., Zhao, T., Dubbel-Hulsman, L.O.M., Wouters, C.H., de Graaff, E., Oyen, W.J.G., Simons, E.J., Breedveld, G.J., Oostra, B.A., Horstink, M.W., Bonifati, V., 2009. FBXO7 mutations cause autosomal recessive, early-onset parkinsonian-pyramidal syndrome. *Neurology* 72, 240–5. doi:10.1212/01.wnl.0000338144.10967.2b
- Dopeso-Reyes, I.G., Rico, A.J., Roda, E., Sierra, S., Pignataro, D., Lanz, M., Sucunza, D., Chang-Azancot, L., Lanciego, J.L., 2014. Calbindin content and differential vulnerability of midbrain efferent dopaminergic neurons in macaques. *Front. Neuroanat.* 8, 146. doi:10.3389/fnana.2014.00146
- Dubois, B., Pillon, B., 1996. Cognitive deficits in Parkinson's disease. *J. Neurol.* 244, 2–8. doi:10.1007/PL00007725
- Eletr, Z.M., Wilkinson, K.D., 2014. Regulation of proteolysis by human deubiquitinating enzymes. *Biochim. Biophys. Acta* 1843, 114–28. doi:10.1016/j.bbamcr.2013.06.027
- Fleming, L., Mann, J.B., Bean, J., Briggles, T., Sanchez-Ramos, J.R., 1994. Parkinson's disease and brain levels of organochlorine pesticides. *Ann. Neurol.* 36, 100–3. doi:10.1002/ana.410360119

- Foehring, R.C., Zhang, X.F., Lee, J.C.F., Callaway, J.C., 2009. Endogenous Calcium Buffering Capacity of Substantia Nigral Dopamine Neurons. *J. Neurophysiol.* 102, 2326–2333. doi:10.1152/jn.00038.2009
- Gelb, D., Oliver, E., Gilman, S., 1999. Diagnostic criteria for Parkinson disease. *Arch. Neurol.* 56, 33–39.
- Goker-Alpan, O., Schiffmann, R., LaMarca, M.E., Nussbaum, R.L., McInerney-Leo, A., Sidransky, E., 2004. Parkinsonism among Gaucher disease carriers. *J. Med. Genet.* 41, 937–940. doi:10.1136/jmg.2004.024455
- Gong, B., Cao, Z., Zheng, P., Vitolo, O. V, Liu, S., Staniszewski, A., Moolman, D., Zhang, H., Shelanski, M., Arancio, O., 2006. Ubiquitin hydrolase Uch-L1 rescues beta-amyloid-induced decreases in synaptic function and contextual memory. *Cell* 126, 775–88. doi:10.1016/j.cell.2006.06.046
- Gorell, J.M., Johnson, C.C., Rybicki, B.A., Peterson, E.L., Richardson, R.J., 1998. The risk of Parkinson's disease with exposure to pesticides, farming, well water, and rural living. *Neurology* 50, 1346–50.
- Goto, A., Wang, Y.L., Kabuta, T., Setsuie, R., Osaka, H., Sawa, A., Ishiura, S., Wada, K., 2009. Proteomic and histochemical analysis of proteins involved in the dying-back-type of axonal degeneration in the gracile axonal dystrophy (gad) mouse. *Neurochem. Int.* 54, 330–338. doi:10.1016/j.neuint.2008.12.012
- Group, T.D.-B.S. for P.D.S., 2001. Deep-Brain Stimulation of the Subthalamic Nucleus or the Pars Interna of the Globus Pallidus in Parkinson's Disease. *N. Engl. J. Med.* 345, 956–963. doi:10.1056/NEJMoa000827
- Hastings, T.G., Lewis, D.A., Zigmond, M.J., 1996. Role of oxidation in the neurotoxic effects of intrastriatal dopamine injections. *Proc. Natl. Acad. Sci.* 93, 1956–1961.
- Hill-Burns, E.M., Ross, O.A., Wissemann, W.T., Soto-Ortolaza, A.I., Zarepari, S., Siuda, J., Lynch, T., Wszolek, Z.K., Silburn, P.A., Mellick, G.D., Ritz, B., Scherzer, C.R., Zabetian, C.P., Factor, S.A., Breheny, P.J., Payami, H., 2016. Identification of genetic modifiers of age-at-onset for familial Parkinson's disease. *Hum. Mol. Genet.* 0, ddw206. doi:10.1093/hmg/ddw206
- Hornykiewicz, O., 1966. Dopamine (3-hydroxytyramine) and brain function. *Pharmacol.Rev.* 18, 925–964.
- Hruska, K.S., LaMarca, M.E., Scott, C.R., Sidransky, E., 2008. Gaucher disease: mutation and polymorphism spectrum in the glucocerebrosidase gene (GBA). *Hum. Mutat.* 29, 567–583. doi:10.1002/humu.20676
- Hung, H.-C., Lee, E.H., 1998. MPTP Produces Differential Oxidative Stress and Antioxidative Responses in the Nigrostriatal and Mesolimbic Dopaminergic Pathways. *Free Radic. Biol. Med.* 24, 76–84. doi:10.1016/S0891-5849(97)00206-2
- Hurst-Kennedy, J., Chin, L.S., Li, L., 2012. Ubiquitin C-terminal hydrolase L1 in

- tumorigenesis. *Biochem. Res. Int.* 2012. doi:10.1155/2012/123706
- Ichihara, N., Wu, J., Hua Chui, D., Yamazaki, K., Wakabayashi, T., Kikuchi, T., 1995. Axonal degeneration promotes abnormal accumulation of amyloid β -protein in ascending gracile tract of gracile axonal dystrophy (GAD) mouse. *Brain Res.* 695, 173–178. doi:10.1016/0006-8993(95)00729-A
- Jara, J.H., Schultz, M.C., Manuel, M., Stanford, M.J., Gautam, M., Klessner, J.L., Sekerkova, G., Heller, D.B., Cox, G.A., 2016. Absence of UCHL 1 function leads to selective motor neuropathy 331–345. doi:10.1002/acn3.298
- Johannessen, J.N., Adams, J.D., Schuller, H.M., Bacon, J.P., Markey, S.P., 1986. 1-methyl-4-phenylpyridine (MPP+) induces oxidative stress in the rodent. *Life Sci.* 38, 743–749. doi:10.1016/0024-3205(86)90589-8
- Kabuta, T., Furuta, A., Aoki, S., Furuta, K., Wada, K., 2008. Aberrant interaction between Parkinson disease-associated mutant UCH-L1 and the lysosomal receptor for chaperone-mediated autophagy. *J. Biol. Chem.* 283, 23731–8. doi:10.1074/jbc.M801918200
- Kampa, M., Castanas, E., 2008. Human health effects of air pollution. *Environ. Pollut.* 151, 362–367. doi:10.1016/j.envpol.2007.06.012
- Kish, S.J., Shannak, K., Hornykiewicz, O., 1988. Uneven Pattern of Dopamine Loss in the Striatum of Patients with Idiopathic Parkinson's Disease. *N. Engl. J. Med.* 318, 876–880. doi:10.1056/NEJM198804073181402
- Kitada, T., Asakawa, S., Hattori, N., Matsumine, H., Yamamura, Y., Minoshima, S., Yokochi, M., Mizuno, Y., Shimizu, N., 1998. Mutations in the parkin gene cause autosomal recessive juvenile parkinsonism. *Nature* 392, 605–8. doi:10.1038/33416
- Klingelhoefer, L., Reichmann, H., 2015. Pathogenesis of Parkinson disease—the gut–brain axis and environmental factors. *Nat. Rev. Neurol.* 11, 625–636. doi:10.1038/nrneurol.2015.197
- Kuzuhara, S., Mori, H., Izumiyama, N., Yoshimura, M., Ihara, Y., 1988. Lewy bodies are ubiquitinated. *Acta Neuropathol.* 75, 345–353. doi:10.1007/BF00687787
- Langston, J., Ballard, P., Tetrud, J., Irwin, I., 1983. Chronic Parkinsonism in humans due to a product of meperidine-analog synthesis. *Science* (80-.). 219, 979–980. doi:10.1126/science.6823561
- Langston, J.W., Forno, L.S., Rebert, C.S., Irwin, I., 1984. Selective nigral toxicity after systemic administration of 1-methyl-4-phenyl-1,2,5,6-tetrahydropyridine (MPTP) in the squirrel monkey. *Brain Res.* 292, 390–4.
- Langston, J.W., Irwin, I., Langston, E.B., Forno, L.S., 1984. 1-Methyl-4-phenylpyridinium ion (MPP+): Identification of a metabolite of MPTP, a toxin selective to the substantia nigra. *Neurosci. Lett.* 48, 87–92. doi:10.1016/0304-3940(84)90293-3

- Lee, H.-J., Bae, E.-J., Lee, S.-J., 2014. Extracellular α -synuclein—a novel and crucial factor in Lewy body diseases. *Nat. Rev. Neurol.* 10, 92–8. doi:10.1038/nrneurol.2013.275
- Leroy, E., Boyer, R., Auburger, G., Leube, B., Ulm, G., Mezey, E., Harta, G., Brownstein, M.J., Jonnalagada, S., Chernova, T., Dehejia, A., Lavedan, C., Gasser, T., Steinbach, P.J., Wilkinson, K.D., Polymeropoulos, M.H., 1998. The ubiquitin pathway in Parkinson's disease. *Nature*. doi:10.1038/26652
- Li, J.-Y., Englund, E., Holton, J.L., Soulet, D., Hagell, P., Lees, A.J., Lashley, T., Quinn, N.P., Rehncrona, S., Björklund, A., Widner, H., Revesz, T., Lindvall, O., Brundin, P., 2008. Lewy bodies in grafted neurons in subjects with Parkinson's disease suggest host-to-graft disease propagation. *Nat. Med.* 14, 501–3. doi:10.1038/nm1746
- Li, W., Englund, E., Widner, H., Mattsson, B., van Westen, D., Lätt, J., Rehncrona, S., Brundin, P., Björklund, A., Lindvall, O., Li, J.-Y., 2016. Extensive graft-derived dopaminergic innervation is maintained 24 years after transplantation in the degenerating parkinsonian brain. *Proc. Natl. Acad. Sci.* 113, 6544–6549. doi:10.1073/pnas.1605245113
- Liu, J., Mori, a, 1999. Stress, aging, and brain oxidative damage. *Neurochem. Res.* 24, 1479–97.
- Liu, Y., Fallon, L., Lashuel, H.A., Liu, Z., Lansbury, P.T., 2002. The UCH-L1 Gene Encodes Two Opposing Enzymatic Activities that Affect α -Synuclein Degradation and Parkinson's Disease Susceptibility 111, 209–218.
- Lookingland, K.J., Moore, K.E., 2005. Chapter VIII Functional neuroanatomy of hypothalamic dopaminergic neuroendocrine systems. *Handb. Chem. Neuroanat.* 21, 435–523. doi:10.1016/S0924-8196(05)80012-0
- Lowe, J., McDermott, H., Landon, M., Mayer, R.J., Wilkinson, K.D., 1990. Ubiquitin carboxyl-terminal hydrolase (PGP 9.5) is selectively present in ubiquitinated inclusion bodies characteristic of human neurodegenerative diseases. *J. Pathol.* 161, 153–160. doi:10.1002/path.1711610210
- Lu, C.-S., Lai, S.-C., Wu, R.-M., Weng, Y.-H., Huang, C.-L., Chen, R.-S., Chang, H.-C., Wu-Chou, Y.-H., Yeh, T.-H., 2012. PLA2G6 mutations in PARK14-linked young-onset parkinsonism and sporadic Parkinson's disease. *Am. J. Med. Genet. Part B Neuropsychiatr. Genet.* 159B, 183–191. doi:10.1002/ajmg.b.32012
- Maingay, M., Romero-Ramos, M., Carta, M., Kirik, D., 2006. Ventral tegmental area dopamine neurons are resistant to human mutant alpha-synuclein overexpression. *Neurobiol. Dis.* 23, 522–32. doi:10.1016/j.nbd.2006.04.007
- McKeon, J.E., Sha, D., Li, L., Chin, L.-S., 2014. Parkin-mediated K63-polyubiquitination targets ubiquitin C-terminal hydrolase L1 for degradation by the autophagy-lysosome system. *Cell. Mol. Life Sci.* doi:10.1007/s00018-014-1781-2

- Mellick, G.D., Silburn, P. a., 2000. The ubiquitin carboxy-terminal hydrolase-L1 gene S18Y polymorphism does not confer protection against idiopathic Parkinson's disease. *Neurosci. Lett.* 293, 127–130. doi:10.1016/S0304-3940(00)01510-X
- MIZUNO, Y., SONE, N., SAITOH, T., 1986. Dopaminergic neurotoxins, MPTP and MPP+, inhibit activity of mitochondrial NADH-ubiquinone oxidoreductase. *Proc. Japan Acad. Ser. B Phys. Biol. Sci.* 62, 261–263. doi:10.2183/pjab.62.261
- Mogenson, G.J., Jones, D.L., Yim, C.Y., 1980. From motivation to action: Functional interface between the limbic system and the motor system. *Prog. Neurobiol.* 14, 69–97. doi:http://dx.doi.org/10.1016/0301-0082(80)90018-0
- Nagley, P., Higgins, G.C., Atkin, J.D., Beart, P.M., 2010. Multifaceted deaths orchestrated by mitochondria in neurones. *Biochim. Biophys. Acta - Mol. Basis Dis.* 1802, 167–185. doi:http://dx.doi.org/10.1016/j.bbadis.2009.09.004
- Oda, K., Yamazaki, K., Miura, H., Shibasaki, H., Kikuchi, T., 1992. Dying back type axonal degeneration of sensory nerve terminals in muscle spindles of the gracile axonal dystrophy (GAD) mutant mouse. *Neuropathol. Appl. Neurobiol.* 18, 265–281. doi:10.1111/j.1365-2990.1992.tb00789.x
- Osaka, H., Wang, Y.L., Takada, K., Takizawa, S., Setsuie, R., Li, H., Sato, Y., Nishikawa, K., Sun, Y.J., Sakurai, M., Harada, T., Hara, Y., Kimura, I., Chiba, S., Namikawa, K., Kiyama, H., Noda, M., Aoki, S., Wada, K., 2003. Ubiquitin carboxy-terminal hydrolase L1 binds to and stabilizes monoubiquitin in neuron. *Hum. Mol. Genet.* 12, 1945–1958. doi:10.1093/hmg/ddg211
- Parkinson, J., 1817. *Essay on the Shaking Palsy*. Printed by Whittingham and Rowland for Sherwood, Neely, and Jones, London.
- Philippart, F., Destreel, G., Merino-Sepúlveda, P., Henny, P., Engel, D., Seutin, V., 2016. Differential Somatic Ca²⁺ Channel Profile in Midbrain Dopaminergic Neurons. *J. Neurosci.* 36, 7234 LP-7245.
- Politis, M., Wu, K., Loane, C., Quinn, N.P., Brooks, D.J., Oertel, W.H., Bjorklund, A., Lindvall, O., Piccini, P., 2012. Serotonin Neuron Loss and Nonmotor Symptoms Continue in Parkinson's Patients Treated with Dopamine Grafts. *Sci. Transl. Med.* 4, 128ra41-128ra41. doi:10.1126/scitranslmed.3003391
- Polymeropoulos, M.H., Lavedan, C., Leroy, E., Ide, S.E., Dehejia, A., Dutra, A., Pike, B., Root, H., Rubenstein, J., Boyer, R., Stenroos, E.S., Chandrasekharappa, S., Athanassiadou, A., Papapetropoulos, T., Johnson, W.G., Lazzarini, A.M., Duvoisin, R.C., Di Iorio, G., Golbe, L.I., Nussbaum, R.L., 1997. Mutation in the alpha-synuclein gene identified in families with Parkinson's disease. *Science* 276, 2045–7.
- Ramirez, A., Heimbach, A., Gründemann, J., Stiller, B., Hampshire, D., Cid, L.P., Goebel, I., Mubaidin, A.F., Wriekat, A.L., Roeper, J., Al-Din, A., Hillmer, A.M., Karsak, M., Liss, B., Woods, C.G., Behrens, M.I., Kubisch, C., 2006. Hereditary

- parkinsonism with dementia is caused by mutations in ATP13A2, encoding a lysosomal type 5 P-type ATPase. *Nat Genet* 38, 1184–1191. doi:10.1038/ng1884
- Ross, C. a., Pickart, C.M., 2004. The ubiquitin-proteasome pathway in Parkinson's disease and other neurodegenerative diseases. *Trends Cell Biol.* 14, 703–711. doi:10.1016/j.tcb.2004.10.006
- Saigoh, K., Wang, Y., Suh, J., Yamanishi, T., 1999. Intragenic deletion in the gene encoding ubiquitin carboxy-terminal hydrolase in *gad* mice. *Nat.* ... 23, 47–51.
- Saucedo-Cardenas, O., Quintana-Hau, J.D., Le, W.-D., Smidt, M.P., Cox, J.J., De Mayo, F., Burbach, J.P.H., Conneely, O.M., 1998. Nurr1 is essential for the induction of the dopaminergic phenotype and the survival of ventral mesencephalic late dopaminergic precursor neurons. *Proc. Natl. Acad. Sci.* 95, 4013–4018.
- Schapira, A.H. V., Cooper, J.M., Dexter, D., Clark, J.B., Jenner, P., Marsden, C.D., 1990. Mitochondrial Complex I Deficiency in Parkinson's Disease. *J. Neurochem.* 54, 823–827. doi:10.1111/j.1471-4159.1990.tb02325.x
- Scheperjans, F., Aho, V., Pereira, P.A.B., Koskinen, K., Paulin, L., Pekkonen, E., Haapaniemi, E., Kaakkola, S., Eerola-Rautio, J., Pohja, M., Kinnunen, E., Murros, K., Auvinen, P., 2015. Gut microbiota are related to Parkinson's disease and clinical phenotype. *Mov. Disord.* 30, 350–358. doi:10.1002/mds.26069
- Schott, B.H., Niehaus, L., Wittmann, B.C., Schütze, H., Seidenbecher, C.I., Heinze, H.J., Düzel, E., 2007. Ageing and early-stage Parkinson's disease affect separable neural mechanisms of mesolimbic reward processing. *Brain* 130, 2412–2424. doi:10.1093/brain/awm147
- Setsuie, R., Wang, Y.-L., Mochizuki, H., Osaka, H., Hayakawa, H., Ichihara, N., Li, H., Furuta, A., Sano, Y., Sun, Y.-J., Kwon, J., Kabuta, T., Yoshimi, K., Aoki, S., Mizuno, Y., Noda, M., Wada, K., 2007. Dopaminergic neuronal loss in transgenic mice expressing the Parkinson's disease-associated UCH-L1 I93M mutant. *Neurochem. Int.* 50, 119–29. doi:10.1016/j.neuint.2006.07.015
- Singaram, C., Gaumnitz, E.A., Torbey, C., Ashraf, W., Quigley, E.M., Sengupta, A., Pfeiffer, R., 1995. Dopaminergic defect of enteric nervous system in Parkinson's disease patients with chronic constipation. *Lancet* 346, 861–864. doi:10.1016/S0140-6736(95)92707-7
- Singleton, A.B., Farrer, M., Johnson, J., Singleton, A., Hague, S., Kachergus, J., Hulihan, M., Peuralinna, T., Dutra, A., Nussbaum, R., Lincoln, S., Crawley, A., Hanson, M., Maraganore, D., Adler, C., Cookson, M.R., Muenter, M., Baptista, M., Miller, D., Blancato, J., Hardy, J., Gwinn-Hardy, K., 2003. α -Synuclein Locus Triplication Causes Parkinson's Disease. *Science* (80-). 302.
- Sonsalla, P.K., Heikkila, R.E., 1986. The influence of dose and dosing interval on MPTP-induced dopaminergic neurotoxicity in mice. *Eur. J. Pharmacol.* 129, 339–45.

- Spillantini, M.G., Schmidt, M.L., Lee, V.M.-Y., Trojanowski, J.Q., Jakes, R., Goedert, M., 1997. [alpha]-Synuclein in Lewy bodies 388, 839–840.
- Strauss, K.M., 2005. Loss of function mutations in the gene encoding Omi/HtrA2 in Parkinson's disease. *Hum. Mol. Genet.* 14, 2099–2111. doi:10.1093/hmg/ddi215
- Surmeier, D.J., Obeso, J.A., Halliday, G.M., 2017. Selective neuronal vulnerability in Parkinson disease. *Nat. Rev. Neurosci.* 18, 101–113. doi:10.1038/nrn.2016.178
- Tanner, C.M., Kamel, F., Ross, G.W., Hoppin, J.A., Goldman, S.M., Korell, M., Marras, C., Bhudhikanok, G.S., Kasten, M., Chade, A.R., Comyns, K., Richards, M.B., Meng, C., Priestley, B., Fernandez, H.H., Cambi, F., Umbach, D.M., Blair, A., Sandler, D.P., Langston, J.W., 2011. Rotenone, Paraquat, and Parkinson's Disease. *Environ. Health Perspect.* 119, 866–872. doi:10.1289/ehp.1002839
- Thompson, R.J., Doran, J.F., Jackson, P., Dhillon, a P., Rode, J., 1983. PGP 9.5--a new marker for vertebrate neurons and neuroendocrine cells. *Brain Res.* 278, 224–228. doi:10.1016/0006-8993(83)90241-X
- Todi, S. V, Paulson, H.L., 2011. Balancing act: deubiquitinating enzymes in the nervous system. *Trends Neurosci.* 34, 370–82. doi:10.1016/j.tins.2011.05.004
- Ulusoy, A., Rusconi, R., Pérez-Revuelta, B.I., Musgrove, R.E., Helwig, M., Winzen-Reichert, B., Monte, D.A. Di, 2013. Caudo-rostral brain spreading of α -synuclein through vagal connections. *EMBO Mol. Med.* 5, 1119–1127. doi:10.1002/emmm.201302475
- Valente, E.M., Abou-Sleiman, P.M., Caputo, V., Muqit, M.M.K., Harvey, K., Gispert, S., Ali, Z., Del Turco, D., Bentivoglio, A.R., Healy, D.G., Albanese, A., Nussbaum, R., González-Maldonado, R., Deller, T., Salvi, S., Cortelli, P., Gilks, W.P., Latchman, D.S., Harvey, R.J., Dallapiccola, B., Auburger, G., Wood, N.W., 2004. Hereditary Early-Onset Parkinson's Disease Caused by Mutations in PINK1. *Science (80-.).* 304, 1158–1160. doi:10.1126/science.1096284
- Virnau, P., Mirny, L. a., Kardar, M., 2006. Intricate knots in proteins: Function and evolution. *PLoS Comput. Biol.* 2, 1074–1079. doi:10.1371/journal.pcbi.0020122
- Wakabayashi, K., Takahashi, H., Takeda, S., Ohama, E., Ikuta, F., 1988. Parkinson's disease: the presence of Lewy bodies in Auerbach's and Meissner's plexuses. *Acta Neuropathol.* 76, 217–221.
- Walters, B.J., Campbell, S.L., Chen, P.C., Taylor, A.P., Schroeder, D.G., Dobrunz, L.E., Artavanis-Tsakonas, K., Ploegh, H.L., Wilson, J.A., Cox, G.A., Wilson, S.M., 2008. Differential effects of Usp14 and Uch-L1 on the ubiquitin proteasome system and synaptic activity. *Mol. Cell. Neurosci.* 39, 539–48. doi:10.1016/j.mcn.2008.07.028
- Walters, B.J., Campbell, S.L., Chen, P.C., Taylor, a. P., Schroeder, D.G., Dobrunz, L.E., Artavanis-Tsakonas, K., Ploegh, H.L., Wilson, J. a., Cox, G. a., Wilson, S.M., 2008. Differential effects of Usp14 and Uch-L1 on the ubiquitin proteasome system

and synaptic activity. *Mol. Cell. Neurosci.* 39, 539–548.
doi:10.1016/j.mcn.2008.07.028

- Wilkinson, K.D., Lee, K.M., Deshpande, S., Duerksen-Hughes, P., Boss, J.M., Pohl, J., 1989. The neuron-specific protein PGP 9.5 is a ubiquitin carboxyl-terminal hydrolase. *Science* 246, 670–673. doi:10.1126/science.2530630
- Xilouri, M., Kyratzi, E., Pitychoutis, P.M., Papadopoulou-Daifoti, Z., Perier, C., Vila, M., Maniati, M., Ulusoy, A., Kirik, D., Park, D.S., Wada, K., Stefanis, L., 2012. Selective neuroprotective effects of the S18Y polymorphic variant of UCH-L1 in the dopaminergic system. *Hum. Mol. Genet.* 21, 874–89. doi:10.1093/hmg/ddr521
- Zhang, J., Hattori, N., Leroy, E., Morris, H.R., Kubo, S.I., Kobayashi, T., Wood, N.W., Polymeropoulos, M.H., Mizuno, Y., 2000. Association between a polymorphism of ubiquitin carboxy-terminal hydrolase L1 (UCH-L1) gene and sporadic Parkinson's disease. *Park. Relat. Disord.* 6, 195–197. doi:10.1016/S1353-8020(00)00015-8
- Zhang, M., Cai, F., Zhang, S., Zhang, S., Song, W., 2014. Overexpression of ubiquitin carboxyl-terminal hydrolase L1 (UCHL1) delays Alzheimer's progression in vivo. *Sci. Rep.* 4, 7298. doi:10.1038/srep07298
- Zimprich, A., Benet-Pagès, A., Struhal, W., Graf, E., Eck, S.H., Offman, M.N., Haubenberger, D., Spielberger, S., Schulte, E.C., Lichtner, P., Rossle, S.C., Klopp, N., Wolf, E., Seppi, K., Pirker, W., Presslauer, S., Mollenhauer, B., Katzenschlager, R., Foki, T., Hotzy, C., Reinthaler, E., Harutyunyan, A., Kralovics, R., Peters, A., Zimprich, F., Brücke, T., Poewe, W., Auff, E., Trenkwalder, C., Rost, B., Ransmayr, G., Winkelmann, J., Meitinger, T., Strom, T.M., 2011. A Mutation in VPS35, Encoding a Subunit of the Retromer Complex, Causes Late-Onset Parkinson Disease. *Am. J. Hum. Genet.* 89, 168–175. doi:10.1016/j.ajhg.2011.06.008
- Zimprich, A., Biskup, S., Leitner, P., Lichtner, P., Farrer, M., Lincoln, S., Kachergus, J., Hulihan, M., Uitti, R.J., Calne, D.B., Stoessl, A.J., Pfeiffer, R.F., Patenge, N., Carbajal, I.C., Vieregge, P., Asmus, F., Müller-Myhsok, B., Dickson, D.W., Meitinger, T., Strom, T.M., Wszolek, Z.K., Gasser, T., 2004. Mutations in LRRK2 Cause Autosomal-Dominant Parkinsonism with Pleomorphic Pathology. *Neuron* 44, 601–607. doi:10.1016/j.neuron.2004.11.005

Chapter 2: Materials and Methods

Animals, drugs, and brain tissue collection

Mice were either bred in house (GFP-TH, Park2^{-/-}; Parkin KO) or purchased from Jackson Labs. All mice were either transgenic on a C57bl6j background or wild type (WT) C57bl6j. Mice were housed in a temperature (22 ± 1 °C) and light controlled (12 h light/dark cycle) room and provided with food and water *ad libitum*. The Michigan State University Institutional Animal Care and Use Committee approved all experiments using live animals (AUF 10/14-183-00). For studies presented in **Chapters 6 and 7**, young mice were 3-8 months old, mature mice were 9-12 months old, old mice were 12.5-14 months old, and aged mice were 22-28 months old.

In studies involving acute MPTP, mice were injected with either saline VH or 20 mg/kg MPTP (Santa Cruz) dissolved in saline (s.c.). For studies involving LDN-57444 (Tocris), mice were injected with either DMSO VH (Sigma) or LDN-57444 (0.5 mg/kg or 5 mg/kg) dissolved in DMSO (i.p.). For all other studies, mice were 8-10 weeks old.

Mice were randomly assigned to study groups. Upon completion of all experimental time points, mice were decapitated via guillotine and the brain rapidly removed and placed on ice. If no ST synaptosomes were collected, brains were frozen on labeled squares of aluminum foil rostral end up on dry ice and stored at -80 °C until further analysis. Brains were sliced to 500 µm coronal sections using a cryostat at -9 °C and sections were placed on a labeled glass slide. Based on brain morphology using the Mouse Brain Atlas (Paxinos and Franklin, 2004) tissue punches were microdissected for the ST (18 gauge round), NAc (18 gauge round),

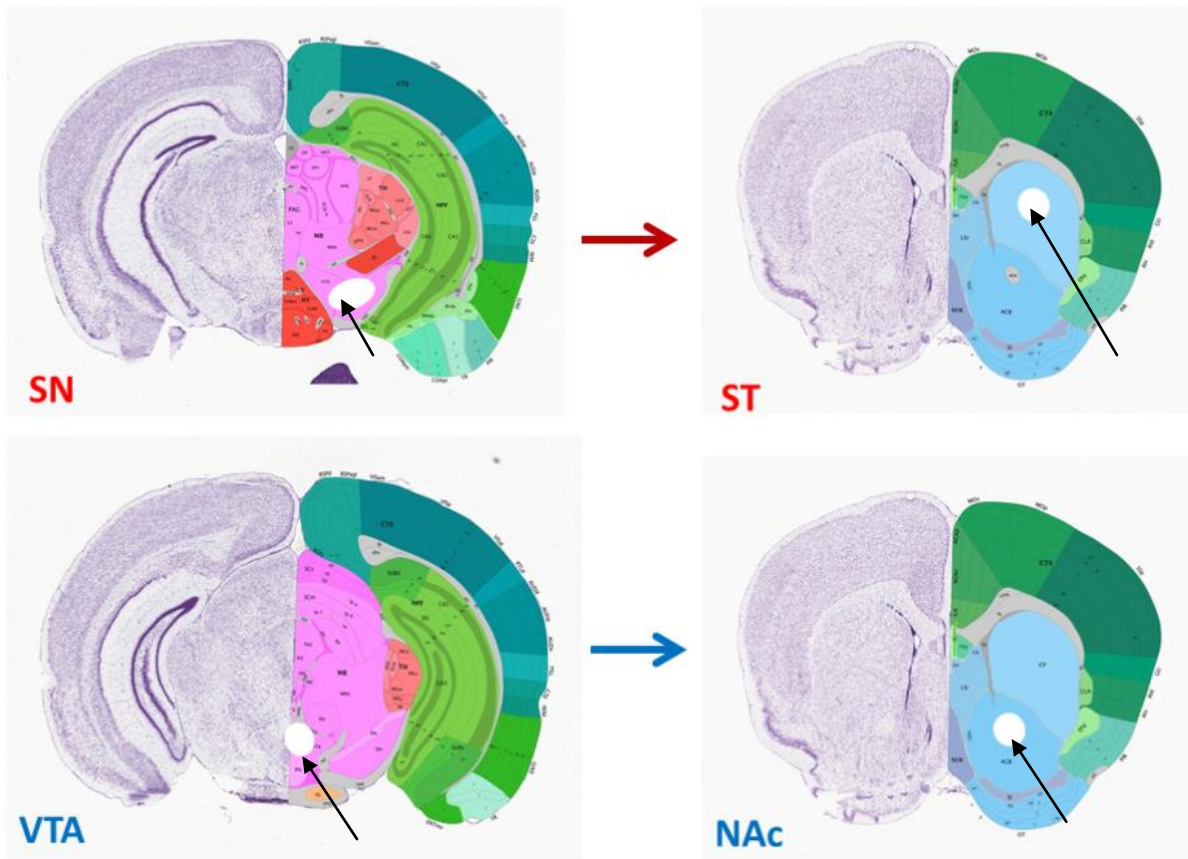


Figure 2.1. Images from the online Allen Brain Atlas (mouse.brain-map.org). Top images represent the cell body (SN, left) and axon terminal (ST, right) regions of NSDA neurons. Lower images represent the cell body (VTA, left) and axon terminal (NAc, right) regions of MLDA. White space in the tissue (designated by arrows) represents the microdissected neurons sampled from a mouse coronal brain section.

SN (21 gauge round), and VTA (18 gauge round) (**Fig. 2.1**) and placed in buffer appropriate for downstream analyses and stored at -80 °C until further use.

Preparation of crude synaptosomes

Chilled fresh brains were sectioned using a brain matrix (Zivic Instruments) at 1 mm thick slices onto a cold stainless steel razorblade. Synaptosomes were isolated from the ST tissue according to a method modified from Dunkley (Dunkley et al., 2008).

Unilateral dorsal ST (approximately 75-100 µg) was collected in 1 mL homogenization buffer (300 mM Sucrose, 10 mM HEPES, 1 mM EGTA, pH 7.4 at 4 °C) and homogenized with a pre-chilled Teflon/glass homogenizer by 10 strokes over ice, resting each sample on ice after 5 strokes. The homogenizer was rinsed with an additional 1 mL of MIB and homogenates were transferred to 2 mL microcentrifuge tubes and centrifuged at low speed (1000 x g) for 10 min. After centrifugation, the supernatant was retained in a separate tube and centrifuged at 17,968 x g at 4 °C for 10 min in fixed-angle rotor. The resulting P2 pellets were re-suspended in 100 µL sucrose buffer (300 mM sucrose and 10 mM HEPES, pH 7.4 at 4 °C). Synaptosomes were stored at -80 °C until further use.

Bicinchoninic acid assay for protein concentrations

The reagents (bicinchoninic acid and copper sulfate) were mixed in a ratio of 50:1 and used to analyze protein content per sample. Samples were diluted as follows: 48 µL of ddH₂O to 2 µL (1:25 dilution) of sample for Western blotting and 25 µL of ddH₂O to 25 µL (1:1 dilution) of sample for neurochemistry analysis. Serial dilutions of bovine serum albumin (BSA) were used as standards (500 ng/µL, 250 ng/µL, 125 ng/µL... etc.).

Samples mixed with BCA reagent were incubated for 15 min at 60 °C and protein concentrations were determined by a Tecan Infinite M1000 Pro Microplate Reader.

Neurochemical analyses via HPLC-ED

Tissue samples in acidic HPLC tissue buffer (0.1 M phosphate, 0.1 M citrate buffer, pH 2.5) were sonicated for three short bursts and centrifuged at 10,000 x g for 1 min at 4 °C. Resulting supernatants were prepared by diluting in tissue buffer up to 100 µL. Mobile phase for detection of neurochemicals was 10% methanol, 0.02% SOS, pH 2.65. Sample content of DA, 3,4-hydroxyphenylacetic acid (DOPAC), homovanillic acid (HVA) and 3-methoxytyramine (3-MT) was determined by high pressure liquid chromatography coupled with electrochemical detection (HPLC-ED) and the concentration of neurochemicals was expressed in nanogram (ng) per milligram (mg) protein.

Immunoblot analyses

Micropunch or cell culture lysates were processed and Western blots were performed as previously described (Benskey et al., 2012). Briefly, tissue or cells were collected in ice cold 1 X RIPA containing phosphatase and protease inhibitors (Thermo) and sonicated for 20 s twice. Samples were centrifuged at 10,000 x g for 10 min and the supernatant was removed and placed in a new labeled tube. Protein content per sample was determined via BCA assay. Five or 10 µg protein was loaded in each well of a 4-20% precast gel (BioRad) diluted in 4X sample buffer (BioRad) containing 5% v/v β-mercaptoethanol and separated by electrophoresis. After the run was complete, the proteins on the gel were transferred to a PVDF membrane by activating the PVDF in methanol for 20 s and washing in ddH₂O. The membrane and thick paper blocks were

soaked in transfer buffer for 15 min and assembled onto the transfer cell. A semi-dry transfer method was used to transfer the proteins from the gel to the PVDF membrane where 15 V were applied for 30 min.

Upon completion of the transfer, the membrane was air-dried for 1 h and blocking was performed for 1 h with 5% non-fat milk. After blocking, membranes were probed with various primary antibodies in 5% BSA in TBS-T at 4 °C overnight, shaking (**Table 2-1**). Membranes were rinsed and incubated at room temperature with appropriate secondary antibodies in 5% non-fat milk in TBS-T for 1 h, shaking. Signal was visualized using a PICO or FEMTO Chemiluminescence substrate (ThermoFisher) kit on a LI-COR Odyssey imager. Bands from each lane of the protein of interest were normalized to the loading controls β -actin or GAPDH using Image Studio version 5.2.

Table 2.1. Primary and secondary antibodies used for Western blotting

Target	Host	Dilution	Product Number
UCH-L1	Rabbit	1:1000	Cell Signaling 11896S
TH	Rabbit	1:1000	Millipore MAB152
Ser40 p-TH	Rabbit	1:1000	Cell Signaling 2791
Ubiquitin	Rabbit	1:500	Cell Signaling
DAT	Rat	1:1000	Millipore MAB369
VMAT2	Rabbit	1:1000	Millipore AB1598
COMT	Rabbit	1:1000	Abcam ab126618
UCH-L3	Rabbit	1:1000	Cell Signaling 8141
USP14	Rabbit	1:1000	Cell Signaling 11931
GAPDH	Mouse	1:4000	Sigma G8795
Rabbit	Goat	1:4000	Cell Signaling 7074S
Mouse	Horse	1:4000	Cell Signaling 7076

Immunohistochemistry

For IHC experiments, mice were perfused with 0.9% saline followed by 4% paraformaldehyde in 0.1 M phosphate buffer. Brains were removed and placed in 4% paraformaldehyde to continue fixation overnight at 4 °C. When brains sunk to the bottom of the glass container, brains were cryoprotected in 0.1 M phosphate buffer containing 20% sucrose. Brains were sliced at 20 µm in a cryostat at -21 °C and free-floating sections were stored in 0.5 M phosphate buffer (PB) in 12-well culture dishes. Sections in each well were 100 µm apart.

Free-floating sections were permeabilized in 0.5 M phosphate buffer containing 0.1% Triton X-100 (PB-TX) and blocked in 5% BSA for 1 h. Sections were incubated in primary antibody overnight in 5% BSA PB-TX at 4 °C with shaking. The next day, sections were rinsed in PB-TX and incubated in secondary antibody for 1 h at room temperature. Next, sections were rinsed in PB-TX with a final rinse in PB before mounting. Brain sections were delicately mounted onto slides subbed with gelatin and coverslipped with anti-fade mounting medium (Invitrogen) and allowed to dry overnight. Slides were stored at 4 °C until imaging.

Confocal analysis of colocalization

Slides were imaged using a FV1000 Olympus inverted confocal microscope. A Cy3 conjugated secondary antibody (Jackson ImmunoResearch) was used to visualize UCH-L1 staining in brain sections using a 543 nm laser for excitation. An Alexa Fluor 488 conjugated secondary antibody was used to visualize TH staining using a 488 nm laser for excitation. Sequential Kalman averaging was employed during acquisition. A z-

series of 20 μm depth through the tissue was captured (average of 8 slices) and the Pearson's and Mander's coefficients for colocalization of the fluorophores were collected using unbiased thresholding where experimenter was blinded to treatment group and compared between VH and MPTP treatment.

DCF-DA assay

For *ex vivo* measurement of ROS production, tissue from the ST and NAc was removed from mice ($n=3$), lysed, and exposed to either VH or 1 μM H_2O_2 for 30 min at 37 $^\circ\text{C}$. Samples were then assayed for DCF-DA fluorescence. Samples were diluted in 10 μM DCF-DA reagent and incubated at 37 $^\circ\text{C}$ for 1 h. Samples were plated in a black 96 well plate and relative fluorescence measured at Ex 485/Em 520.

In tissue from MPTP-treated mice, the ST and NAc were dissected fresh and processed for the DCF-DA assay. Samples were diluted in 10 μM DCF-DA reagent and incubated at 37 $^\circ\text{C}$ for 1 h. Samples were plated in a black 96 well plate and relative fluorescence measured at Ex 485/Em 520.

MN9D cell culture and drug treatment

MN9D immortalized cells were cultured in DMEM containing 10% of fetal bovine serum (FBS) and 1 mM n-butyrate and grown on plates (6, 12, 96 well plates) coated with 50 $\mu\text{g}/\text{mL}$ poly-D-lysine (PDL) for 5-7 days to ensure a differentiated phenotype. Cells were maintained in a 37 $^\circ\text{C}$, 5% CO_2 incubator and fed every other day. Differentiated MN9D cells were treated with the following concentrations of MPP+ dissolved in culture media: 0, 50, 100, and 200 μM in 12 or 6 well plates ($n=6$ wells per group). MPP+ exposure on

media was allowed to continue for 2 h or 8 h (n=6 wells per group). Additional wells were used for subsequent ICC staining and analysis.

Cytotoxicity assay

The cytotoxicity of the MPP⁺ treatment was evaluated using a CytoTox-ONE kit from Promega. Briefly, cells were plated in 96 well plates at a corresponding density as the treatment groups and treated identically. Immediately before the reaction, medium containing serum was removed and replaced with serum-free medium. Reagents from the kit were mixed and applied to the cells. Ten minutes later, the reaction was stopped and the plate was assayed for fluorescent resorufin product, the amount of which is proportional to lactate dehydrogenase (LDH) leaked from dead cells. LDH release is a common indicator of membrane permeability associated with cell death (Cummings et al., 2004).

UCH-L1 hydrolase activity

ST synaptosomes placed in UCH-L1 assay buffer (100 mM NaCl, 0.5 mM EDTA, 50 mM HEPES pH 7.5) containing 0.1% Triton X-100 and sonicated for 20 s twice. Samples were centrifuged at 10,000 x g for 10 min and supernatant was placed into a new tube. One µg protein per sample was plated in duplicate in a black 384-well plate with 1 mM DTT and 0.5 µM Ub-AMC substrate. Kinetic readings for AMC fluorescence (Ex/Em 380/460 nm) were collected over 30 min and the RFU/min slope was determined and compared between groups.

Cayman total glutathione measurements

Total glutathione (GSH + GSSG) was measured using a kit from Cayman. Briefly, samples were deproteinized using metaphosphoric acid. Once samples were deproteinized and neutralized, the assay was performed according to kit instructions. The data was collected as end point absorbance values at 405 nm and expressed as μM total glutathione per μg protein.

Abcam GSH/GSSG ratio measurements

Brain tissue samples in 1 X RIPA were deproteinized using a kit from Abcam. Briefly, 2 μL cold trichloroacetic acid was added to each sample and samples were allowed to incubate on ice for 15 min. Tubes were centrifuged at 12,000 x g for 5 min and the supernatant was transferred to a new tube. Samples were then neutralized by adding 2 μL Neutralization Solution and incubated on ice for 5 min. Samples were stored at -80°C before use in the GSH/GSSG assay.

The GSH/GSSG ratio was performed using a kit from Abcam. Briefly, samples were diluted in PBS/0.5% NP-40 and placed in two 384-well plates (one for GSH and one for GSH + GSSG). Results were obtained using a fluorescence microplate reader with an excitation of 490 and emission of 520 nm. Resulting concentrations of GSH and GSSG were normalized to protein values and expressed as μM GSH or μM GSSG per μg protein.

HA-Ub-VME DUB labeling assay

HA-Ub-VME substrate was purchased from UBPBio and reconstituted according to product instructions. Samples in 1 X RIPA containing no protease or phosphatase inhibitors were prepared as if for Western blot. Ten μg of sample was used in the assay and diluted to 20 μL with labeling buffer (50 mM Tris pH 7.4, 5 mM MgCl_2 , 250 mM sucrose, 1 mM DTT, 1 mM ATP). Samples were incubated with 0.5 μM HA-Ub-VME at 37 °C for 1 h and prepared for Western blotting. Samples were run on 4-20% gels and transferred to PVDF. Membranes were probed for UCH-L1.

Statistical analyses

All statistical analyses were performed using SigmaPlot v. 12 software. In studies where only one factor is examined (i.e., drug treatment or age), a one-way ANOVA was performed with a post hoc Holm-Sidak test to determine if there is a statistically significant difference between groups ($p < 0.05$). For experiments containing two factors (such as genotype and treatment or age and treatment), a two-way ANOVA was performed with a post hoc Holm-Sidak test to determine if there is a statistically significant difference between groups ($p < 0.05$). At least 6 mice per sample group were used for each analysis to yield a power of $\geq 80\%$. Outliers in each experimental group were removed before statistical analysis using a Grubbs outlier test (graphpad.com/quickcalcs/Grubbs1.cfm) for significance level $p < 0.05$. All graphical representations of data denote the mean + SEM. Refer to each individual chapter and figure legends for final n values.

REFERENCES

REFERENCES

- Cummings, B.S., Schnellmann, R.G., Schnellmann, R.G., 2004. Measurement of cell death in mammalian cells. *Curr. Protoc. Pharmacol.* Chapter 12, Unit 12.8.
doi:10.1002/0471141755.ph1208s25
- Dunkley, P.R., Jarvie, P.E., Robinson, P.J., 2008. A rapid Percoll gradient procedure for preparation of synaptosomes. *Nat. Protoc.* 3, 1718–1728.
doi:10.1038/nprot.2008.171
- Paxinos, G., Franklin, K.B.J., 2004. *The Mouse Brain in Stereotaxic Coordinates*, 2nd ed. Elsevier Science.

Chapter 3: Oxidative Stress, Dopaminergic Phenotypic Markers, and UCH-L1 Expression in NSDA and MLDA Neurons after Exposure to Acute MPTP

Introduction

In PD, NSDA neurons progressively degenerate while MLDA neurons are spared (Braak and Braak, 2000). This differential susceptibility is likely influenced by a number of different factors, including vulnerability to oxidative stress, which is heavily implicated in development and progression of PD (Sun and Chen, 1998). However, one factor yet to be examined in detail is expression of PD-linked proteins in pathways known to be compromised in both human PD and animal models. UCH-L1 is differentially expressed between NSDA and TIDA neurons after acute MPTP exposure: UCH-L1 is decreased in the SN but maintained in the ARC 24 h after MPTP (Benskey et al., 2012), suggesting that UCH-L1 maintenance in TIDA neurons could protect these neurons from neurotoxicant-induced injury. However, there are caveats associated with comparing NSDA and TIDA neurons, namely that they are somewhat phenotypically dissimilar: TIDA neurons do not express much DAT (Meister and Elde, 1993), while NSDA neurons highly express the transporter. DAT expression is a major factor in determining MPTP susceptibility, since MPP^+ is taken up by DAT into DA neuron terminals. The two populations also differ in terms of axon length: axons are much shorter in TIDA neurons compared to NSDA and MLDA neurons. In addition, NSDA and MLDA neuronal activity is mediated by DA autoreceptors (Lookingland and Moore, 2005).

Therefore, since TIDA and NSDA neurons are so different, the third type of DA neurons in the CNS, the MLDA neurons, should be evaluated in relation to their response to

acute MPTP. Previous studies have established that MLDA neurons are less susceptible to damage from both chronic (Hung and Lee, 1998) and acute (B. Behrouz et al., 2007) MPTP with respect to DA loss, but individual pathways such as the UPS have not yet been studied to determine what factors (such as dysfunction in protein degradation) could contribute to the resistance of MLDA neurons to neurotoxicant exposure and PD. The purpose of these studies was to determine if UCH-L1 expression is maintained in MLDA neurons after acute MPTP.

Results

Oxidative stress in brain regions containing NSDA vs. MLDA neurons

Because MPP^+ , the active metabolite of MPTP, causes oxidative stress and an increase in ROS (Johannessen et al., 1986), we predict that the differential susceptibilities of NSDA and MLDA neurons could be linked to differential production of ROS. We first used an *ex vivo* approach to compare production of ROS in ST and NAc tissue by hydrogen peroxide (H_2O_2). **Fig. 3.1** shows that H_2O_2 produces different amounts of ROS in tissue from the ST and NAc. This approach directly delivers the oxidant to the tissue, so no questions of tissue penetration impede interpretation of the response. The same amount of H_2O_2 produced more ROS in equal amounts of tissue from the ST than in the NAc, suggesting that the antioxidant capacity of the NAc is likely greater than in the ST. The greater antioxidant capacity in the NAc could explain why these neurons are less susceptible, since the response of DA neurons to toxicant-induced acute oxidative stress is predicted to play a substantial role in development and

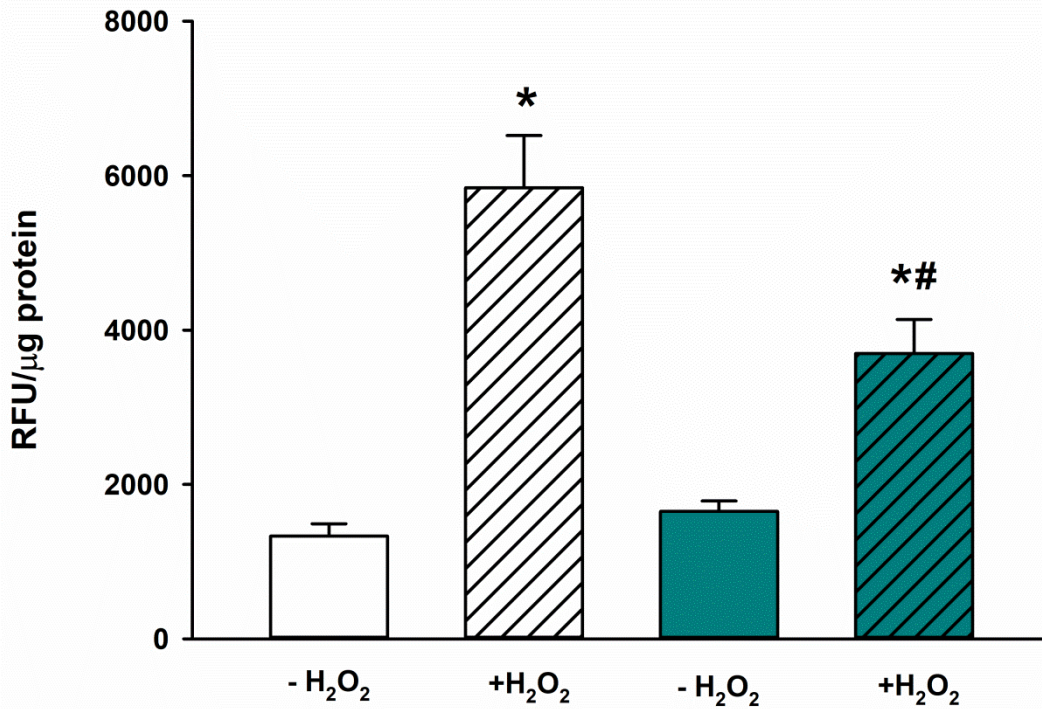


Figure 3.1. Ex vivo ROS production in ST (white) and NAc (teal) lysates. Five mice were decapitated and the brains sectioned fresh (n=5). The ST and NAc were microdissected. Tissue was lysed and treated with 1 μM H_2O_2 . A DCF-DA assay for detection of ROS was performed and the resulting fluorescence in relative fluorescence units (RFU) was normalized to protein content. Data is plotted as mean + SEM. Asterisk (*) indicates difference from respective (-) H_2O_2 control, whereas pound (#) represents difference from ST (+) H_2O_2 via Repeated Measures ANOVA and post hoc Holm-Sidak test.

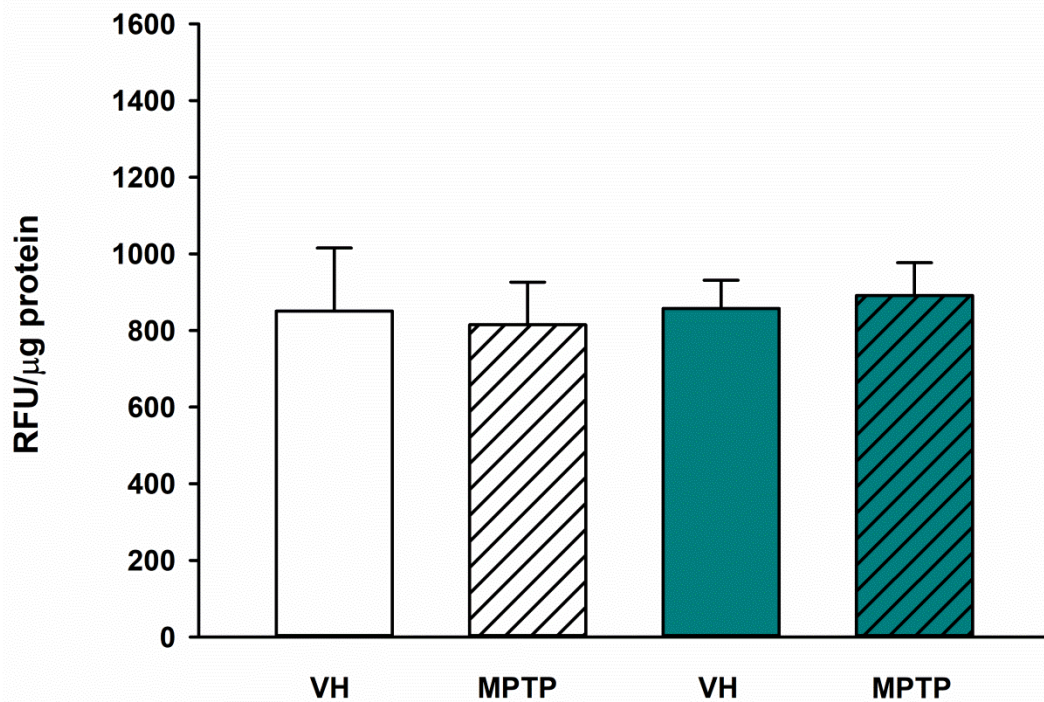


Figure 3.2. *In vivo* ROS levels in the ST (white) and NAc (teal) 6 after MPTP exposure. ROS was measured using a DCF-DA assay in ST and NAc from either VH or MPTP treated mice. ST VH n=7; ST MPTP n=10; NAc VH n=8; NAc MPTP n=10. Six hours after injection, mice were decapitated and the ST and NAc microdissected from fresh brain tissue. The DCF-DA assay was performed to yield relative amounts of ROS between brain regions and treatments. Data is plotted as mean + SEM. No statistically significant differences were detected between treatment groups ($p > 0.05$) via two-way ANOVA.

progression of PD (Sun and Chen, 1998). A limit of this technique is that we currently do not know if the antioxidant capacity within the neurons themselves is increased, or whether it could be due to glial cells present in the NAc. Next, since the peak concentration of MPP⁺ in the ST occurs at 6 h (Benskey et al., 2012), *in vivo* production of ROS was examined in the ST and NAc 6 h after MPTP exposure. In **Fig. 3.2**, the amount of DCF-DA fluorescence was found to be equivalent between brain regions and between treatment groups. This result is somewhat unexpected based on previous research with chronic MPTP, where increased lipid peroxidation and other markers of oxidative stress were evident in the ST but not the NAc (Hung and Lee, 1998). It appears that MPTP exposure results in the same amount of ROS generation between the ST and NAc at the 6 h time point. However, just because ROS levels are not elevated does not indicate that ROS-induced damage did not occur, since one of our indices of DA neuronal damage, DA levels in the ST, was decreased at 6 h (**Fig. 3.3**). Furthermore, since microdissected ST and NAc tissue includes MSNs and glial cells, a change in the production of ROS specifically in axon terminals of DA neurons is less likely to be detectable with the present methods. One way to specifically examine endpoints in NSDA axon terminals is to prepare synaptosomes (Dunkley et al., 2008), or pinched off axon terminals using special homogenization steps with buffers that create a sphere from the tip of an axon. However, this technique is limited by the amount of tissue available and cannot be used with much smaller brain regions like the NAc (~20 µg protein from bilateral punches). It is readily done with the ST, however, and axon-terminal specific analyses in the ST are presented in **Chapter 4** of this dissertation.

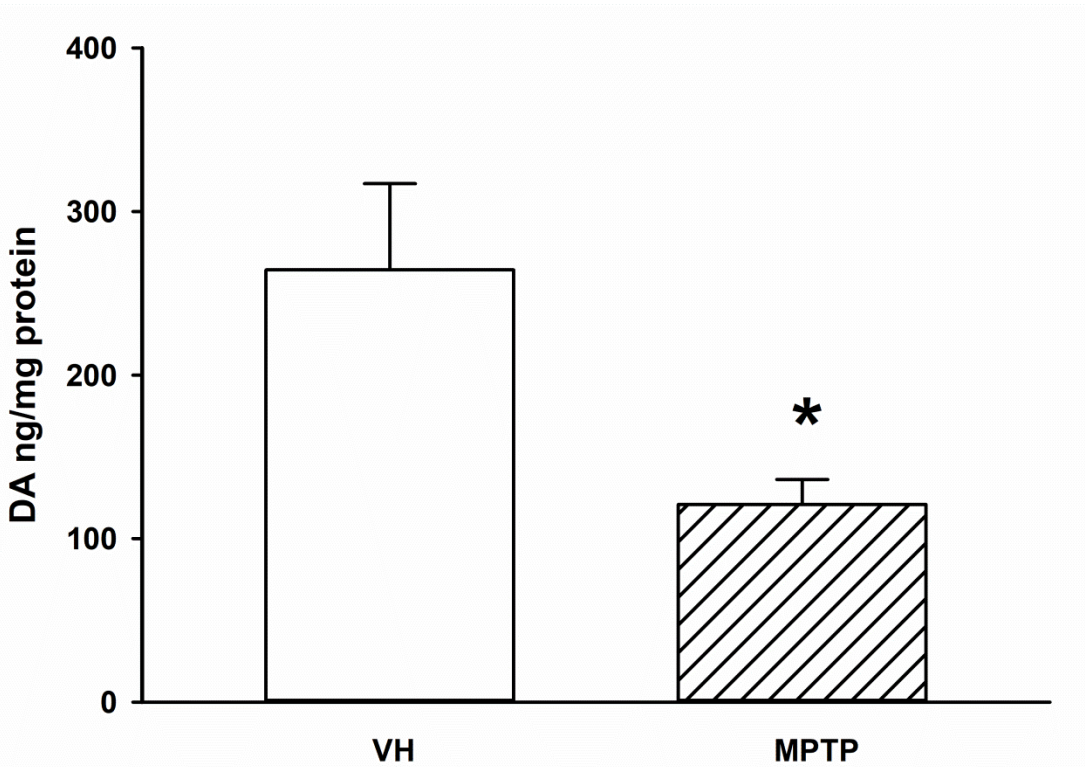


Figure 3.3. DA in the ST 6 h post MPTP exposure. Mice were injected with VH (n=10) or MPTP (n=9) and killed 6 h later. The ST was dissected and DA was measured via HPLC-ED. Data is plotted as mean + SEM. Asterisk (*) signifies a significant difference where $p < 0.05$ via t-test.

Differential susceptibility of NSDA and MLDA neurons to MPTP: DA, DOPAC, and TH

The MPTP model of DA depletion recapitulates early events thought to underlie mechanisms related to loss of NSDA neurons in PD. In a paper published previously by our laboratory, DA is not decreased in the NAc to the same extent as the ST after acute MPTP (Behrouz et al., 2007). We sought to replicate this differential responsiveness of MLDA and NSDA neurons and to further examine DA metabolism and expression of TH, the rate-limiting enzyme of DA synthesis. In **Fig. 3.4 (Left Panel)**, DA is decreased in the both the ST and NAc 24 h after MPTP exposure. However, the extent of DA loss is greater in the ST compared to the NAc, which can be more easily seen by expressing the data as percent control **Fig. 3.4 (Right Panel)**. Since the ST and NAc are located in similar regions of the brain, it is also likely that the ST and NAc are exposed to the same concentration of MPTP, since MPTP is lipid soluble and readily penetrates the BBB. Therefore, MLDA neurons are resistant to loss of DA after MPTP exposure. These results make sense in the context of antioxidant response if MLDA neurons are able to mount a more successful defense of ROS compared to NSDA neurons in the *ex vivo* experiment with equal amounts of hydrogen peroxide.

The primary intracellular metabolite of DA, DOPAC, is an index of DA that has been released, recaptured, and metabolized by MAO-B in presynaptic axon terminals (Meiser et al., 2013). In **Fig. 3.5**, DOPAC is decreased in both the ST and NAc to an equal extent, reflecting less DA release after acute MPTP exposure in both regions. This result makes sense if DA is being displaced from synaptic vesicles by MPP⁺ since it cannot be released unless packaged (Sulzer et al., 2016). The DOPAC/DA

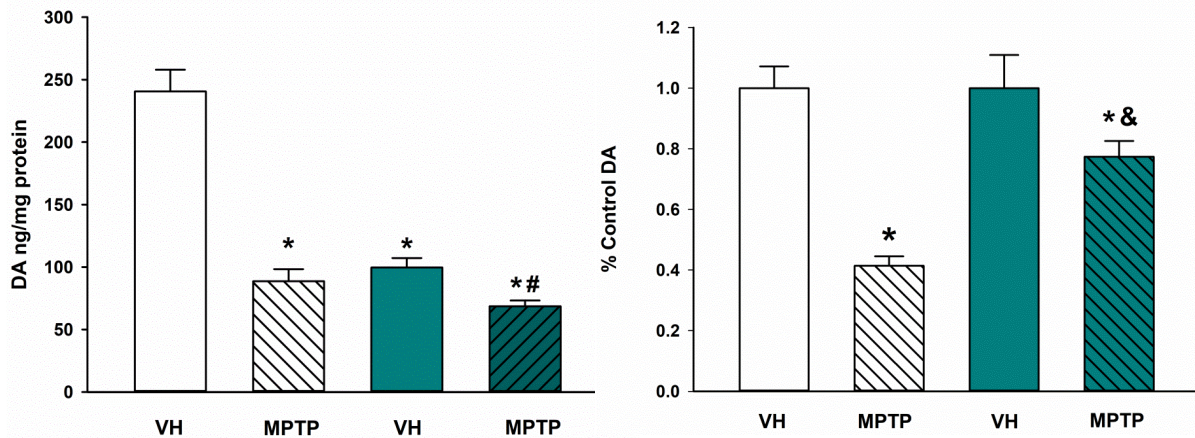


Figure 3.4. DA in the ST (white) and NAc (teal) 24 h after MPTP exposure. Mice were injected with VH or MPTP and killed 24 h later. The ST and NAc were dissected and DA was measured via HPLC-ED. ST VH n=9; ST MPTP n=8; NAc VH n=10; NAc MPTP n=10. Data is plotted as mean + SEM. Asterisk (*) signifies a significant difference from respective VH control where $p < 0.05$ via two-way ANOVA with post hoc Holm-Sidak test. Pound sign (#) or ampersand (&) signifies a significant difference from ST MPTP via two-way ANOVA with post hoc Holm-Sidak test.

ratio is an index of the rate of DA release, reuptake and metabolism relative to packaging into synaptic storage vesicles. The DOPAC/DA ratio is elevated in the NAc compared to the ST under basal conditions (**Fig. 3.6**), reflecting a higher rate of DA release in the NAc compared to the ST. MPTP caused a decrease in the DOPAC/DA ratio in the NAc but not the ST (**Fig. 3.6**).

TH, the rate-limiting enzyme of DA synthesis, is an important phenotypic marker for DA neurons and is highly expressed in both the ST and NAc. Previous studies have shown that TH expression is impaired in the ST after MPTP (Benskey et al., 2012), but the effects of MPTP on TH expression in the NAc has not been examined. Total TH in the ST and NAc 6 h (**Fig. 3.7**) and 24 h (**Fig. 3.8**) after MPTP was measured. Six h after MPTP exposure, TH expression is not changed in the ST or NAc (**Fig. 3.7**). However, 24 h after MPTP exposure, TH is decreased in both the ST and NAc, but to a lesser extent in the NAc (**Fig. 3.8**). Loss of TH protein expression likely is associated with the loss of DA stores in axon terminals, since more DA synthesis would be impaired with a deficiency of this key catalytic enzyme responsible for DA synthesis. These results show that MLDA neurons are more resilient to MPTP-induced decreases in DA stores and TH expression.

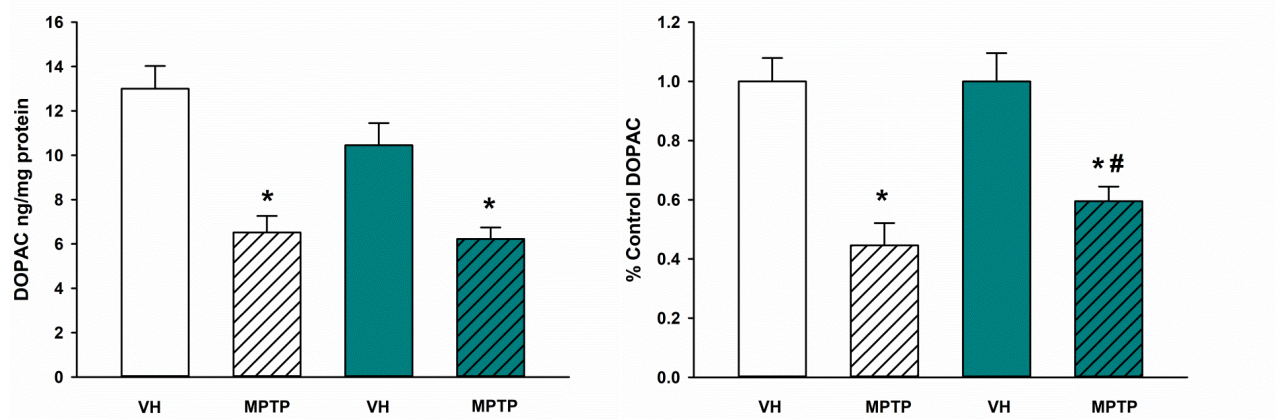


Figure 3.5. DOPAC in the ST (white) and NAc (teal) 24 h after MPTP exposure.

Mice were injected with VH or MPTP and killed 24 h later. The ST and NAc were dissected and DOPAC was measured via HPLC-ED. ST VH n=9; ST MPTP n=8; NAc VH n=10; NAc MPTP n=10. Data is plotted as mean + SEM. Asterisk (*) signifies a significant difference from respective VH control, where $p < 0.05$ via two-way ANOVA with a post hoc Holm-Sidak test. Pound sign (#) signifies a significant difference from ST MPTP via two-way ANOVA with a post hoc Holm-Sidak test.

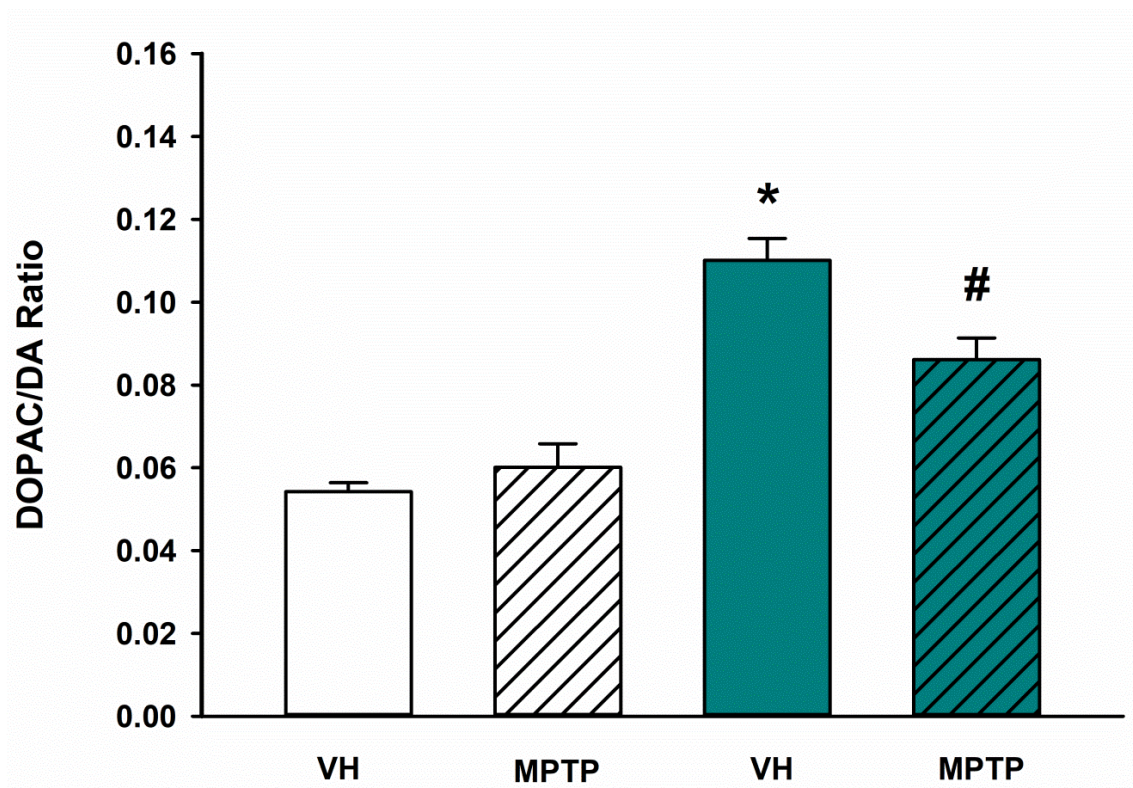


Figure 3.6. DOPAC/DA ratio in the ST (white) and NAc (teal) 24 h after MPTP exposure. Mice were injected with VH or MPTP and killed 24 h later. The ST and NAc were dissected and DA and DOPAC were measured via HPLC-ED. ST VH n=9; ST MPTP n=8; NAc VH n=10; NAc MPTP n=10. Data is plotted as mean + SEM. Asterisk (*) signifies a significant difference from ST VH control where $p < 0.05$ via two-way ANOVA and a post hoc Holm-Sidak test. Pound sign (#) signifies a significant difference from NAc

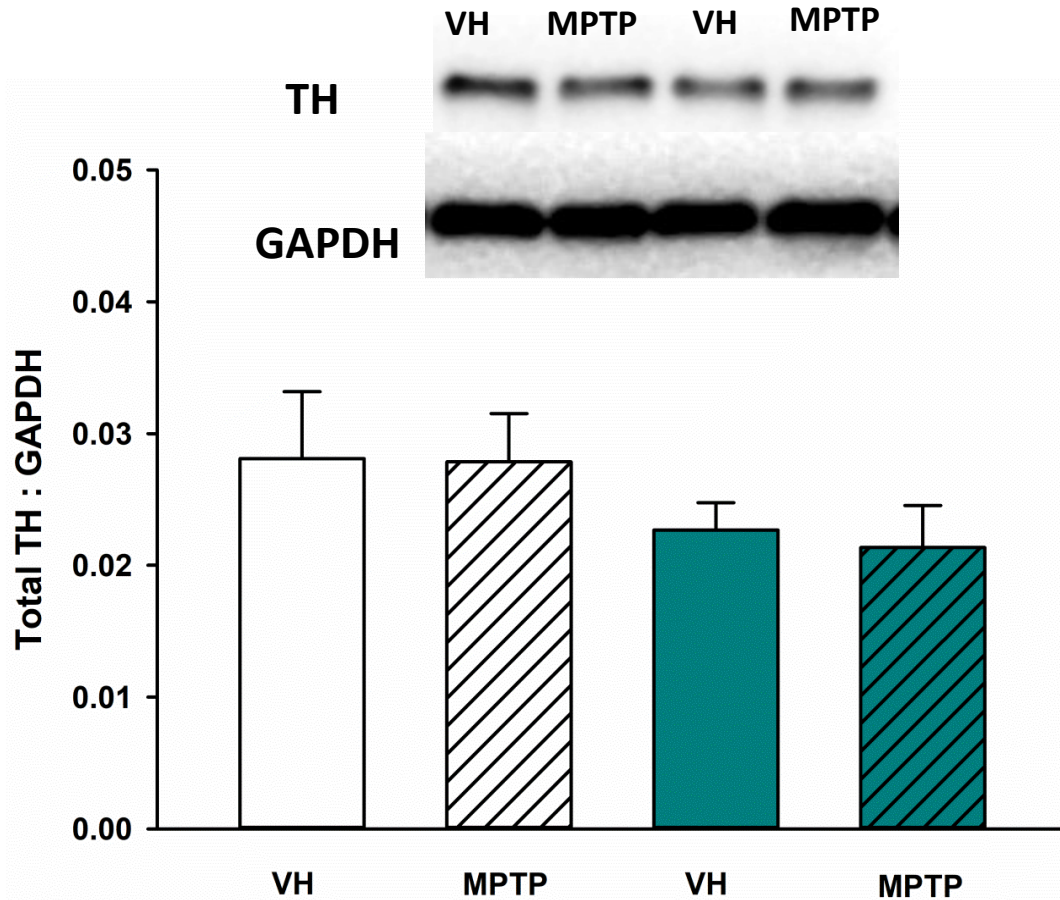


Figure 3.7. Total TH protein expression in the ST (white) and NAc (teal) 6 h after MPTP exposure. Mice were injected with VH or MPTP and killed 6 h later (n=10 each group). The ST and NAc were dissected and total TH protein was measured via Western blot. Data is plotted as mean + SEM. No statistically significant differences were detected in either brain region or treatment group ($p > 0.05$) via two-way ANOVA with post hoc Holm-Sidak test.

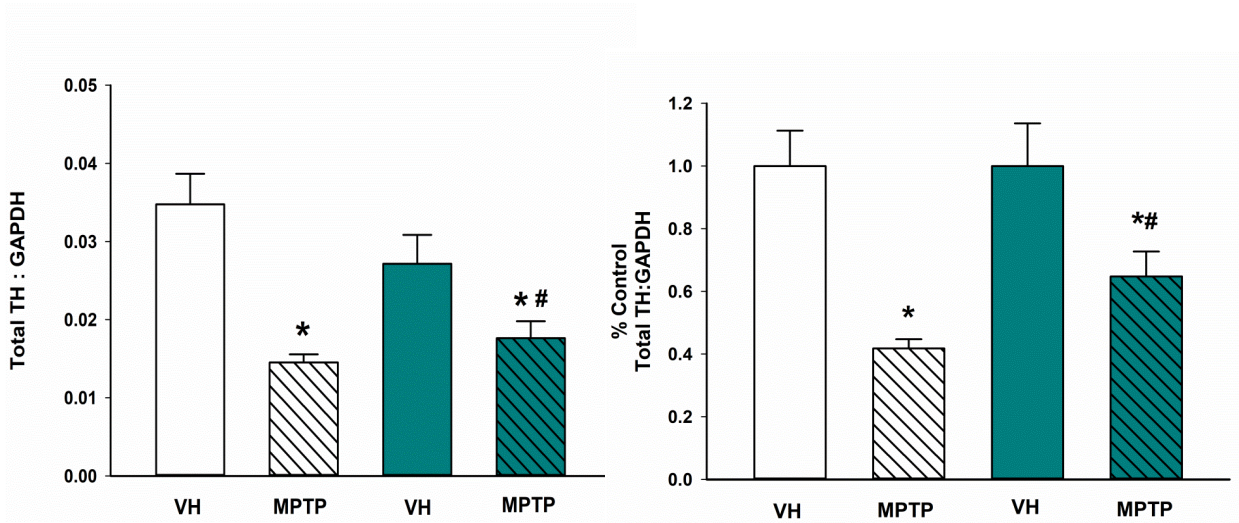


Figure 3.8. Total TH protein expression in the ST (white) and NAc (teal) 24 h after MPTP exposure. Mice were injected with VH or MPTP and killed 24 h later. The ST and NAc were dissected and total TH protein was measured via Western blot. ST VH n=10; ST MPTP n=9; NAc VH n=10; NAc MPTP n=9. Data is plotted as mean + SEM. Asterisk (*) signifies a significant difference from respective VH control. where $p < 0.05$ via two-way ANOVA and post hoc Holm-Sidak test. Pound sign (#) signifies a significant difference from ST MPTP where $p < 0.05$ via two-way ANOVA

UCH-L1 and mono-Ub in MLDA neurons after MPTP exposure

Twenty four h after MPTP exposure, UCH-L1 is decreased in the SN (Benskey et al., 2012), which is the cell body region of NSDA neurons that degenerate in PD. However, the expression of UCH-L1 protein in the ST and NAc has not been reported. UCH-L1 expression in the ST and NAc is not changed 6 h (**Fig. 3.9**) or 24 h (**Fig. 3.10**) after MPTP exposure.

The decrease in UCH-L1 in the SN was recapitulated over time after a single injection of MPTP in **Fig. 3.11**. Prior to the present experiments, the expression of UCH-L1 had not been examined in MLDA neurons, whether in the cell body region (VTA) or the axon terminal region (NAc). UCH-L1 protein expression was measured at various time points after MPTP exposure and was found to be maintained after neurotoxicant-induced injury in the VTA (**Fig. 3.12**). The ability to maintain UCH-L1 expression in the VTA may confer resistance to MLDA neurons to MPTP. Since UCH-L1 was decreased in the SN but maintained in the VTA 24 h after MPTP exposure, the 24 h time point was considered to be the most relevant and was used for subsequent experiments.

The main function of UCH-L1 activity is to replenish pools of free mono-Ub, which can be activated by E1 and E2 ligases and passed to an E3 ligase, which attaches Ub to protein substrates (Ciechanover, 1994). Therefore, it is hypothesized that if UCH-L1 levels decrease, so should levels of mono-Ub. In **Fig. 3.13**, mono-Ub was not changed in the ST or NAc 24 h after MPTP exposure, which is congruent with maintenance of UCH-L1 expression in the two brain regions 24 h after MPTP. However, in the SN, mono-Ub was decreased 24 h after MPTP exposure (**Fig. 3.14**).

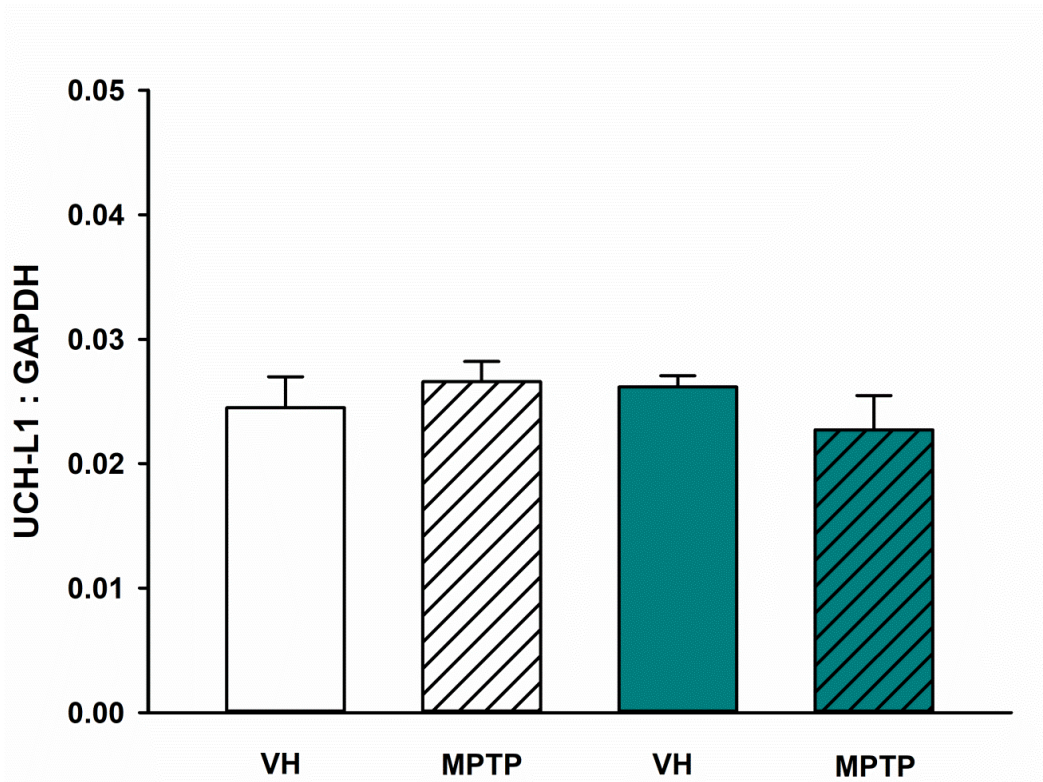


Figure 3.9. UCH-L1 protein expression in the ST (white) and NAc (teal) 6 h after MPTP exposure. Mice were injected with VH or MPTP and killed 6 h later (n=10 each group). The ST and NAc were dissected and UCH-L1 protein was measured via Western blot. Data is plotted as mean + SEM. No statistically significant differences between brain region or treatment group were found ($p > 0.05$) via two-way ANOVA.

In contrast, 24 h after MPTP exposure, mono-Ub was not decreased in the VTA (**Fig. 3.15**). This congruence between UCH-L1 expression and levels of free mono-Ub in the cell body region of MLDA neurons agrees well with the proposed function of UCH-L1.

Total glutathione concentrations in brain regions containing NSDA and MLDA neurons

The exact mechanism by which UCH-L1 could contribute to protection of MLDA neurons is as yet unknown, but could involve a relationship of UCH-L1 to regulation of reduced glutathione (GSH): UCH-L1 is predicted to have activity toward Ub-GSH and can help scavenge free GSH (Rose and Warms, 1983). GSH is an important free radical scavenger that is converted to its reduced form GSSG when encountering ROS. Mice lacking functional UCH-L1 (*gad* phenotype) have less GSH in brain tissue (Coulombe et al., 2014). Therefore, if UCH-L1 has a protective function to maintain levels of GSH in mouse brain, it is predicted that we should observe that GSH decreases when UCH-L1 decreases and GSH is maintained when UCH-L1 is maintained.

Total GSH (both GSH + GSSG forms) was measured in NSDA and MLDA neurons 24 h after MPTP. In the ST and NAc, no changes in total GSH concentration were observed (**Fig. 3.16**). Similarly, in the SN and VTA, no changes in total GSH were observed after MPTP (**Fig. 3.17**). These results are unexpected based on the findings in UCH-L1 null mice (Coulombe et al., 2014) but can be explained by introducing two caveats: 1) the phenotype of a UCH-L1 null mouse is expected to be much more severe than in a WT mouse that still expresses functional (if reduced levels of) UCH-L1, so it could be difficult to compare the magnitude of the response, and 2) the kit used for this assay

measures total GSH, which may not be the best indicator for perturbations of the GSH antioxidant system. Rather, it would be better to use an assay that measures both GSH and GSSG and can yield a GSH/GSSG ratio. Future measurements of GSH homeostasis will utilize a kit that measures both forms of GSH.

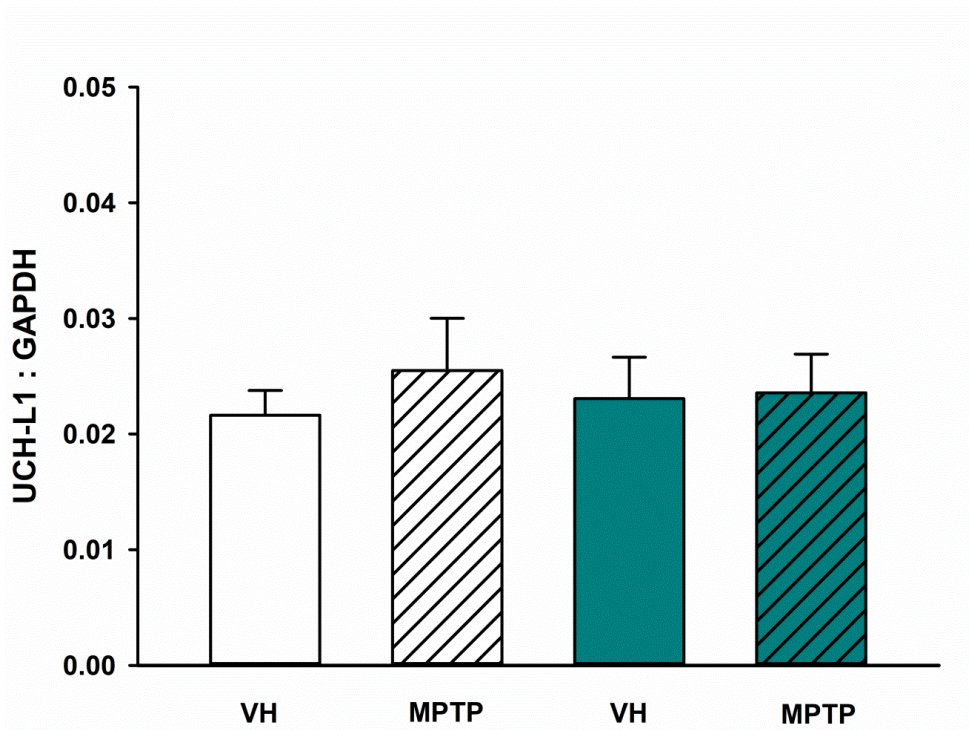


Figure 3.10. UCH-L1 protein expression in the ST (white) and NAc (teal) 24 h after MPTP exposure. Mice were injected with VH or MPTP and killed 24 h later (n=10 each group). The ST and NAc were dissected and UCH-L1 protein was measured via Western blot. Data is plotted as mean + SEM. No statistically significant differences between brain region or treatment group were found ($p > 0.05$) via two-way ANOVA.

Expression of UCH-L1 in NSDA and MLDA neurons

Thus far, we have examined UCH-L1 protein expression in microdissected mouse brain tissue containing cell bodies and axon terminals of NSDA and MLDA neurons. While the sampling technique is relatively specific based on brain region morphology, these tissue samples also contain glial cells and other non-TH neuron types. Fortunately, UCH-L1 is expressed solely in neurons (Lowe et al., 1990), so glial expression of this DUB is not an issue in this case. To determine if UCH-L1 protein expression is changing specifically in DA neurons, dual labeling IHC can be used to visualize TH neurons and UCH-L1 staining can be employed to relatively determine how many TH neurons express UCH-L1 in the SN and VTA after MPTP. **Fig. 3.18** shows UCH-L1 staining in the SN and VTA. The results reveal that UCH-L1 is robustly expressed in both brain regions co-localized in TH⁺ neurons under basal, control conditions.

Initial determination of UCH-L1 expression in the SN by IHC (**Fig. 3.19**) yielded the finding that the percent of TH neurons expressing UCH-L1 decreased 24 h after MPTP. This result is congruent with the microdissected tissue sample results and indicates that the decrease in UCH-L1 in the SN observed 24 h after MPTP exposure is occurring in the TH neurons present in the same brain region captured by the microdissection. There was no difference in numbers of TH neurons after acute MPTP in either brain region. Similarly, the percent of TH neurons expressing UCH-L1 was not changed in the VTA (**Fig. 3.20**), which is similar to the observed result that UCH-L1 protein is not altered after MPTP exposure in the VTA. The method of analyzing numbers of neurons in images captured by an epifluorescence microscope was developed for ImageJ and involved using thresholding for both size and

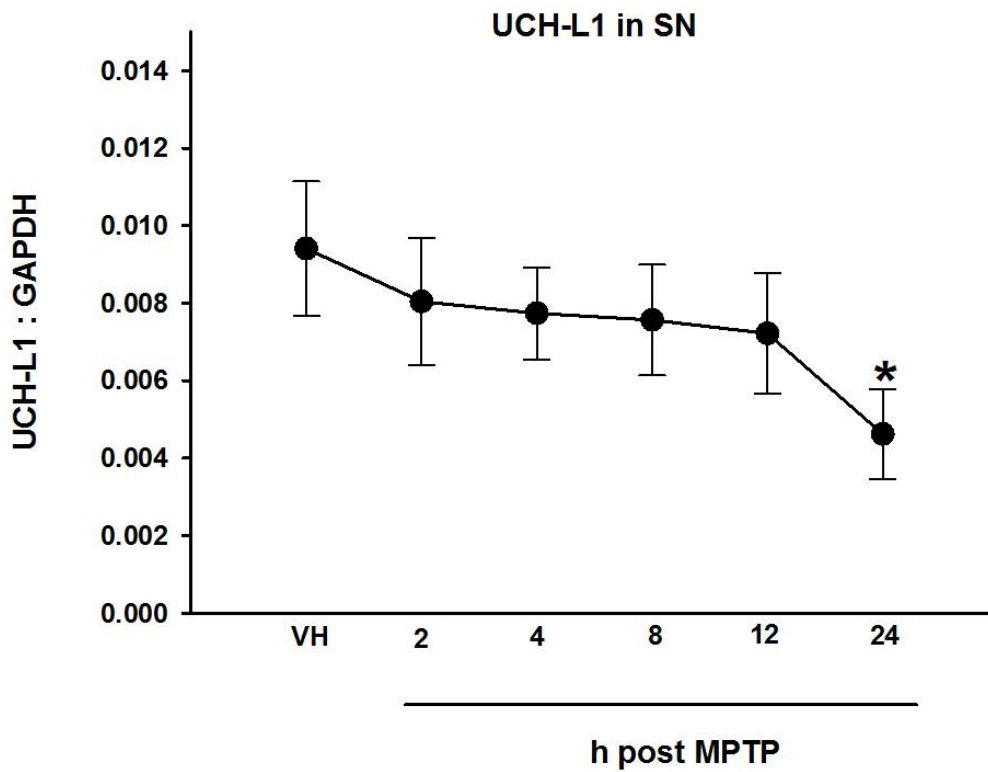


Figure 3.11. UCH-L1 protein expression in the SN after MPTP exposure. Mice were injected with MPTP and killed various times after MPTP. The SN was dissected and UCH-L1 protein was measured via Western blot. VH n=8; 2 h n=10; 4 h n=10; 8 h n=10; 12 h n=9; 24 h n=7. Data is plotted as mean + SEM. Asterisk (*) signifies a significant difference from VH control where $p < 0.05$ via one-way ANOVA with a post hoc Holm-Sidak test.

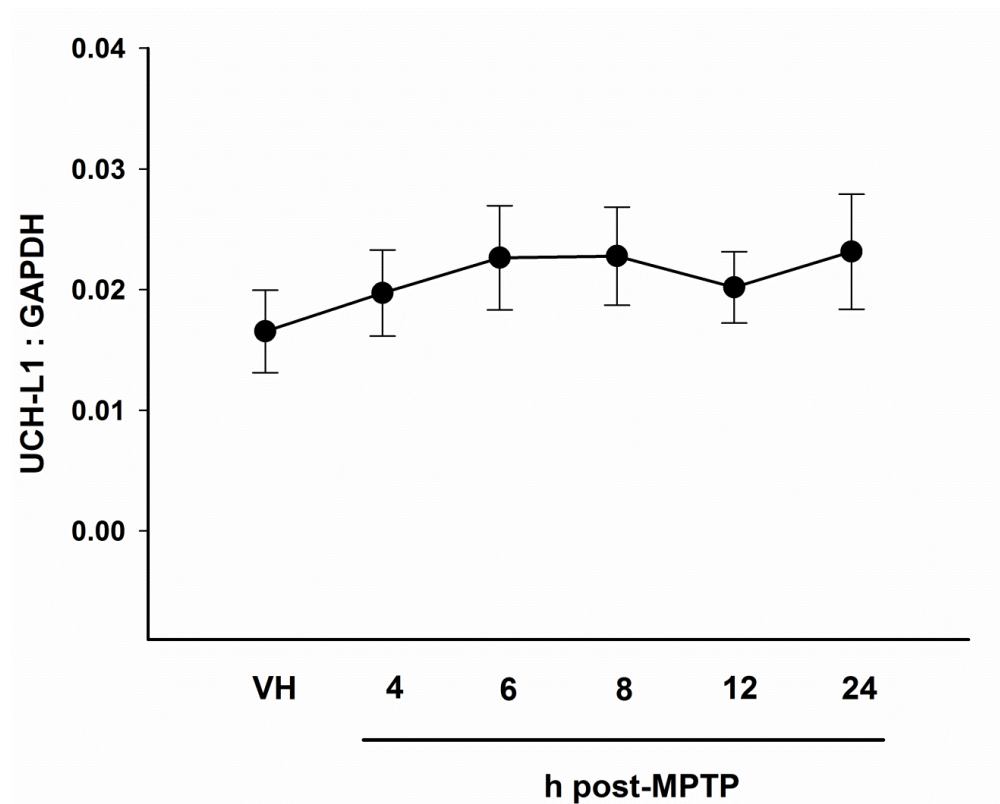


Figure 3.12. UCH-L1 protein expression in the VTA after MPTP exposure. Mice were injected with MPTP and killed various times after MPTP (n=10 each group). The VTA was dissected and UCH-L1 protein was measured via Western blot. Data is plotted as mean + SEM. No significant difference was detected between groups ($p > 0.05$) via one-way ANOVA.

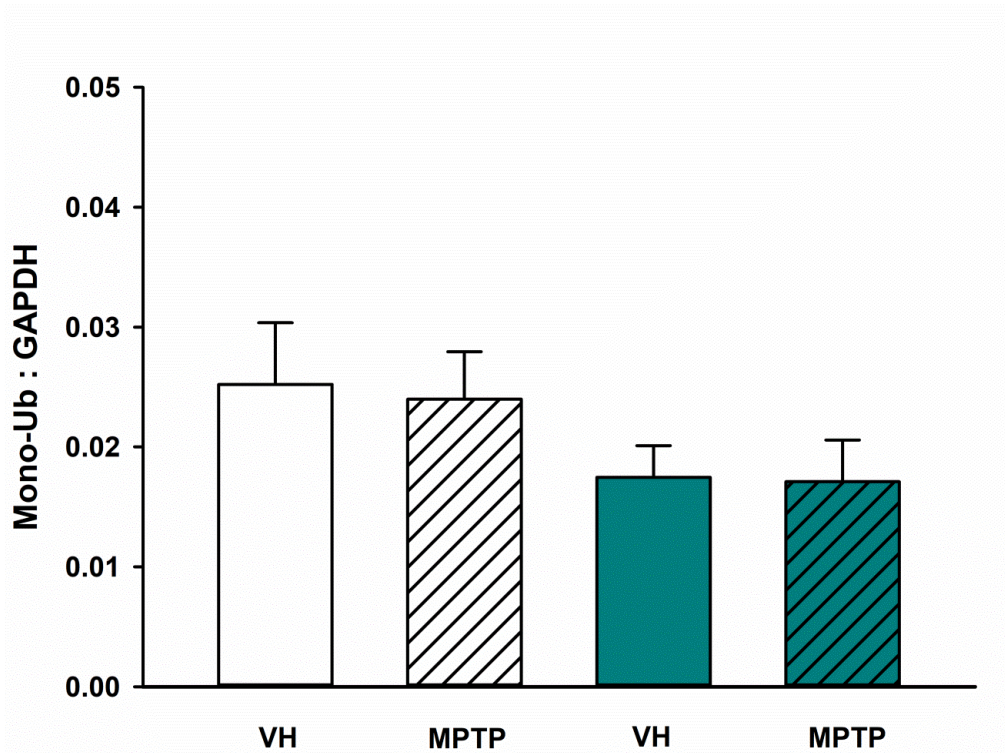


Figure 3.13. Mono-Ub protein expression in the ST (white) and NAc (teal) 24 h after MPTP exposure. Mice were injected with VH or MPTP and killed 24 h later. The ST and NAc were dissected and mono-Ub protein was measured via Western blot. ST VH n=10; ST MPTP n=10; NAc VH n=10; NAc MPTP n=9. Data is plotted as mean + SEM. No statistically significant differences between brain region or treatment group were found ($p > 0.05$) via two-way ANOVA.

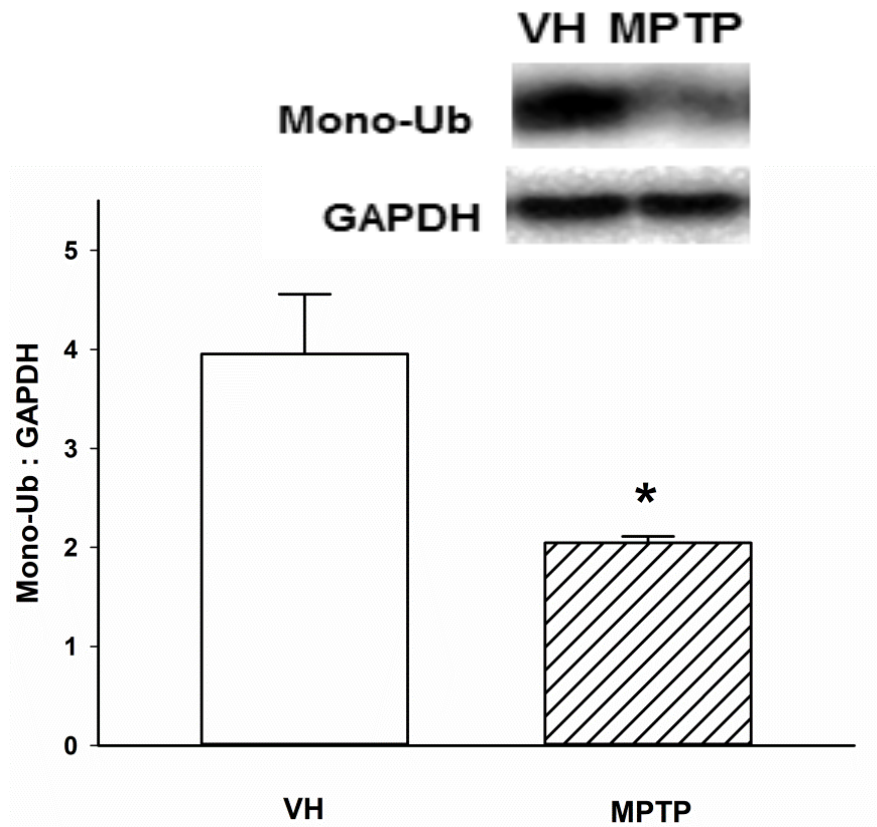


Figure 3.14. Mono-Ub protein expression in the SN 24 h after MPTP exposure. Mice were injected with VH or MPTP and killed 24 h later (n=8 each group). The SN was dissected and mono-Ub protein was measured via Western blot. Data is plotted as mean + SEM. Asterisk (*) signifies a statistically significant difference from VH control where $p < 0.05$ via t-test.

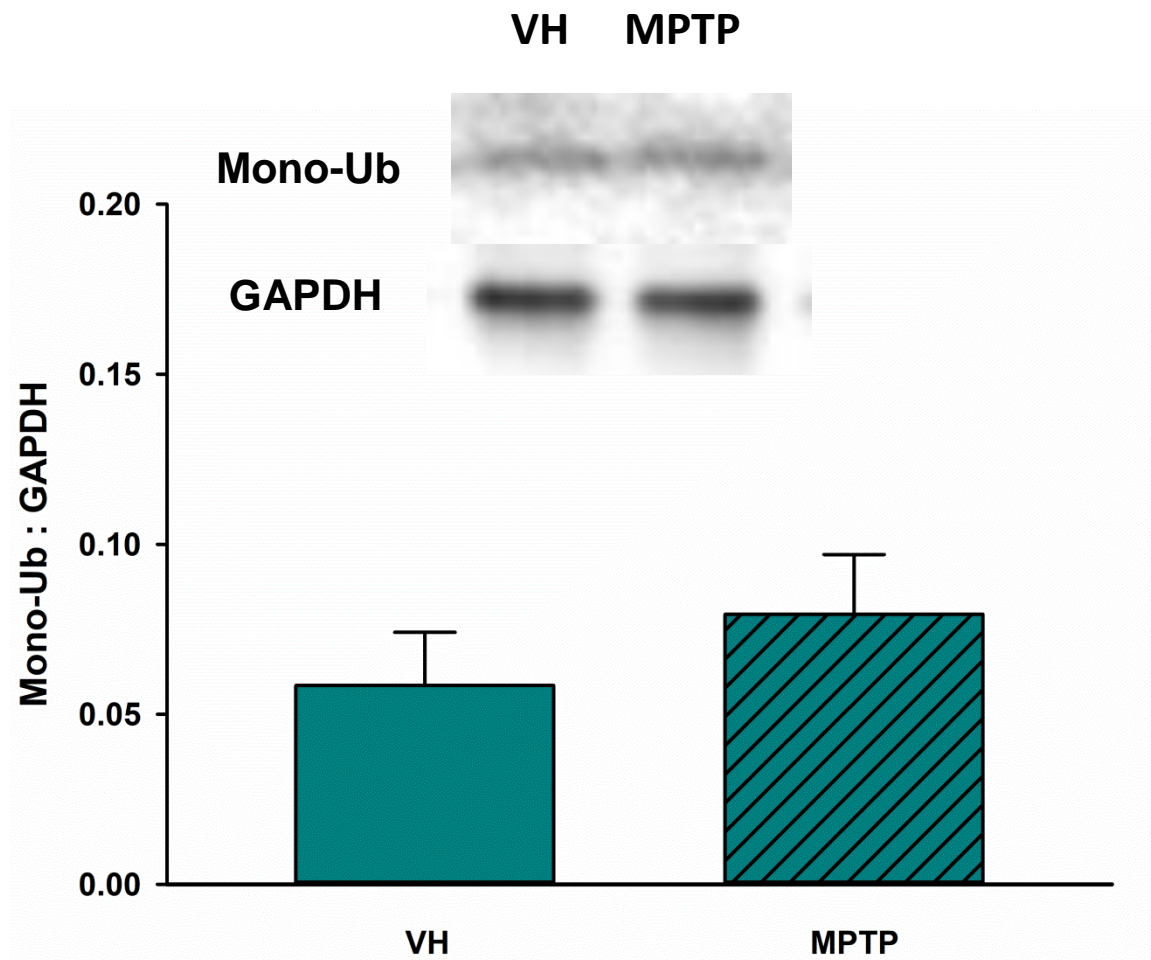


Figure 3.15. Mono-Ub protein expression in the VTA 24 h after MPTP exposure. Mice were injected with VH or MPTP and killed 24 h later (n=10 each group). The VTA was dissected and mono-Ub protein was measured via Western blot. Data is plotted as mean + SEM. No statistically significant difference was detected between groups ($p > 0.05$) via t-test.

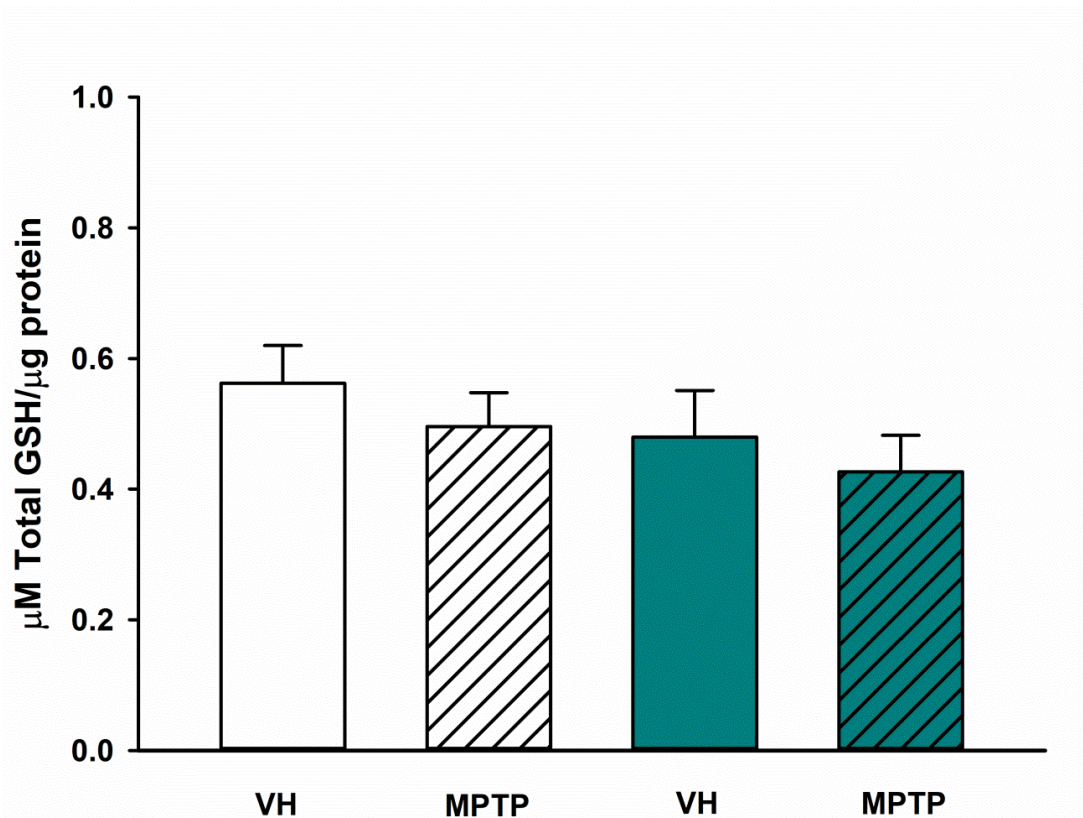


Figure 3.16. Total GSH concentrations in the ST (white) and NAc (teal). Mice were injected with VH or MPTP and killed 24 h later (n=10 each group). Brains were removed and ST and NAc were dissected and assayed for total GSH (GSH + GSSG) content. Data is plotted as mean + SEM. No statistically significant differences between brain region or treatment group were found ($p > 0.05$) via two-way ANOVA.

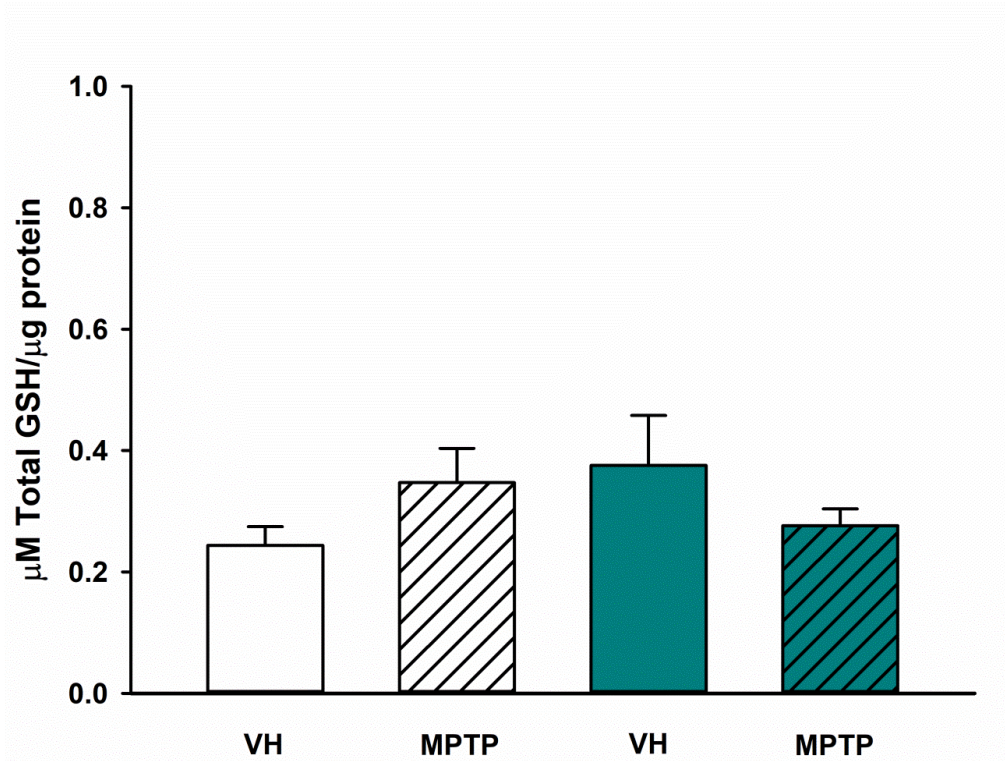


Figure 3.17. Total GSH concentrations in the SN (white) and VTA (teal). Mice were injected with VH or MPTP and killed 24 h later. SN VH n=9; SN MPTP n=10; VTA VH n=8; VTA MPTP n=10. Brains were removed and SN and VTA were dissected and assayed for total GSH (GSH + GSSG) content. Data is plotted as mean + SEM. No statistically significant differences between brain region or treatment group were found ($p > 0.05$) via two-way ANOVA.

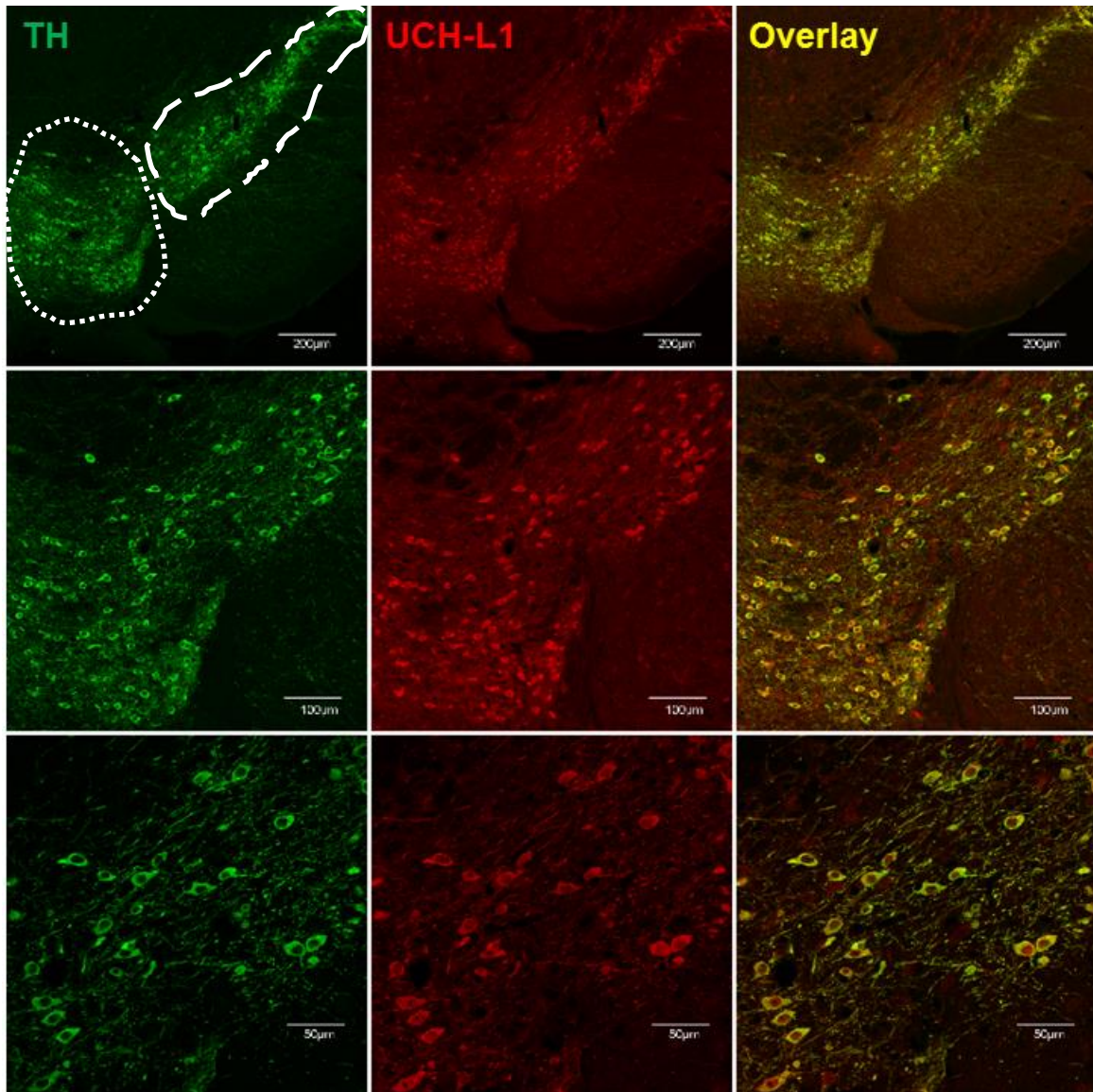


Figure 3.18. Immunohistochemical staining for UCH-L1 and TH in the SN (white dashed oval) and VTA (white dotted circle). Mice were perfused with paraformaldehyde and brains sectioned at 20 μm . Brain sections were stained and mounted onto slides. Slides were imaged using an Olympus FV1000 confocal microscope. Top tier images are 10X magnification (scale bar = 200 μm). Middle tier images are 20X magnification (scale bar = 100 μm). Bottom tier images are 40X magnification (scale bar = 50 μm).

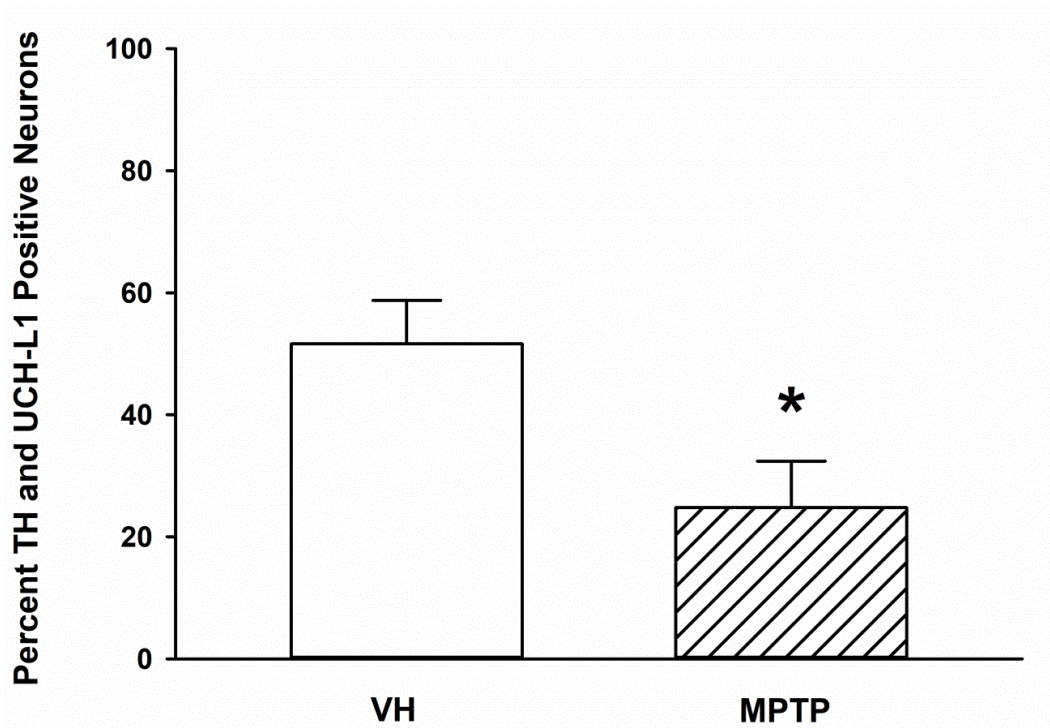


Figure 3.19. Percent of TH and UCH-L1 positive neurons in the SN 24 h after MPTP. Mice were injected with VH or MPTP and perfused 24 h later with paraformaldehyde (n=4 each group). The brain was sectioned and stained for UCH-L1. Images were analyzed using an ImageJ method to count double-labeled cells. Data is plotted as mean + SEM. Asterisk (*) signifies a statistically significant difference where $p < 0.05$ via t-test.

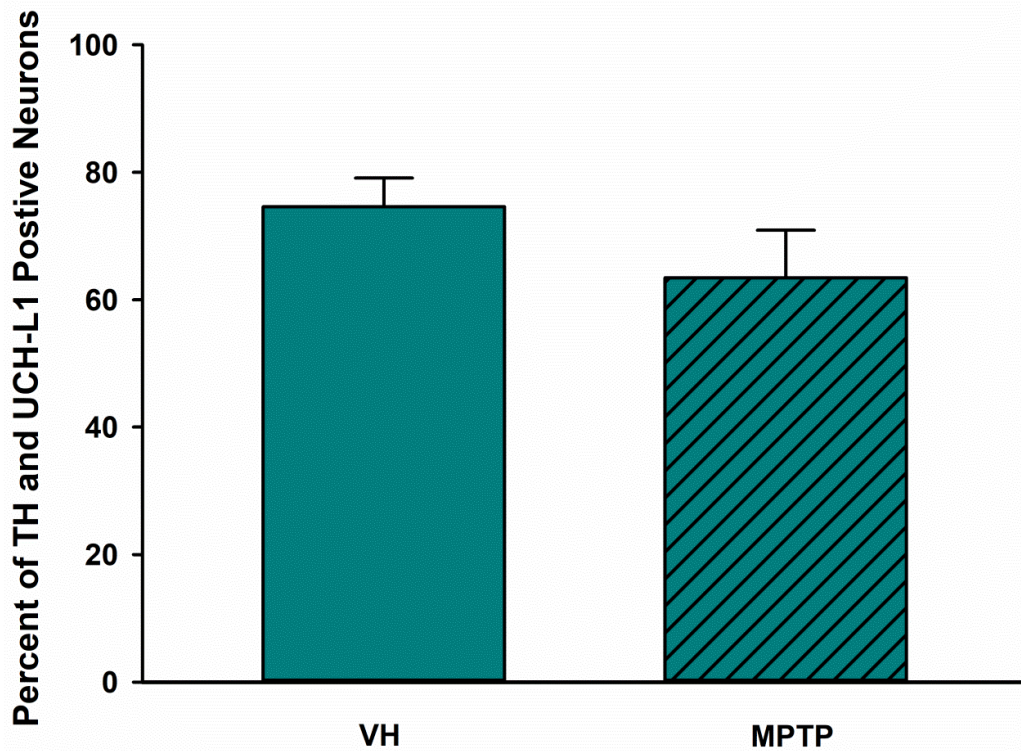


Figure 3.20. Percent of TH and UCH-L1 positive neurons in the VTA 24 h after MPTP. Mice were injected with VH or MPTP and perfused 24 h later with paraformaldehyde (n=5 each group). The brain was sectioned and stained for UCH-L1. Images were analyzed using an ImageJ method to count double-labeled cells. Data is plotted as mean + SEM. No significant difference between groups was detected ($p > 0.05$) via t-test.

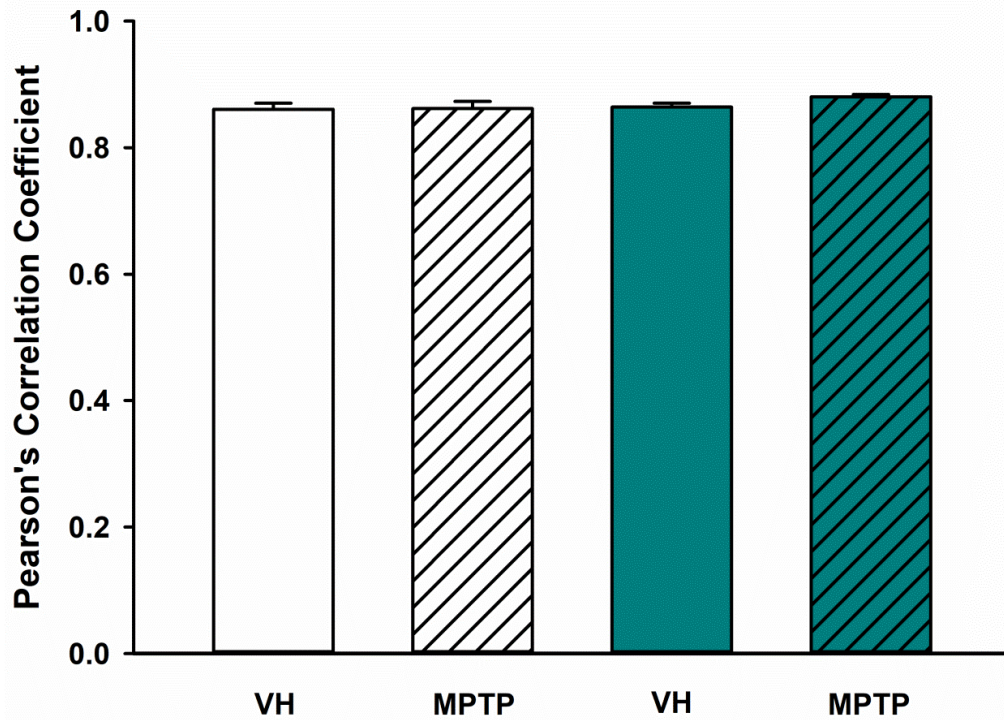


Figure 3.21. Pearson's correlation coefficient values for co-localization of UCH-L1 and TH signal in the SN (white) and VTA (teal). Mice were injected with VH or MPTP and perfused 24 h later with paraformaldehyde. SN VH n=6; SN MPTP n=7; VTA VH n=5; VTA MPTP n=6. The brain was sectioned and stained for UCH-L1. Images were analyzed using FV1000 software to determine the PCC for overlap of UCH-L1 and TH signal. Data is plotted as mean + SEM. No statistically significant difference was detected between groups ($p > 0.05$) via two-way ANOVA.

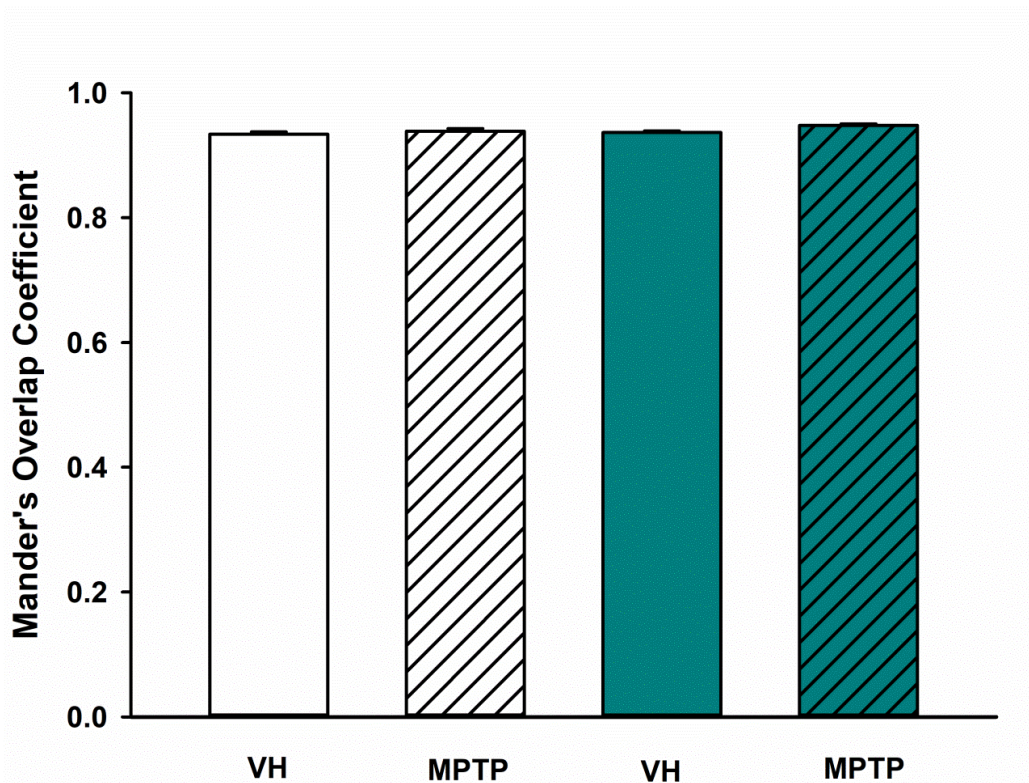


Figure 3.22. Mander's overlap correlation values for co-localization of UCH-L1 and TH signal in the SN (white) and VTA (teal). Mice were injected with VH or MPTP and perfused 24 h later with paraformaldehyde. SN VH n=6; SN MPTP n=7; VTA VH n=5; VTA MPTP n=5. The brain was sectioned and stained for UCH-L1. Images were analyzed using FV1000 software to determine the MOC for overlap of UCH-L1 and TH signal. Data is plotted as mean + SEM. No statistically significant difference was detected between groups ($p > 0.05$) via two-way ANOVA.

intensity, where visualization of the fluorophore signal is only taken into account if it is above a certain threshold and the region of signal corresponds to the actual size of a neuron. A caveat for this method is that relatively thicker (20 μm) specimens imaged using an epifluorescence microscope can show fluorescence bleed through, due to a wide area of tissue being excited by the mercury lamp bulb. One way to get around this issue is to use confocal microscopy.

The experiment was repeated and images captured via confocal microscopy. Images were analyzed for co-localization of pixels corresponding to TH and UCH-L1 staining. To measure the degree of co-localization, the Pearson's correlation coefficient (PCC) and Mander's Overlap Coefficient (MOC) were analyzed for SN and VTA images and between VH and MPTP treated mice (**Fig. 3.21**).

Discussion

In this chapter, evidence for differential response to MPTP between two differentially susceptible DA neuron populations was presented. In addition, MLDA neurons showed partial resistance to MPTP toxicity with respect to a decrease in DA and TH expression. This observed decreased susceptibility to MPTP has been demonstrated both here and in previous studies (Behrouz et al., 2007; Hung and Lee, 1998; Hung et al., 1995) and likely involves a difference in MLDA neuron response to oxidative stress. Although the actual production of ROS in ST and NAc are not different 6 h after MPTP, the response to downstream effects of ROS toxicity could be different.

To understand pathways that could compensate in MLDA neurons to combat neurotoxic injury, we examined a protein found to be mutated in rare familial PD—UCH-L1, a

neuron specific DUB. Although UCH-L1 expression is decreased in the SN, UCH-L1 protein is maintained in the VTA. This preservation of UCH-L1 expression is accompanied by maintenance of UCH-L1 function, as evidenced by maintenance of free mono-Ub levels after neurotoxicant exposure. However, there is a mismatch between UCH-L1 changes between the cell body regions and the axon terminals: UCH-L1 is only decreased in the SN rather than the ST. Since the axon terminal regions are considered to be the primary site of action to MPP⁺ because MPP⁺ relies on DAT to enter the cell, we would have predicted that UCH-L1 would be decreased in the ST as well as the SN. UCH-L1 expression over time after MPTP in the axon terminals of NSDA neurons is more closely examined in **Chapter 4**.

The number of DA neurons expressing UCH-L1 was decreased in the SN but not the VTA 24 h after MPTP, matching the protein expression found in whole tissue and demonstrating that the decrease in UCH-L1 protein observed in whole SN tissue is not obscured by changes in UCH-L1 in other neuronal populations. However, the co-localization of TH and UCH-L1 signal was not changed in either region after MPTP treatment. It should be noted that although PCC and MOC indices are widely accepted as a valid method for determining co-localization of fluorophores (Dunn et al., 2011), it may be of limited use in determine how many DA neurons express UCH-L1 because these only determine that there is no difference in co-incidence of red and green pixels between VH and MPTP treated mice. Accordingly, it would be expected that the number of red pixels corresponding to UCH-L1 protein would decrease in brain sections from MPTP-treated mice. But fluorescence intensity is not generally a good measure of protein abundance, since there are many factors that can affect fluorescence intensity

(Dunn et al., 2011) that are independent of the amount of protein present (such as binding affinity and abundance of the secondary antibody, which contains the fluorophore). However, this method of determining the PCC and MOC with thresholding is one way to avoid observer bias.

The most ideal method for determining numbers of TH neurons would be stereology (West, 1999), but most investigators use stereology for bright field microscopic analysis of tissues rather than fluorescence, and determination of dual-labeled cells is limited. Therefore, the ImageJ method may be a new acceptable way to determine numbers of neurons expressing a particular protein as evidenced by presence of a fluorophore. This is the first time that UCH-L1 expression and function has been measured in the MLDA neurons, especially in the context of neurotoxicant-induced stress. Maintenance of UCH-L1 expression in the VTA may confer resistance of MLDA neurons to neurotoxicant-induced injury. Further work to inhibit UCH-L1 will help to elucidate whether this effect is UCH-L1 specific.

Summary and conclusions

In this chapter, we recapitulated the differential susceptibility of NSDA and MLDA neurons to acute MPTP with respect to DA and TH expression. We also examined response to oxidative stress by production of ROS. UCH-L1 was discovered to be maintained in the VTA, both in whole tissue samples and in DA neurons by IHC. These studies provide evidence that UCH-L1 is differentially regulated between NSDA and MLDA neurons and maintenance of UCH-L1 is associated with decreased susceptibility to MPTP.

REFERENCES

REFERENCES

- Behrouz, B., Drolet, R.E., Sayed, Z.A., Lookingland, K.J., Goudreau, J.L., 2007. Unique responses to mitochondrial complex I inhibition in tuberoinfundibular dopamine neurons may impart resistance to toxic insult. *Neuroscience* 147, 592–8. doi:10.1016/j.neuroscience.2007.05.007
- Behrouz, B., Drolet, R.E., Sayed, Z. a., Lookingland, K.J., Goudreau, J.L., 2007. Unique responses to mitochondrial complex I inhibition in tuberoinfundibular dopamine neurons may impart resistance to toxic insult. *Neuroscience* 147, 592–598. doi:10.1016/j.neuroscience.2007.05.007
- Benskey, M., Behrouz, B., Sunryd, J., Pappas, S.S., Baek, S.-H.H., Huebner, M., Lookingland, K.J., Goudreau, J.L., 2012. Recovery of hypothalamic tuberoinfundibular dopamine neurons from acute toxicant exposure is dependent upon protein synthesis and associated with an increase in parkin and ubiquitin carboxy-terminal hydrolase-L1 expression. *Neurotoxicology* 33, 321–31. doi:10.1016/j.neuro.2012.02.001
- Braak, H., Braak, E., 2000. Pathoanatomy of Parkinson's disease. *J. Neurol.* 247 Suppl, I13-10. doi:10.1007/PL00007758
- Ciechanover, A., 1994. The ubiquitin-proteasome proteolytic pathway. *Cell* 79, 13–21. doi:10.1016/0092-8674(94)90396-4
- Coulombe, J., Gamage, P., Gray, M.T., Zhang, M., Tang, M.Y., Woulfe, J., Saffrey, M.J., Gray, D.A., 2014. Loss of UCHL1 promotes age-related degenerative changes in the enteric nervous system . *Front. Aging Neurosci.* .
- Dunkley, P.R., Jarvie, P.E., Robinson, P.J., 2008. A rapid Percoll gradient procedure for preparation of synaptosomes. *Nat. Protoc.* 3, 1718–1728. doi:10.1038/nprot.2008.171
- Dunn, K.W., Kamocka, M.M., McDonald, J.H., 2011. A practical guide to evaluating colocalization in biological microscopy. *AJP Cell Physiol.* 300, C723–C742. doi:10.1152/ajpcell.00462.2010
- Hung, H.-C., Lee, E.H., 1998. MPTP Produces Differential Oxidative Stress and Antioxidative Responses in the Nigrostriatal and Mesolimbic Dopaminergic Pathways. *Free Radic. Biol. Med.* 24, 76–84. doi:10.1016/S0891-5849(97)00206-2
- Hung, H.C., Tao, P.L., Lee, E.H., 1995. 1-Methyl-4-phenyl-pyridinium (MPP+) uptake does not explain the differential toxicity of MPP+ in the nigrostriatal and mesolimbic dopaminergic pathways. *Neurosci. Lett.* 196, 93–6.
- Johannessen, J.N., Adams, J.D., Schuller, H.M., Bacon, J.P., Markey, S.P., 1986. 1-

- methyl-4-phenylpyridine (MPP+) induces oxidative stress in the rodent. *Life Sci.* 38, 743–749. doi:10.1016/0024-3205(86)90589-8
- Lookingland, K.J., Moore, K.E., 2005. Chapter VIII Functional neuroanatomy of hypothalamic dopaminergic neuroendocrine systems. *Handb. Chem. Neuroanat.* 21, 435–523. doi:10.1016/S0924-8196(05)80012-0
- Lowe, J., McDermott, H., Landon, M., Mayer, R.J., Wilkinson, K.D., 1990. Ubiquitin carboxyl-terminal hydrolase (PGP 9.5) is selectively present in ubiquitinated inclusion bodies characteristic of human neurodegenerative diseases. *J. Pathol.* 161, 153–160. doi:10.1002/path.1711610210
- Meiser, J., Weindl, D., Hiller, K., 2013. Complexity of dopamine metabolism. *Cell Commun. Signal.* 11, 34. doi:10.1186/1478-811X-11-34
- Meister, B., Elde, R., 1993. Dopamine Transporter mRNA in Neurons of the Rat Hypothalamus. *Neuroendocrinology* 58, 388–395. doi:10.1159/000126568
- Rose, I.A., Warms, J.V.B., 1983. An enzyme with ubiquitin carboxy-terminal esterase activity from reticulocytes. *Biochemistry* 22, 4234–4237. doi:10.1021/bi00287a012
- Sulzer, D., Cragg, S.J., Rice, M.E., 2016. Striatal dopamine neurotransmission: Regulation of release and uptake. *Basal Ganglia* 6, 123–148. doi:10.1016/j.baga.2016.02.001
- Sun, A., Chen, Y., 1998. Oxidative stress and neurodegenerative disorders. *J. Biomed. Sci.* 65212, 401–414.
- West, M.J., 1999. Stereological methods for estimating the total number of neurons and synapses: issues of precision and bias. *Trends Neurosci.* 22, 51–61. doi:10.1016/S0166-2236(98)01362-9

Chapter 4: Effects of Neurotoxicant and UCH-L1 Inhibitor in MN9D Cells and ST Synaptosomes, and a Potential Interaction between UCH-L1 and Parkin with Relevance to Autophagy

Introduction

One approach to the determination of whether expression of UCH-L1 in populations of DA neurons influences susceptibility to neurotoxicant-induced injury is to use tools and techniques targeting only NSDA neurons. This chapter takes a closer look at mechanistic aspects of UCH-L1 function in an *in vitro* model of NSDA neurons and in ST synaptosomes containing axon terminals of NSDA neurons. A potential interaction between UCH-L1 and parkin is also investigated, with potential consequences for another major avenue of protein degradation: the ALP.

The “MN9D” cell line is derived from a fusion of mouse mesencephalic DA neurons with murine neuroblastoma cells (Choi et al., 1991), and is extensively used in PD research. Utilization of this immortalized cell line affords many benefits to studying mechanisms of DA neuronal loss in PD or MPTP toxicity because of its ease of neurotoxicant exposure to a culture, the ease of collection of samples, the shorter time frame and less cost for an experiment as compared to *in vivo* models, and last but certainly not least, the conservation of rodent life while performing “proof of principle” experiments. MN9D cells express high levels of TH and DAT (Choi et al., 1992), which are prerequisites for evaluating MPP⁺ induced toxicity. The active metabolite of MPTP, MPP⁺, has been used in MN9D cell cultures to examine its cytotoxic effect under varying conditions (Choi et al., 1999). It is currently unknown if UCH-L1 is highly expressed in MN9D cells, and

further, if UCH-L1 expression is altered with MPP⁺ exposure. The purpose of studies using MN9D cells described in this chapter is to determine if these cells model inhibition of NSDA neuronal UCH-L1 expression after toxicant exposure. In addition, pharmacological inhibitors of UCH-L1 and the UPS will be used to examine the effects of UCH-L1 and proteasome inhibition on DA phenotypic markers.

A hallmark pathology of PD is the presence of Lewy bodies in NSDA neurons, which are proteinaceous deposits of α -syn (Spillantini et al., 1997) (Baba et al., 1998) and Ub (Meredith et al., 2004) linked to disruption in protein homeostasis. Indeed, within the family of human genes with the PARK denotation, a few code for enzymes involved in protein degradation such as UCH-L1 (PARK5) and parkin (PARK2). UCH-L1's role in maintaining proteasome function is not well understood, as it removes Ub from small substrates and could potentially prevent proteasomal degradation of those substrates. On the other hand, UCH-L1 helps to recycle free mono-Ub to be used by E3 ligases to tag misfolded protein substrates. Parkin, a 465 amino acid protein, is an E3 ligase (Shimura et al., 2000) responsible for tagging specific substrates with mono-Ub and building poly-Ub chains that target substrates for degradation via the 26S proteasome. In addition to its ligase activity, parkin has been shown to bind to the Rpn10 domain of the 26S proteasome via its ubiquitin-like domain (UBL) to directly modulate 26S proteasome activity (Um et al., 2010).

Although parkin's PD-related substrates *in vivo* are only partially known, loss of functional parkin causes widespread neurodegeneration in the human brain (Shimura et al., 2000). Mutations in parkin are the second most common cause of autosomal-recessive juvenile parkinsonism (Kitada et al., 1998) and parkin has also been shown to

contribute to mitophagy (Narendra et al., 2008), which is a critical process of mitochondrial quality control. In fact, recent evidence shows that parkin is critical for recovery of SN neurons after mitochondrial stress (Pickrell et al., 2015). However, since the generation of the parkin null mouse (Goldberg et al., 2003), a puzzling lack of degenerative phenotype (Perez and Palmiter, 2005) has been observed in these mice, begging the question of compensation since the mice have coped with lack of parkin protein from birth. How these mice compensate for loss of UPS function and whether that compensation involves down-regulation of UCH-L1 will be examined in this chapter.

Death of NSDA neurons is likely due at least in part to failure of both the UPS and the ALP since pathology in PD is highly associated with aggregated proteins (Ross and Poirier, 2004). The UPS and ALP represent the two major pathways of protein degradation in the cell tasked with recycling amino acids from degraded proteins and maintaining proteostasis. The 26S proteasome primarily degrades small, short-lived proteins in a highly specific manner, requiring the use of a K48-linked poly-Ub chain attached to a substrate protein to signal degradation (Thrower et al., 2000). It is important to note that another form of the proteasome may play a role in degrading proteins and aggregates: the 20S proteasome can degrade proteins that are not ubiquitinated and can also degrade oxidatively modified proteins (Davies, 2001). In contrast to 26S proteasome activity, macroautophagy, one of the pathways broadly described as the ALP, is relatively non-selective and can degrade larger complexes or even organelles, of which mitophagy (self-eating of mitochondria) is a prominent example (Ross et al., 2015).

In another branch of the ALP pathway, chaperone mediated autophagy (CMA), proteins containing a specific amino acid motif (KFERQ) bind to the chaperone hsc70, which shuttles the substrate to the LAMP-2A receptor located on the exterior of the lysosome which forms a multimeric complex to induce unfolding and endocytosis of the substrate (Bandyopadhyay et al., 2008). An important protein relevant to PD, α -syn, has been demonstrated to be degraded by CMA in its monomeric form and mutant forms of α -syn impair the ability of CMA to clear other substrates (Cuervo et al., 2004).

A K63-linked poly-Ub chain may act to signal a protein to be degraded by macroautophagy, but it is unclear whether these chains are required for all types and situations of macroautophagy. It is also unclear which E3 ligase is responsible for conjugating K63-linked chains on specific substrates though parkin has been shown to create K63-linked poly-Ub chains, especially with respect to mitophagy (Olzmann and Chin, 2008). Indeed, evidence of failure of the ALP has been shown in post-mortem brain samples from PD patients where NSDA neurons display many autophagic vacuoles (Anglade et al., 1997). Although the UPS and ALP were once considered functionally separate, emerging evidence suggests that crosstalk between the two systems exist such that if one pathway becomes dysfunctional, the other's activity may be upregulated to compensate to maintain proteostasis (Ross and Pickart, 2004).

Since degradation of substrates by the 26S proteasome canonically requires a K48-linked poly-Ub chain, 26S proteasome function may be dependent on E3 ligases that can perform this ubiquitination. In the case of parkin deficient mice, total UPS activity has been shown in our laboratory to be decreased in the SN, suggesting that proteasome activity is impaired in Park2^{-/-} mice compared to wild-type mice (Lansdell,

2017). If 26S proteasome activity is at least partially dependent on parkin E3 ligase activity and/or parkin UBL domain binding to the Rpn10 subunit (Um et al., 2010) and parkin regulation of UCH-L1 plays a role, perhaps the ALP is upregulated to compensate and degrade UPS substrates *sans* poly-Ub chains. This hypothesis will be tested in this chapter.

Results

MN9D expression of DA phenotypic markers and UCH-L1

To determine if the MN9D cells grown and differentiated in our laboratory express DA phenotypic markers after differentiation, IHC was performed to stain for TH, DAT, and UCH-L1. **Fig. 4.1** shows a phase contrast bright field image of differentiated MN9D cells as well as MN9D cells stained for TH, DAT, and UCH-L1. It is critical for differentiated MN9D cells to express DAT because it is the avenue through which the neurotoxicant MPP⁺ can gain access to the cell and cause oxidative damage (Dauer and Przedborski, 2003). In addition, in order to use these cells as a model for NSDA neurons *in vitro*, they also need to highly express UCH-L1. These results confirmed expression of these proteins.

Next, MN9D cell cultures were treated with the neurotoxicant MPP⁺ to determine a concentration dependent response with respect to depletion of DA levels. In **Fig. 4.2**, incremental concentrations of MPP⁺ cause a corresponding increased loss of intracellular DA content from MN9D cells at 2 h and 8 h, showing that the effects of MPP⁺ in MN9D cells mirrors the effects of MPTP in mice. The lowest concentration of MPP⁺ had no effect at 2 h, whereas the higher concentration did have an effect on

intracellular DA. Next, DA and DOPAC were measured in MN9D cells exposed to 100 μM MPP⁺ (**Fig. 4.3**). This decrease in intracellular DA was accompanied by a concurrent decrease in UCH-L1 protein (**Fig. 4.4**) showing that MN9D cells closely model the decrease in UCH-L1 protein in the NSDA neurons after neurotoxicant treatment (Benskey et al., 2012) (**Fig. 3.11**). When UCH-L1 hydrolase activity was analyzed, it was found that MPP⁺ does not appear to directly inhibit UCH-L1 activity in MN9D cells (**Fig. 4.5**). Next, we sought to treat MN9D cells with the UCH-L1 inhibitor, LDN-57444 (LDN) (Liu et al., 2003). We wanted to understand the effects of direct inhibition of UCH-L1 would have on an *in vitro* model of NSDA neurons. When we treated MN9D cells with MPP⁺, varying concentrations of LDN, and MPP⁺ + LDN, we found that intracellular DA was decreased in MPP⁺, 5 μM LDN, and MPP⁺ + LDN treatment groups (**Fig. 4.6**). These results point to potential toxicity of LDN or impairment of UCH-L1 hydrolase activity on MN9D cells that cause perturbations of the DA phenotype of the cells. The main metabolite of recaptured DA, DOPAC, however, was not decreased with LDN treatment alone. DA was decreased only in the MPP⁺ treated and the MPP⁺ + LDN treated groups.

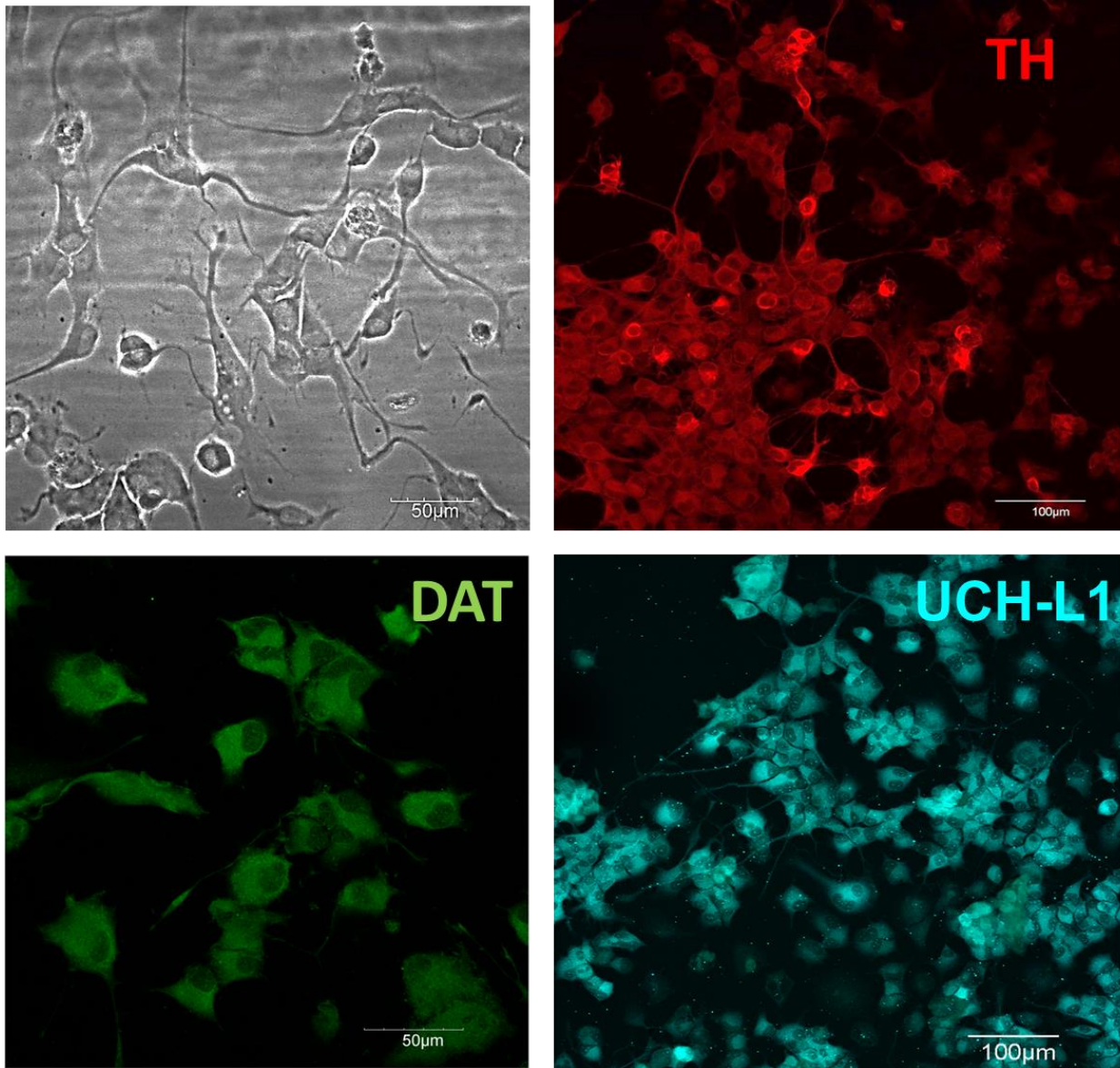


Figure 4.1. Images of differentiated MN9D cells: phase contrast (top left), TH (top right), DAT (bottom left) and UCH-L1 (bottom right). MN9D cells were grown and differentiated on glass coverslips coated with PDL and stained for TH, DAT, and UCH-L1. Images were captured via an Olympus FV1000 confocal microscope.

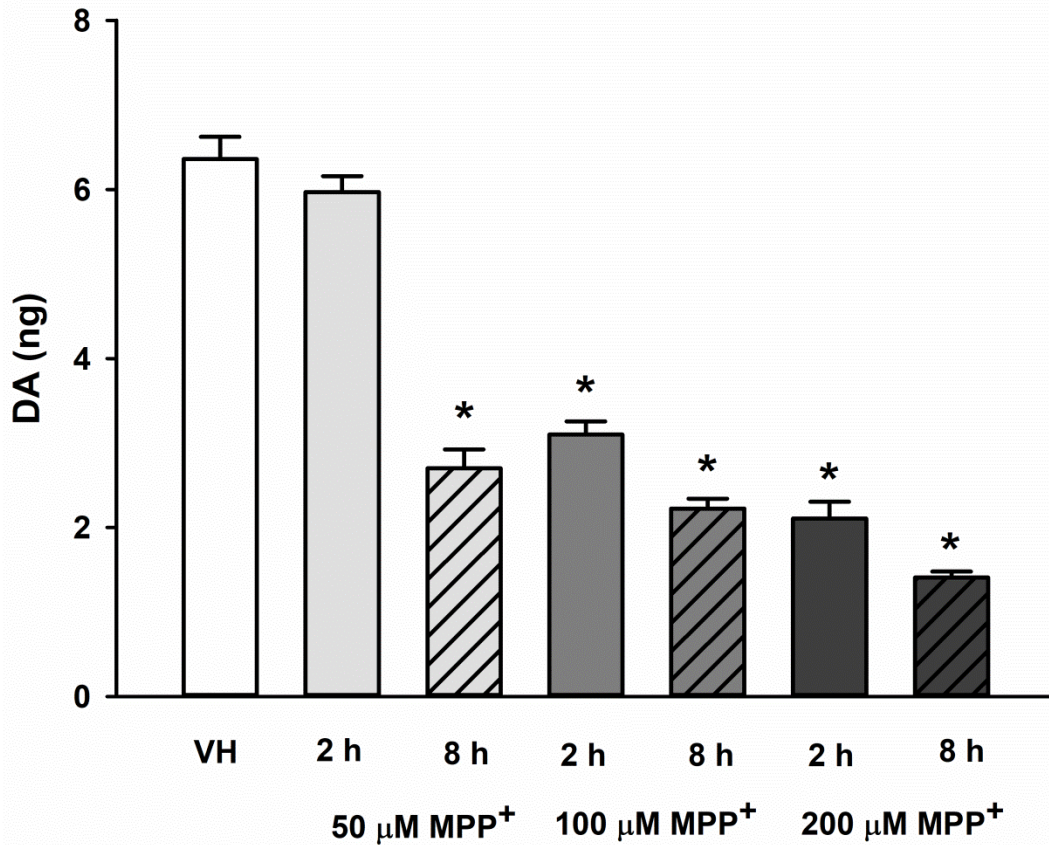


Figure 4.2. DA content in MN9D cells exposed to various concentrations of MPP⁺ at 2 and 8 h. Differentiated MN9D cells were grown on PDL-coated plates and exposed to varying concentrations of MPP⁺ for 2 or 8 h (n=6 each group). Data is plotted as mean + SEM and asterisk (*) indicates a significant difference from VH control where $p < 0.05$ via one-way ANOVA and post hoc Holm-Sidak test.

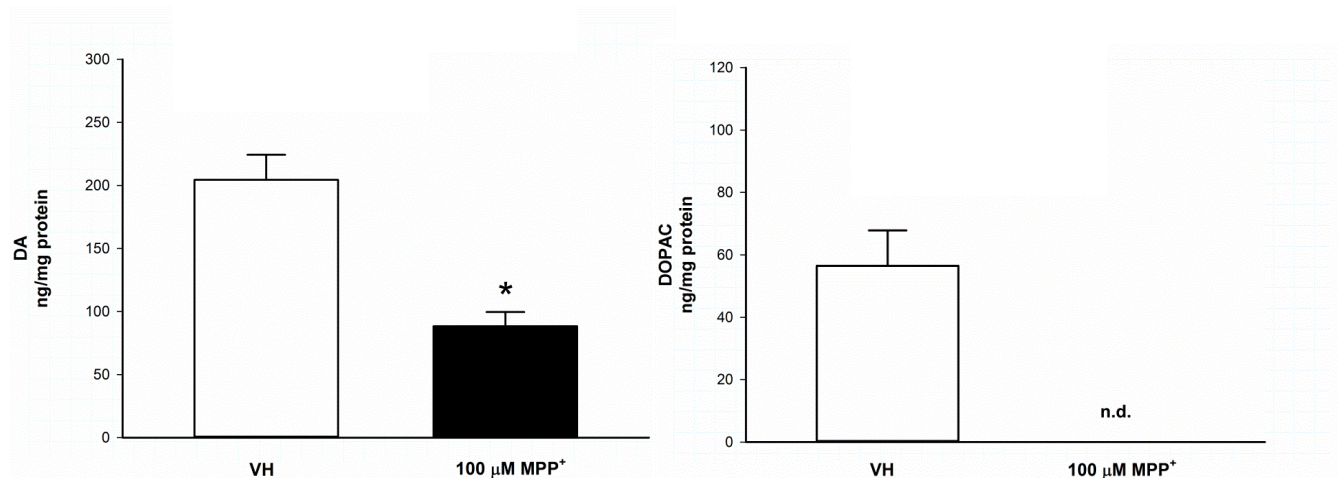


Figure 4.3. DA and DOPAC concentrations in MN9D cells exposed to 100 μM MPP⁺ for 2 h. Differentiated MN9D cells were treated with 100 μM MPP⁺ for 2 h and collected for HPLC-ED analysis of DA and DOPAC (n=6 each group). Data is plotted as mean + SEM and asterisk (*) indicates a statistically significant difference from VH where $p < 0.05$ via t-test. The term “n.d.” indicates that DOPAC content was not detectable.

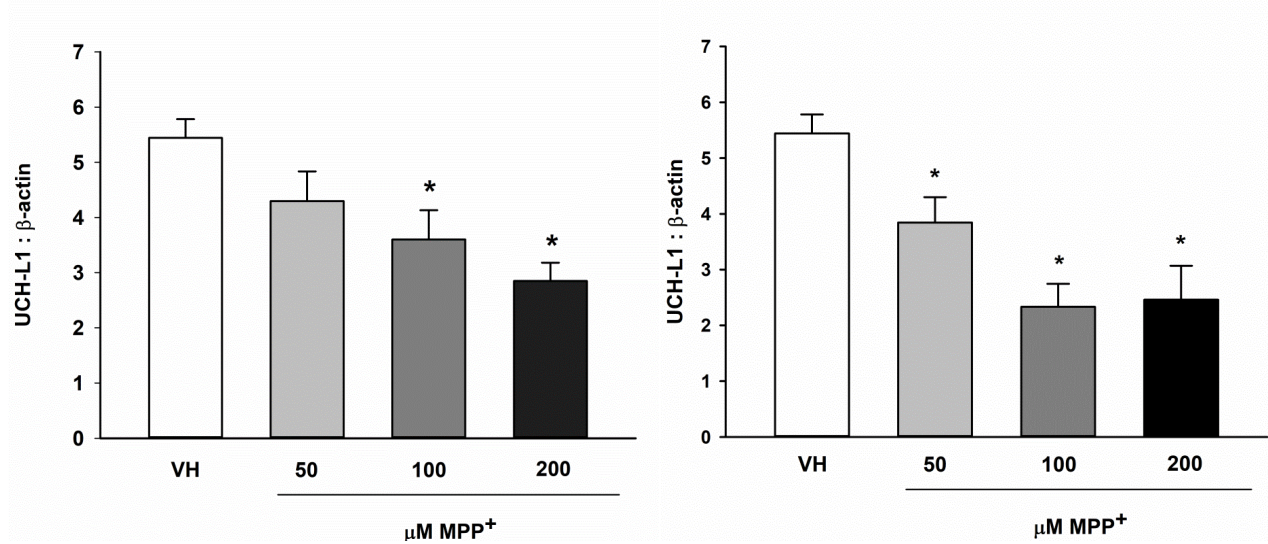


Figure 4.4. UCH-L1 expression in MN9D cells exposed to various concentrations of MPP⁺ at 2 h (left) and 8 h (right). Cells were differentiated and treated with varying concentrations of MPP⁺ for 2 h and 8 h (n=6 each group). UCH-L1 expression was measured via Western blot. Data is plotted as mean + SEM and asterisk (*) indicates a statistically significant difference from VH control where $p < 0.05$ via one-way ANOVA and post hoc Holm-Sidak test.

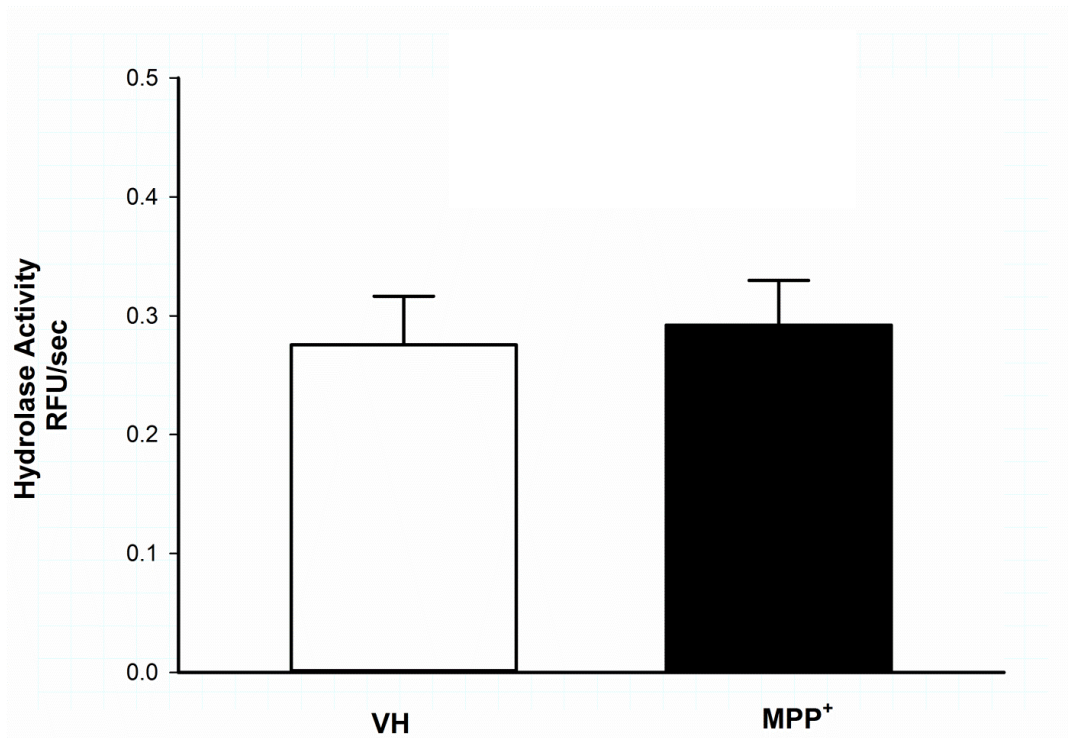


Figure 4.5. UCH-L1 hydrolase activity in MN9D cells 2 h after 100 μ M MPP⁺ exposure. Cells were differentiated and treated with 100 μ M MPP⁺ and hydrolase activity was measured (n=6). Data is plotted as mean + SEM and no statistically significant differences between groups was detected ($p > 0.05$) via t-test.

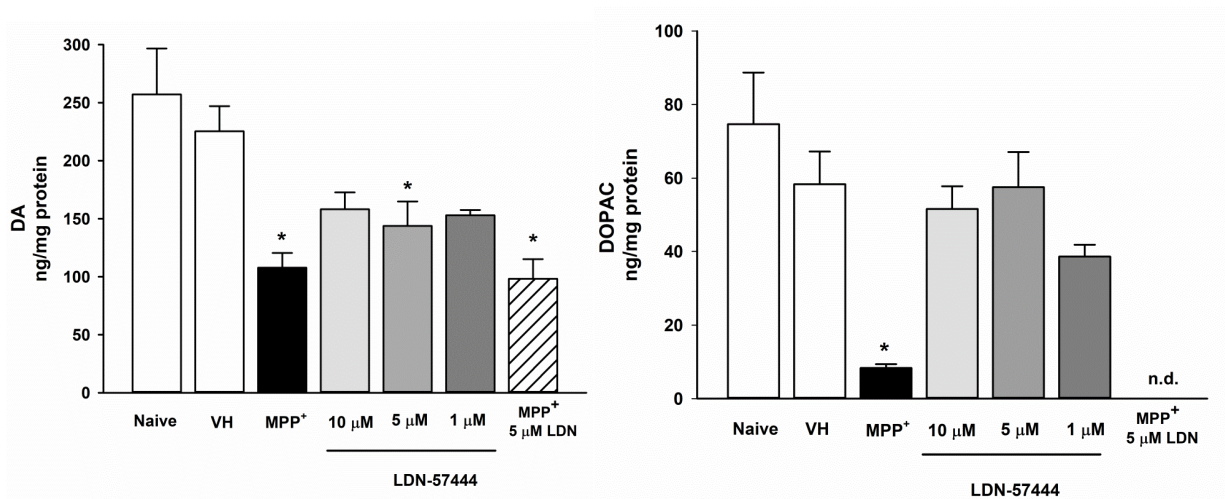


Figure 4.6. DA (left) and DOPAC (right) in MN9D cells treated with MPP⁺, LDN-57444, or a combination for 2 h. Differentiated cells were treated with 100 μM MPP⁺, various concentrations of the UCH-L1 inhibitor LDN-57444, or a combination of MPP⁺ and LDN (n=6 each group). DA and DOPAC were measured via HPLC-ED. Data is expressed as mean + SEM and asterisk (*) indicates a statistically significant difference between groups and VH control where p < 0.05 via one-way ANOVA and a post hoc Holm-Sidak test.

Therefore, DA release was likely not affected by LDN treatment in MN9D cells even though DA stores pools were depleted. The DOPAC/DA ratio was decreased with MPP⁺ treatment, but increased with LDN treatment (**Fig. 4.7**). LDN appears to have an effect on DA homeostasis in MN9D cells that is distinct from effects of MPP⁺. Whether this decrease in DA occurs specifically due to UCH-L1 inhibition is not known, since we did not measure UCH-L1 function after exposure to LDN. Another possibility is that LDN is having a non-specific effect on DA homeostasis, though the drug itself does not decrease cell viability.

Since UCH-L1 is a DUB and is hypothesized to function within the UPS, the proteasome inhibitor bortezomib (BZ) was used along with the autophagy inducer chloroquine (CQ) to examine effects of major direct perturbations of the UPS and ALP on MN9D cells as compared with inhibition of UCH-L1 hydrolase activity (**Fig. 4.8**). Although LDN treatment did not alter intracellular DA concentrations in this experiment, the UPS inhibitor BZ and the ALP inducer CQ caused a decrease in intracellular DA. None of these inhibitors produced any changes in TH (**Fig. 4.9**), suggesting that a decrease in availability of the key enzyme required for DA synthesis is not responsible for the decrease in DA stores in these cells. The cytotoxicity profile of these inhibitors in MN9D cells is not readily available in the literature, so we performed a cytotoxicity assay to determine if these concentrations of inhibitors are toxic to MN9D cells. In fact, no other groups have examined dynamics of the UPS or ALP in MN9D cells.

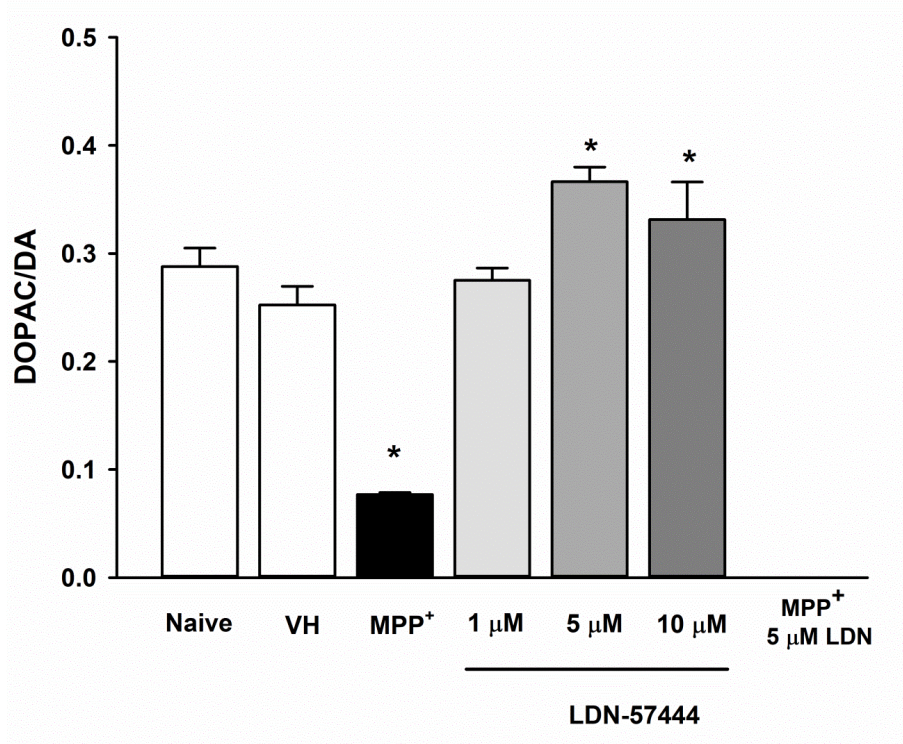


Figure 4.7. DOPAC/DA ratio in MN9D cells treated with MPP⁺, LDN-57444, or a combination for 2 h. Differentiated cells were treated with 100 μM MPP⁺, various concentrations of the UCH-L1 inhibitor LDN-57444, or a combination of MPP⁺ and LDN (n=6 each group). DA and DOPAC were measured via HPLC-ED and the ratio between the two was calculated. Data is expressed as mean + SEM and asterisk (*) indicates a statistically significant difference between groups and VH control where p < 0.05 via one-way ANOVA and a post hoc Holm-Sidak test.

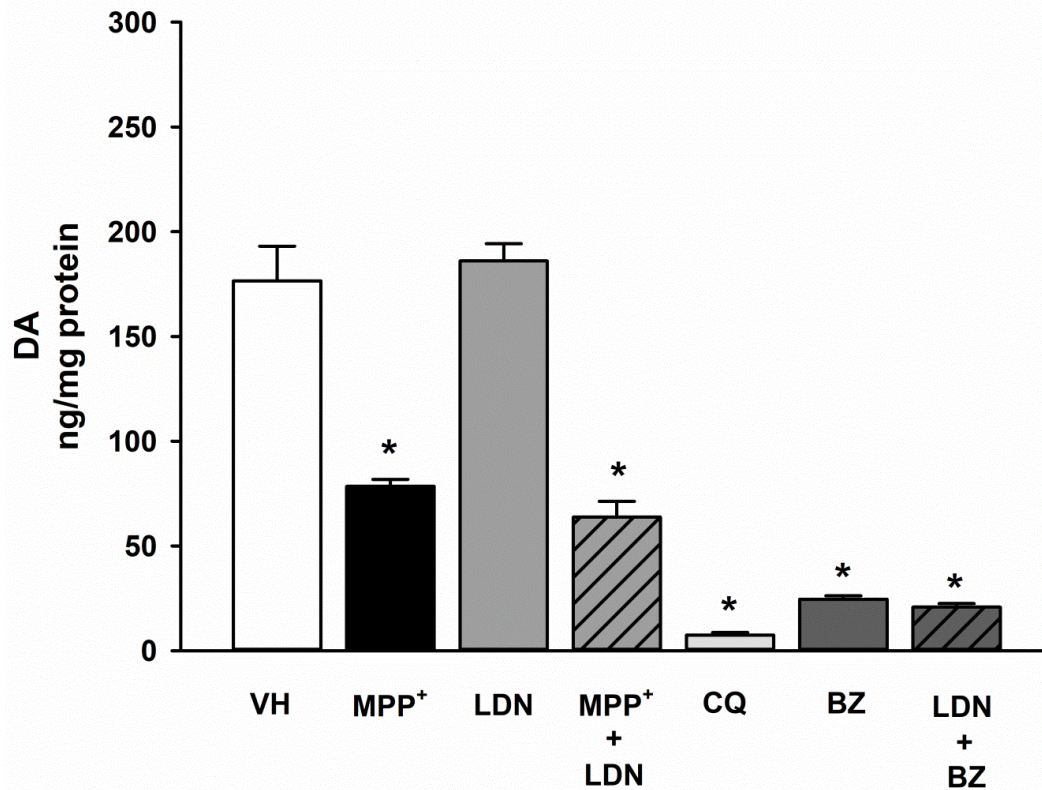


Figure 4.8. DA concentration in MN9D cells exposed to various inhibitors for 2 h. Differentiated cells were treated with 100 μM MPP⁺, 5 μM LDN, 10 μM CQ, 100 nM BZ, and a combination of LDN + BZ (n=6 each group). DA and DOPAC were measured via HPLC-ED and the ratio between the two was calculated. Data is expressed as mean + SEM and asterisk (*) indicates a statistically significant difference between groups and VH control where $p < 0.05$ via one-way ANOVA and a post hoc Holm-Sidak test.

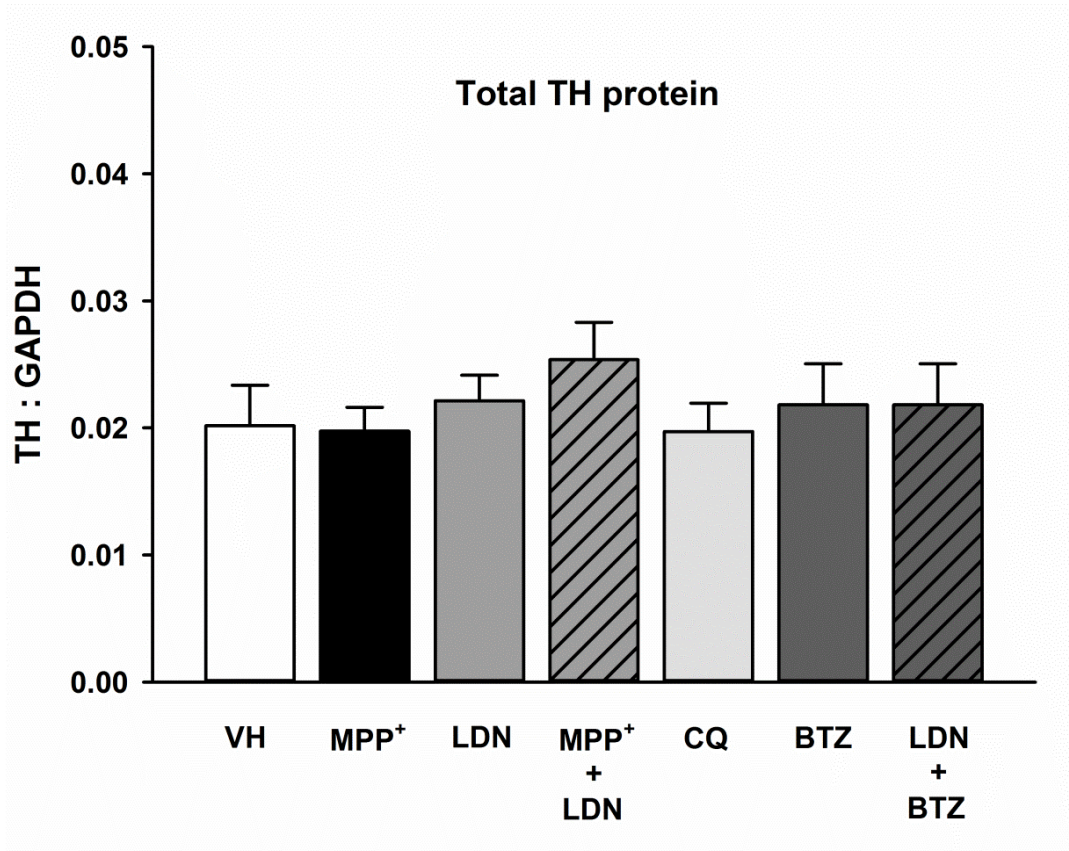


Figure 4.9. TH protein in MN9D cells exposed to various inhibitors for 2 h. Differentiated cells were treated with 100 μ M MPP⁺, 5 μ M LDN, 10 μ M CQ, 100 nM BZ, and a combination of LDN + BZ (n=6 each group). TH protein was measured via western blot. Data is expressed as mean + SEM and asterisk (*) indicates a statistically significant difference between groups and VH control where $p < 0.05$ via one-way ANOVA and a post hoc Holm-Sidak test.

In **Fig. 4.10**, we show that none of the inhibitors assayed previously caused cytotoxicity at these doses in differentiated MN9D cells. Since CQ is an autophagy inducer, we sought to measure target engagement of the drug by measuring the levels of microtubule-associated protein 1 light chain 3 B-II (LC3B-II), a protein that is required for autophagic degradation of substrates via the ALP. Indeed, CQ treatment caused an increase in expression of LC3B-II (**Fig. 4.11**), which is conjugated to phosphatidylethanolamine from LC3B-I and associates closely with the autophagosome membrane, making it a good indication of the number of autophagosomes (Barth et al., 2010).

These experiments show that MN9D cells replicate the results seen in mouse NSDA neurons with respect to loss of DA after neurotoxicant treatment and loss of UCH-L1 expression. In addition, we have examined the effects of UCH-L1 and UPS inhibitors and an autophagy inducer on DA concentration and phenotype without causing cytotoxic effects.

Effects of MPTP UCH-L3 and USP14 in NSDA neurons in vivo

Although UCH-L1 is the most highly expressed DUB in the nervous system (Lowe et al., 1990) other DUBs have similar functions with respect to recycling of mono-Ub within the UPS (**Fig. 4.12**). UCH-L3 has a structure very similar to UCH-L1 and is >50% homologous (Kurihara et al., 2001). USP14, on the other hand, is associated with the 26S proteasome and belongs to a different family than the DUB enzymes. Loss of USP14 function has also been linked to neurodegenerative phenotype (the ataxia mouse) (Walters et al., 2008). The function of these other DUBs includes maintaining

the pool of free mono-Ub, so we sought to determine if these other DUBs are altered after MPTP exposure in mice. In **Figs. 4.13** and **4.14**, both UCH-L3 and USP-14 (respectively) are expressed in TH SN NSDA neurons. After MPTP treatment protein levels of UCH-L3 (**Fig. 4.15**) and USP14 (**Fig. 4.16**) were not altered in the SN, suggesting that the decrease in mono-Ub observed after MPTP is likely related to the decrease in UCH-L1 rather than UCH-L3 or USP14. These results confirm that UCH-L1 is the correct DUB to examine in the context of neurotoxicant-induced damage to NSDA neurons.

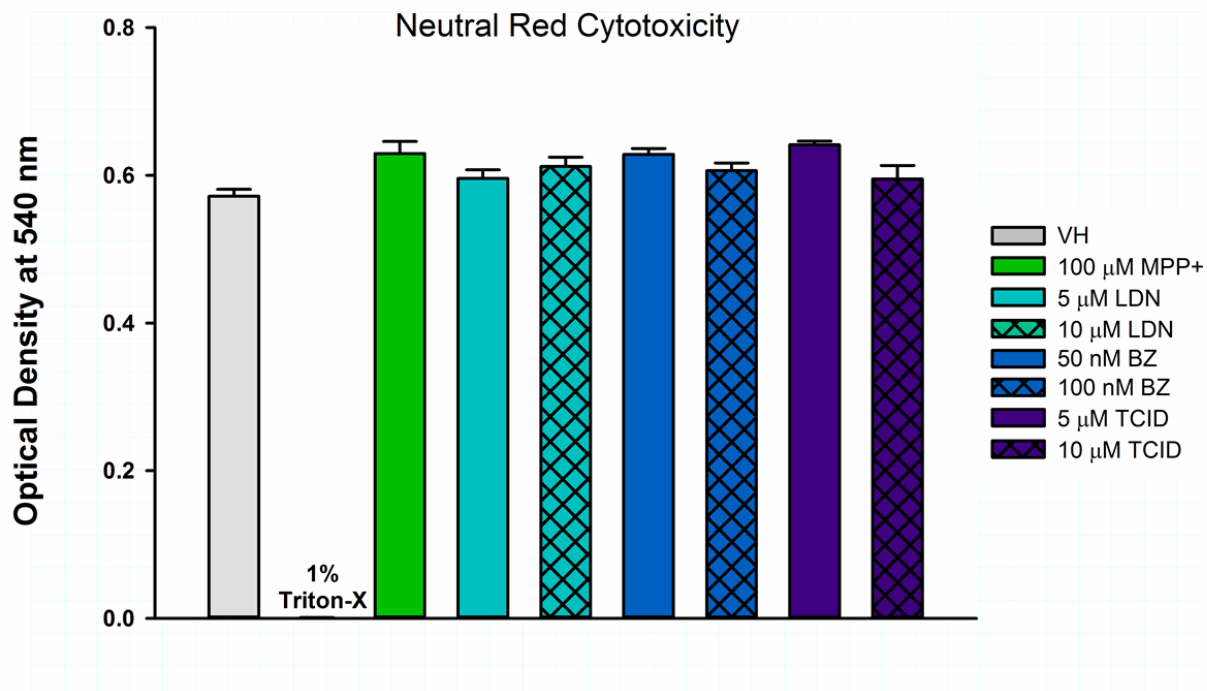


Figure 4.10. Cytotoxicity profile of MN9D cells exposed to various inhibitors for 2 h.

Differentiated cells were treated with 100 μM MPP⁺, 5 and 10 μM LDN, 50 and 100 nM BZ, and 5 and 10 μM TCID (a UCH-L3 inhibitor) (n=6). A neutral red assay was performed to determine if the concentrations of compounds caused significant cytotoxicity, where 1% triton-x100 was used as a positive control. Data is plotted as mean + SEM. No significant difference between compounds and VH control were detected ($p > 0.05$) via one-way ANOVA.

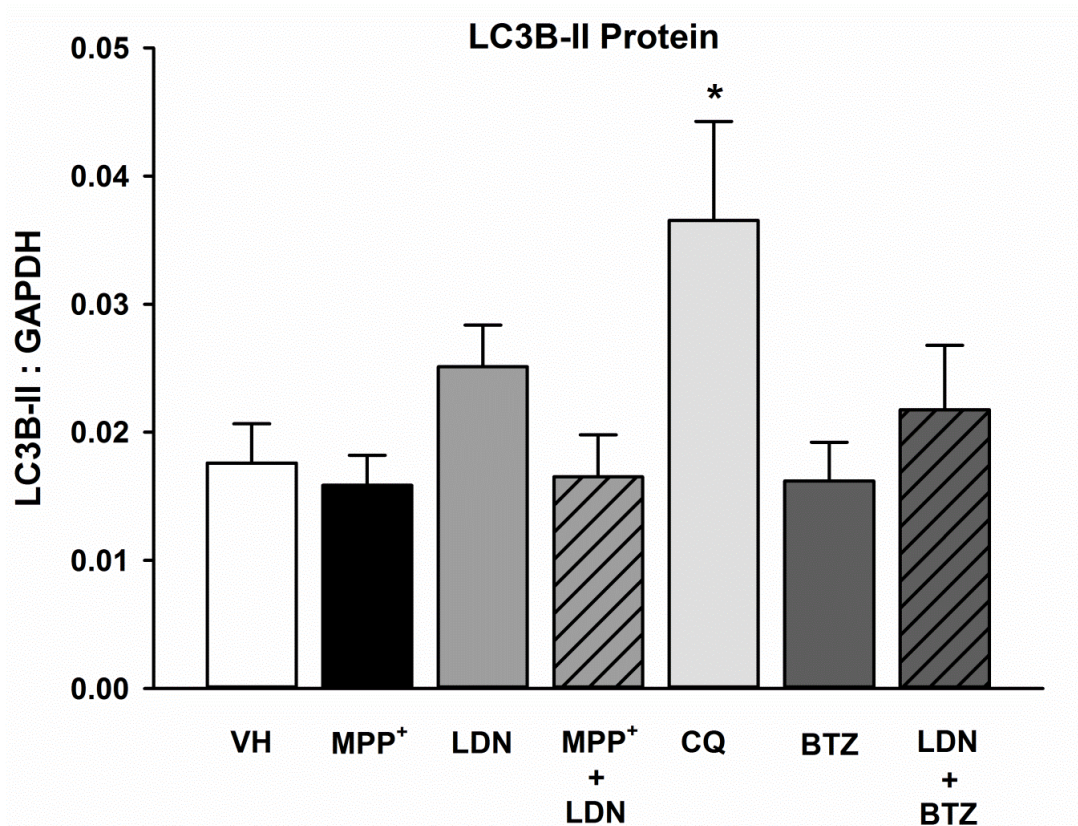


Figure 4.11. LC3B-II protein in MN9D cells exposed to various inhibitors for 2 h. Differentiated cells were treated with 100 μ M MPP⁺, 5 μ M LDN, MPP⁺ + LDN, 10 μ M CQ, 100 nM BZ, and LDN + BZ (n=6 each group). LC3B-II protein was measured via western blot. Data is plotted as mean + SEM and asterisk (*) indicates a statistically significant difference where $p < 0.05$ via one-way ANOVA and a post hoc Holm-Sidak test.

Effects of MPTP on UCH-L1 expression in NSDA axon terminals

Thus far, expression of UCH-L1 has been measured in tissue microdissections from the ST and SN of mice. However, a caveat of measuring protein expression from microdissected ST tissue is that other cell types are present in the sample, so it may be erroneous to infer specific changes occurring in NSDA axon terminals. One method to isolate axon terminals is to produce synaptosomes (Dunkley et al., 2008), which are pinched off axon terminals made by homogenizing tissue and using sucrose to allow the membrane to fold, making a spherical shape and preserving terminal constituents within. UCH-L1 and mono-Ub expression were measured in ST synaptosomes at various times after in vivo MPTP injection (**Fig. 4.17**). UCH-L1 protein in ST synaptosomes is decreased after 6 h and appears to recover by 24 h post MPTP treatment. Similarly, mono-Ub protein levels closely follows that of UCH-L1 and the

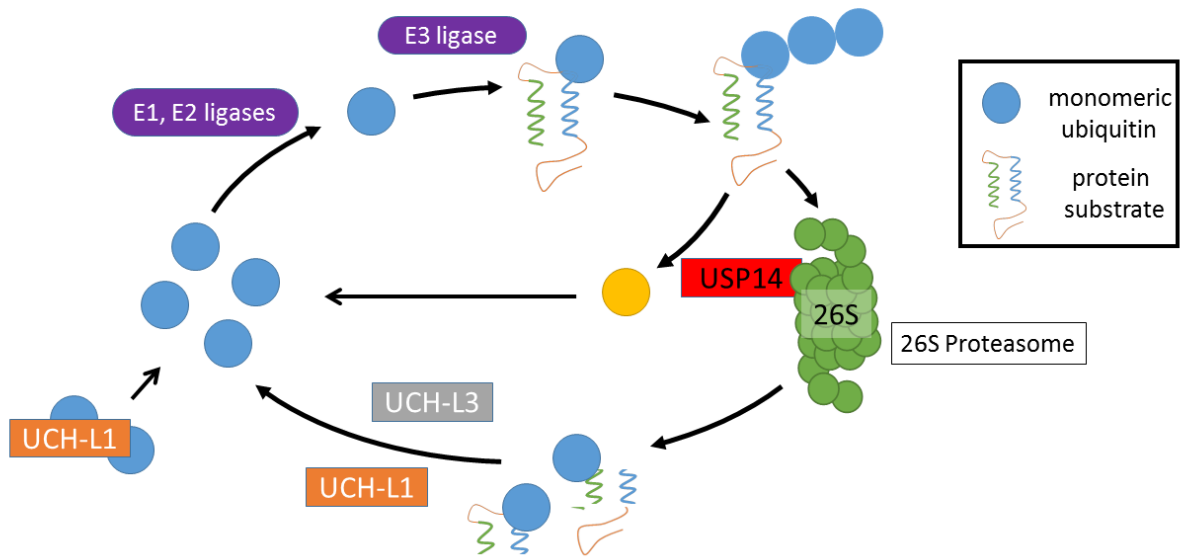


Figure 4.12. Diagram showing three relevant DUBs in the context of mono-Ub recycling: UCH-L1, UCH-L3, and USP14. UCH-L1 and UCH-L3 have very similar functions, but UCH-L3 has not been demonstrated to bind and sequester mono-Ub, which is the main difference between the proposed function of the two closely-related DUBs. USP14, on the other hand, is closely associated with the 26S proteasome and can remove Ub from substrates destined for proteasomal degradation.

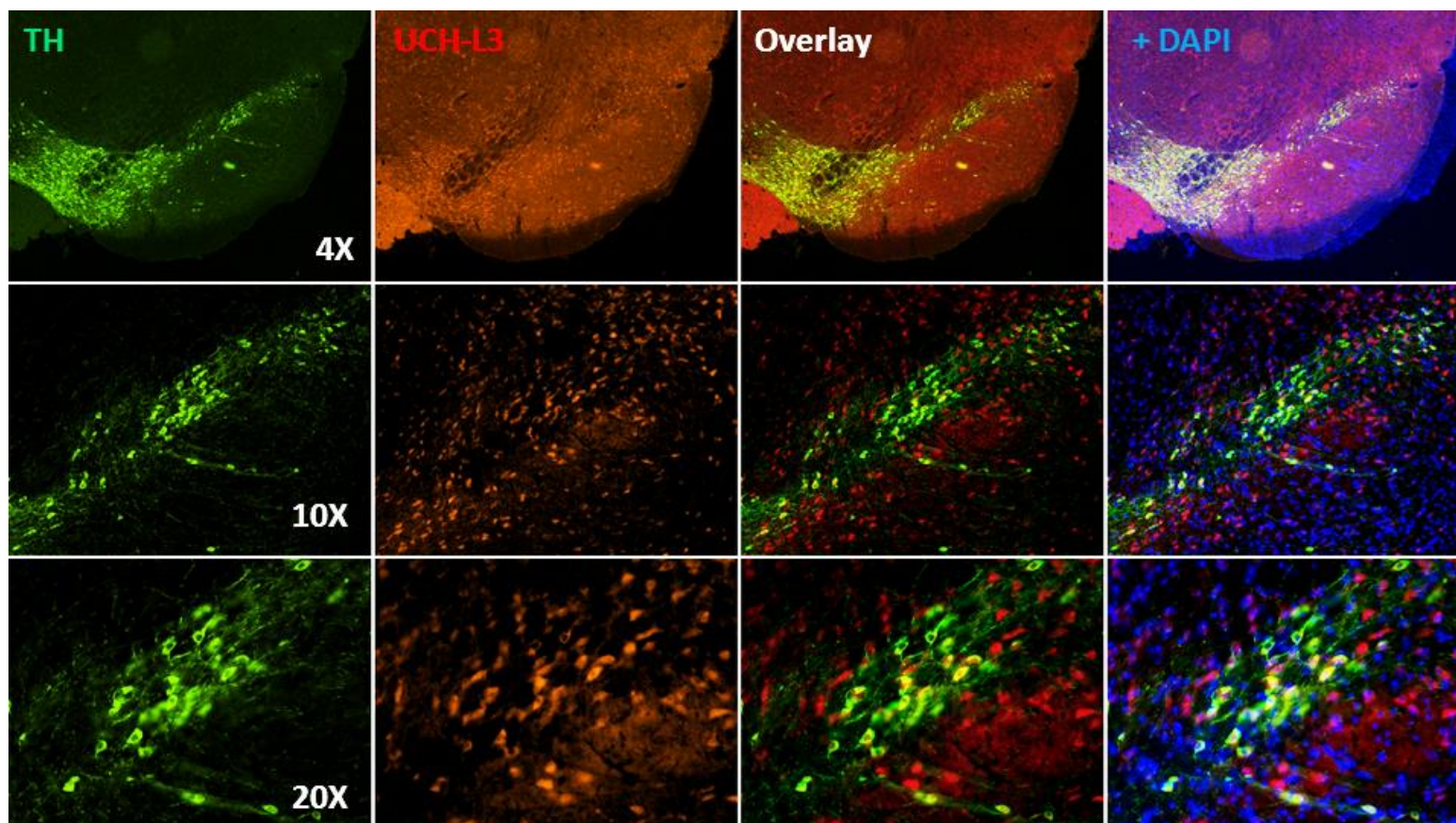


Figure 4.13. UCH-L3 staining in TH neurons in the SN of mice. 20 μm thick mouse brain sections were stained for TH and UCH-L3 and images were captured via epifluorescence microscopy. Overlays for TH + UCH-L3 and a triple overlay including the nuclear stain DAPI were generated.

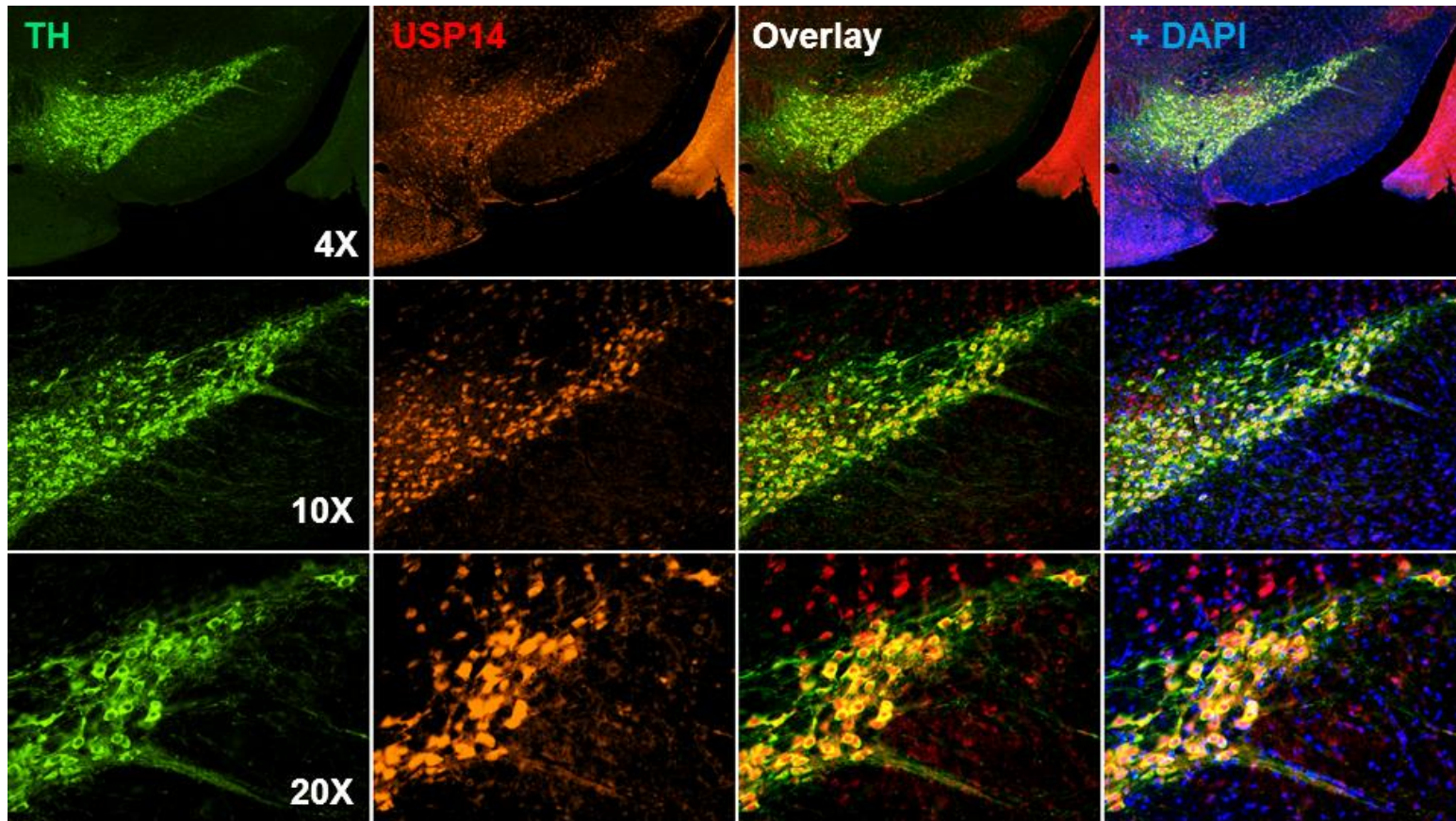


Figure 4.14. USP14 staining in TH neurons in the SN of mice. 20 μ m thick mouse brain sections were stained for TH and USP14 and images were captured via epifluorescence microscopy. Overlays for TH + USP14 and a triple overlay including the nuclear stain DAPI were generated.

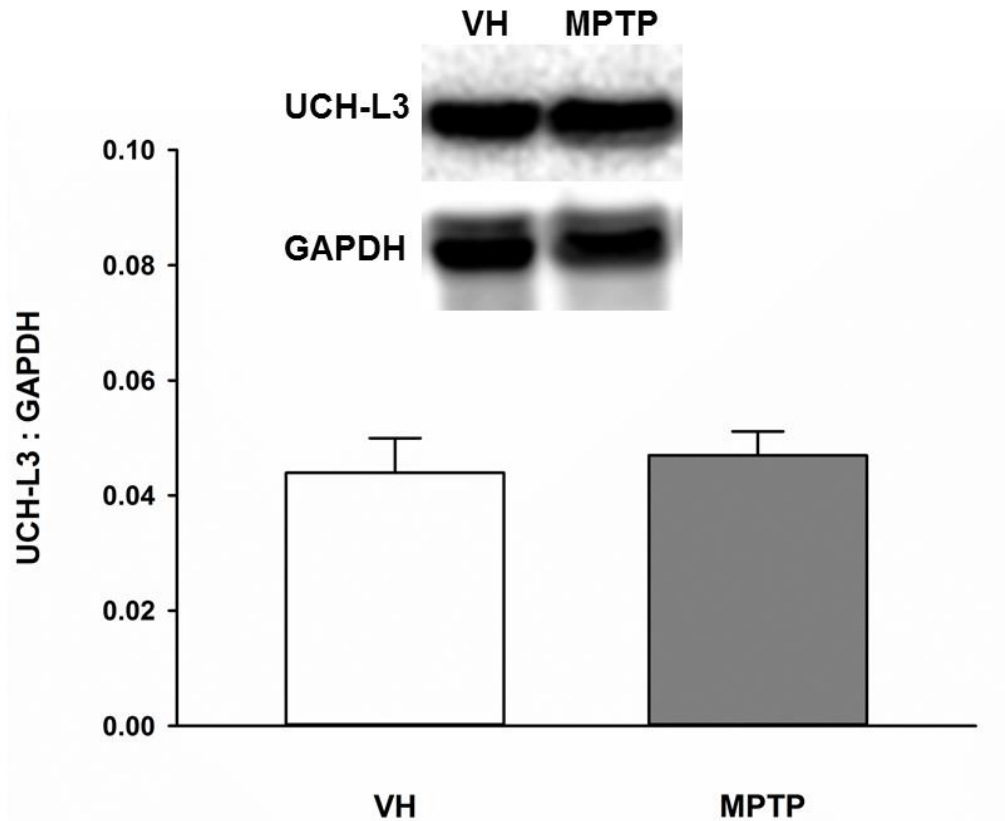


Figure 4.15. UCH-L3 levels in the mouse SN 24 h after MPTP exposure. Mice were treated with VH or acute MPTP and sacrificed 24 h later (n=10 each group). Brains were removed and analyzed via western blot for UCH-L3 expression in the SN. No statistically significant difference between groups was detected ($p > 0.05$) via t-test.

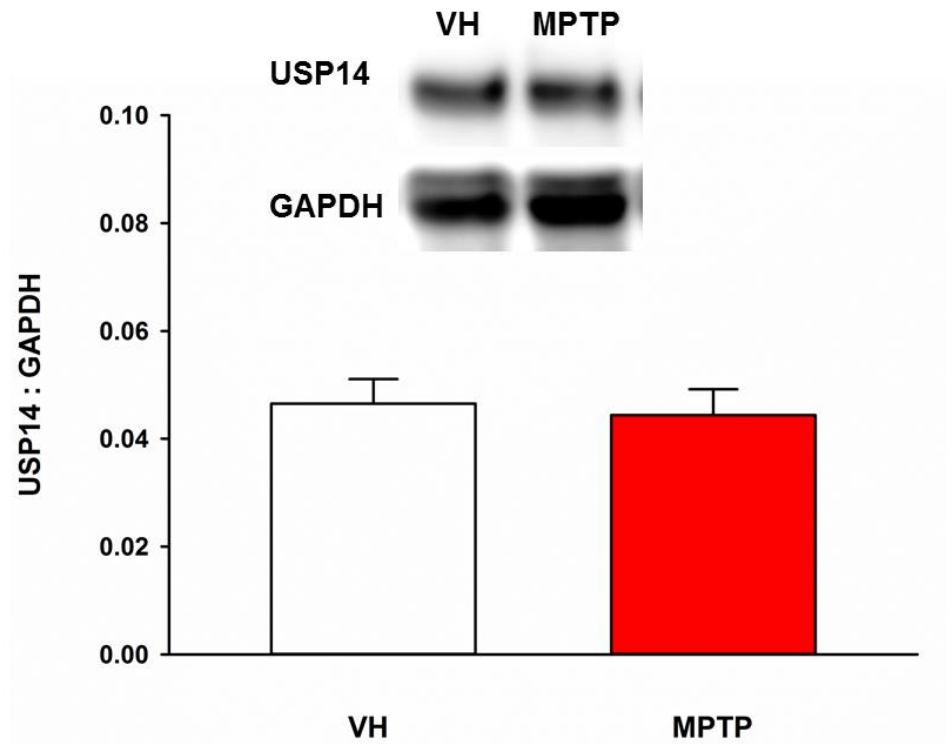


Figure 4.16. USP14 levels in the mouse SN 24 h after MPTP exposure. Mice were treated with VH or acute MPTP and sacrificed 24 h later (n=10 each group). Brains were removed and analyzed via western blot for USP14 expression in the SN. No statistically significant difference between groups was detected ($p > 0.05$) via t-test.

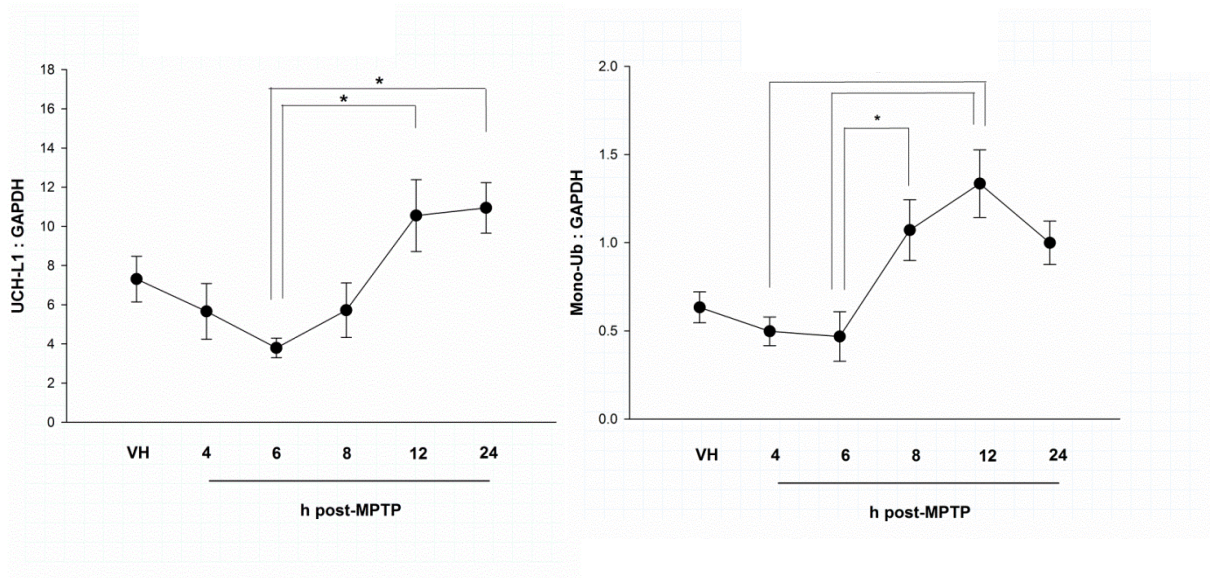


Figure 4.17. UCH-L1 (left) and mono-Ub (right) protein levels in ST synaptosomes various time points after acute MPTP exposure. Mice were killed 4, 6, 8, 12, or 24 h after a single injection of MPTP (n=10 each group). Levels of UCH-L1 and mono-Ub were measured via western blot. Data is plotted as mean \pm SEM and asterisk (*) indicates a statistically significant difference between points connected by lines where $p < 0.05$ via one-way ANOVA and a post hoc Holm-Sidak test.

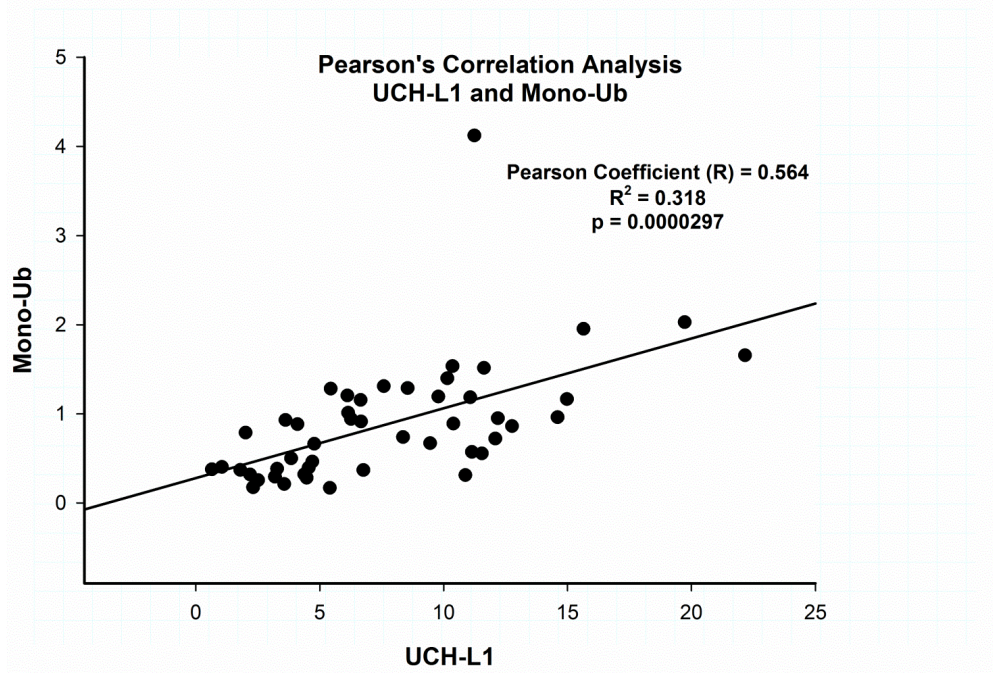


Figure 4.18. Pearson correlation analysis of UCH-L1 and mono-Ub levels after acute MPTP exposure. Protein expression levels of UCH-L1 and mono-Ub determined by western blotting were plotted on the x and y axis and a correlation analysis was performed.

expression profiles of UCH-L1 and mono-Ub after acute MPTP are well correlated (**Fig. 4.18**).

Relationship between UCH-L1 and parkin

Since both UCH-L1 and parkin operate in the context of the UPS, it is conceivable that these enzymes interact and potentially oppose each other's actions since de-ubiquitination and ubiquitination are reverse processes. Indeed, it was demonstrated that parkin can add poly-Ub to UCH-L1 via a K63-linked chain to target UCH-L1 degradation via autophagy (McKeon et al., 2014), suggesting that parkin may regulate UCH-L1 expression and activity to promote 26S proteasome function. This proposed mechanism to decrease UCH-L1 in cases where the neuron requires increased protein degradation via the 26S proteasome could be an attempt at compensation under conditions of oxidative stress, as UCH-L1 has been shown to decrease in the SN of mice treated with MPTP (Benskey et al., 2012) (**Fig. 3.11**). On the other hand, in parkin-deficient (*Parkin*^{-/-}) mice, UCH-L1 is not decreased in the SN (**Fig. 4.19**), pointing to the fact that the decrease in UCH-L1 protein in the SN of WT mice may be parkin dependent. In addition, **Fig. 4.20** shows that under basal conditions, UCH-L1 is elevated in the SN of *Parkin*^{-/-} mice. However, elevated levels of UCH-L1 in the SN did not correspond to elevated levels of mono-Ub in *Parkin*^{-/-} mice (**Fig. 4.21**). These data suggest that parkin may cause the decrease in UCH-L1 expression in conditions of oxidative stress to promote 26S function, but that the levels of mono-Ub are not affected in mice lacking parkin.

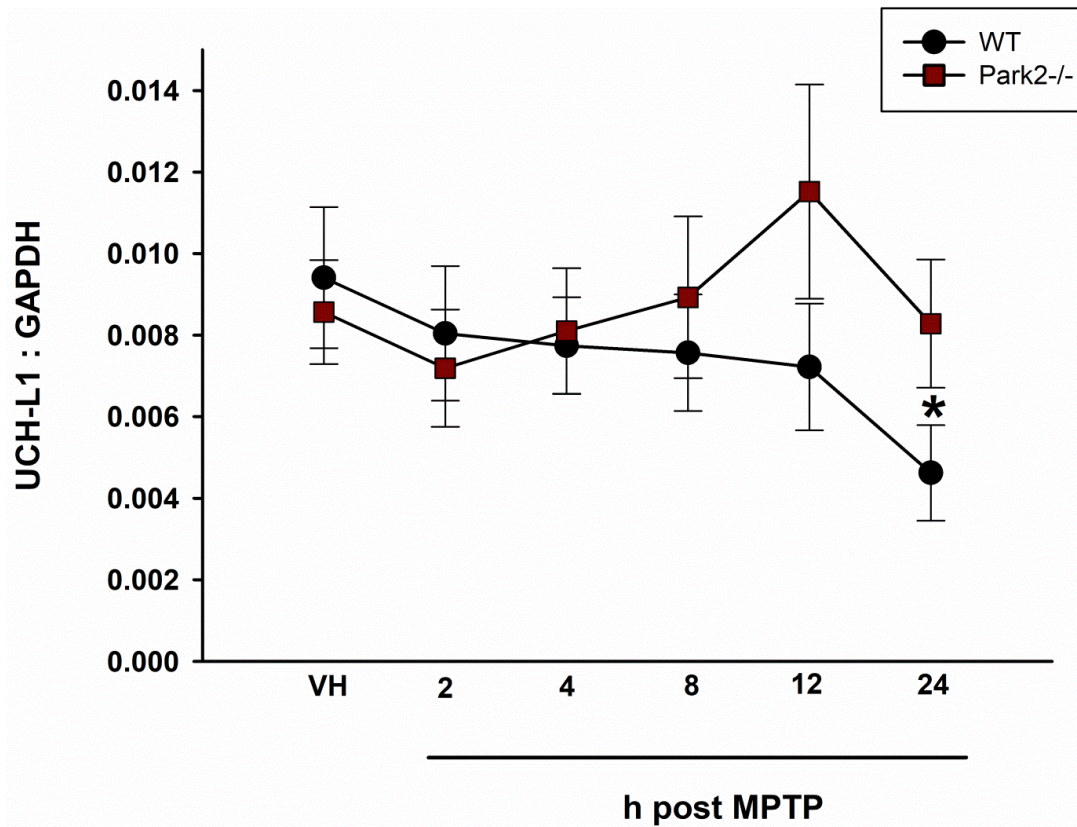


Figure 4.19. UCH-L1 protein expression in the SN of WT (black) and Park2^{-/-} (red) mice various points after single injection of MPTP. WT and Park2^{-/-} mice were injected with MPTP and sacrificed at various time points (n=10 each group). Brains were sectioned and the SN was analyzed for UCH-L1 expression via western blotting. Data is plotted as mean \pm SEM and asterisk (*) indicates a difference from VH control where $p < 0.05$ via one-way ANOVA and a post hoc Holm-Sidak test.

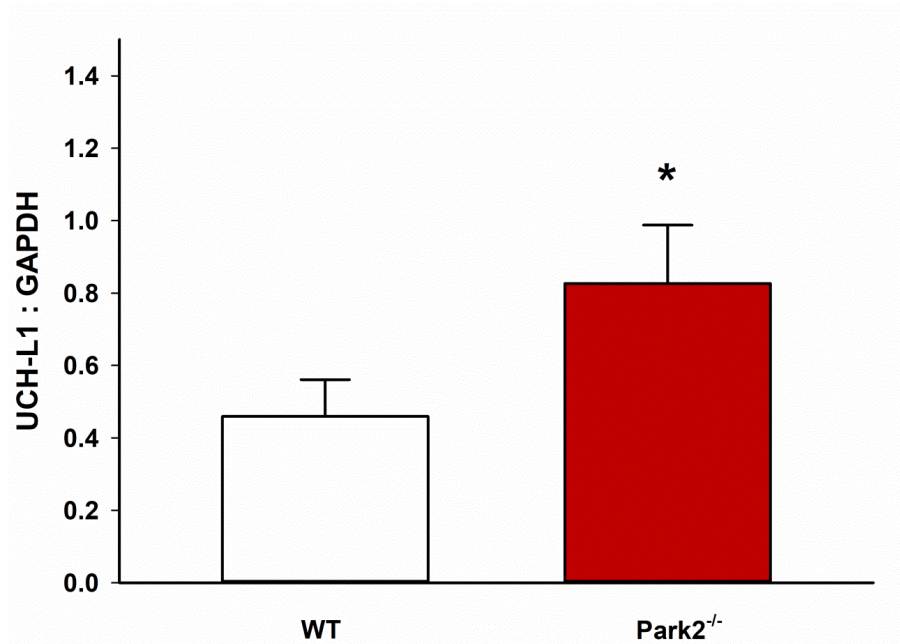


Figure 4.20. UCH-L1 protein expression in the SN of WT (white) and Park2^{-/-} (red) mice. WT and Park2^{-/-} mice were sacrificed and brains were sectioned (n=10 each group). The SN was analyzed for UCH-L1 expression via western blotting. Data is plotted as mean + SEM and asterisk (*) indicates a difference from WT SN where p < 0.05 via t-test.

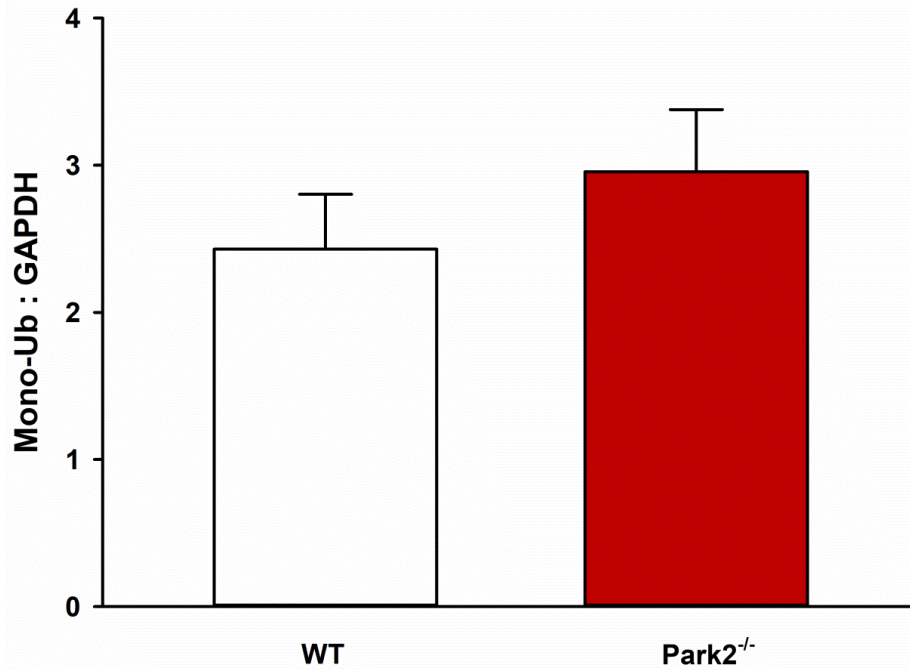


Figure 4.21. Mono-Ub protein expression in the SN of WT (white) and Park2^{-/-} (red) mice. WT and Park2^{-/-} mice were sacrificed and brains were sectioned (n=10 each group). The SN was analyzed for mono-Ub expression via western blotting. Data is plotted as mean + SEM and no statistically significant differences were detected between genotypes ($p > 0.05$) via t-test.

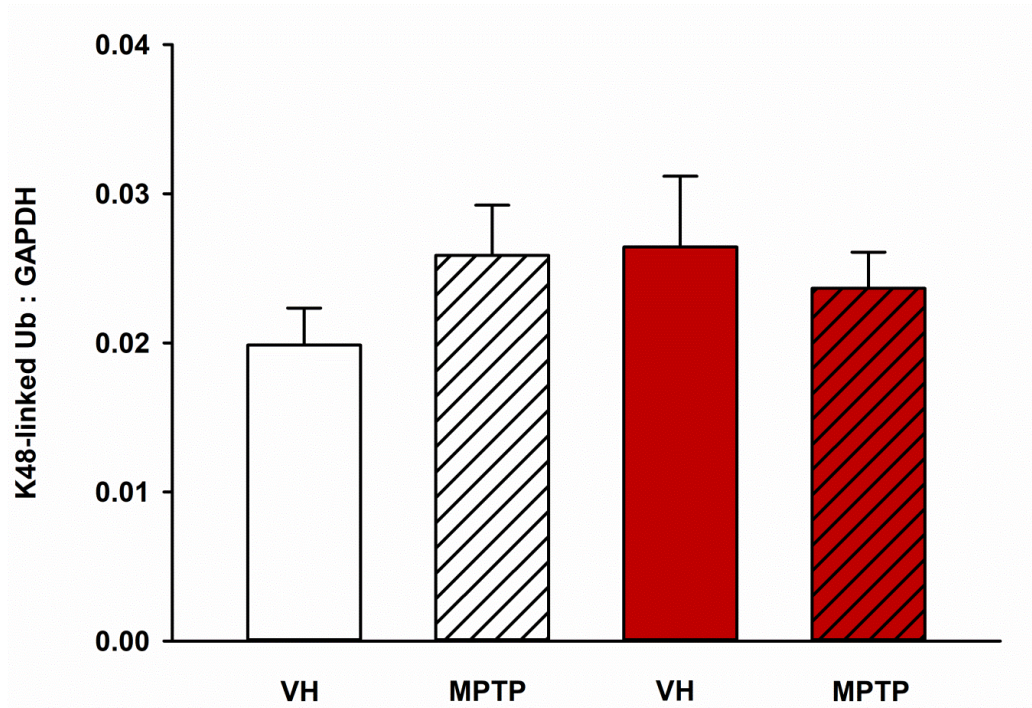


Figure 4.22. K48-linked ubiquitinated proteins in the SN of WT (white) and Park2^{-/-} (red) mice exposed to MPTP. WT and Park2^{-/-} mice were injected with MPTP and sacrificed 24 h later (n=10 each group). Brains were sectioned and the SN was analyzed for K48-linked Ub-proteins via western blotting. Data is plotted as mean + SEM and no statistically significant differences were detected between genotypes ($p > 0.05$) via two-way ANOVA.

In the case of a toxic insult to the SN, with exposure to a neurotoxicant such as MPTP (Langston et al., 1983) substrates and toxic proteins may overwhelm the UPS, especially in the absence of functional parkin. In WT and Park2^{-/-} mice exposed to MPTP, levels of K48-linked proteins were not elevated (**Fig. 4.22**), suggesting that there is likely no critical accumulation of Ub-substrates. However, minor perturbations in UPS function are not likely to be measurable using this method, so perhaps 26S function is still compromised in Park2^{-/-} mice. We next investigated whether the ALP could be upregulated in Park2^{-/-} mice by measuring LC3B-II in the ST at various times after MPTP treatment (**Fig. 4.23**). Park2^{-/-} mice have more LC3B-II in ST synaptosomes compared to WT under basal conditions, indicating the presence of more autophagosomes. By 2 h after MPTP exposure LC3B-II expression was decreased to that seen in WT mice, and this effect persisted for at least 24 h. However, increased expression of LC3B-II could mean two very different things: either that the ALP is induced, thereby creating more autophagosomes, or that the ALP is inhibited, and that the autophagosomes do not break down properly and accumulate.

To distinguish between these possibilities, an important substrate of the ALP, sequestome 1 (also known as p62), was measured to determine if inhibition of the ALP occurs in the SN of Park2^{-/-} mice since p62 accumulates when the ALP is inhibited (Barth et al., 2010) (**Fig. 4.24**). Since p62 protein was not accumulated, we interpret this result to mean that the ALP is not inhibited in Park2^{-/-} mice and is likely upregulated. We took this analysis further and looked over time after MPTP to ensure that the ALP was not inhibited in ST synaptosomes (**Fig. 4.25**) and found that p62 expression in WT and Park2^{-/-} was constant over the time course measured. Finally, to give us an idea of

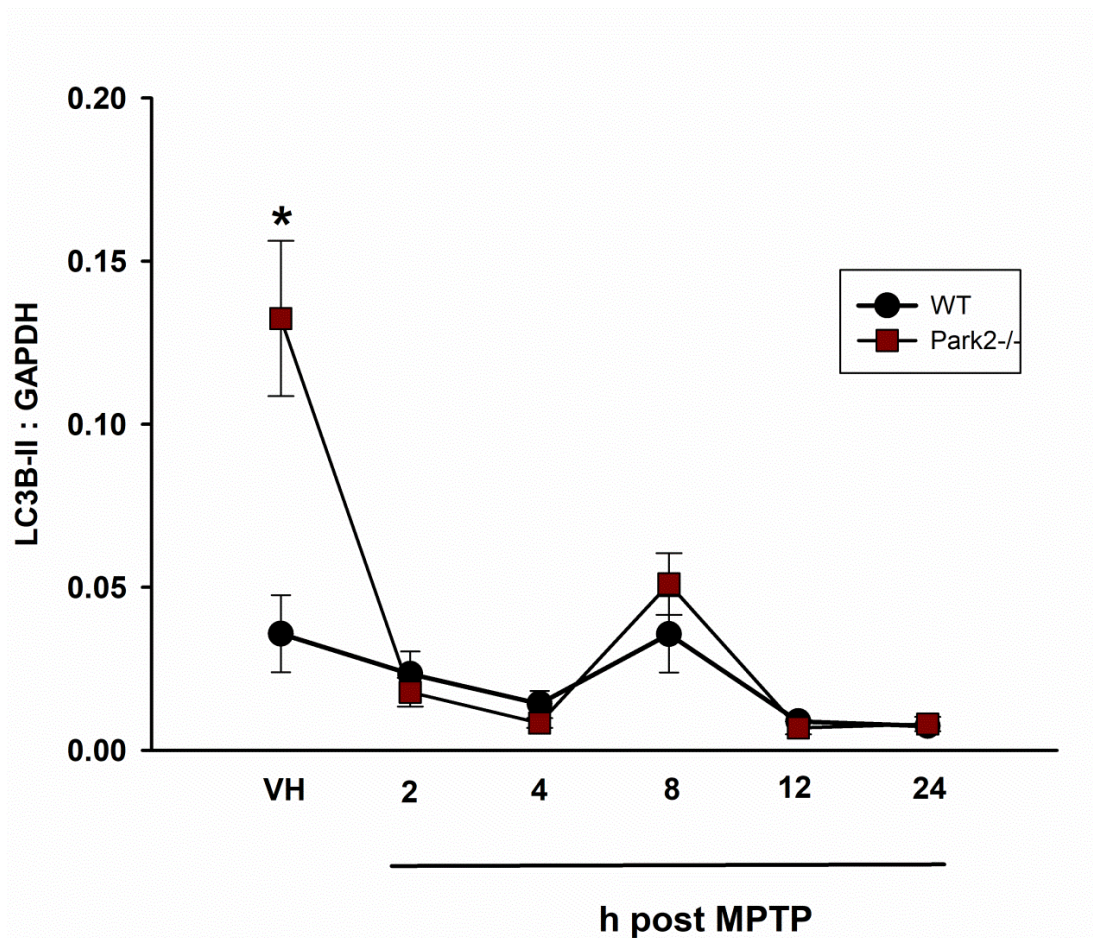


Figure 4.23. LC3B-II protein levels in ST synaptosomes between WT (black) and Park2^{-/-} (red) mice at various time points after MPTP injection. Mice were injected with MPTP and killed at various time points after MPTP (n=10 each group). Brains were removed and ST synaptosomes collected and analyzed for LC3B-II expression via western blotting. Data is plotted as mean \pm SEM and asterisk (*) indicates statistically significant difference from WT VH where $p < 0.05$ via one-way ANOVA and a post hoc Holm-Sidak test.

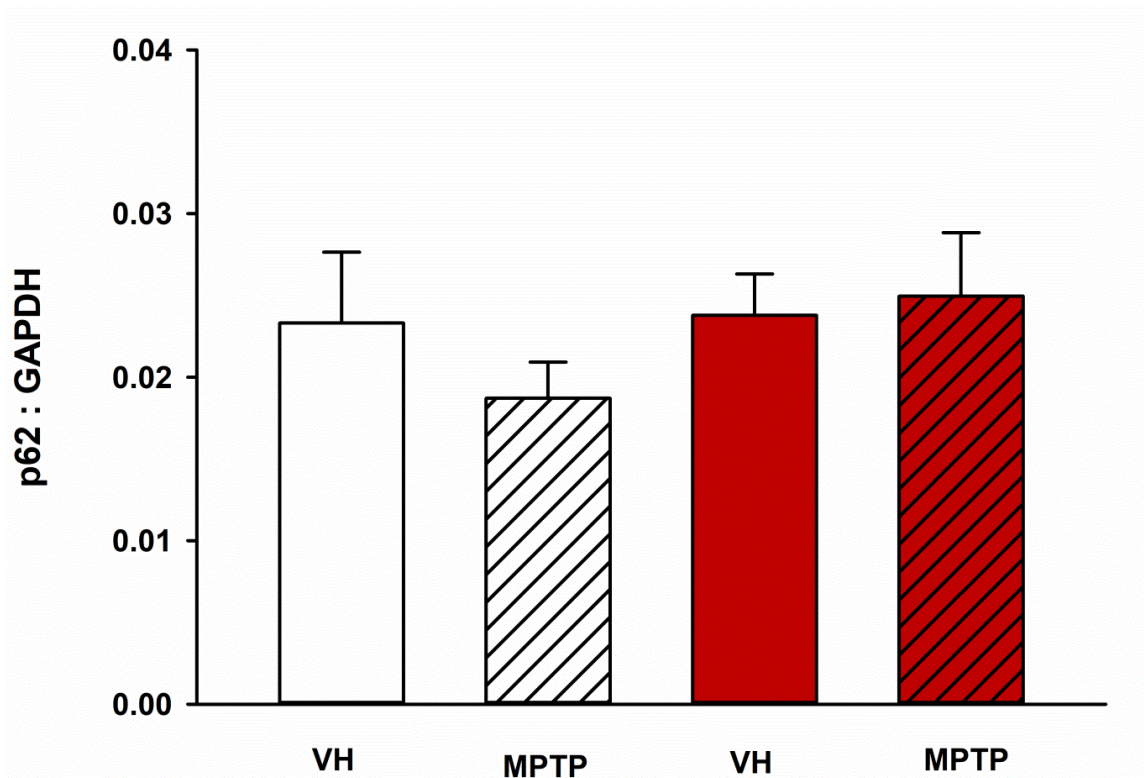


Figure 4.24. p62 protein levels in the SN between WT (black) and Park2^{-/-} (red) mice 24 h after MPTP injection. Mice were injected with MPTP and killed at 24 h after MPTP (n=10 each group). Brains were removed and SN collected and analyzed for p62 expression via western blotting. Data is plotted as mean + SEM and no statistically significant differences were detected between genotypes and drug treatment ($p > 0.05$) via two-way ANOVA.

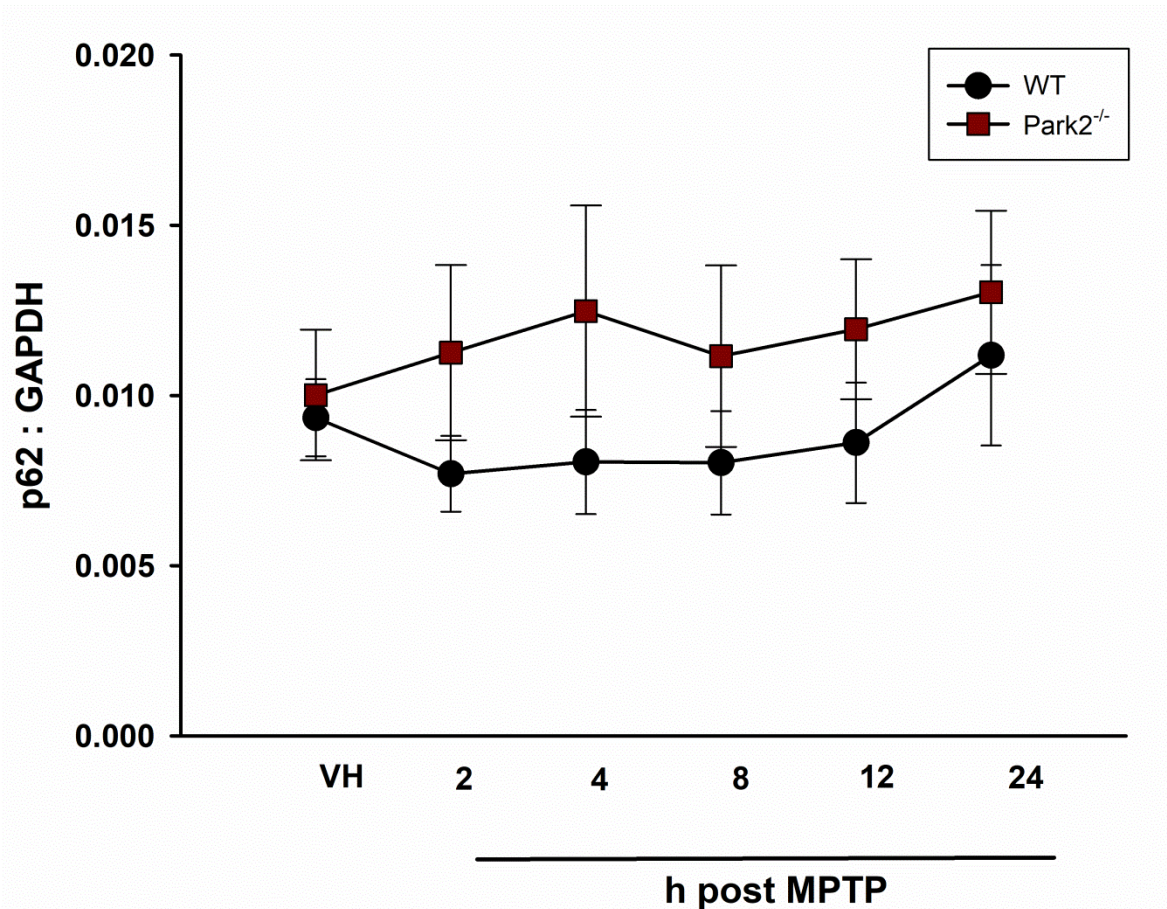


Figure 4.25. p62 protein levels in ST synaptosomes between WT (black) and Park2^{-/-} (red) mice at various time points after MPTP injection. Mice were injected with MPTP and killed at various time points after MPTP (n=10 each group). Brains were removed and ST synaptosomes collected and analyzed for p62 expression via western blotting. Data is plotted as mean \pm SEM and no significant differences between groups were detected ($p > 0.05$) via one-way ANOVA.

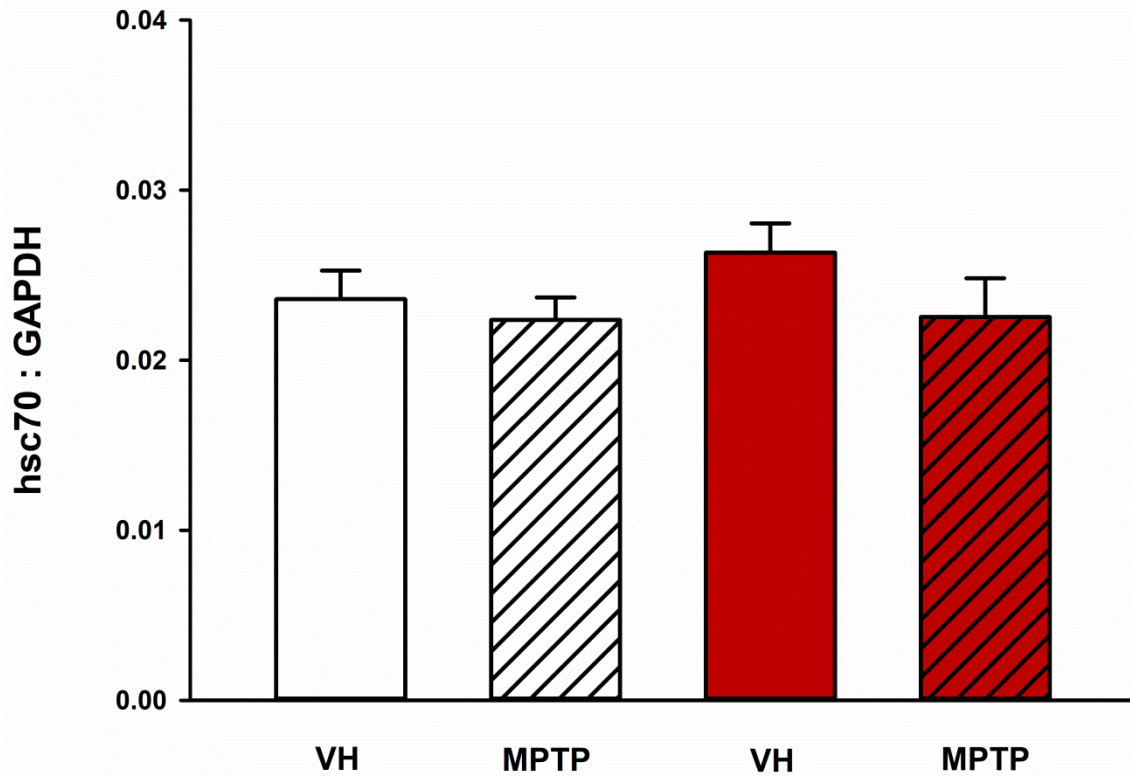


Figure 4.26. hsc70 protein levels in the SN between WT (black) and Park2^{-/-} (red) mice 24 h after MPTP injection. Mice were injected with MPTP and killed at 24 h after MPTP (n=10 each group). Brains were removed and SN collected and analyzed for hsc70 expression via western blotting. Data is plotted as mean + SEM and no statistically significant differences were detected between genotypes and drug treatment ($p > 0.05$) via two-way ANOVA.

which arm of the ALP (CMA or macroautophagy) could be upregulated, we measured hsc70, which is a vital chaperone used in CMA (Cuervo and Wong, 2014) (**Fig. 4.26**). No differences in hsc70 expression between genotypes or neurotoxicant treatment were found, suggesting that CMA is not the type of autophagy upregulated in *Park2*^{-/-} mice. Rather, it appears that macroautophagy is induced in *Park2*^{-/-} mice, which could be a key factor to why these mice do not have any overt neurodegenerative phenotype.

Discussion

MN9D cells were used to model NSDA neurons *in vitro*, with special relevance to UCH-L1 expression after neurotoxicant exposure. MN9D cells express TH and DAT, which are required for sensitivity to MPP⁺ exposure (Choi et al., 1999). Many analyses can be performed on MN9D cells before attempting an *in vivo* study with rodents such as treatment with the UCH-L1 inhibitor, LDN. Inhibition of UCH-L1 activity with LDN in MN9D cells decreased DA concentration, though this effect was not repeated consistently between experiments. However, treatment with LDN was not cytotoxic at the concentrations used. Further study with the inhibitor *in vivo* may yield more reproducible and relevant results. Studies employing LDN *in vivo* are described in **Chapter 6** of this Dissertation.

Although the MN9D cell line is among the most useful and relevant *in vitro* models for murine ventral midbrain toxicity, it has a few inherent disadvantages. First, the cell line is not commercially available and is nigh impossible to acquire, which also could mean that each batch of MN9D cells distributed to collaborators are different. Second, the cell

line is a fusion of neuroblastoma cells and murine ventral midbrain DA neurons, which means that it possesses qualities of each cell type. The neuroblastoma phenotype may make the cell line likely to respond differently to toxic insult compared to *in vivo* DA neurons. Third, the cell line is derived from murine cells, which may be quite different from human NSDA neurons, considering that mice do not naturally develop PD. Despite these caveats, MN9D cells are a decent model for NSDA neurons especially in their response to neurotoxicant exposure and their use has contributed to the existing evidence that a decrease in UCH-L1 expression accompanies oxidative stress in NSDA neurons.

For the first time, UCH-L1 and mono-Ub protein were measured in ST synaptosomes, which are isolated axon terminals of NSDA neurons. Although UCH-L1 is decreased in the SN 24 h after MPTP (**Fig 3.11**), UCH-L1 is not decreased in ST synaptosomes 24 h after MPTP. The fact that UCH-L1 appears to recover at 24 h in ST synaptosomes but is decreased in the SN brings up a question about potential transport of UCH-L1 from its synthesis site in the cell body region to the axon terminals, as if in an attempt to compensate during injury. No information on how UCH-L1 is transported from the cell body to the axon terminal is available in the literature, but it is reasonable to hypothesize that UCH-L1 could be transported from the SN to the ST at an accelerated rate in response to neurotoxic insult. Although purely conjecture at this point, it appears that such efforts of NSDA neurons challenged with MPTP are futile and maintaining UCH-L1 protein to the ST may not be sufficient to protect against toxicity. Therefore, a better approach would be to pharmacologically inhibit UCH-L1 hydrolase activity in MLDA neurons to determine if UCH-L1 is the factor that protects non-susceptible

neurons from injury. The results from using the UCH-L1 inhibitor LDN *in vivo* are presented in **Chapter 6**.

A possible interaction between two UPS-related genes mutated in familial PD, UCH-L1 and parkin, was explored. A previous report in the literature suggested that parkin activity causes degradation of UCH-L1 (McKeon et al., 2014), so we sought to explain the functional consequences of absence of parkin in the context of this interaction. UCH-L1 is not decreased in the SN of parkin deficient mice, suggesting that that parkin may be important (and perhaps even necessary) for regulating UCH-L1 in the context of MPTP-induced injury. In parkin deficient mice, UCH-L1 and macroautophagy are upregulated in the SN, consistent with the hypothesis that dysregulation of the UPS in the absence of parkin may be compensated for by upregulation of the ALP. Notably, CMA, a specific type of autophagy, was not upregulated in parkin deficient mice. Rather, it appears that macroautophagy, the ALP mechanism with less substrate specificity than CMA, could be more useful for compensating for reduced UPS activity.

It is important to not only consider the UPS but also the ALP when examining pathways mediating protein degradation, so this chapter also sought to understand the interplay of these proteins in the context of autophagic protein degradation. The role of UCH-L1 in the ALP is less clear and has not been fully studied, but if UCH-L1 removes Ub from substrates to promote autophagic degradation in the face of UPS impairment, increased UCH-L1 expression could be part of the mechanism by which Park2^{-/-} mice compensate for lack of parkin and consequentially, avoid a detrimental phenotype resembling humans with mutated parkin.

Summary and conclusions

Taken together, these studies provide evidence for a unique role for UCH-L1 in potentially mediating autophagic degradation of substrates in the absence of parkin, and a hypothesis for how Park2^{-/-} mice compensate for reduced UPS activity.

REFERENCES

REFERENCES

- Anglade, P., Vyas, S., Javoy-Agid, F., Herrero, M.T., Michel, P.P., Marquez, J., Mouatt-Prigent, A., Ruberg, M., Hirsch, E.C., Agid, Y., 1997. Apoptosis and autophagy in nigral neurons of patients with Parkinson's disease. *Histol. Histopathol.* 12, 25–31.
- Baba, M., Nakajo, S., Tu, P.H., Tomita, T., Nakaya, K., Lee, V.M., Trojanowski, J.Q., Iwatsubo, T., 1998. Aggregation of alpha-synuclein in Lewy bodies of sporadic Parkinson's disease and dementia with Lewy bodies. *Am. J. Pathol.* 152, 879–84.
- Bandyopadhyay, U., Kaushik, S., Varticovski, L., Cuervo, A.M., 2008. The chaperone-mediated autophagy receptor organizes in dynamic protein complexes at the lysosomal membrane. *Mol. Cell. Biol.* 28, 5747–63. doi:10.1128/MCB.02070-07
- Barth, S., Glick, D., Macleod, K.F., 2010. Autophagy: assays and artifacts. *J. Pathol.* 221, 117–24. doi:10.1002/path.2694
- Benskey, M., Behrouz, B., Sunryd, J., Pappas, S.S., Baek, S.-H.H., Huebner, M., Lookingland, K.J., Goudreau, J.L., 2012. Recovery of hypothalamic tuberoinfundibular dopamine neurons from acute toxicant exposure is dependent upon protein synthesis and associated with an increase in parkin and ubiquitin carboxy-terminal hydrolase-L1 expression. *Neurotoxicology* 33, 321–31. doi:10.1016/j.neuro.2012.02.001
- Choi, H.K., Won, L. a, Kontur, P.J., Hammond, D.N., Fox, a P., Wainer, B.H., Hoffmann, P.C., Heller, a, 1991. immortalization of embryonic mesencephalic dopaminergic neurons by somatic cell fusion. *Brain Res.* 552, 67–76. doi:10.1016/0006-8993(91)90661-E
- Choi, H.K., Won, L., Roback, J.D., Wainer, B.H., Heller, A., 1992. Specific modulation of dopamine expression in neuronal hybrid cells by primary cells from different brain regions. *Proc. Natl. Acad. Sci.* 89, 8943–8947. doi:10.1073/pnas.89.19.8943
- Choi, W.-S., Canzoniero, L.M.T., Sensi, S.L., O'Malley, K.L., Gwag, B.J., Sohn, S., Kim, J.-E., Oh, T.H., Lee, E.B., Oh, Y.J., 1999. Characterization of MPP+-Induced Cell Death in a Dopaminergic Neuronal Cell Line: Role of Macromolecule Synthesis, Cytosolic Calcium, Caspase, and Bcl-2-Related Proteins. *Exp. Neurol.* 159, 274–282. doi:10.1006/exnr.1999.7133
- Cuervo, A.M., Stefanis, L., Fredenburg, R., Lansbury, P.T., Sulzer, D., 2004. Impaired degradation of mutant alpha-synuclein by chaperone-mediated autophagy. *Science* 305, 1292–5. doi:10.1126/science.1101738
- Cuervo, A.M., Wong, E., 2014. Chaperone-mediated autophagy: roles in disease and aging. *Cell Res.* 24, 92–104. doi:10.1038/cr.2013.153

- Dauer, W., Przedborski, S., 2003. Parkinson ' s Disease : Mechanisms and Models 39, 889–909.
- Davies, K.J.A., 2001. Degradation of oxidized proteins by the 20S proteasome. *Biochimie* 83, 301–310. doi:10.1016/S0300-9084(01)01250-0
- Dunkley, P.R., Jarvie, P.E., Robinson, P.J., 2008. A rapid Percoll gradient procedure for preparation of synaptosomes. *Nat. Protoc.* 3, 1718–1728. doi:10.1038/nprot.2008.171
- Goldberg, M.S., Fleming, S.M., Palacino, J.J., Cepeda, C., Lam, H. a., Bhatnagar, A., Meloni, E.G., Wu, N., Ackerson, L.C., Klapstein, G.J., Gajendiran, M., Roth, B.L., Chesselet, M.F., Maidment, N.T., Levine, M.S., Shen, J., 2003. Parkin-deficient Mice Exhibit Nigrostriatal Deficits but not Loss of Dopaminergic Neurons. *J. Biol. Chem.* 278, 43628–43635. doi:10.1074/jbc.M308947200
- Kitada, T., Asakawa, S., Hattori, N., Matsumine, H., Yamamura, Y., Minoshima, S., Yokochi, M., Mizuno, Y., Shimizu, N., 1998. Mutations in the parkin gene cause autosomal recessive juvenile parkinsonism. *Nature* 392, 605–8. doi:10.1038/33416
- Kurihara, L.J., Kikuchi, T., Wada, K., Tilghman, S.M., 2001. Loss of Uch-L1 and Uch-L3 leads to neurodegeneration, posterior paralysis and dysphagia. *Hum. Mol. Genet.* 10, 1963–70.
- Langston, J., Ballard, P., Tetrud, J., Irwin, I., 1983. Chronic Parkinsonism in humans due to a product of meperidine-analog synthesis. *Science* (80-.). 219, 979–980. doi:10.1126/science.6823561
- Lansdell, T., 2017. THE ROLE OF PARKIN IN MAINTAINING PROTEASOME ACTIVITY FOLLOWING NEUROTOXICANT EXPOSURE (Dissertation).
- Liu, Y., Lashuel, H.A., Choi, S., Xing, X., Case, A., Ni, J., Yeh, L.A., Cuny, G.D., Stein, R.L., Lansbury, P.T., 2003. Discovery of inhibitors that elucidate the role of UCH-L1 activity in the H1299 lung cancer cell line. *Chem. Biol.* 10, 837–846. doi:10.1016/j.chembiol.2003.08.010
- Lowe, J., McDermott, H., Landon, M., Mayer, R.J., Wilkinson, K.D., 1990. Ubiquitin carboxyl-terminal hydrolase (PGP 9.5) is selectively present in ubiquitinated inclusion bodies characteristic of human neurodegenerative diseases. *J. Pathol.* 161, 153–160. doi:10.1002/path.1711610210
- McKeon, J.E., Sha, D., Li, L., Chin, L.-S., 2014. Parkin-mediated K63-polyubiquitination targets ubiquitin C-terminal hydrolase L1 for degradation by the autophagy-lysosome system. *Cell. Mol. Life Sci.* doi:10.1007/s00018-014-1781-2
- Meredith, G.E., Halliday, G.M., Totterdell, S., 2004. A critical review of the development and importance of proteinaceous aggregates in animal models of Parkinson's disease: new insights into Lewy body formation. *Parkinsonism Relat. Disord.* 10, 191–202. doi:10.1016/j.parkreldis.2004.01.001

- Narendra, D., Tanaka, A., Suen, D.-F., Youle, R.J., 2008. Parkin is recruited selectively to impaired mitochondria and promotes their autophagy. *J. Cell Biol.* 183, 795–803. doi:10.1083/jcb.200809125
- Olzmann, J.A., Chin, L.-S., 2008. Parkin-mediated K63-linked polyubiquitination: a signal for targeting misfolded proteins to the aggresome-autophagy pathway. *Autophagy* 4, 85–7.
- Perez, F.A., Palmiter, R.D., 2005. Parkin-deficient mice are not a robust model of parkinsonism. *Proc. Natl. Acad. Sci. U. S. A.* 102, 2174–9. doi:10.1073/pnas.0409598102
- Pickrell, A.M., Huang, C.-H., Kennedy, S.R., Ordureau, A., Sideris, D.P., Hoekstra, J.G., Harper, J.W., Youle, R.J., 2015. Endogenous Parkin Preserves Dopaminergic Substantia Nigral Neurons following Mitochondrial DNA Mutagenic Stress. *Neuron* 87, 371–381. doi:10.1016/j.neuron.2015.06.034
- Ross, C.A., Poirier, M.A., 2004. Protein aggregation and neurodegenerative disease.
- Ross, C. a., Pickart, C.M., 2004. The ubiquitin-proteasome pathway in Parkinson's disease and other neurodegenerative diseases. *Trends Cell Biol.* 14, 703–711. doi:10.1016/j.tcb.2004.10.006
- Ross, J.M., Olson, L., Coppotelli, G., 2015. Mitochondrial and Ubiquitin Proteasome System Dysfunction in Ageing and Disease: Two Sides of the Same Coin? *Int. J. Mol. Sci.* 16, 19458–76. doi:10.3390/ijms160819458
- Shimura, H., Hattori, N., Kubo, S.I., Mizuno, Y., Asakawa, S., Minoshima, S., Shimizu, N., Iwai, K., Chiba, T., Tanaka, K., Suzuki, T., 2000. Familial Parkinson disease gene product, parkin, is a ubiquitin-protein ligase. *Nat. Genet.* 25, 302–305. doi:10.1038/77060
- Spillantini, M.G., Schmidt, M.L., Lee, V.M.-Y., Trojanowski, J.Q., Jakes, R., Goedert, M., 1997. [alpha]-Synuclein in Lewy bodies 388, 839–840.
- Thrower, J.S., Hoffman, L., Rechsteiner, M., Pickart, C.M., 2000. Recognition of the polyubiquitin proteolytic signal. *EMBO J.* 19, 94–102. doi:10.1093/emboj/19.1.94
- Um, J.W., Im, E., Lee, H.J., Min, B., Yoo, L., Yoo, J., Lübbert, H., Stichel-Gunkel, C., Cho, H.-S., Yoon, J.B., Chung, K.C., 2010. Parkin directly modulates 26S proteasome activity. *J. Neurosci.* 30, 11805–14. doi:10.1523/JNEUROSCI.2862-09.2010
- Walters, B.J., Campbell, S.L., Chen, P.C., Taylor, A.P., Schroeder, D.G., Dobrunz, L.E., Artavanis-Tsakonas, K., Ploegh, H.L., Wilson, J.A., Cox, G.A., Wilson, S.M., 2008. Differential effects of Usp14 and Uch-L1 on the ubiquitin proteasome system and synaptic activity. *Mol. Cell. Neurosci.* 39, 539–48. doi:10.1016/j.mcn.2008.07.028

Chapter 5: Effects of Inhibition of UCH-L1 on Susceptibility of NSDA and MLDA Neurons to Neurotoxicant Exposure

Introduction

MLDA neurons are resistant to cell death in PD while NSDA neurons progressively degenerate (Braak and Braak, 2000). The differential susceptibility between NSDA and MLDA neurons can be recapitulated using the neurotoxicant MPTP (Behrouz et al., 2007; Hung and Lee, 1998) (**Figs. 3.4-3.6**). To understand which pathways could be protective in MLDA neurons and impaired in NSDA neurons, we examined the UPS-related DUB, UCH-L1, which has been found to be mutated in familial PD (Leroy et al., 1998). UCH-L1 is decreased in the SN 24 h after MPTP exposure while UCH-L1 is maintained in the SN 24 h after MPTP exposure (**Figs. 3.11 and 3.12**). Since maintenance of UCH-L1 protein expression is hypothesized to protect MLDA neurons from neurotoxic injury, while loss of UCH-L1 expression contributes to vulnerability of NSDA neurons, this idea implies that UCH-L1 hydrolase activity may provide a protective function against neurotoxicity.

One way to influence UCH-L1 hydrolase activity without changing the amount of UCH-L1 protein is to use a pharmacological inhibitor of UCH-L1. An inhibitor of UCH-L1 was developed for the purpose of studying the role of UCH-L1 hydrolase activity in cancer cell lines (Liu et al., 2003). UCH-L1 is neuron specific but has been found to be ectopically expressed in some cancers and cancer-derived cell lines (Hurst-Kennedy et al., 2012). The most potent inhibitor discovered in the study, LDN-57444, is an isatin oxime compound that binds competitively and reversibly and targets the active site of

UCH-L1. Importantly, LDN-57444 shows a 28-fold higher specificity for UCH-L1 over its closely related DUB UCH-L3 (Liu et al., 2003), which is important since the two DUBs are thought to have distinct but potentially overlapping functions.

Once LDN-57444 became commercially available other groups began using it in neurodegeneration research, especially with regard to AD and PD. One of the first AD studies to use LDN-57444 to inhibit UCH-L1 examined synaptic transmission in hippocampal slices and found that decreasing UCH-L1 impairs function of hippocampal neurons (Gong et al., 2006). The consequences of LDN-57444 administration were shown to be UCH-L1-specific since overexpressing UCH-L1 protein rescued the effects of LDN-57444, demonstrating that UCH-L1 is necessary for synaptic transmission and cognitive function (Gong et al., 2006). This study also examined UCH-L1 inhibition *in vivo* using LDN-57444 and demonstrated reduced contextual learning in mice injected with the UCH-L1 inhibitor (Gong et al., 2006). Another study showed that UCH-L1 inhibition in hippocampal neurons causes a decrease in synaptic spine density, concurrent with a depletion of mono-Ub pools (Cartier et al., 2009). This decrease in spine density translated to deficits in synaptic transmission and long-term potentiation and strengthened the relationship between UCH-L1 and memory and cognition.

A study with relevance to PD from the same group used LDN-57444 *in vivo* and observed that inhibition of UCH-L1 in mice expressing normal amounts of the PD-linked protein α -syn caused an abnormal accumulation of α -synuclein (Cartier et al., 2012). However, DA neuron-specific effects of LDN-57444 administration were not explored in these previous studies. Since maintenance of UCH-L1 expression and function is hypothesized to protect MLDA neurons from MPTP-induced injury, experiments

described in this chapter sought to determine if inhibition of UCH-L1 hydrolase activity with LDN-57444 renders MLDA neurons more vulnerable to MPTP, and whether inhibition of UCH-L1 would exacerbate the extent of MPTP-induced injury in NSDA neurons.

Results

Characterization of effects of LDN-57444 under basal conditions

The compound LDN-57444 proved challenging to work with because it is highly lipophilic and requires DMSO for its dissolution. On one hand, these physicochemical properties of LDN-57444 are advantageous because it is predicted that LDN will readily cross the BBB due to its high lipophilicity (**Fig. 5.1**) and that some proportion of LDN-57444 administered to mice will reach the targeted brain regions. The BOILED egg diagram modeled from compiled Swiss ADME pharmacokinetics data shows LDN-57444 placement within the “yolk”, which signifies that it is predicted to cross the BBB as plotted against the logP (lipophilicity) on the Y-axis and topological polar surface area (TPSA) on the X-axis. Since LDN-57444 is highly lipophilic and has a relatively small TPSA, it is predicted to cross the BBB. The “egg white” of the diagram signifies human intestinal absorption (HIA). LDN-57444 is predicted to not be a substrate for p-glycoprotein (PGP) present on the BBB, which can actively pump out drugs from the brain (Daina and Zoete, 2016).

On the other hand, a disadvantage for using LDN-57444 is that DMSO is not a commonly used vehicle for *in vivo* studies. DMSO can, however, be used in very small amounts (i.e., < 100 μ L) without substantial toxicity to the mouse (Kelava et al., 2011).

Therefore, a pilot study was performed that would examine the effects of DMSO administration and two previously employed doses of LDN-57444: 0.5 mg/kg (Cartier et al., 2012) and 5 mg/kg. Mice were injected at time zero and 4 h later mice

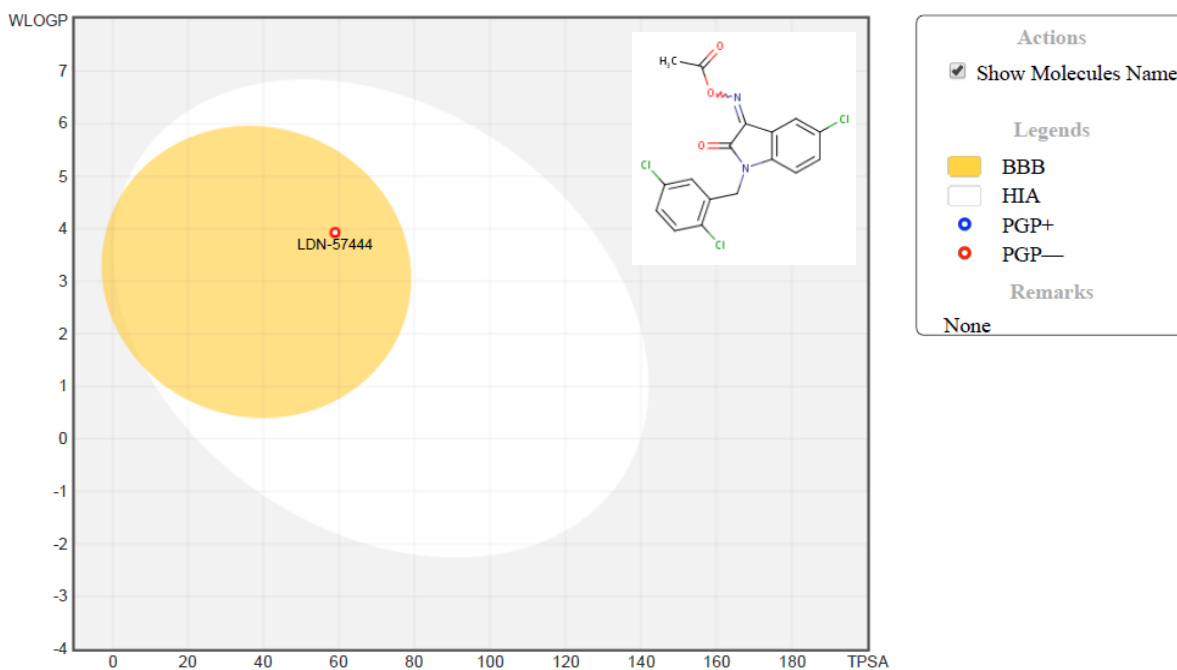


Figure 5.1. The UCH-L1 inhibitor LDN-57444 is predicted to cross the blood brain barrier (BBB). Using SwissADME (SwissADME: a free web tool to evaluate pharmacokinetics, drug-likeness and medicinal chemistry friendliness of small molecules. *Sci. Rep.* (2017) 7:42717.) the physicochemical properties of LDN-57444 were predicted. In particular, the BOILED-Egg simulation was used to predict blood-brain barrier permeability of LDN.

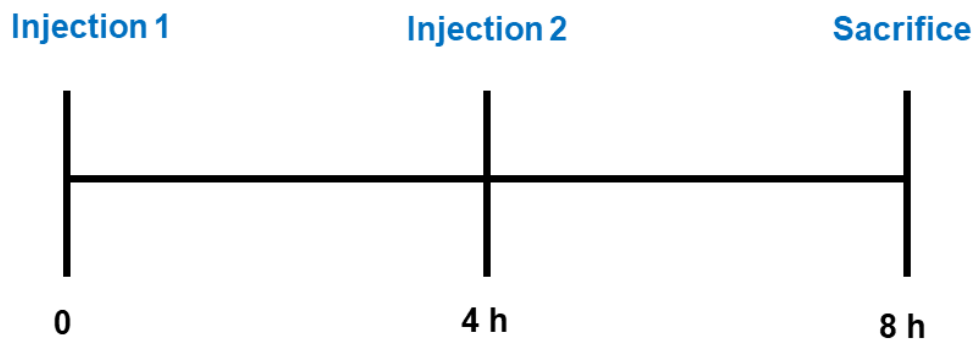


Figure 5.2. Injection paradigm for LDN dose response study. Mice were injected with saline VH, DMSO VH, 0.5 mg/kg LDN, or 5 mg/kg LDN at time point zero. Four h later, mice received a second injection of VH or LDN identical to the first injection and sacrificed 4 h later.

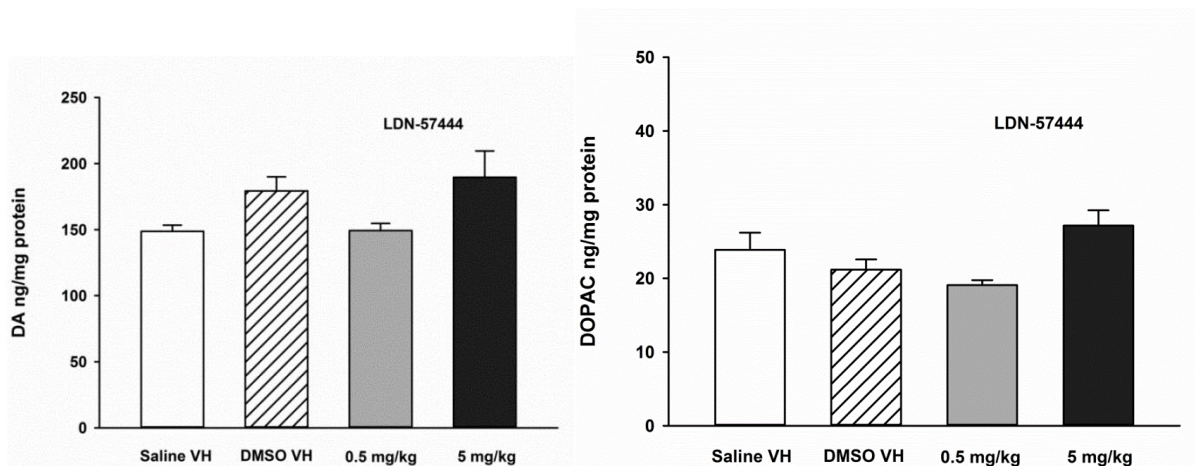


Figure 5.3. DA (left) and DOPAC (right) concentrations in the ST following saline VH, DMSO VH, 0.5 mg/kg LDN, or 5 mg/kg LDN. Mice received two injections of LDN and were sacrificed as described in **Fig. 5.2** (n=10 each group). The ST was microdissected from brain tissue and analyzed via HPLC-ED for DA and DOPAC. Data is plotted as mean + SEM. No significant differences between groups were detected ($p > 0.05$) via one-way ANOVA.

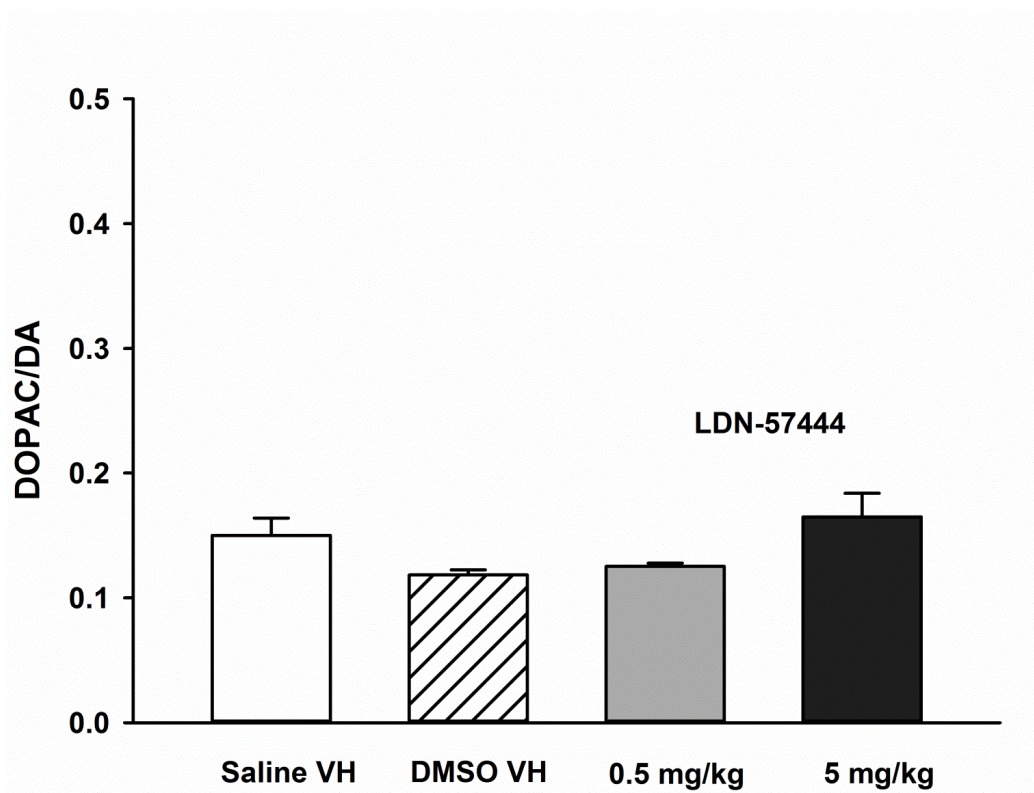


Figure 5.4. DOPAC/DA ratio in the ST after saline VH, DMSO VH, and 0.5 and 5 mg/kg LDN. Mice received two injections of LDN and were sacrificed as described in **Fig. 5.2**. The ST was microdissected from brain tissue and analyzed via HPLC-ED for DA and DOPAC (n=10 each group). The DOPAC/DA ratio was calculated. Data is plotted as mean + SEM. No significant differences between groups were detected ($p > 0.05$) via one-way ANOVA.

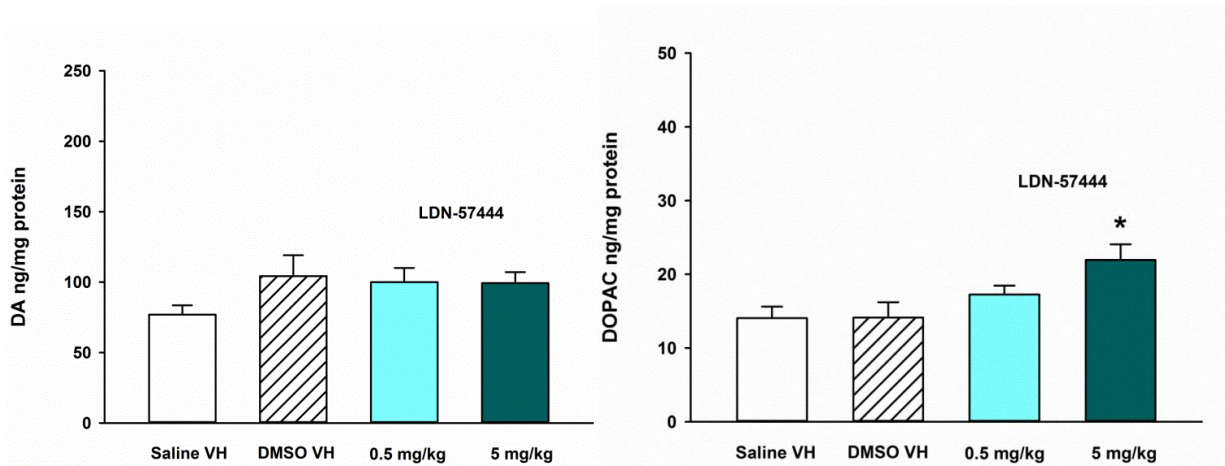


Figure 5.5. DA (left) and DOPAC (right) concentrations in the NAc following saline VH, DMSO VH, 0.5 mg/kg LDN, or 5 mg/kg LDN. Mice received two injections of LDN and were sacrificed as described in **Fig. 5.2**. The NAc was microdissected from brain tissue and analyzed via HPLC-ED for DA and DOPAC (n=10 each group). Data is plotted as mean + SEM. Asterisk (*) indicates statistically significant difference from DMSO VH where $p < 0.05$ via one-way ANOVA and a post hoc Holm-Sidak test.

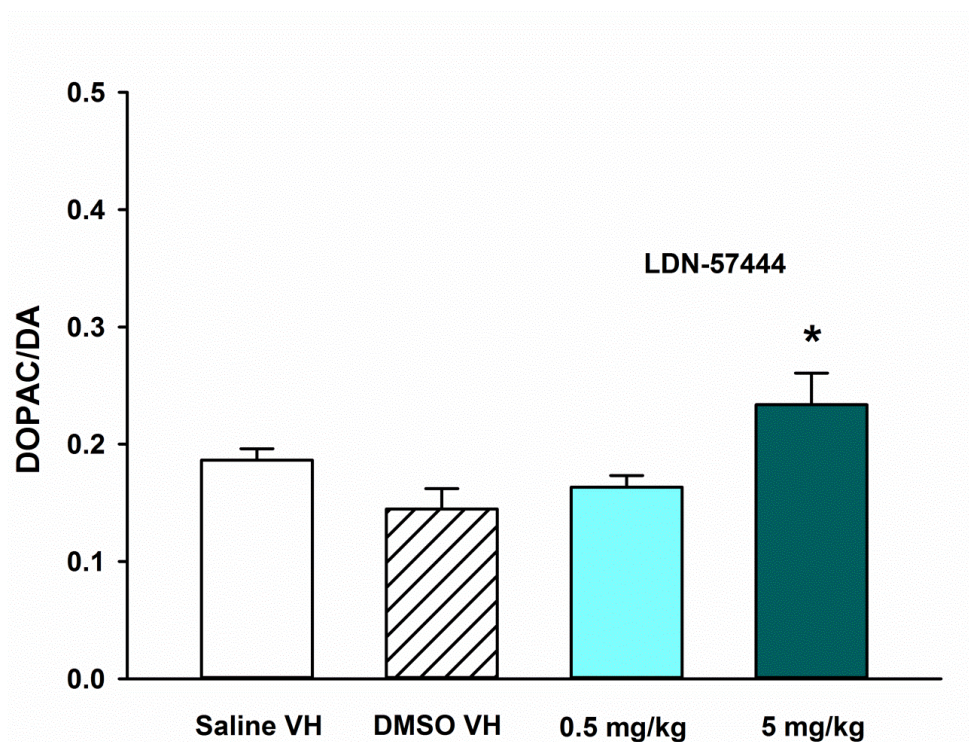


Figure 5.6. DOPAC/DA ratio in the NAc after saline VH, DMSO VH, and 0.5 and 5 mg/kg LDN. Mice received two injections of LDN and were sacrificed as described in **Fig. 5.2**. The NAc was microdissected from brain tissue and analyzed via HPLC-ED for DA and DOPAC (n=10 each group). The DOPAC/DA ratio was calculated. Data is plotted mean + SEM. Asterisk (*) indicates a statistically significant difference from DMSO VH where $p < 0.05$ via one-way ANOVA and a post hoc Holm-Sidak test.

Table 5.1. Mono-Ub and Total Ub proteins in the ST. Mice received two injections of LDN and were sacrificed as described in **Fig. 5.2**. The ST was microdissected from brain tissue and analyzed via western blotting for mono-Ub and total Ub proteins (n=10 each group). Data (densitometry of mono-Ub and total Ub compared to GAPDH loading control) is shown as mean + SEM. No significant difference between groups was detected ($p > 0.05$) via one-way ANOVA.

Treatment Group	Endpoint	Mean \pm SEM
Saline VH	Mono-Ub	0.0173 \pm 0.00215
DMSO VH	Mono-Ub	0.0258 \pm 0.00375
0.05 mg/kg LDN	Mono-Ub	0.0195 \pm 0.00193
5 mg/kg LDN	Mono-Ub	0.0167 \pm 0.00320
Saline VH	Total Ub	0.0281 \pm 0.00545
DMSO VH	Total Ub	0.0329 \pm 0.00398
0.05 mg/kg LDN	Total Ub	0.0273 \pm 0.00388
5 mg/kg LDN	Total Ub	0.0288 \pm 0.00424

Table 5.2. Mono-Ub and Total Ub proteins in the NAc. Mice received two injections of LDN and were sacrificed as described in **Fig. 5.2**. The NAc was microdissected from brain tissue and analyzed via western blotting for mono-Ub and total Ub proteins (n=10 each group). Data (densitometry of mono-Ub and total Ub compared to GAPDH loading control) is shown as mean + SEM. No significant difference between groups was detected ($p > 0.05$) via one-way ANOVA.

Treatment Group	Endpoint	Mean \pm SEM
Saline VH	Mono-Ub	0.00569 \pm 0.000716
DMSO VH	Mono-Ub	0.00618 \pm 0.000629
0.05 mg/kg LDN	Mono-Ub	0.00663 \pm 0.000597
5 mg/kg LDN	Mono-Ub	0.00579 \pm 0.000792
Saline VH	Total Ub	0.0216 \pm 0.00260
DMSO VH	Total Ub	0.0276 \pm 0.00479
0.05 mg/kg LDN	Total Ub	0.0290 \pm 0.00323
5 mg/kg LDN	Total Ub	0.0227 \pm 0.00176

Table 5.3. Mono-Ub and Total Ub proteins in the SN. Mice received two injections of LDN and were sacrificed as described in **Fig. 5.2**. The SN was microdissected from brain tissue and analyzed via western blotting for mono-Ub and total Ub proteins (n=10 each group). Data (densitometry of mono-Ub or total Ub compared to GAPDH loading control) is shown as mean + SEM. No significant difference between groups was detected ($p > 0.05$) via one-way ANOVA.

Treatment Group	Endpoint	Mean \pm SEM
Saline VH	Mono-Ub	0.0294 \pm 0.00544
DMSO VH	Mono-Ub	0.0237 \pm 0.00266
0.05 mg/kg LDN	Mono-Ub	0.0255 \pm 0.00360
5 mg/kg LDN	Mono-Ub	0.0259 \pm 0.00344
Saline VH	Total Ub	0.0306 \pm 0.00411
DMSO VH	Total Ub	0.0305 \pm 0.00427
0.05 mg/kg LDN	Total Ub	0.0271 \pm 0.00554
5 mg/kg LDN	Total Ub	0.0233 \pm 0.00379

Table 5.4. Mono-Ub and Total Ub proteins in the VTA. Mice received two injections of LDN and were sacrificed as described in **Fig. 5.2**. The VTA was microdissected from brain tissue and analyzed via western blotting for mono-Ub and total Ub proteins (n=10 each group). Data (densitometry of mono-Ub and total Ub compared to GAPDH loading control) is shown as mean + SEM. No significant difference between groups was detected ($p > 0.05$) via one-way ANOVA.

Treatment Group	Endpoint	Mean \pm SEM
Saline VH	Mono-Ub	0.0281 \pm 0.00839
DMSO VH	Mono-Ub	0.0298 \pm 0.00651
0.05 mg/kg LDN	Mono-Ub	0.0177 \pm 0.00310
5 mg/kg LDN	Mono-Ub	0.0372 \pm 0.00837
Saline VH	Total Ub	0.0201 \pm 0.00131
DMSO VH	Total Ub	0.0215 \pm 0.00183
0.05 mg/kg LDN	Total Ub	0.0184 \pm 0.00106
5 mg/kg LDN	Total Ub	0.0254 \pm 0.00627

received a second injection. Four h after the second injection mice were sacrificed (**Fig. 5.2**).

First, potential toxicity to DA neurons was examined, since the inhibitor would not be useful for future studies if it caused overt injury to DA neurons. As shown in **Fig. 5.3**, DA and DOPAC in the ST were not affected by any drug treatments and DMSO did not have an effect compared to saline VH. Similarly, the DOPAC/DA ratio is not affected by drug treatments in the ST (**Fig. 5.4**). In the NAc, DA was not different between drug treatments, but DOPAC was increased in the 5 mg/kg group (**Fig. 5.5**). This increase in DOPAC in the NAc contributed to an increase in the DOPAC/DA ratio (**Fig. 5.6**) suggesting increased activity of MLDA neurons in mice treated with 5 mg/kg LDN-57444.

After establishing that DMSO and up to 5 mg/kg doses of LDN-57444 are not toxic to either NSDA or MLDA neurons, we measured target engagement and UPS function by measuring mono-Ub levels and total Ub conjugated proteins (total Ub). In the ST (**Table 5.1**), NAc (**Table 5.2**), SN (**Table 5.3**) and VTA (**Table 5.4**) mono-Ub levels or UPS function were not affected by DMSO or either dose of LDN administration. **Fig. 5.7** shows the point at which LDN-57444 is expected to act within the scheme of the UPS, which is anticipated to decrease levels of available mono-Ub.

Effects of LDN-57444 on susceptibility of NSDA and MLDA neurons to MPTP

Next, the question of whether inhibition of UCH-L1 affects susceptibility to MPTP was addressed. To do this, early events that occur following MPTP that would be related to UCH-L1 function were examined (**Table 5.5**). At time zero, mice received a s.c. injection

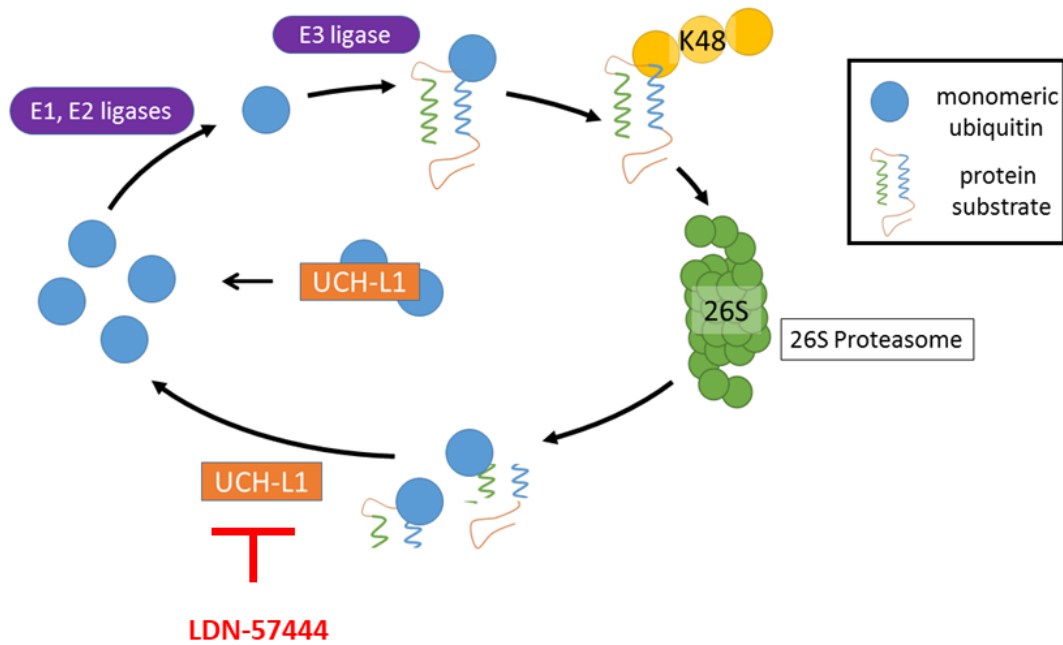


Figure 5.7. Proposed mechanism of action of the UCH-L1 inhibitor LDN in the context of UCH-L1 activity and the UPS. LDN is expected to inhibit UCH-L1 hydrolase activity, one of the ways in which UCH-L1 is hypothesized to replenish mono-Ub pools. However, the ability to bind and stabilize mono-Ub may not be affected by the inhibitor, which could result in no loss of mono-Ub when LDN is administered.

Table 5.5. Injection paradigm for LDN-57444 + MPTP study. Mice were administered either saline VH or 20 mg/kg MPTP s.c. at time zero. Immediately after mice were given an injection of either DMSO VH or 0.5 mg/kg LDN-57444 i.p. and 4 h later, mice were given a repeat of the same drug injected i.p. Four h after the last injection, mice were sacrificed and brain tissue processed for analyses of DA neurochemistry and protein expression.

Group	Injection 1	Injection 2
DMSO Saline	DMSO + Saline	DMSO
LDN Saline	LDN + Saline	LDN
DMSO MPTP	DMSO + MPTP	DMSO
LDN MPTP	LDN + MPTP	LDN

of either saline VH or 20 mg/kg MPTP, then immediately after received an i.p. injection of either DMSO VH or 0.05 mg/kg LDN-57444. Four h later, mice received a second i.p. injection of DMSO VH or 0.05 mg/kg LDN-57444 and were sacrificed 4 h after the second injection and 8 h after MPTP. We used the lower dose of LDN to potentially avoid inhibiting UCH-L3.

Fig. 5.8 shows DA concentrations in the ST. LDN-57444 treatment alone did not have any effects on DA content in the ST. MPTP administration caused a decrease in DA, which is expected at the 8 h time point (Behrouz et al., 2007). LDN-57444 blocked the inhibitory effect of MPTP on ST DA concentrations. This result was recapitulated in the NAc (**Fig. 5.9**).

Next, to ensure that any effects of LDN-57444 or MPTP on mono-Ub and UPS activity are not simply due to decreased levels of UCH-L1 protein, UCH-L1 was measured in each brain region. In the ST (**Table 5.6**), NAc (**Table 5.7**), SN (**Table 5.8**) and VTA (**Table 5.9**) UCH-L1 protein was not affected by LDN-57444, MPTP, or the combination of LDN-57444 and MPTP. This finding allows us to interpret any further results apart from changes in UCH-L1 protein expression.

To address the question of target engagement and inhibition of the UPS, mono-Ub levels and total Ub-proteins were measured via Western blot. In the ST (**Table 5.10**), NAc (**Table 5.11**), SN (**Table 5.12**), and VTA (**Table 5.13**) mono-Ub and UPS function remain unchanged in all groups. This result suggests that if inhibition of UCH-L1 has occurred, there are no effects on mono-Ub or UPS activity. An alternative method to measure target engagement is using a DUB labeling assay (Borodovsky et al., 2002). In

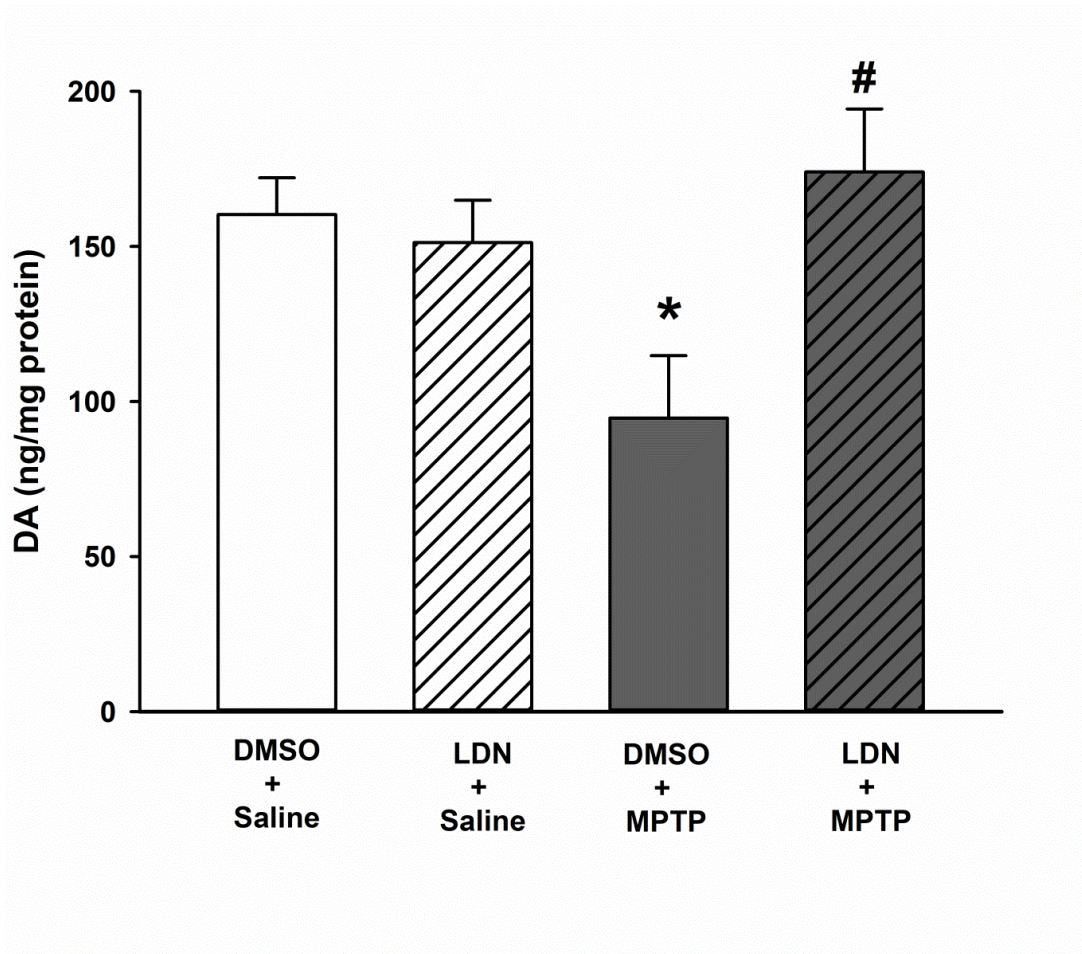


Figure 5.8. DA concentrations in the ST of mice and various drug treatments.

Mice were injected with saline or 20 mg/kg MPTP, DMSO VH or 0.5 mg/kg LDN. Four h after mice received the second i.p. injection, mice were sacrificed and the ST microdissected. DMSO + Saline n=9; LDN + Saline n=9; DMSO + MPTP n=6; LDN + MPTP n=7. DA was measured via HPLC-ED. Data is plotted as mean + SEM and asterisk (*) indicates a statistically significant difference from DMSO + Saline group where $p < 0.05$ via one-way ANOVA with a post hoc Holm-Sidak test. Pound (#) indicates statistically significant difference from DMSO + MPTP group where $p < 0.05$ via one-way ANOVA and a post hoc Holm-Sidak test.

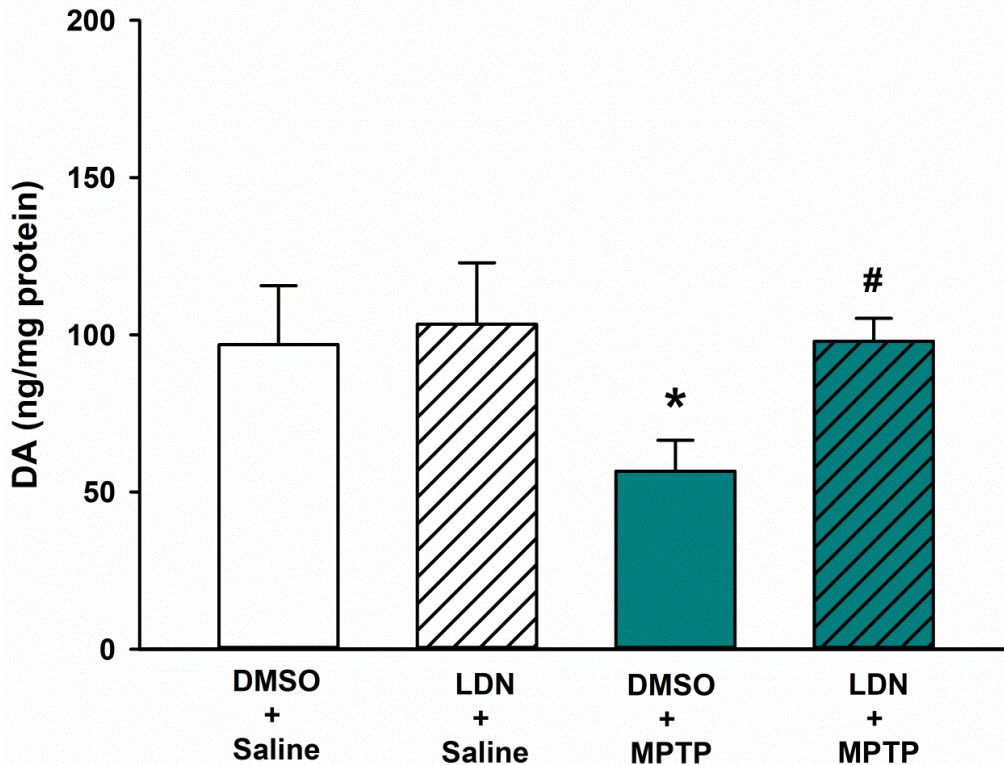


Figure 5.9. DA concentrations in the NAc of mice and various drug treatments. Mice were injected with saline or 20 mg/kg MPTP, DMSO VH or 0.5 mg/kg LDN. Four h after mice received the second i.p. injection, mice were sacrificed and the NAc microdissected. DMSO + Saline n=9; LDN + Saline n=10; DMSO + MPTP n=9; LDN + MPTP n=9. DA was measured via HPLC-ED. Data is plotted as mean + SEM and asterisk (*) indicates a statistically significant difference from DMSO + Saline group where $p < 0.05$ via one-way ANOVA and a post hoc Holm-Sidak test. Pound (#) indicates statistically significant difference from DMSO + MPTP group where $p < 0.05$ via one-way ANOVA and a post hoc Holm-Sidak test.

Table 5.6. UCH-L1 protein expression in the ST. Mice were injected with saline or 20 mg/kg MPTP, DMSO VH or 0.5 mg/kg LDN-57444 as described in **Table 5.5**. The ST was microdissected from brain tissue and analyzed via Western blotting for UCH-L1 (n=10 each group). Data (densitometry of UCH-L1 compared to GAPDH loading control) is shown as mean \pm SEM. No significant difference between groups was detected ($p > 0.05$) via one-way ANOVA.

Treatment Group	Endpoint	Mean \pm SEM
DMSO + Saline	UCH-L1	0.0295 \pm 0.00253
LDN + Saline	UCH-L1	0.0276 \pm 0.00181
DMSO + MPTP	UCH-L1	0.0249 \pm 0.00273
LDN + MPTP	UCH-L1	0.0227 \pm 0.00187

Table 5.7. UCH-L1 protein expression in the NAc. Mice were injected with saline or 20 mg/kg MPTP, DMSO VH or 0.5 mg/kg LDN-57444 as described in **Table 5.5**. The NAc was microdissected from brain tissue and analyzed via Western blotting for UCH-L1 (n=10 each group). Data (densitometry of UCH-L1 compared to GAPDH loading control) is shown as mean \pm SEM. No significant difference between groups was detected ($p > 0.05$) via one-way ANOVA.

Treatment Group	Endpoint	Mean \pm SEM
DMSO + Saline	UCH-L1	0.0282 \pm 0.00267
LDN + Saline	UCH-L1	0.0271 \pm 0.00129
DMSO + MPTP	UCH-L1	0.0241 \pm 0.00209
LDN + MPTP	UCH-L1	0.0255 \pm 0.00284

Table 5.8. UCH-L1 protein expression in the SN. Mice were injected with saline or 20 mg/kg MPTP, DMSO VH or 0.5 mg/kg LDN-57444 as described in **Table 5.5**. The SN was microdissected from brain tissue and analyzed via Western blotting for UCH-L1 (n=10 each group). Data (densitometry of UCH-L1 compared to GAPDH loading control) is shown as mean \pm SEM. No significant difference between groups was detected ($p > 0.05$) via one-way ANOVA.

Treatment Group	Endpoint	Mean \pm SEM
DMSO + Saline	UCH-L1	0.0250 \pm 0.00175
LDN + Saline	UCH-L1	0.0251 \pm 0.00185
DMSO + MPTP	UCH-L1	0.0265 \pm 0.00209
LDN + MPTP	UCH-L1	0.0289 \pm 0.00322

Table 5.9. UCH-L1 protein expression in the VTA. Mice were injected with saline or 20 mg/kg MPTP, DMSO VH or 0.5 mg/kg LDN-57444 as described in **Table 5.5**. The VTA was microdissected from brain tissue and analyzed via Western blotting for UCH-L1 (n=10 each group). Data (densitometry of UCH-L1 compared to GAPDH loading control) is shown as mean \pm SEM. No significant difference between groups was detected ($p > 0.05$) via one-way ANOVA.

Treatment Group	Endpoint	Mean \pm SEM
DMSO + Saline	UCH-L1	0.0255 \pm 0.00204
LDN + Saline	UCH-L1	0.0262 \pm 0.00225
DMSO + MPTP	UCH-L1	0.0276 \pm 0.00265
LDN + MPTP	UCH-L1	0.0260 \pm 0.00187

Table 5.10. Mono-Ub and total Ub protein in the ST. Mice were injected with saline or 20 mg/kg MPTP, DMSO VH or 0.5 mg/kg LDN-57444 as described in **Table 5.5**. The ST was microdissected from brain tissue and analyzed via Western blotting for UCH-L1 (n=10 each group). Data (densitometry of mono-Ub and total Ub compared to GAPDH loading control) is shown as mean \pm SEM. No significant difference between groups was detected ($p > 0.05$) via one-way ANOVA.

Treatment Group	Endpoint	Mean \pm SEM
DMSO + Saline	Mono-Ub	0.0304 \pm 0.00687
LDN + Saline	Mono-Ub	0.0346 \pm 0.00988
DMSO + MPTP	Mono-Ub	0.0310 \pm 0.00999
LDN + MPTP	Mono-Ub	0.0239 \pm 0.00694
DMSO + Saline	Total Ub	0.0229 \pm 0.00340
LDN + Saline	Total Ub	0.0172 \pm 0.00266
DMSO + MPTP	Total Ub	0.0380 \pm 0.00449
LDN + MPTP	Total Ub	0.0307 \pm 0.00259

Table 5.11. Mono-Ub and total Ub protein in the NAc. Mice were injected with saline or 20 mg/kg MPTP, DMSO VH or 0.5 mg/kg LDN-57444 as described in **Table 5.5**. The NAc was microdissected from brain tissue and analyzed via Western blotting for UCH-L1 (n=10 each group). Data (densitometry of mono-Ub and total Ub compared to GAPDH loading control) is shown as mean \pm SEM. No significant difference between groups was detected ($p > 0.05$) via one-way ANOVA.

Treatment Group	Endpoint	Mean \pm SEM
DMSO + Saline	Mono-Ub	0.0261 \pm 0.00442
LDN + Saline	Mono-Ub	0.0182 \pm 0.00238
DMSO + MPTP	Mono-Ub	0.0202 \pm 0.00315
LDN + MPTP	Mono-Ub	0.0235 \pm 0.00327
DMSO + Saline	Total Ub	0.0248 \pm 0.00435
LDN + Saline	Total Ub	0.0279 \pm 0.00435
DMSO + MPTP	Total Ub	0.0284 \pm 0.00606
LDN + MPTP	Total Ub	0.0331 \pm 0.00582

Table 5.12. Mono-Ub and total Ub protein in the SN. Mice were injected with saline or 20 mg/kg MPTP, DMSO VH or 0.5 mg/kg LDN-57444 as described in **Table 5.5**. The SN was microdissected from brain tissue and analyzed via Western blotting for UCH-L1 (n=10 each group). Data (densitometry of mono-Ub and total Ub compared to GAPDH loading control) is shown as mean \pm SEM. No significant difference between groups was detected ($p > 0.05$) via one-way ANOVA.

Treatment Group	Endpoint	Mean \pm SEM
DMSO + Saline	Mono-Ub	0.0230 \pm 0.00179
LDN + Saline	Mono-Ub	0.0266 \pm 0.00263
DMSO + MPTP	Mono-Ub	0.0306 \pm 0.00507
LDN + MPTP	Mono-Ub	0.0255 \pm 0.00383
DMSO + Saline	Total Ub	0.0209 \pm 0.00275
LDN + Saline	Total Ub	0.0219 \pm 0.00394
DMSO + MPTP	Total Ub	0.0364 \pm 0.00442
LDN + MPTP	Total Ub	0.0320 \pm 0.00529

Table 5.13. Mono-Ub and total Ub protein in the VTA. Mice were injected with saline or 20 mg/kg MPTP, DMSO VH or 0.5 mg/kg LDN-57444 as described in **Table 5.5**. The VTA was microdissected from brain tissue and analyzed via Western blotting for UCH-L1 (n=10 each group). Data (densitometry of mono-Ub and total Ub compared to GAPDH loading control) is shown as mean \pm SEM. No significant difference between groups was detected ($p > 0.05$) via one-way ANOVA.

Treatment Group	Endpoint	Mean \pm SEM
DMSO + Saline	Mono-Ub	0.0199 \pm 0.00686
LDN + Saline	Mono-Ub	0.0210 \pm 0.00633
DMSO + MPTP	Mono-Ub	0.0324 \pm 0.00380
LDN + MPTP	Mono-Ub	0.0249 \pm 0.00733
DMSO + Saline	Total Ub	0.0256 \pm 0.0034
LDN + Saline	Total Ub	0.0185 \pm 0.00372
DMSO + MPTP	Total Ub	0.0270 \pm 0.00427
LDN + MPTP	Total Ub	0.0299 \pm 0.00205

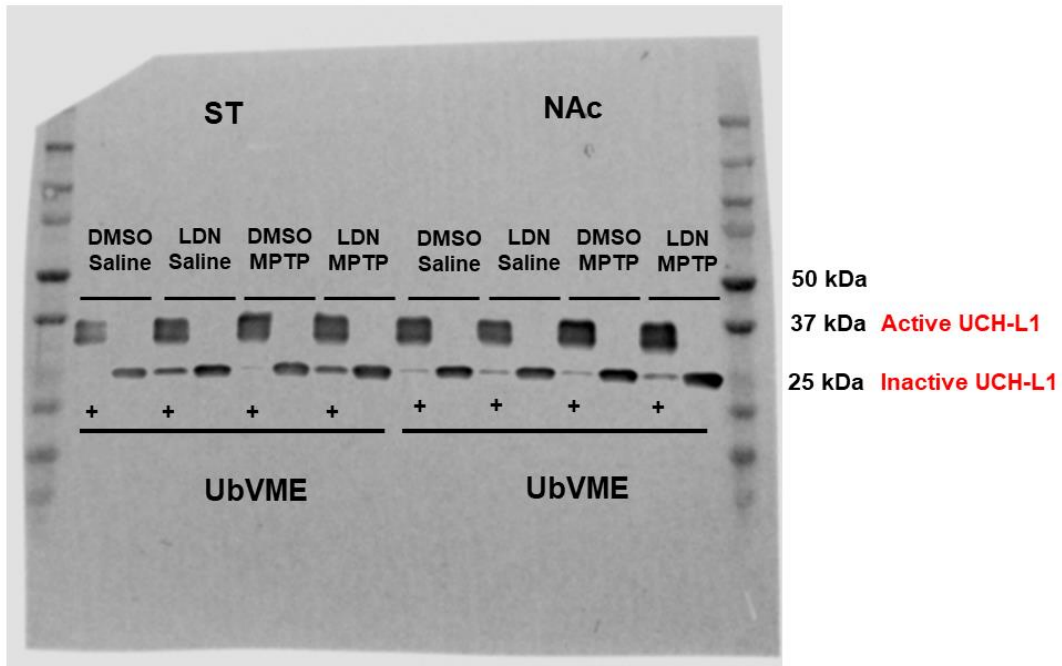


Figure 5.10. Gel image representing Ub-VME DUB labeling assay for the ST and NAc. Mice were injected with saline or 20 mg/kg MPTP, DMSO VH or 0.5 mg/kg LDN-57444 as described in **Table 5.5**. Lysates from the ST and NAc were incubated with the suicide substrate, Ub-VME (+) or with buffer. Samples were denatured and run on a gel and membranes were probed for UCH-L1. No qualitative difference between DMSO and LDN-57444 samples were observed.

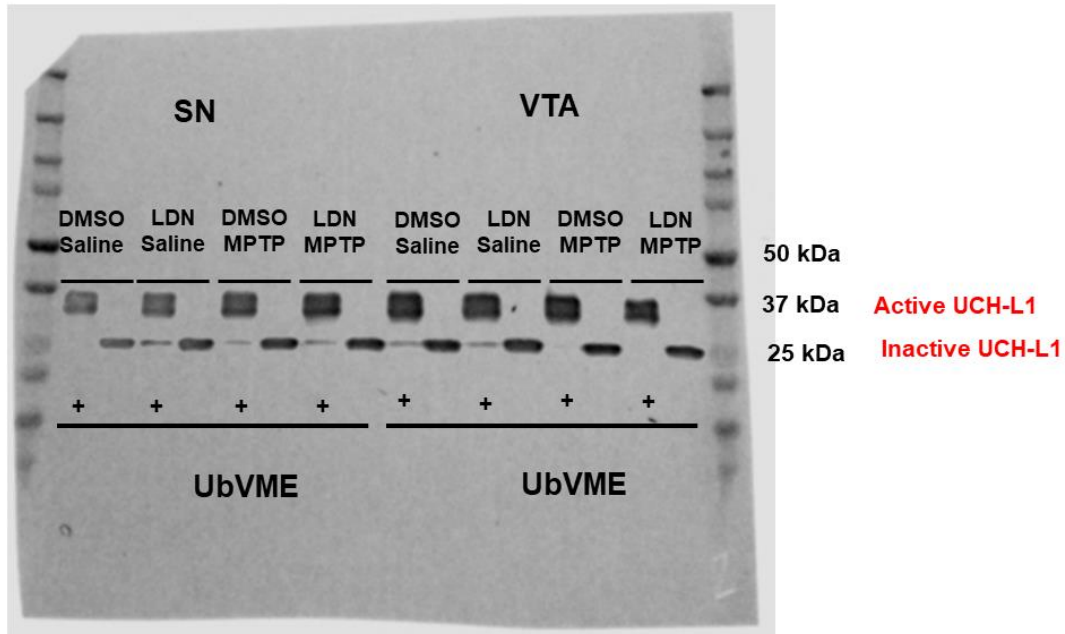


Figure 5.11. Gel image representing Ub-VME DUB labeling assay for the SN and VTA. Mice were injected with saline or 20 mg/kg MPTP, DMSO VH or 0.5 mg/kg LDN-57444 as described in **Table 5.5**. Lysates from the SN and VTA were incubated with the suicide substrate, Ub-VME (+) or with buffer. Samples were denatured and run on a gel and membranes were probed for UCH-L1. No qualitative differences between DMSO and LDN-57444 were observed.

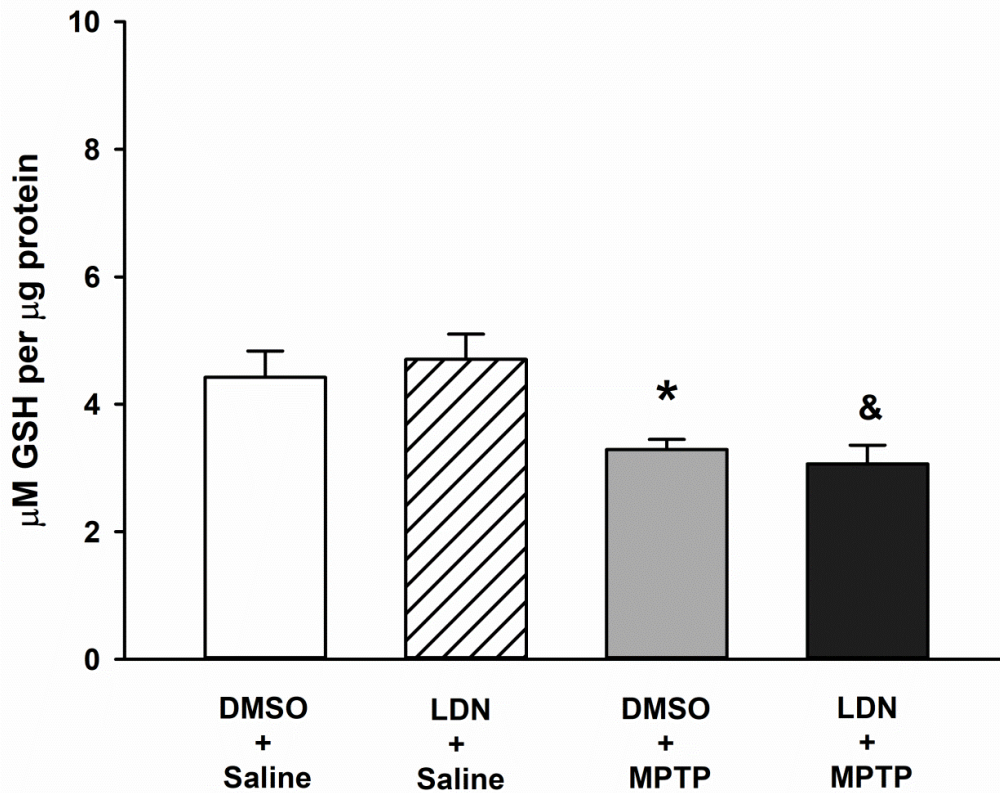


Figure 5.12. Reduced GSH concentration in the ST. Mice were injected with saline or 20 mg/kg MPTP, DMSO VH or 0.5 mg/kg LDN-57444 as described in **Table 5.5**. The ST was microdissected and assayed for reduced GSH. DMSO + Saline n=10; LDN + Saline n=10; DMSO + MPTP n=8; LDN + MPTP n=9. The concentration of reduced GSH was normalized to protein. Data is plotted mean + SEM. Asterisk (*) indicates a statistically significant difference from DMSO + saline group and ampersand (&) indicates a statistically significant difference from LDN + Saline group where $p < 0.05$ via one-way ANOVA and a post hoc Holm-Sidak test.

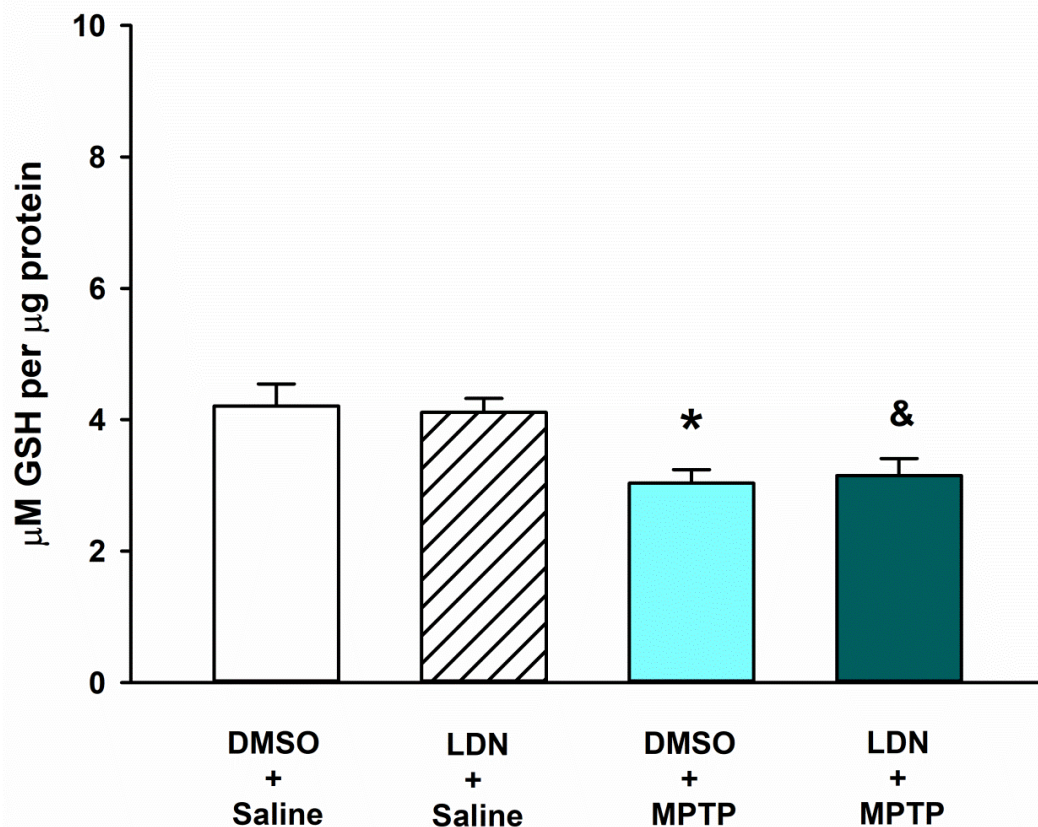


Figure 5.13. Reduced GSH concentration in the NAc. Mice were injected with saline or 20 mg/kg MPTP, DMSO VH or 0.5 mg/kg LDN-57444 as described in **Table 5.5**. The NAc was microdissected and assayed for reduced GSH. DMSO + Saline n=7; LDN + Saline n=9; DMSO + MPTP n=8; LDN + MPTP n=9. The concentration of reduced GSH was normalized to protein. Data is plotted mean + SEM. Asterisk (*) indicates a statistically significant difference from DMSO + saline group and ampersand (&) indicates a statistically significant difference from LDN + Saline group where $p < 0.05$ via one-way ANOVA and a post hoc Holm-Sidak test.

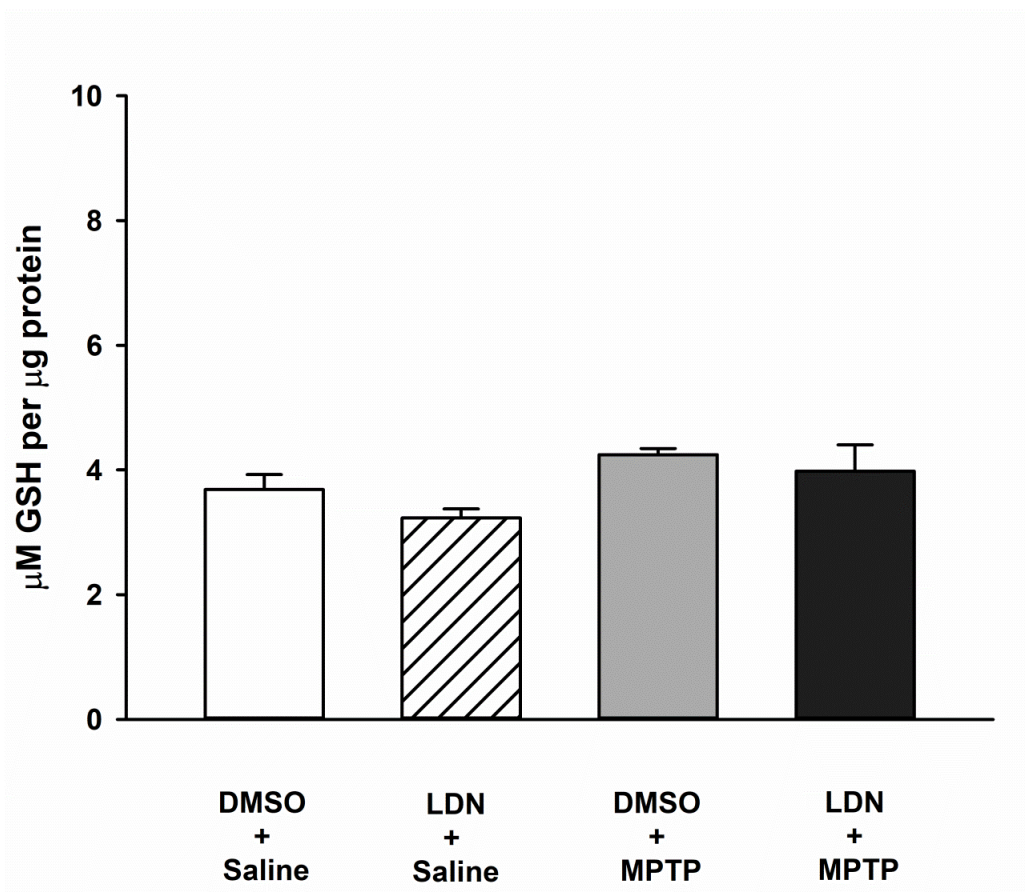


Figure 5.14. Reduced GSH concentration in the SN. Mice were injected with saline or 20 mg/kg MPTP, DMSO VH or 0.5 mg/kg LDN-57444 as described in **Table 5.5**. The SN was microdissected and assayed for reduced GSH. DMSO + Saline n=10; LDN + Saline n=9; DMSO + MPTP n=8; LDN + MPTP n=6. The concentration of reduced GSH was normalized to protein. Data is plotted mean + SEM. No statistically significant differences were detected between groups ($p > 0.05$) via one-way ANOVA.

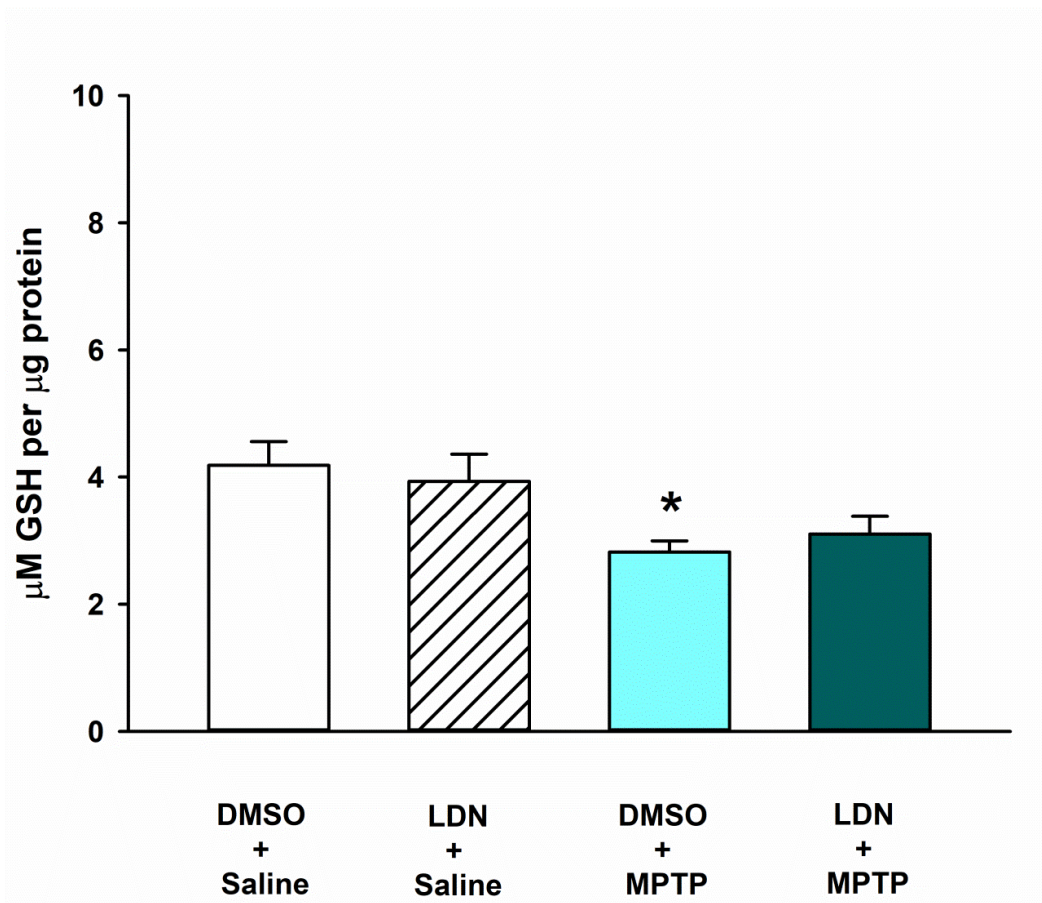


Figure 5.15. Reduced GSH concentration in the VTA. Mice were injected with saline or 20 mg/kg MPTP, DMSO VH or 0.5 mg/kg LDN as described in **Table 5.5**. The VTA was microdissected and assayed for reduced GSH. DMSO + Saline n=8; LDN + Saline n=10; DMSO + MPTP n=9; LDN + MPTP n=9. The concentration of reduced GSH was normalized to protein. Data is plotted mean + SEM. Asterisk (*) indicates a statistically significant difference from DMSO + saline group where $p < 0.05$ via one-way ANOVA and a post hoc Holm-Sidak test.

this assay tissue lysates are incubated with the suicide inhibitor, Ub-VME. Ub-VME attaches covalently to active DUBs, since Ub-VME can only bind if the active site is unoccupied by an inhibitor. In the ST and NAc, the amount of inactive UCH-L1 appeared to be the same between DMSO- and LDN-57444-treated mice (**Fig. 5.10**). Similarly, in the SN and VTA, LDN treatment did not have any effect on whether Ub-VME bound to UCH-L1 (**Fig. 5.11**).

The last endpoint in this experiment is reduced GSH, the levels of which are predicted to be affected by UCH-L1 function (Rose and Warms, 1983). In **Fig. 5.12**, reduced GSH levels are maintained in the LDN + saline group, but decreased in both groups exposed to MPTP in the ST. A similar pattern is followed in the NAc (**Fig. 5.13**). In the SN, however, reduced GSH is maintained following MPTP treatment (**Fig. 5.14**). In the VTA, reduced GSH is not affected by LDN treatment but is decreased in mice exposed to MPTP (**Fig. 5.15**).

Discussion

In this chapter, data from a dose response study with the UCH-L1 inhibitor LDN and a study combining LDN drug treatment with MPTP exposure were presented. These experiments sought to understand effects of UCH-L1 inhibition on both NSDA and MLDA neurons, which has not previously been demonstrated in the literature. It was hypothesized that a decrease in UCH-L1 activity would render MLDA neurons more vulnerable to MPTP-induced oxidative injury, and that the effects of MPTP would be exacerbated in NSDA neurons. LDN administration alone did not affect DA levels at

either doses (5 mg/kg or 0.5 mg/kg) administered and did not appear to have any overt toxic effects.

However, LDN administration did increase the DOPAC/DA ratio in the NAc, which we interpret as an increase in firing rate. Since there have been no previous reports in the literature that UCH-L1 inhibition results in higher firing rate of neurons (in fact, the opposite was demonstrated in hippocampal neurons and slices (Cartier et al., 2009; Gong et al., 2006)). We surmise this result could be a nonspecific effect of the higher dose of LDN, since it did not occur at the lower dose. It is possible that at the higher dose of LDN, inhibition of UCH-L3 occurred, but this possibility is somewhat unlikely based on the demonstrated specificity of the inhibitor for UCH-L1 over UCH-L3 (Liu et al., 2003). In addition, UCH-L3 modulation has not previously been shown to have effects on DA neurochemistry. LDN administration did not alter levels of mono-Ub or UPS function, calling into question whether target engagement was achieved. Caveats for interpretation of these data are discussed below.

Combination treatment with LDN and MPTP was used to determine if vulnerability of MLDA neurons to MPTP was achieved with inhibition of UCH-L1. To our surprise, LDN appeared to protect NSDA and MLDA neurons from loss of DA after MPTP exposure. UCH-L1 inhibition in hippocampal neurons results in less synaptic activity and deleterious effects in mice with respect to cognition and learning (Cartier et al., 2009; Gong et al., 2006), which are in contrast to our results. LDN administration could potentially have differential effects in different types of neurons, or differential effects on neurotransmitter dynamics versus synaptic structure since only the latter has been previously characterized in brain slices *ex vivo* and mice *in vivo*.

The observation that MLDA neurons are susceptible to loss of reduced GSH upon MPTP exposure was also unanticipated, and even more surprising still is that reduced GSH is not decreased in the SN. Previous studies employing chronic MPTP have shown that MLDA neurons are less susceptible to lipid peroxidation than NSDA neurons (Hung and Lee, 1998), which is a downstream consequence of oxidative stress, highlighting a potential difference in antioxidant capacity between NSDA and MLDA neurons. It is possible that at the acute time point and relatively low dose of MPTP used, reduced GSH levels are not indicative of the overall response to oxidative stress. In addition, with the techniques currently used to isolate tissue from the ST, NAc, SN, and VTA, it cannot be definitively stated that the effects on reduced GSH are specifically happening in NSDA or MLDA neurons. Contribution of glial GSH could be masking any DA neuron-specific effects, even though UCH-L1 is only expressed in neurons. What is clear, however, is that administration of LDN does not cause a decrease in reduced GSH by itself in any of the brain regions examined. Assuming that UCH-L1 inhibition did occur, these results suggest that UCH-L1 may not play a major role in regulation of the available amount of reduced GSH in neurons.

The use of a pharmacological inhibitor appeared to be a promising strategy to modulate UCH-L1 hydrolase activity without affecting total UCH-L1 protein levels. However, using LDN to accomplish this goal has a few inherent caveats. One, the compound was described as a reversible inhibitor (Liu et al., 2003), which means that perhaps it could have dissociated from UCH-L1 at the time of collecting the brain tissue and tissue processing and we simply missed the window of inhibition. Two, the effects of administration of LDN on DA axon terminals could not be directly examined due to the

fact that the NAc is too small a brain region to generate adequate sample for synaptosomes without pooling samples from multiple animals. Three, pharmacologically inhibiting UCH-L1 may not have an impact on its ability to bind and sequester mono-Ub, calling into question how useful the inhibitor may be to adequately model what effects loss of UCH-L1 function could have in the context of MPTP-induced injury. However, any changes in mono-Ub levels could be masked by glial cells. Our methods of target engagement, while addressing possible functional consequences of inhibition of UCH-L1, do not include measurements of LDN in mouse brain. Although we expect LDN to distribute in brain tissue due to its high lipophilicity, we cannot definitively without a shadow of a doubt say that in each mouse, LDN-57444 reached the brain region of interest. However, we did see effects of LDN-57444 in mouse brain, which strongly suggests that LDN-57444 did reach the targeted tissue.

The previously published study using LDN *in vivo* described a differential effect of UCH-L1 inhibition depending on the genotype of the mice used: in WT animals, inhibition of UCH-L1 caused UPS inhibition and subsequent accumulation of α -syn, while in α -syn overexpressing mice, UCH-L1 inhibition was protective due to upregulation of autophagic clearance of α -syn (Cartier et al., 2012). It is reasonable, therefore, to surmise that perhaps UCH-L1 inhibition could have a protective function in pathological conditions.

The contribution of UCH-L1 function in autophagic clearance was explored in **Chapter 4**, and it is not unreasonable to link a PD-related enzyme to the other major protein degradation pathway. In this context, downregulation of UCH-L1 function could result in upregulation of autophagy to promote degradation of toxic species, since we know that

MPTP causes an accumulation of Ub-proteins. The effects of LDN-57444 on autophagy have not yet been studied in either NSDA or MLDA neurons.

Further characterization of this effect would help clarify these data, but during the execution of the experiment unexpected toxicity of the combination of DMSO and MPTP was observed, which resulted in approximately 30-40% mortality of animals. On the other hand, DMSO alone did not cause any issues with endpoints measured or the overall well-being of the animals in the experiment. This toxic effect of the combination of DMSO and MPTP severely limits the feasibility of follow up experiments using the UCH-L1 inhibitor in combination with MPTP unless development of a different vehicle for LDN can be employed. Nevertheless, the results presented in this chapter have demonstrated that LDN administration did not have the expected effect on mono-Ub and UPS activity, but did appear to be protective against DA loss after MPTP in both NSDA and MLDA neurons. Potential mechanisms for how inhibition of UCH-L1 could protect DA neurons from MPTP are currently unclear but open to speculation.

Summary and conclusions

The UCH-L1 inhibitor, LDN-57444, was used *in vivo* to examine the effects of UCH-L1 inhibition in NSDA and MLDA neurons with respect to DA neurochemical and UPS-related endpoints. LDN itself was not toxic to DA neurons in either brain region as evidenced by no observed decrease in DA in either brain region with LDN treatment alone. When combined with MPTP exposure, however, LDN-57444 was protective against neurotoxicant-induced loss of DA in both brain regions. These results indicate

that the contribution of UCH-L1 activity to differential susceptibility of NSDA and MLDA neurons is currently not clear and needs further investigation.

REFERENCES

REFERENCES

- Behrouz, B., Drolet, R.E., Sayed, Z.A., Lookingland, K.J., Goudreau, J.L., 2007. Unique responses to mitochondrial complex I inhibition in tuberoinfundibular dopamine neurons may impart resistance to toxic insult. *Neuroscience* 147, 592–8. doi:10.1016/j.neuroscience.2007.05.007
- Behrouz, B., Drolet, R.E., Sayed, Z. a., Lookingland, K.J., Goudreau, J.L., 2007. Unique responses to mitochondrial complex I inhibition in tuberoinfundibular dopamine neurons may impart resistance to toxic insult. *Neuroscience* 147, 592–598. doi:10.1016/j.neuroscience.2007.05.007
- Borodovsky, A., Ovaa, H., Kolli, N., Gan-Erdene, T., Wilkinson, K.D., Ploegh, H.L., Kessler, B.M., 2002. Chemistry-Based Functional Proteomics Reveals Novel Members of the Deubiquitinating Enzyme Family. *Chem. Biol.* 9, 1149–1159. doi:10.1016/S1074-5521(02)00248-X
- Braak, H., Braak, E., 2000. Pathoanatomy of Parkinson's disease. *J. Neurol.* 247 Suppl, I13-10. doi:10.1007/PL00007758
- Cartier, A.E., Djakovic, S.N., Salehi, A., Wilson, S.M., Masliah, E., Patrick, G.N., 2009. Regulation of synaptic structure by ubiquitin C-terminal hydrolase L1. *J. Neurosci.* 29, 7857–68. doi:10.1523/JNEUROSCI.1817-09.2009
- Cartier, A.E., Ubhi, K., Spencer, B., Vazquez-Roque, R. a., Kosberg, K.A., Fourgeaud, L., Kanayson, P., Patrick, C., Rockenstein, E., Patrick, G.N., Masliah, E., 2012. Differential effects of UCHL1 modulation on alpha-synuclein in PD-like models of alpha-synucleinopathy. *PLoS One* 7. doi:10.1371/journal.pone.0034713
- Daina, A., Zoete, V., 2016. A BOILED-Egg To Predict Gastrointestinal Absorption and Brain Penetration of Small Molecules. *ChemMedChem* 1117–1121. doi:10.1002/cmdc.201600182
- Gong, B., Cao, Z., Zheng, P., Vitolo, O. V, Liu, S., Staniszewski, A., Moolman, D., Zhang, H., Shelanski, M., Arancio, O., 2006. Ubiquitin hydrolase Uch-L1 rescues beta-amyloid-induced decreases in synaptic function and contextual memory. *Cell* 126, 775–88. doi:10.1016/j.cell.2006.06.046
- Hung, H.-C., Lee, E.H., 1998. MPTP Produces Differential Oxidative Stress and Antioxidative Responses in the Nigrostriatal and Mesolimbic Dopaminergic Pathways. *Free Radic. Biol. Med.* 24, 76–84. doi:10.1016/S0891-5849(97)00206-2
- Hurst-Kennedy, J., Chin, L.S., Li, L., 2012. Ubiquitin C-terminal hydrolase L1 in tumorigenesis. *Biochem. Res. Int.* 2012. doi:10.1155/2012/123706
- Kelava, T., Čavar, I., Čulo, F., 2011. Biological actions of drug solvents. *Period. Biol.*

113, 311–320. doi:10.18054

- Leroy, E., Boyer, R., Auburger, G., Leube, B., Ulm, G., Mezey, E., Harta, G., Brownstein, M.J., Jonnalagada, S., Chernova, T., Dehejia, A., Lavedan, C., Gasser, T., Steinbach, P.J., Wilkinson, K.D., Polymeropoulos, M.H., 1998. The ubiquitin pathway in Parkinson's disease. *Nature*. doi:10.1038/26652
- Liu, Y., Lashuel, H.A., Choi, S., Xing, X., Case, A., Ni, J., Yeh, L.A., Cuny, G.D., Stein, R.L., Lansbury, P.T., 2003. Discovery of inhibitors that elucidate the role of UCH-L1 activity in the H1299 lung cancer cell line. *Chem. Biol.* 10, 837–846. doi:10.1016/j.chembiol.2003.08.010
- Rose, I.A., Warms, J.V.B., 1983. An enzyme with ubiquitin carboxy-terminal esterase activity from reticulocytes. *Biochemistry* 22, 4234–4237. doi:10.1021/bi00287a012

Chapter 6: Effects of Aging on DA Metabolic Homeostasis in NSDA and MLDA Neurons and Susceptibility to MPTP Toxicity

Introduction

Advanced age is the greatest risk factor for certain neurodegenerative diseases including PD (Calne and William Langston, 1983). In PD, motor symptoms such as bradykinesia, resting tremor, postural instability, and shuffling gait (Gelb et al., 1999) occur due to loss of NSDA neurons (Hornykiewicz, 1966) which are vital for the proper function of the basal ganglia pathway. Although NSDA neurons are lost over time as PD progresses, other DA neurons are relatively spared: TIDA neurons and MLDA neurons resist degeneration (Braak and Braak, 2000). DA loss is more pronounced in the putamen of PD patients versus other regions in the ST (Kish et al., 1988). MLDA neurons are often compared to NSDA neurons since they are phenotypically and anatomically similar, with soma in the ventral midbrain and axon terminals in the ventral striatum (Demarest and Moore, 1979). MLDA neurons in the VTA project to the NAc and release DA as part of the reward pathway. How dissimilarities between NSDA and MLDA neurons translate into differential susceptibility between the two DA neuron populations has recently been well-reviewed (Surmeier et al., 2017). Despite the available understanding about factors that underlie the differential susceptibility of NSDA and MLDA neurons, few studies have focused on the role of aging.

Studies with the neurotoxicant MPTP have shown that aged mice demonstrate greater motor deficits and have more loss of DA in the ST when compared to younger mice following chronic MPTP exposure (Gupta et al., 1986). While neurotoxicant treated mice

have limitations in modeling every aspect of PD, the MPTP model of DA depletion and oxidative stress can recapitulate differential susceptibility between NSDA and MLDA neurons (Hung and Lee, 1998; Behrouz et al., 2007). The differential susceptibility of MLDA and NSDA neurons observed in toxicant models has also been demonstrated in transgenic rodent models of PD-like pathology. In addition, studies in nonhuman primates have also recapitulated the resistance of VTA DA neurons to MPTP (Dopeso-Reyes et al., 2014). MLDA neurons are not susceptible to damage in rats after rAAV-mediated overexpression of α -syn in the ventral midbrain (Maingay et al., 2006), which indicates MLDA neurons are resistant to neurodegeneration elicited by distinct, but likely convergent etiologies of PD.

While these studies highlight intrinsic properties of MLDA neurons that enable survival in PD, there are non-neuronal cells in the cell body and axon terminal regions that likely play a role in differential responses to injury. While the synthesis and metabolism of DA in the presynaptic DA neuron is well understood, the role of glial cells has only relatively recently been appreciated and contribution of astrocytes to diseases such as PD should be explored (Forno et al., 1992). Astrocytes express the catabolic enzymes MAO-B and COMT and are the main non-neuronal cell type to metabolize DA (Levitt et al., 1982). Some studies suggest that astrocyte-mediated DA metabolism removes excessive synaptic DA, thus decreasing DA available for re-uptake, which would reduce cytoplasmic DA in the axon terminal available for toxic DA adduct formation. Other studies, however, indicate that astrocytes may also have pro-inflammatory functions that could exacerbate neuron death (Teismann et al., 2003). Mice treated with chronic MPTP display abnormal proliferation of astrocytes in the ST, a process known as

astrogliosis (Dervan et al., 2004). There is also emerging evidence that astrocytes may play a role in MLDA mechanisms related to drug abuse (Miguel-Hidalgo, 2009). If astrocytes safeguard MLDA neurons in aging and under neurotoxic stress, therapeutic strategies to promote protective functions of astrocytes in regions affected by PD could be developed.

The involvement of astrocytes in age-related decline of DA neuronal function in the NAc has not yet been explored. To this end, a series of experiments in various ages of mice were conducted to determine if DA synthesis, release, and metabolism are altered in MLDA neurons or astrocytes from aged mice and whether MLDA neurons are rendered susceptible to MPTP exposure with aging. We hypothesize that presynaptic synthesis and metabolism of DA by astrocytes is preserved in the NAc in younger but not aged mice, and that MLDA neurons are resistant to the effects of toxicant exposure in young, but not aged mice. Our study addresses the contribution of presynaptic metabolism and metabolism of DA by astrocytes in the aged NAc to better understand neuronal and astrocyte susceptibility to aging.

Results

Aged mice have less stored DA in the NAc, but astroglial metabolism of DA remains intact

We first sought to determine the basal neurochemical profile for DA in the NAc and ST in young, mature, old and aged mice. In the ST, DA was not altered in any of the various age groups compared to young control (**Fig. 6.1A**). In the NAc, however, DA is

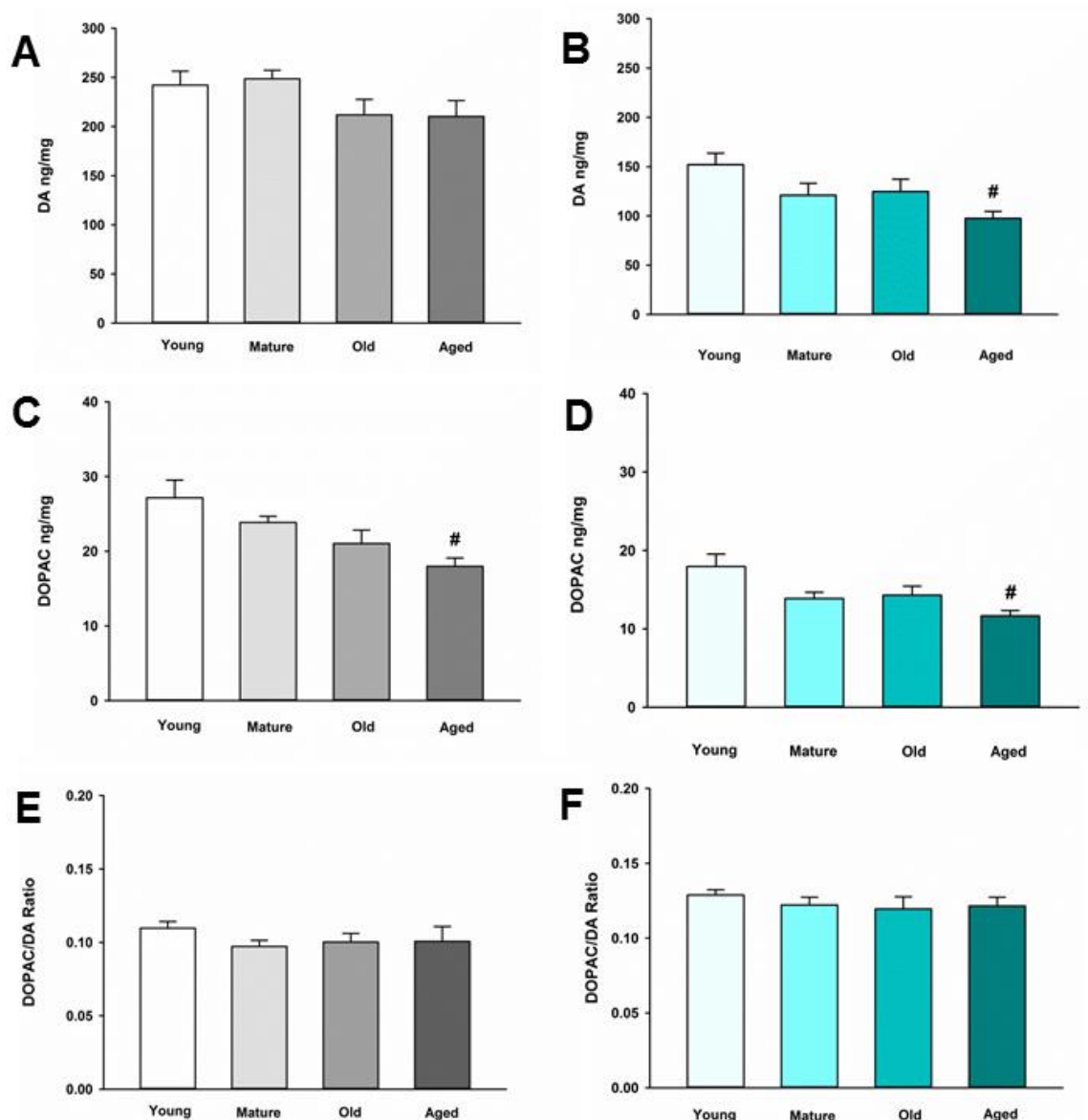


Figure 6.1. DA and DOPAC concentrations and DOPAC/DA ratio in ST (A, C, E) and NAc (B, D, F) in Young, Mature, Old, and Aged mice. Young, Mature, Old, and Aged mice were decapitated, brains were sectioned, and ST (Young n=7; Mature n=13; Old n=11; Aged n=10) and NAc (Young n=7; Mature n=13; Old n=10; Aged n=10) were collected in tissue buffer for HPLC-ED analysis. DA and DOPAC were measured and normalized to mg protein per sample. Concentrations for DOPAC were divided by DA to give the DOPAC/DA ratio. Data is expressed as mean + SEM. Data was analyzed via One-Way ANOVA with post hoc Holm-Sidak test. Pound symbol (#) indicates statistically significant difference ($p < 0.05$) from Young age group.

decreased in aged mice compared to young mice (**Fig. 6.1B**). The main metabolite of recaptured DA by MAO-B, DOPAC, also decreased in an age-dependent manner in the ST (**Fig. 6.1C**) and the NAc (**Fig. 6.1D**). The DOPAC/DA ratio is a measure of the relative rate of DA metabolism via MAO-B compared to release, uptake and storage in synaptic vesicles. The DOPAC/DA ratio is not changed in the ST (**Fig. 6.1E**) or the NAc between age groups (**Fig. 6.1F**). This latter observation indicates that the rate of DA metabolism relative to storage and release of recaptured DA from the synapse is not affected by aging in DA axon terminals in either brain region.

Given the observed age-related decrease DA stored in the NAc, we next sought to determine if synthesis and vesicular storage of DA in presynaptic axon terminals are also decreased in the NAc and ST of aged mice compared to younger mice. Total TH and Ser40 phosphorylated TH (p-TH) were measured in the NAc (**Fig. 6.4**). TH is the rate-limiting enzyme of DA synthesis and requires phosphorylation of serine residue 40 to become active (Campbell et al., 1986). To determine if reuptake or vesicular storage of DA could be affected by aging in the ST and NAc, DAT, and vesicular monoamine transporter 2 (VMAT2) were measured. We observed no change in levels of these proteins between young and aged mice in either brain region (**Fig. 6.4** and **Fig. 6.5**).

Extraneuronal metabolism of DA released from the pre-synaptic axon terminal produces HVA and 3-MT. To determine if age alters extraneuronal metabolism of released DA, HVA and 3-MT were measured in young and aged mice (**Fig. 6.2**). HVA was decreased with age in both the ST (**Fig. 6.2A**) and the NAc (**Fig. 6.2B**). 3-MT, however, was decreased with age in the ST (**Fig. 6.2C**) but not in the NAc (**Fig. 6.2D**). These results suggest that extraneuronal astrocyte metabolism of DOPAC to HVA by COMT or DA to

3-MT by MAO-B could be compromised in aged mice in the ST. In contrast, the extraneuronal (astroglial) metabolism of released DA does not appear to be diminished in the NAc as mice get older. We measured total COMT

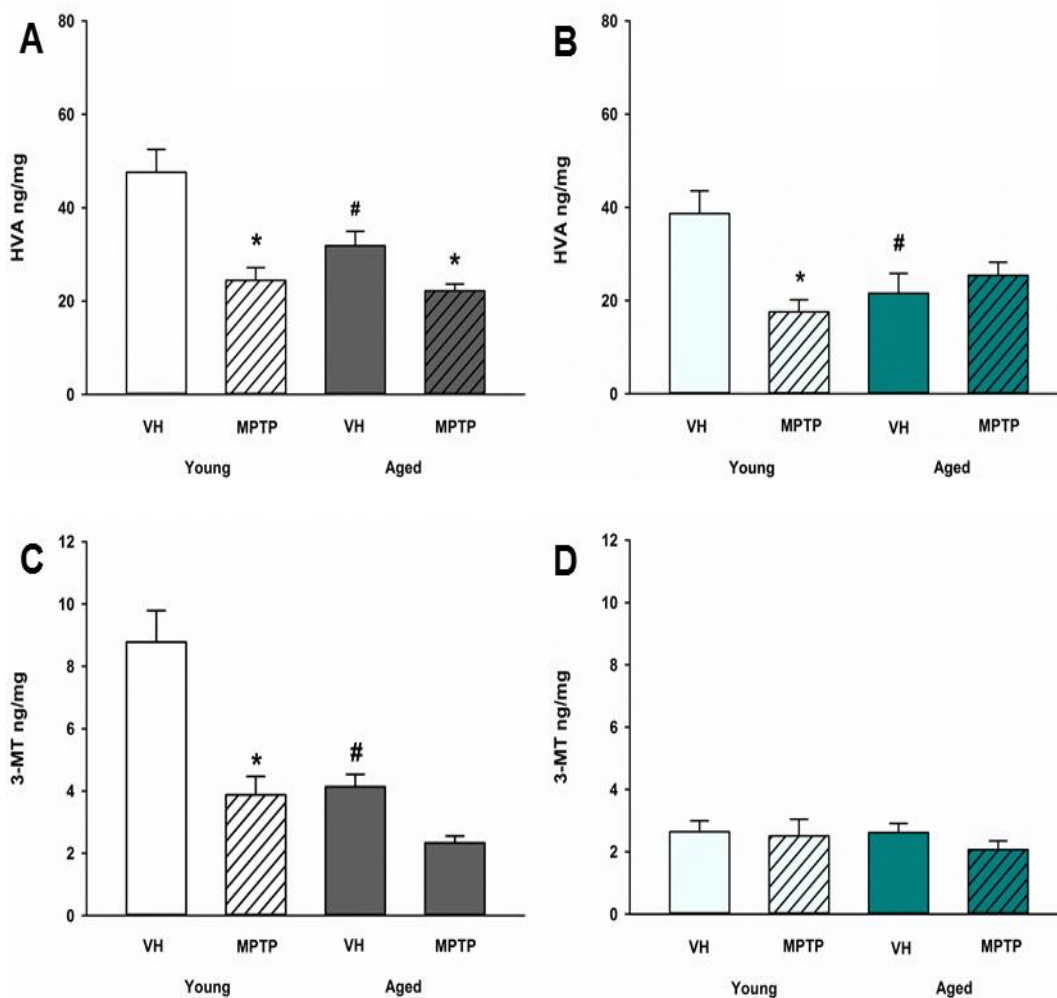


Figure 6.2. HVA and 3-MT concentrations after MPTP in Young and Aged ST (A, C) and NAc (B, D). Young and aged mice were treated with vehicle (VH) or 20 mg/kg MPTP and sacrificed 24 h later. Brains were sectioned and ST (Young VH n=7; Young MPTP n=8; Aged VH n=10; Aged MPTP n=10) and NAc (Young VH n=9; Young MPTP n=8; Aged VH n=8; Aged MPTP n=9) were collected in tissue buffer for HPLC-ED analysis. HVA and 3-MT were measured and normalized to mg protein per sample. Data is expressed as mean + SEM. Data was analyzed via Two Way ANOVA with post hoc Holm-Sidak test. Asterisk (*) indicates statistically significant difference ($p < 0.05$) from VH control, while pound symbol (#) represents statistically significant difference from Young VH.

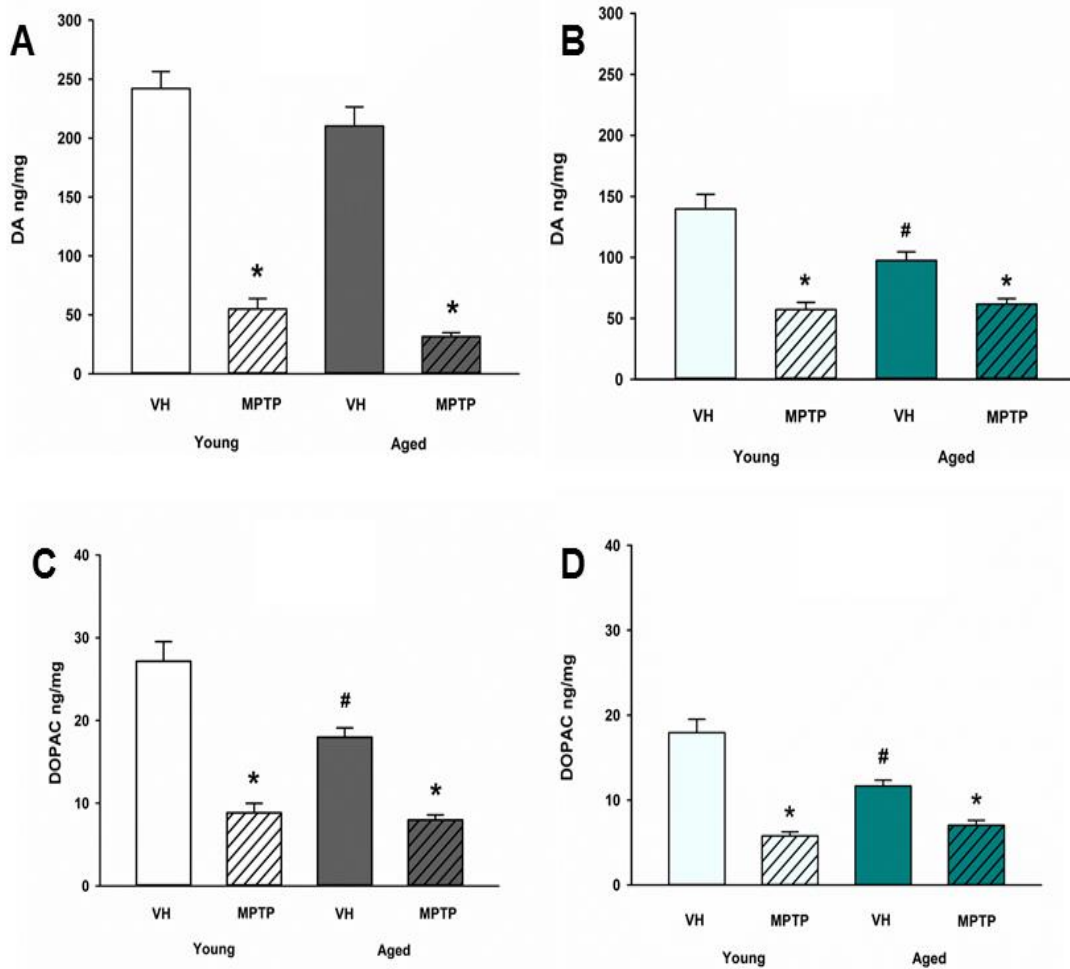


Figure 6.3. DA and DOPAC concentrations after MPTP in Young and Aged ST (A, C) and NAc (B, D). Young and aged mice were treated with vehicle (VH) or 20 mg/kg MPTP and sacrificed 24 h later. Brains were sectioned and ST (Young VH n=7; Young MPTP n=8; Aged VH n=10; Aged MPTP n=10) and NAc (Young VH n=7; Young MPTP n=8; Aged VH n=10; Aged MPTP n=8) were collected in tissue buffer for HPLC-ED analysis. DA and DOPAC were measured and normalized to mg protein per sample. Data is expressed as mean + SEM. Data was analyzed via Two Way ANOVA with post hoc Holm-Sidak test. Asterisk (*) indicates statistically significant difference ($p < 0.05$) from respective VH control within age group, while pound symbol (#) represents statistically significant difference from Young VH control.

protein in the ST and NAc in young and aged mice and found no significant difference between age groups (**Fig. 6.6**).

Acute MPTP exposure decreases DA, DOPAC, and astroglial DA metabolites in ST and NAc of both young and aged mice

Next, mice were challenged with the neurotoxicant MPTP to determine if loss of DA axonal stores in the NAc observed after MPTP exposure is exacerbated in aged mice. Aged mice are not more sensitive to acute MPTP-induced loss of DA in the ST (**Fig. 6.3A**) but aged mice are less susceptible to loss of DA in the NAc compared to young mice (**Fig. 6.3B**). Loss of DOPAC after MPTP is equivalent between age groups in the ST (**Fig. 6.3C**) but the MPTP-induced decrease in DOPAC is reduced in the NAc of aged mice (**Fig. 6.3D**). The diminished MPTP-induced loss of DA and DOPAC in the NAc aged mice compared to young mice may reflect the combined effects of age-dependent and MPTP-induced loss of DA and DOPAC. There may also be a lower limit to the extent of DA and DOPAC loss that can be achieved with a single, acute 20 mg/kg dose of MPTP. This lower limit for toxicant-induced DA impairment may represent a resilient population of NAc DA neurons in advanced age.

A differential effect of MPTP was also observed in the astroglial metabolism of DA in the MLDA and NSDA neurons. HVA, a direct metabolite of DOPAC, decreases in the ST of both young and old mice following acute MPTP treatment (**Fig. 6.2A**). In the NAc, however, HVA decreases in young mice treated with MPTP (**Fig. 6.2B**), but is not further decreased in aged mice treated with MPTP. Following MPTP treatment, the COMT DA metabolite 3-MT decreased in the ST of both young and aged mice (**Fig. 6.2C**) but was unchanged in the NAc of young or aged mice (**Fig. 6.2D**). The

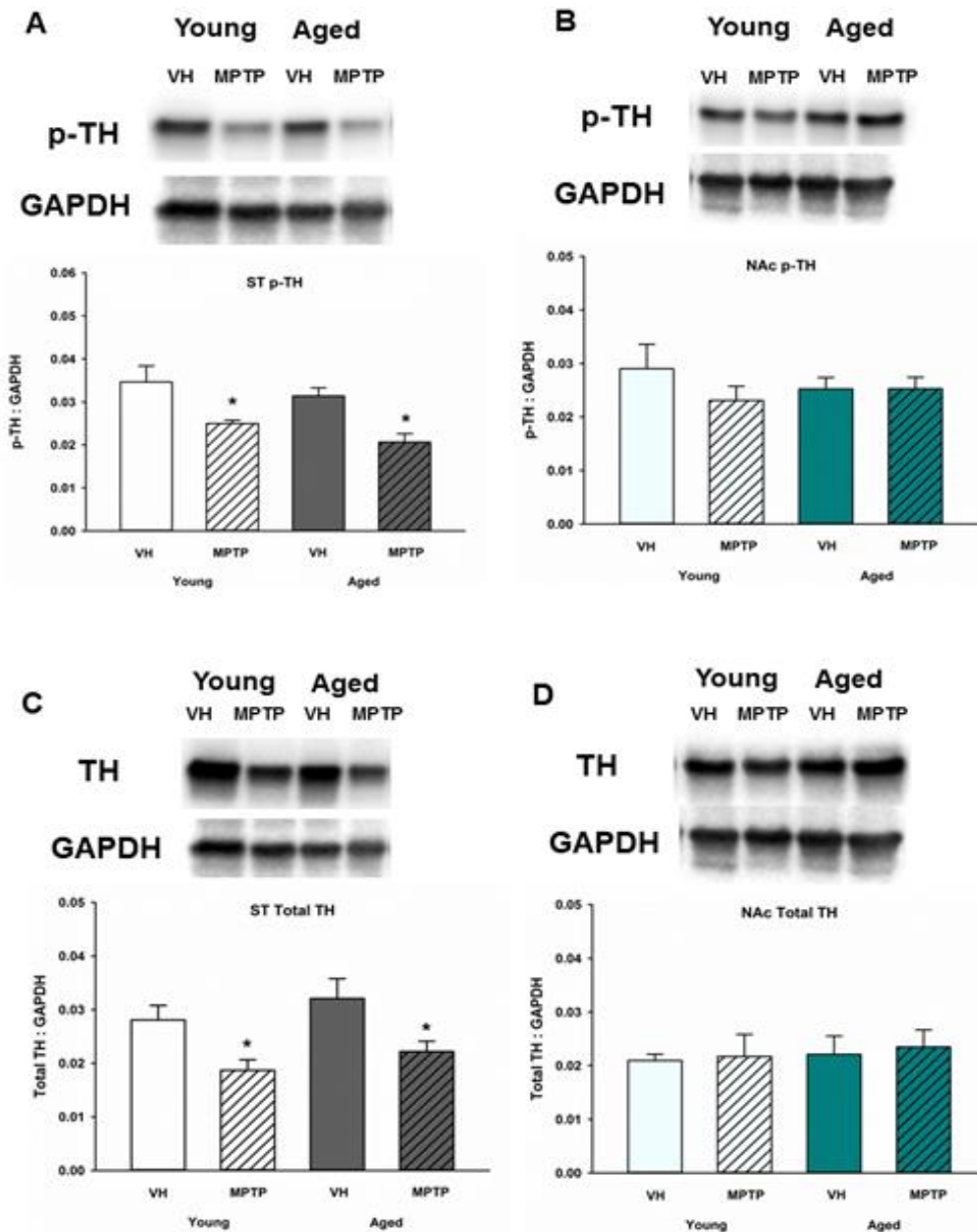


Figure 6.4. Ser40 p-TH and total TH protein levels in ST (A, C) and NAc (B, D). Young and aged mice were treated with vehicle (VH) or 20 mg/kg MPTP and sacrificed 24 h later. Brains were sectioned and ST (Young VH n=8; Young MPTP n=7; Aged VH n=10; Aged MPTP n=10) and NAc (Young VH n=8; Young MPTP n=7; Aged VH n=10; Aged MPTP n=10) were collected in lysis buffer for Western blot analysis. Representatives of immunoblots are shown in figure. Data is expressed as mean + SEM and analyzed via Two Way ANOVA with post hoc Holm-Sidak test. Asterisk (*) indicates statistically significant difference ($p < 0.05$) from VH control.

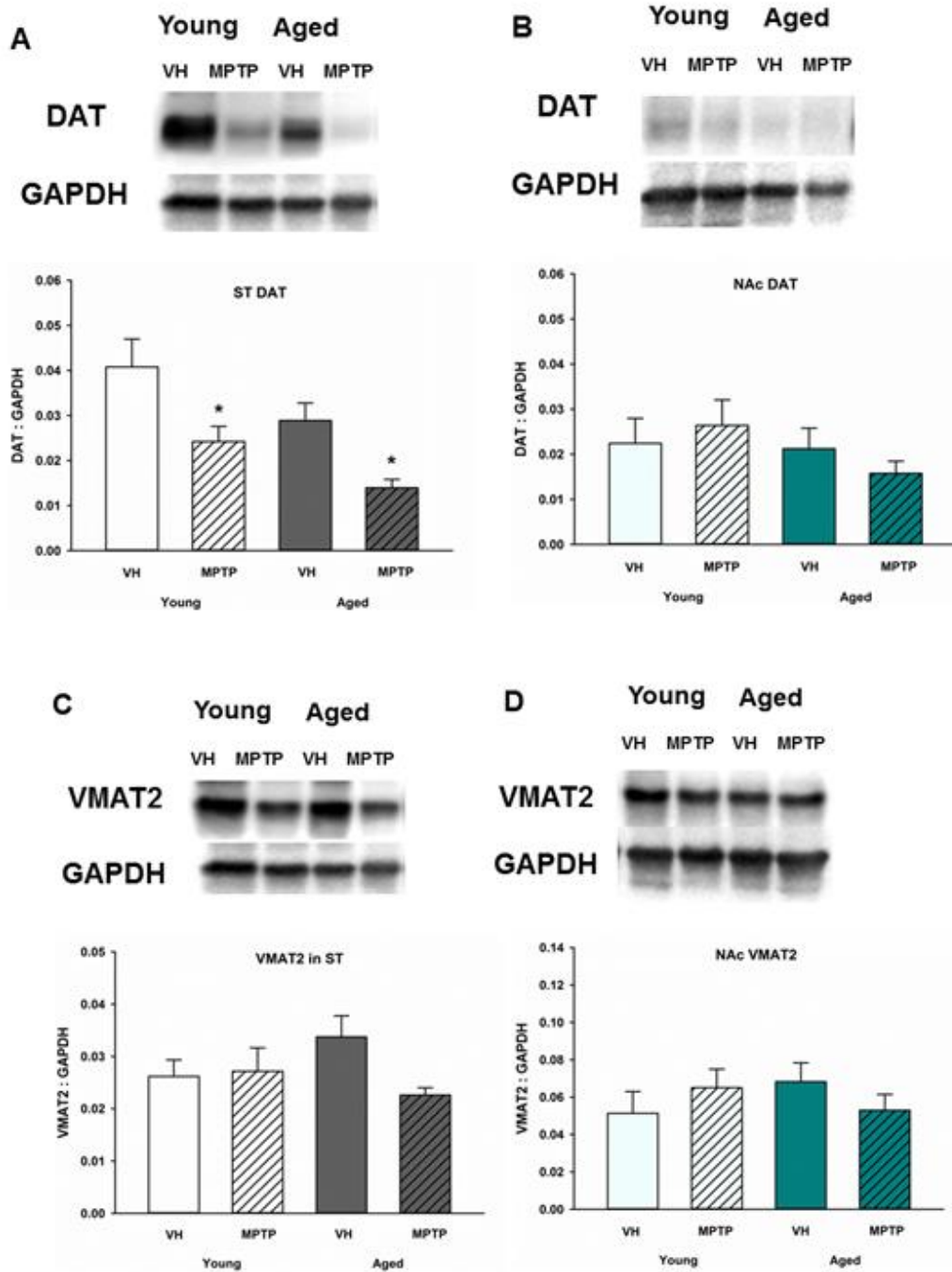


Figure 6.5. DAT and VMAT2 protein levels in ST (A, C) and NAc (B, D). Young and aged mice were treated with vehicle (VH) or 20 mg/kg MPTP and sacrificed 24 h later. Brains were sectioned and ST (Young VH n=8; Young MPTP n=8; Aged VH n=10; Aged MPTP n=9) and NAc (Young VH n=7; Young MPTP n=8; Aged VH n=9; Aged MPTP n=10) were collected in lysis buffer for Western blot analysis. Representatives of immunoblots are shown in figure. Data is expressed as mean + SEM and analyzed via Two Way ANOVA with post hoc Holm-Sidak test. Asterisk (*) indicates statistically significant difference ($p < 0.05$) from VH control.

unique MPTP-induced changes in HVA and 3MT in the ST and NAc of young and aged mice suggests that extraneuronal metabolism of DOPAC and DA in astrocytes are differentially regulated in these two brain regions in the context of acute neurotoxic stress.

Total and phosphorylated TH are decreased in the ST but not the NAc after MPTP in young and aged mice

Both Ser40 p-TH and total TH were decreased in the ST following MPTP treatment in young and aged mice (**Fig. 6.4A** and **Fig. 6.4C**). In the NAc, however, total TH and Ser40 p-TH expression was similar in saline and MPTP treated young and aged mice (**Fig. 6.4B** and **Fig. 6.4D**). Therefore, the MPTP-induced decrease in DA observed in the NAc is not due to a deficit in total or activated TH available for DA synthesis.

DAT is decreased in the ST, but not the NAc, after MPTP while VMAT2 is unchanged in both young and aged mice treated with MPTP

DAT is susceptible to oxidative damage and toxic adduct formation. In addition to synthesis and metabolism, cytoplasmic DA concentrations are regulated by the relative capacity for DA uptake via DAT and vesicular storage via VMAT. In addition to recycling synaptic DA, DAT is also the transporter through which the active MPTP metabolite, MPP⁺ enters into DA neurons and astrocytes. Relative DAT levels reflect the axon terminal DA uptake capacity. As such, measuring DAT expression can assess potential mechanisms for age and region specific differential susceptibility to MPTP and oxidative stress. DAT decreases in the ST following acute MPTP treatment (**Fig. 6.5A**). In contrast, DAT expression in the NAc is similar in vehicle and MPTP treated mice (**Fig. 6.5B**). VMAT2 packages DA into synaptic

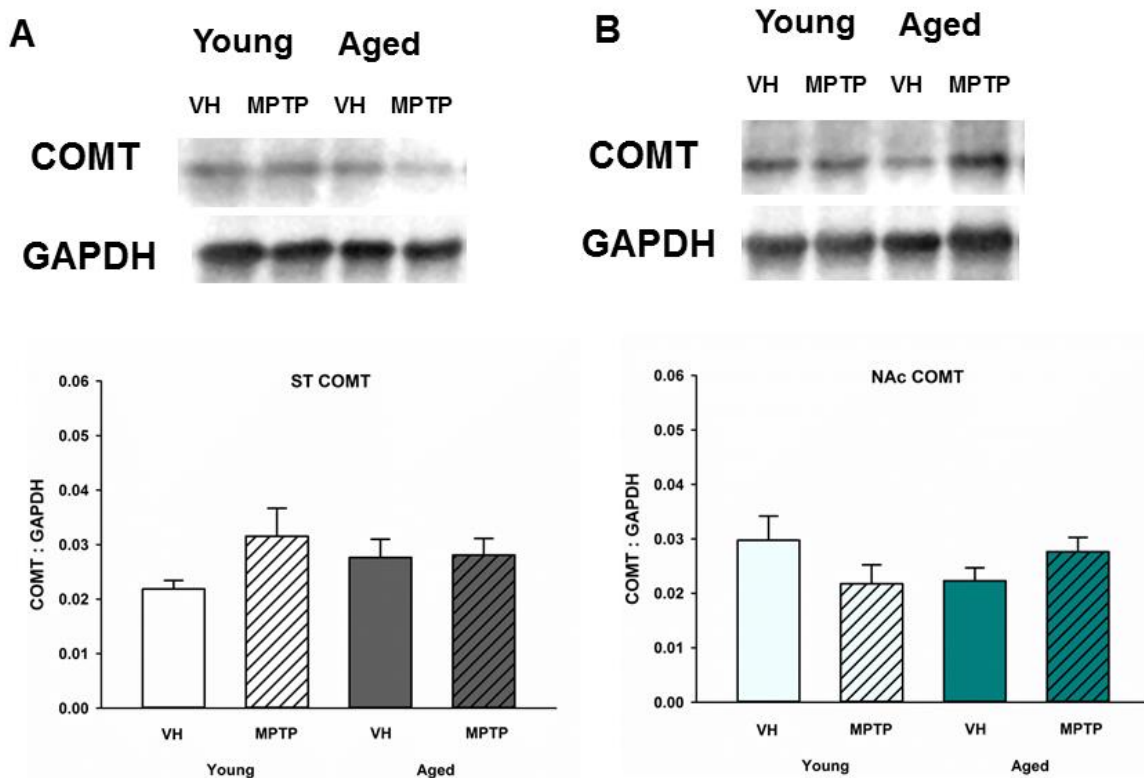


Figure 6.6. COMT protein levels in ST (A, C) and NAc (B, D). Young and aged mice were treated with vehicle (VH) or 20 mg/kg MPTP and sacrificed 24 h later. Brains were sectioned and ST (Young VH n=7; Young MPTP n=6; Aged VH n=9; Aged MPTP n=10) and NAc (Young VH n=7; Young MPTP n=5; Aged VH n=9; Aged MPTP n=10) were collected in lysis buffer for Western blot analysis. Representatives of immunoblots are shown in figure. Data is expressed as mean + SEM and analyzed via Two Way ANOVA with post hoc Holm-Sidak test. No significant differences were detected.

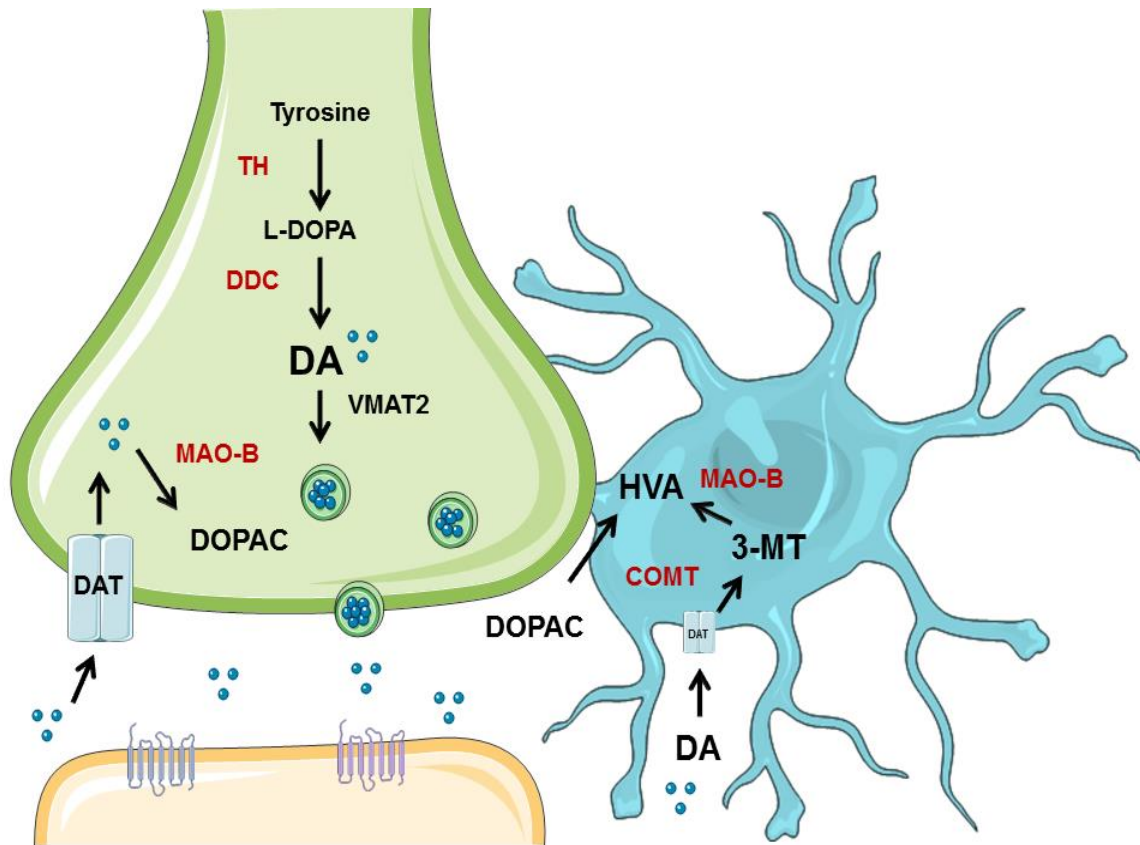


Figure 6.7. Overview of neuronal synthesis of DA and astrocyte metabolism.

DA synthesis occurs in a presynaptic neuron (green) and is metabolized or packaged into vesicles and released into the synapse. DA is synthesized from tyrosine by TH to L-DOPA, which is then metabolized to DA via dopa decarboxylase (DDC). DA can then be metabolized by MAO to DOPAC, which can be exported to astrocytes (blue) for further metabolism into HVA by COMT. If DA is packaged into vesicles by VMAT2, it can be released into the synapse and bind to receptors on the postsynaptic neuron (orange). DA can also be transported back into the axon terminal by DAT. If DA is exported to the astrocyte, it can undergo metabolism by COMT to 3-MT, which then can be metabolized by MAO to HVA. Graphics were adapted from Servier Medical Art (www.servier.com) with a Creative Commons Attribution 3.0 Unported License and edited for use in this figure.

vesicles and reduces the amount of cytoplasmic DA available for oxidative conversion to toxic molecules (e.g., dopamine quinones). VMAT2 was not altered in either brain region in saline and MPTP treated young or aged mice (**Fig.6.5C** and **Fig. 6.5D**).

Discussion

Young animals are frequently used in experiments designed to understand PD, yet have clear limitations in the study of a disease so closely associated with aging. We sought to evaluate age-related changes in two groups of midbrain DA neurons differentially affected in PD under basal conditions and following toxicant exposure to induce oxidative damage. Presynaptic and extraneuronal DA metabolic pathways were assessed in the brain regions containing the nerve terminals of the NSDA and MLDA neurons, the ST and NAc, respectively (**Fig. 6.7**). First, we determined if presynaptic DA metabolism and release are perturbed in aged mice. After investigating changes in DA concentrations between the ST and NAc, we observed that DA was not changed with age in the ST but was decreased in aged mice in the NAc. We examined levels of total and Ser40 p-TH to determine if the shortage of DA stores could be linked to deficient availability of the active form of the rate-limiting enzyme essential for DA synthesis. We did not, however, observe an age-related decrease in p-TH or total TH in the NAc. As such, it appears unlikely that impaired DA synthesis capacity is an explanation for the age-related decrease in MLDA stores.

If synthesis of DA was unperturbed in aged NAc, then perhaps reuptake of DA and presynaptic metabolism of DA to DOPAC increases with age, thus explaining the age-dependent decrease in MLDA stores. Aged mice were found to have less DOPAC than young mice. The majority of DOPAC is produced when DA is taken back up into the

axon terminal (Roth et al., 1976) and metabolized by MAO-B. Thus DOPAC represents an indirect index of DA that has been released and recaptured by the presynaptic neuron. Our observation that aged mice have lower DOPAC concentrations compared to young mice suggests that aged mice release less DA or metabolize less intraneuronal cytoplasmic DA. One study found that aged rats release less DA in the NAc as measured by microdialysis, which is congruent with our results (Huang et al., 1995). DA release is dependent on DA neuronal activity. The ratio of DOPAC/DA is an index of DA metabolism or turnover that is independent of DA nerve terminal density (Lookingland and Moore, 2005). Notably, the ratio of DOPAC/DA was similar in the NAc of young and aged mice, which suggests that there is no age-related change in DA turnover in MLDA neurons.

Changes in DA uptake or synaptic vesicular storage capacity, in part, regulate the pool of cytoplasmic DA that is susceptible to oxidative conversion to toxic molecules (Hastings et al., 1996). To understand whether reuptake or vesicular packaging could affect the concentrations of DA or DOPAC, we measured DAT and VMAT2 in ST and NAc after aging. No significant alterations in DAT and VMAT2 were found in aged mice in either brain region. As such, presynaptic reuptake and synaptic vesicle compartmentalization of DA are not affected by aging in the NAc.

If changes in presynaptic DA synthesis, release-reuptake and intraneuronal metabolism cannot explain the age-dependent decline in mesolimbic DA stores, then alterations in extraneuronal DA metabolism may play a role. We assessed extraneuronal metabolism of DA by astrocytes. Impairment of these glial cells have been reported to contribute to alterations in DA metabolism and progression of PD (Maragakis and Rothstein, 2006).

COMT within astrocytes metabolizes DOPAC to HVA. Measurement of HVA, therefore, provides an index of glial metabolism of extraneuronal DOPAC (Schendzielorz et al., 2013).

In the present study, both the ST and NAc experienced an age-related decrease in HVA, which suggests that less DOPAC is being metabolized into HVA in astrocytes of aged mice. The decrease in HVA could also reflect decreased glial COMT expression or number of glial cells expressing COMT, but COMT protein levels were not decreased in the ST or NAc of aged mice. Also, a prior study by Emsley and Macklis (2006) reported there is approximately the same density of astrocytes in the ST and NAc (Emsley and Macklis, 2006). Another DA metabolite, 3-MT, is the direct product of metabolism of DA by COMT in astrocytes and represents an indirect index of DA release (**Fig. 6.7**). Since 3-MT was not decreased with aging in the NAc, there could be an increase in activity of glial COMT (rather than increase in protein expression) to compensate for decreased substrate. Our results indicate that astrocytes retain the ability to metabolize DA in the NAc in aged mice.

Toxicant-induced oxidative stress results in a decrease in DA in the ST and NAc in addition to loss of axon terminals of NSDA and MLDA neurons. Susceptibility to axon terminal loss and cell body degeneration in NSDA neurons may increase with age (McGeer et al., 1977). We specifically used the acute MPTP dosing paradigm to allow investigation of DA axon terminal and local astrocyte responses in the absence of significant neuronal loss or denervation. Early events occurring following oxidative injury predispose neurons to eventual degeneration but also may represent potentially

reversible steps in the process that may be more amenable to disease modifying therapeutic intervention.

We observed that a single acute dose of MPTP was similar in NSDA and MLDA neurons in young and aged mice. With chronic, repeated exposure to MPTP, the susceptibility of NSDA neurons does appear to increase with age MPTP (Gupta et al., 1986). Chronic, repeated MPTP treatment eventually results in both ST axon terminal and SN cell body loss, while a single acute MPTP treatment causes axon terminal dysfunction but does not produce cell death at the time periods we examined.

DAT mediates the uptake of MPP⁺ and DAT expression is required for MPTP toxicity (Gainetdinov et al., 2002). DAT expression depends, to a large extent, on the number of DA axon terminals, but the overall and surface expression of DAT can change independent of the density of DA nerve terminals (Nirenberg et al., 1996). In the present study total DAT expression decreases to a similar extent in the ST after acute MPTP treatment in both young and aged mice. DAT expression was also similar in saline and MPTP treated mice in the NAc, regardless of age. As previously noted, the acute MPTP paradigm we employ does not result in significant NSDA axon terminal loss (Jackson-Lewis et al., 1995). Indeed, we observed no significant change in the expression a more stable marker of DA nerve terminal density (VMAT2) (Vander Borght et al., 1995) following acute MPTP treatment. Our findings, therefore, suggest that the early and likely dynamic decline in ST DAT expression following acute oxidative injury is not age dependent. Our results also provide some reassurance that capacity for MPP⁺ uptake via DAT does not change significantly with age and is not a likely confounding factor for our observations.

It should be noted that measurement of total DAT protein expression does not always parallel the DAT localized or expressed on the plasma membrane surface. This is an important caveat, since the surface expression of DAT determines the true uptake capacity of this transporter (Mortensen and Amara, 2003). Cytoplasmic DA available for oxidative conversion to more toxic molecules would be expected to be low in brain regions with high storage capacity (VMAT2) relative to re-uptake (DAT) (Uhl, 1998). Basal expression of VMAT2 or the ratio of VMAT2/DAT are inversely correlated with the susceptibility of different brain regions to MPTP (Hall et al., 2014; Lohr et al., 2016). VMAT2 expression was not changed in either brain region in young or aged mice and also did not change following acute MPTP treatment. This observation indicates there was no age-dependent change in the capacity of NSDA and MLDA axon terminals to store DA in synaptic vesicles. Direct or indirect measurement of VMAT2 is closely linked to nerve terminal density. Since the acute MPTP model we employed in the current study does not cause significant cell body or axon loss, then it is not surprising there was no observed change in VMAT2 following MPTP treatment.

Taken together, the above findings indicate alterations in pre-synaptic DA metabolic homeostasis do not appear to change with age in the NAc and are not likely to explain the age-dependent decline in NAc DA stores. Age-dependent changes in astrocyte metabolism of extraneuronal DA, however, may play a role. This is evidenced by impairment of extraneuronal metabolism of DA to 3-MT in the ST, but not the NAc, and that HVA produced by the metabolism of DOPAC via COMT and the conversion of 3MT by MAO, decreases in both the ST and NAc with age.

Since DAT is expressed in astrocytes as well as presynaptic neurons (Schömig et al., 1997), MPP⁺ can be taken up by astrocytes and cause oxidative damage. In the NAc, however, no decrease in 3-MT was observed in mice exposed to MPTP. Our results suggest that astrocytes could be playing a protective role in the NAc. Indeed, under conditions of heightened oxidative stress, astrocytes may be overwhelmed and no longer able to properly protect NSDA neurons terminating in the ST (Episcopo et al., 2013). Perhaps exceeding the protective capacity of glial cells contributes to neurodegeneration in PD. Consistent with this hypothesis, astrocytes are activated in regions containing NSDA neuron in younger primates treated with MPTP, but this is impaired in aged primates in association with impairment of striatal DA metabolism (Kanaan et al., 2008). In the present study we observed that astrocyte metabolism is relatively preserved in the NAc of aged mice and this maintained capacity for extraneuronal DA metabolism may stabilize DA homeostasis by rapidly clearing synaptic DA in MLDA neurons under conditions of oxidative stress-induced injury.

Summary and conclusions

This study was designed to test the hypothesis that MLDA neurons are less susceptible to age-related deficits in DA synthesis, metabolism and reuptake compared to well-characterized NSDA neurons. We measured the components of presynaptic and astrocyte DA synaptic homeostasis including metabolites, enzymes for synthesis, and transporters to understand the impact of aging on DA homeostasis in MLDA and NSDA neurons. We also exposed young and aged mice to acute neurotoxic insult to examine how aged MLDA neurons cope with oxidative stress. We conclude that DA and DOPAC

loss in the NAc is consistent with a decrease in release of DA while DA synthesis remains unaffected. As contributors to metabolism of DA released in the synapse, astrocytes in the NAc retain the ability to metabolize DA into 3-MT, suggesting these cells are capable of fulfilling their neuroprotective role in both young and aged mice. Our study highlights the importance of DA metabolism in astrocytes, which introduces the potential role of astrocytes in differential susceptibility of NSDA and MLDA neurons in PD.

REFERENCES

REFERENCES

- Behrouz, B., Drolet, R.E., Sayed, Z.A., Lookingland, K.J., Goudreau, J.L., 2007. Unique responses to mitochondrial complex I inhibition in tuberoinfundibular dopamine neurons may impart resistance to toxic insult. *Neuroscience* 147, 592–8. doi:10.1016/j.neuroscience.2007.05.007
- Benskey, M., Behrouz, B., Sunryd, J., Pappas, S.S., Baek, S.-H.H., Huebner, M., Lookingland, K.J., Goudreau, J.L., 2012. Recovery of hypothalamic tuberoinfundibular dopamine neurons from acute toxicant exposure is dependent upon protein synthesis and associated with an increase in parkin and ubiquitin carboxy-terminal hydrolase-L1 expression. *Neurotoxicology* 33, 321–31. doi:10.1016/j.neuro.2012.02.001
- Braak, H., Braak, E., 2000. Pathoanatomy of Parkinson's disease. *J. Neurol.* 247 Suppl, I13-10. doi:10.1007/PL00007758
- Calne, D., William Langston, J., 1983. AETIOLOGY OF PARKINSON'S DISEASE. *Lancet* 322, 1457–1459. doi:10.1016/S0140-6736(83)90802-4
- Campbell, D.G., Hardie, D.G., Vulliet, P.R., 1986. Identification of 4 Phosphorylation Sites in the N-Terminal Region of Tyrosine-Hydroxylase. *J. Biol. Chem.* 261, 489–492.
- Caudle, W.M., Richardson, J.R., Wang, M.Z., Taylor, T.N., Guillot, T.S., McCormack, A.L., Colebrooke, R.E., Di Monte, D.A., Emson, P.C., Miller, G.W., 2007. Reduced Vesicular Storage of Dopamine Causes Progressive Nigrostriatal Neurodegeneration. *J. Neurosci.* 27, 8138 LP-8148.
- Chinaglia, G., Alvarez, F.J., Probst, A., Palacios~ li, J.M., 1992. Mesostriatal and Mesolimbic Dopamine Uptake Binding Sites Are Reduced in Parkinson'S Disease and Progressive Supranuclear Palsy: a Quantitative Autoradiographic Study Using [3H]Mazindol. *Neuroscience* 49, 317–327. doi:10.1016/0306-4522(92)90099-N
- Dervan, A.G., Meshul, C.K., Beales, M., McBean, G.J., Moore, C., Totterdell, S., Snyder, A.K., Meredith, G.E., 2004. Astroglial plasticity and glutamate function in a chronic mouse model of Parkinson's disease. *Exp. Neurol.* 190, 145–156. doi:10.1016/j.expneurol.2004.07.004
- Dopeso-Reyes, I.G., Rico, A.J., Roda, E., Sierra, S., Pignataro, D., Lanz, M., Sucunza, D., Chang-Azancot, L., Lanciego, J.L., 2014. Calbindin content and differential vulnerability of midbrain efferent dopaminergic neurons in macaques. *Front. Neuroanat.* 8, 146. doi:10.3389/fnana.2014.00146
- Emsley, J.G., Macklis, J.D., 2006. Astroglial heterogeneity closely reflects the neuronal-

- defined anatomy of the adult murine CNS. *Neuron Glia Biol.* 2, 175–86.
doi:10.1017/S1740925X06000202
- Episcopo, F.L., Tirolo, C., Testa, N., Caniglia, S., Morale, M.C., Marchetti, B., 2013. Reactive astrocytes are key players in nigrostriatal dopaminergic neurorepair in the MPTP mouse model of Parkinson's disease: focus on endogenous neurorestoration. *Curr. Aging Sci.* 6, 45–55. doi:10.1093/pubmed/fdl064
- Forno, L.S., DeLanney, L.E., Irwin, I., Monte, D. Di, Langston, J.W., 1992. Chapter 36: Astrocytes and Parkinson's disease. pp. 429–436. doi:10.1016/S0079-6123(08)61770-7
- Gelb, D., Oliver, E., Gilman, S., 1999. Diagnostic criteria for Parkinson disease. *Arch. Neurol.* 56, 33–39.
- Gupta, M., Gupta, B.K., Thomas, R., Bruemmer, V., Sladek, J.R., Felten, D.L., 1986. Aged mice are more sensitive to 1-methyl-4-phenyl-1,2,3,6-tetrahydropyridine treatment than young adults. *Neurosci. Lett.* 70, 326–331. doi:10.1016/0304-3940(86)90573-2
- Hall, F.S., Itokawa, K., Schmitt, A., Moessner, R., Sora, I., Lesch, K.P., Uhl, G.R., 2014. Decreased vesicular monoamine transporter 2 (VMAT2) and dopamine transporter (DAT) function in knockout mice affects aging of dopaminergic systems. *Neuropharmacology* 76, 146–155. doi:10.1016/j.neuropharm.2013.07.031
- Hastings, T.G., Lewis, D.A., Zigmond, M.J., 1996. Role of oxidation in the neurotoxic effects of intrastriatal dopamine injections. *Proc. Natl. Acad. Sci.* 93, 1956–1961.
- Hornykiewicz, O., 1966. Dopamine (3-hydroxytyramine) and brain function. *Pharmacol.Rev.* 18, 925–964.
- Huang, R., Wang, C., Tai, M., Tsai, Y., Peng, M., 1995. NEUROSCIENCf IEHHIS 200, 61–64.
- Hung, H.-C., Lee, E.H., 1998. MPTP Produces Differential Oxidative Stress and Antioxidative Responses in the Nigrostriatal and Mesolimbic Dopaminergic Pathways. *Free Radic. Biol. Med.* 24, 76–84. doi:10.1016/S0891-5849(97)00206-2
- Jackson-Lewis, V., Jakowec, M., Burke, R.E., Przedborski, S., 1995. Time course and morphology of dopaminergic neuronal death caused by the neurotoxin 1-methyl-4-phenyl-1,2,3,6-tetrahydropyridine. *Neurodegeneration* 4, 257–269. doi:10.1016/1055-8330(95)90015-2
- Jackson-Lewis, V., Przedborski, S., 2007. Protocol for the MPTP mouse model of Parkinson's disease. *Nat. Protoc.* 2, 141–51. doi:10.1038/nprot.2006.342
- Kanaan, N.M., Kordower, J.H., Collier, T.J., 2008. Age and region-specific responses of microglia, but not astrocytes, suggest a role in selective vulnerability of dopamine neurons after 1-methyl-4-phenyl-1,2,3,6-tetrahydropyridine exposure in monkeys. *Glia* 56, 1199–1214. doi:10.1002/glia.20690

- Kish, S.J., Shannak, K., Hornykiewicz, O., 1988. Uneven Pattern of Dopamine Loss in the Striatum of Patients with Idiopathic Parkinson's Disease. *N. Engl. J. Med.* 318, 876–880. doi:10.1056/NEJM198804073181402
- Levitt, P., Pintart, J.E., Breakefield, X. O, 1982. Immunocytochemical demonstration of monoamine oxidase B in brain astrocytes and serotonergic neurons (central nervous system/rat/monoamine) 79, 6385–6389.
- Lohr, K.M., Chen, M., Hoffman, C.A., McDaniel, M.J., Stout, K.A., Dunn, A.R., Wang, M., Bernstein, A.I., Miller, G.W., 2016. Vesicular Monoamine Transporter 2 (VMAT2) Level Regulates MPTP Vulnerability and Clearance of Excess Dopamine in Mouse Striatal Terminals. *Toxicol. Sci.* 153, 79–88.
- Lookingland, K.J., Moore, K.E., 2005. Chapter VIII Functional neuroanatomy of hypothalamic dopaminergic neuroendocrine systems. *Handb. Chem. Neuroanat.* 21, 435–523. doi:10.1016/S0924-8196(05)80012-0
- Maingay, M., Romero-Ramos, M., Carta, M., Kirik, D., 2006. Ventral tegmental area dopamine neurons are resistant to human mutant alpha-synuclein overexpression. *Neurobiol. Dis.* 23, 522–32. doi:10.1016/j.nbd.2006.04.007
- Maragakis, N.J., Rothstein, J.D., 2006. Mechanisms of Disease: astrocytes in neurodegenerative disease. *Nat Clin Pr. Neurol* 2, 679–689. doi:ncpneuro0355 [pii]r10.1038/ncpneuro0355
- McGeer, P.L., McGeer, E.G., Suzuki, J.S., 1977. Aging and Extrapyrmidal Function. *Arch. Neurol.* 34, 33–35. doi:10.1001/archneur.1977.00500130053010
- Miguel-Hidalgo, J.J., 2009. The Role of Glial Cells in Drug Abuse. *Curr. Drug Abuse Rev.* 2, 76–82.
- Mogenson, G.J., Jones, D.L., Yim, C.Y., 1980. From motivation to action: Functional interface between the limbic system and the motor system. *Prog. Neurobiol.* 14, 69–97. doi:http://dx.doi.org/10.1016/0301-0082(80)90018-0
- Mortensen, O. V., Amara, S.G., 2003. Dynamic regulation of the dopamine transporter. *Eur. J. Pharmacol.* 479, 159–170. doi:10.1016/j.ejphar.2003.08.066
- Nirenberg, M.J., Vaughan, R.A., Uhl, G.R., Kuhar, M.J., Pickeli, V.M., 1996. The Dopamine Transporter Is Localized to Dendritic and Axonal Plasma Membranes of Nigrostriatal Dopaminergic Neurons. *J. Neurosci.* 76, 436–447.
- Roth, R.H., Murrin, L.C., Walters, J.R., 1976. Central dopaminergic neurons: Effects of alterations in impulse flow on the accumulation of dihydroxyphenylacetic acid. *Eur. J. Pharmacol.* 36, 163–171. doi:10.1016/0014-2999(76)90268-5
- Sawamoto, K., Nakao, N., Kobayashi, K., Matsushita, N., Takahashi, H., Kakishita, K., Yamamoto, A., Yoshizaki, T., Terashima, T., Murakami, F., Itakura, T., Okano, H., 2001. Visualization, direct isolation, and transplantation of midbrain dopaminergic neurons. *Proc. Natl. Acad. Sci. U. S. A.* 98, 6423–8. doi:10.1073/pnas.111152398

- Schendzielorz, N., Oinas, J.-P., Myöhänen, T.T., Reenilä, I., Raasmaja, A., Männistö, P.T., 2013. Catechol-O-Methyltransferase (COMT) Protein Expression and Activity after Dopaminergic and Noradrenergic Lesions of the Rat Brain. *PLoS One* 8, e61392.
- Schömig, E., Russ, H., Staudt, K., Martel, F., Gliese, M., Gründemann, D., 1997. The Extraneuronal Monoamine Transporter Exists in Human Central Nervous System Glia. pp. 356–359. doi:10.1016/S1054-3589(08)60764-4
- Schott, B.H., Niehaus, L., Wittmann, B.C., Schütze, H., Seidenbecher, C.I., Heinze, H.J., Düzel, E., 2007. Ageing and early-stage Parkinson's disease affect separable neural mechanisms of mesolimbic reward processing. *Brain* 130, 2412–2424. doi:10.1093/brain/awm147
- Surmeier, D.J., Obeso, J.A., Halliday, G.M., 2017. Selective neuronal vulnerability in Parkinson disease. *Nat. Rev. Neurosci.* 18, 101–113. doi:10.1038/nrn.2016.178
- Teismann, P., Tieu, K., Cohen, O., Choi, D.-K., Wu, D.C., Marks, D., Vila, M., Jackson-Lewis, V., Przedborski, S., 2003. Pathogenic role of glial cells in Parkinson's disease. *Mov. Disord.* 18, 121–129. doi:10.1002/mds.10332
- Uhl, G.R., 1998. Hypothesis: The role of dopaminergic transporters in selective vulnerability of cells in Parkinson's disease. *Ann. Neurol.* 43, 555–560. doi:10.1002/ana.410430503
- Vander Borght, T., Kilbourn, M., Desmond, T., Kuhl, D., Frey, K., 1995. The vesicular monoamine transporter is not regulated by dopaminergic drug treatments. *Eur. J. Pharmacol.* 294, 577–83.

Chapter 7: Effects of Aging on UCH-L1 Expression and Function in Brain Regions Containing NSDA and MLDA Neurons

Introduction

A major theme of this Dissertation thus far has been comparing the response of NSDA and MLDA neurons to neurotoxicant treatment in hopes that we can identify protective pathways maintained in non-susceptible neurons to develop new disease modifying therapeutics for PD. Therapeutics that halt or reverse neurodegeneration are currently lacking and represent a major unmet need. One pathway known to be compromised in PD is the UPS (Ross and Pickart, 2004), which is responsible for protein degradation. Two proteins found mutated in familial PD, parkin (Kitada et al., 1998) and UCH-L1 (Leroy et al., 1998), are enzymes associated with the UPS. The association between parkin and UCH-L1 mutations and PD highlights the importance of UPS-mediated protein degradation in neurons. The focus of this Dissertation is UCH-L1, which is a DUB shown to be important in maintaining available pools of mono-Ub (Setsuie and Wada, 2007). In **Chapter 3**, we demonstrated that both UCH-L1 and mono-Ub are decreased in the SN but maintained in the VTA 24 h after MPTP exposure. These results lead to the hypothesis that maintenance of UCH-L1 could be protective in MLDA neurons and that loss of UCH-L1 in NSDA neurons contributes to susceptibility to MPTP.

One of the major risk factors for developing PD is advanced age, and data examining DA metabolic homeostasis in aged NSDA and MLDA neurons was presented in **Chapter 6**. The vast majority of idiopathic PD patients without mutations are diagnosed

in elderly patients (Calne and William Langston, 1983), which suggests that the aging process could contribute to development and progression of PD. Indeed, oxidative stress in the brain is increased with aging (Floyd et al., 2001), and since oxidative stress is predicted to play a substantial role in development and progression of PD (Chen et al., 2008; Sun and Chen, 1998), aging and PD appear to go hand in hand. However, there is clearly a difference between neurodegeneration of NSDA neurons in PD and normal age-related decline of NSDA neurons (Stark and Pakkenberg, 2004). Why some elder patients develop PD while others do not is a critical question in neurodegenerative research. Investigation of differentially susceptible DA neuronal populations represents a valid approach to elucidate potentially protective mechanisms, such as UPS, that could be targeted in the treatment of PD.

In **Chapter 6**, it was demonstrated that NSDA and MLDA neurons in young and old mice are equally susceptible to acute MPTP exposure, and highlighted an important protective role for NAc astrocytes that may account for maintenance of MLDA resistance to toxicity. The function of the UPS, and in particular expression and function of UCH-L1, has not been examined in differentially susceptible neuronal populations of aged mice. In fact, no data is currently available in the literature describing the effects of aging on UCH-L1 expression in NSDA and MLDA neurons. In this chapter, we sought to determine if UCH-L1 expression or function are altered in aged mice, and whether responses of aged mice to MPTP is associated with maintenance of UCH-L1 expression and function in the VTA.

Results

UPS and UCH-L1 function and expression in NSDA and MLDA neurons in aged mice exposed to MPTP

In order to compare responses in brain regions containing NSDA and MLDA axon terminals (the ST and NAc, respectively), whole tissue microdissection was employed. UPS function in the ST (**Fig. 7.1**) is maintained between young and aged mice exposed to MPTP. In the NAc, similarly, UPS function was not impaired in either age or treatment group (**Fig. 7.2**).

UPS function and UCH-L1 expression in ST synaptosomes from young and aged mice following acute MPTP exposure

Using ST synaptosomes, axon terminals from NSDA neurons were isolated to specifically measure endpoints that may be masked by the presence of other neuronal or glial populations in the brain region. Ub protein accumulation was measured in ST synaptosomes and the UPS was found to be impaired in both age groups 24 h after MPTP treatment (**Fig. 7.3**). Next, to determine if UCH-L1 expression is decreased with aging and neurotoxicant treatment in axon terminals of NSDA neurons, UCH-L1 was measured in ST synaptosomes in young and aged mice exposed to MPTP (**Fig. 7.4**). UCH-L1 was not different in either age or neurotoxicant treatment groups.

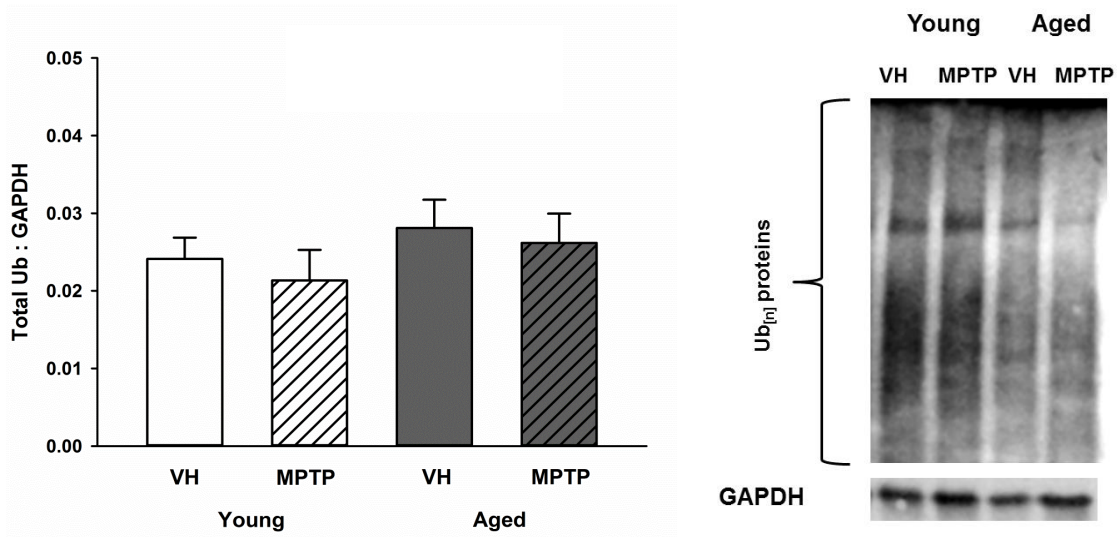


Figure 7.1. Total Ub protein in the ST. Young (VH n=7; MPTP n=5) and Aged (VH n=10; MPTP n=9) mice were injected with VH or MPTP and sacrificed 24 h later. The ST was microdissected and total Ub proteins were measured via Western blotting. Data is plotted as mean + SEM. No statistically significant differences were detected ($p > 0.05$) via two-way ANOVA.

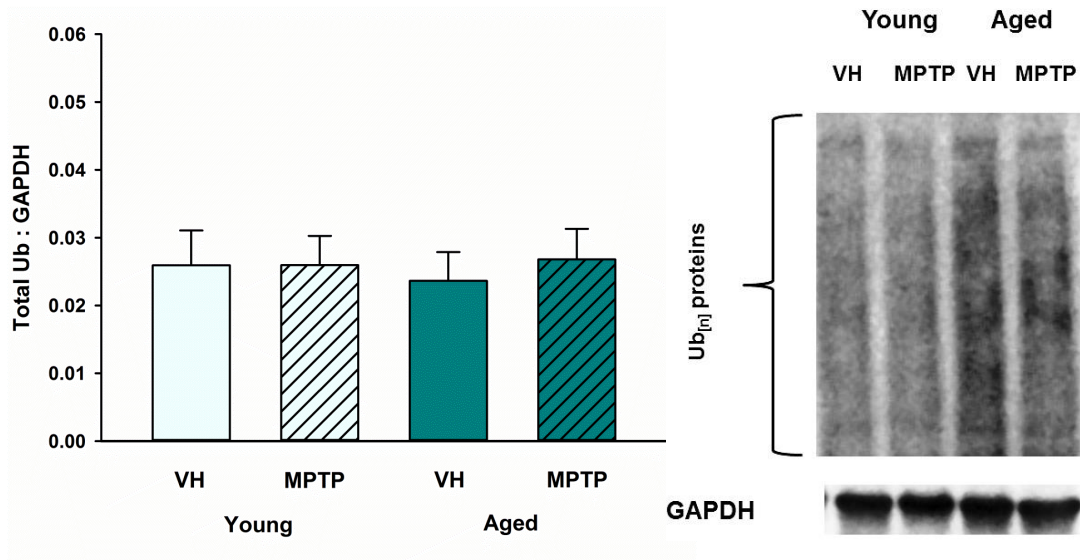


Figure 7.2. Total Ub protein in the NAc. Young (VH n=7; MPTP n=7) and Aged (VH n=9; MPTP n=10) mice were injected with VH or MPTP and sacrificed 24 h later. The NAc was microdissected and total Ub proteins were measured via western blotting. Data is plotted as mean + SEM. No statistically significant differences were detected via two-way ANOVA ($p > 0.05$).

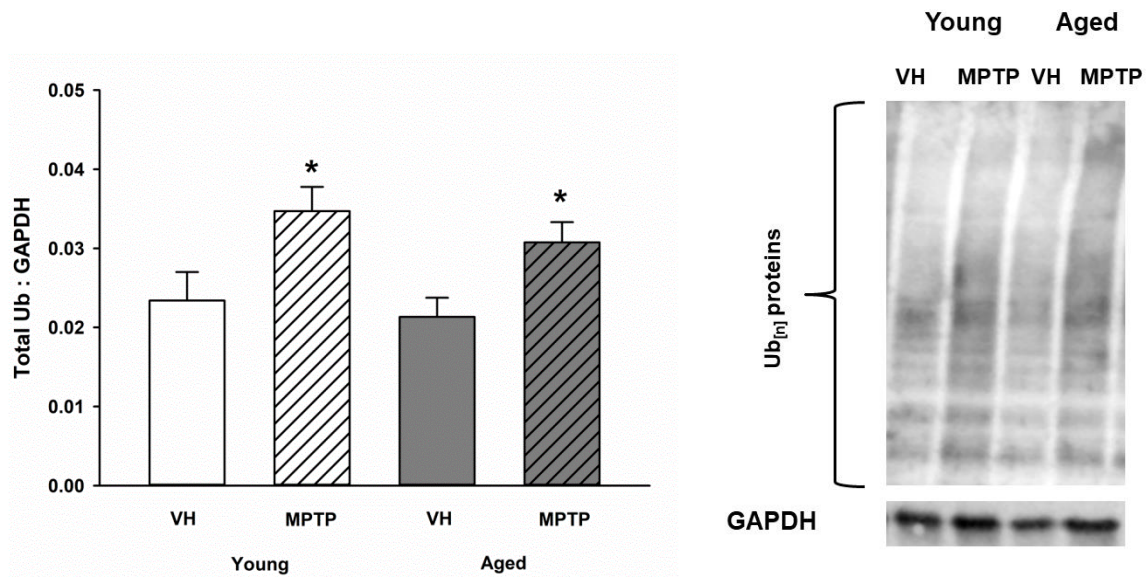


Figure 7.3. Total Ub proteins in ST synaptosomes. Young (VH n=7; MPTP n=8) and Aged (VH n=9; MPTP n=9) mice were injected with VH or MPTP and sacrificed 24 h later. ST synaptosomes were prepared and total Ub was measured via Western blotting. Data is plotted as mean + SEM and asterisk (*) indicates a statistically significant difference where $p < 0.05$ via two-way ANOVA and a post hoc Holm-Sidak test.

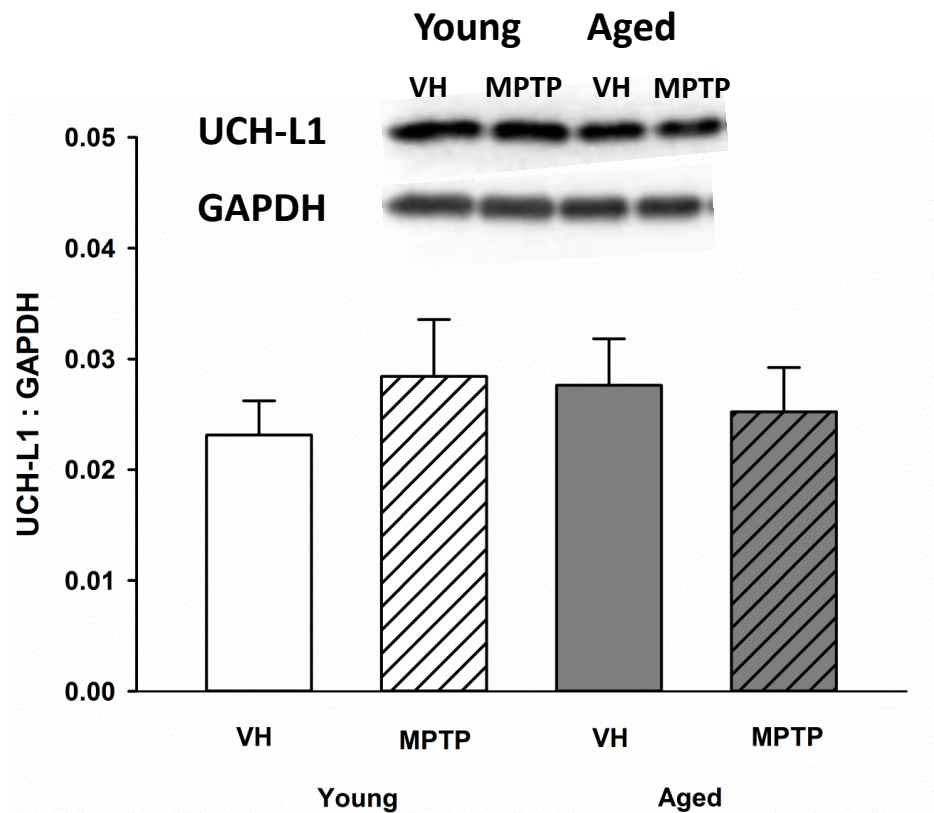


Figure 7.4. UCH-L1 protein in ST synaptosomes. Young (VH n=7; MPTP n=8) and Aged (VH n=10; MPTP n=10) mice were injected with VH or MPTP and sacrificed 24 h later. ST synaptosomes were prepared and UCH-L1 was measured via Western blotting. Data is plotted as mean + SEM. No statistically significant differences were detected via two-way ANOVA ($p > 0.05$).

UPS impairment, UCH-L1 expression and function in SN and VTA in aged mice

To examine the effects of aging on UPS function under basal conditions in the SN and VTA, accumulation of total Ub proteins was measured (**Fig. 7.5**). In both the SN and VTA, aged mice showed increased total Ub proteins and there was no difference in the extent of Ub accumulation between the two brain regions. To determine if expression of UCH-L1 is decreased with advanced age, UCH-L1 protein expression was measured in SN and VTA between young and aged mice (**Fig. 7.6**). There was no age-related change in UCH-L1 protein in either brain region. UCH-L1 function was assessed by measuring mono-Ub levels (**Fig. 7.7**) and there were no differences between brain regions or age groups.

Effects of MPTP on UCH-L1 expression in the SN and VTA of young and aged mice

Although UCH-L1 expression and function do not appear to be impaired with normal aging, it is of interest to determine if the decrease in UCH-L1 observed in the SN (Benskey et al., 2012) (**Fig. 3.11**) in young mice is exacerbated in aged mice. When we measured UCH-L1 in the SN in young and aged mice 24 h after MPTP exposure, we found that UCH-L1 was decreased to the same extent in both young and aged mice (**Fig. 7.8**). In the VTA, where UCH-L1 has previously been demonstrated to be maintained 24 h after MPTP exposure (**Fig. 3.12**), UCH-L1 was measured in young and aged mice exposed to MPTP. UCH-L1 expression was maintained in both young and aged mice 24 h after MPTP expression (**Fig. 7.9**).

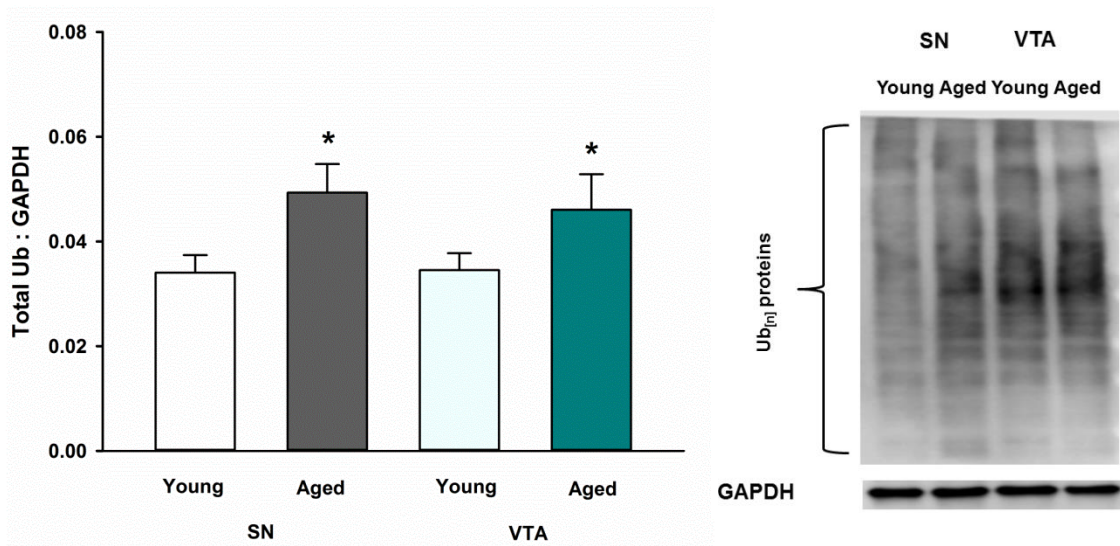


Figure 7.5. Total Ub protein in the SN and VTA in Young and Aged mice. Young and Aged mice were sacrificed and the SN (Young n=7; Aged n=8) and VTA (Young n=9; Aged n=9) were microdissected and total Ub proteins were measured via western blotting. Data is plotted as mean + SEM and asterisk (*) indicates a statistically significant difference between groups via two-way ANOVA and a post hoc Holm-Sidak test.

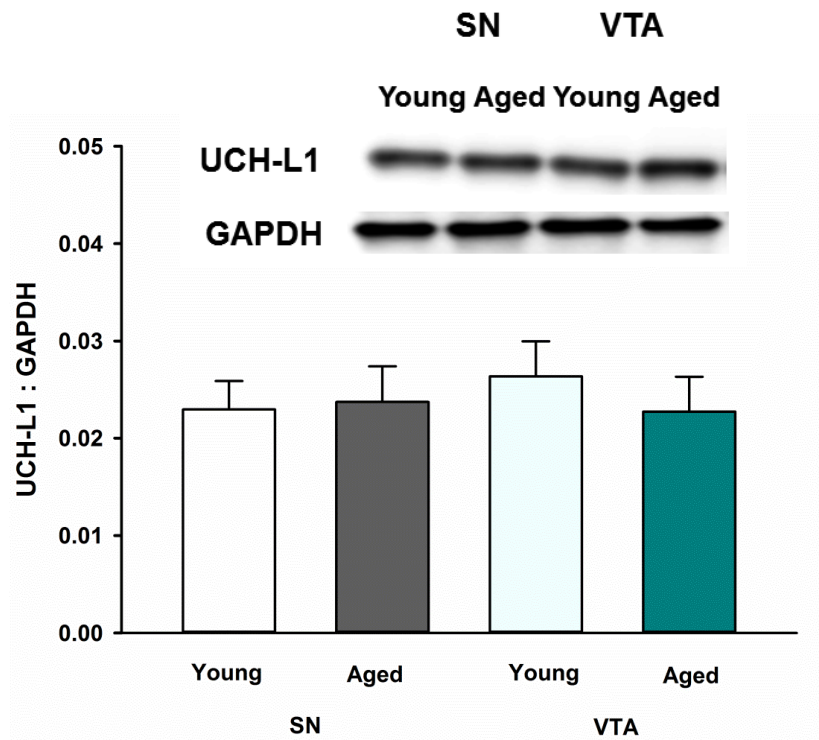


Figure 7.6. UCH-L1 protein in the SN and VTA in Young and Aged mice. Young and aged mice were sacrificed and the ST (Young n=9; Aged n=9) and NAc (Young n=8; Aged n=8) were microdissected and UCH-L1 was measured via western blotting. Data is plotted as mean + SEM. No statistically significant difference was detected via two-way ANOVA ($p > 0.05$).

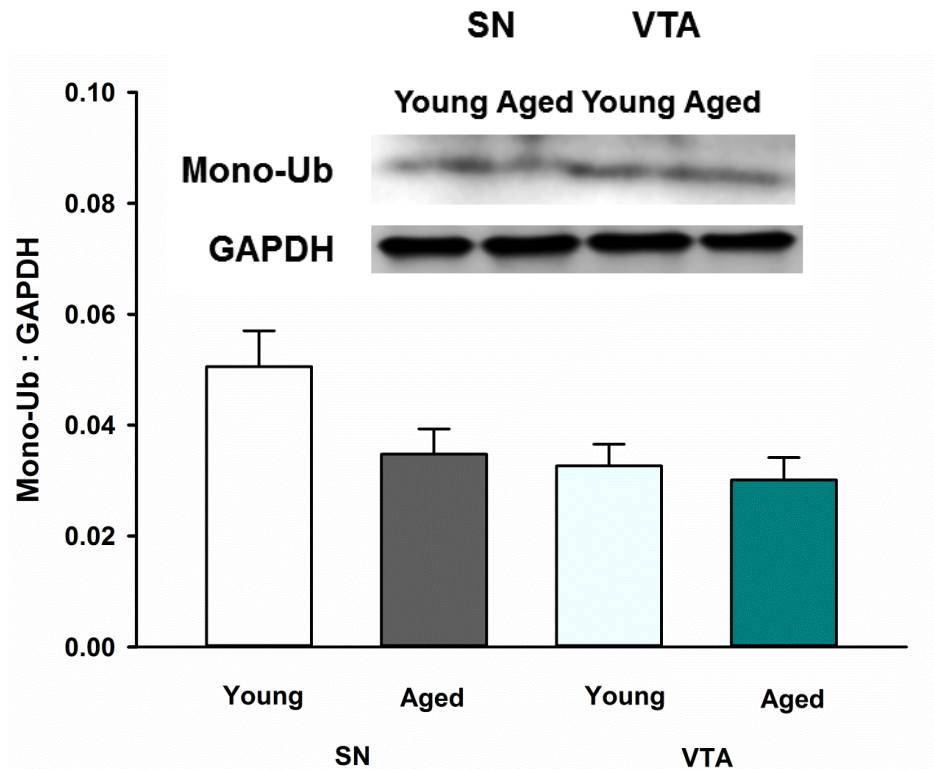


Figure 7.7. Mono-Ub protein in the SN and VTA in Young and Aged mice. Young and aged mice were sacrificed and the SN (Young n=9; Aged n=5) and VTA (Young n=5; Aged n=6) were microdissected and mono-Ub protein was measured via western blotting. Data is plotted as mean + SEM. No statistically significant difference was detected between groups via two-way ANOVA ($p > 0.05$).

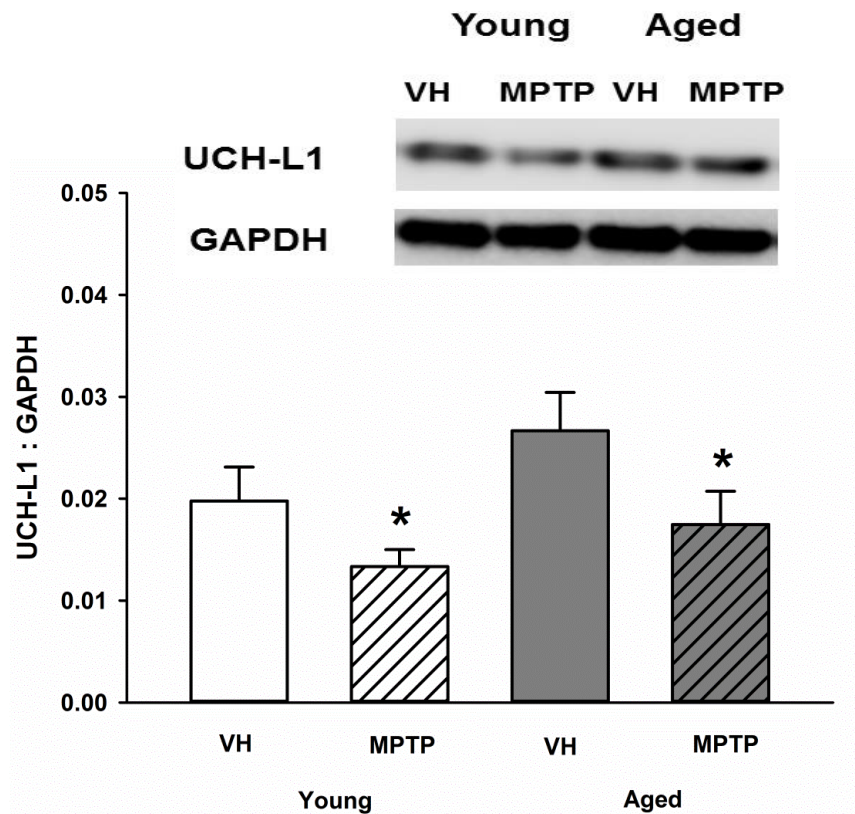


Figure 7.8. UCH-L1 protein in the SN Young and Aged mice treated with VH or MPTP. Young (VH n=7; MPTP n=6) and Aged (VH n=8; MPTP n=8) mice were sacrificed and the SN was microdissected and UCH-L1 was measured via western blotting. Data is plotted as mean + SEM. No statistically significant difference was detected via two-way ANOVA ($p > 0.05$).

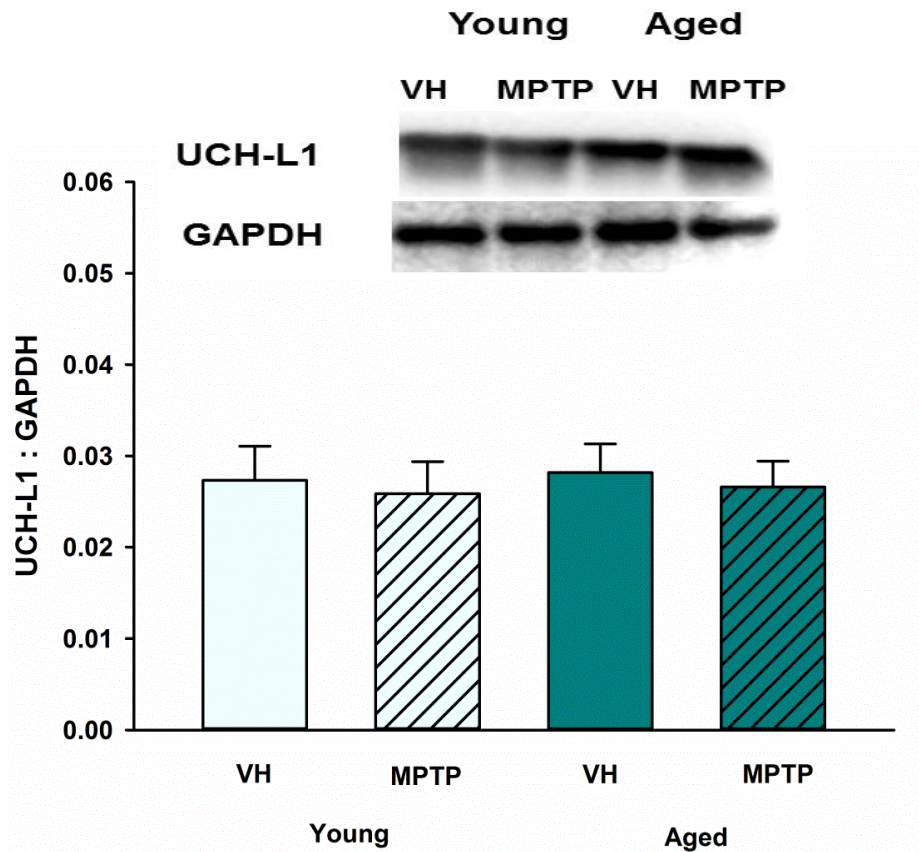


Figure 7.9. UCH-L1 protein in the VTA Young and Aged mice treated with VH or MPTP. Young (VH n=8; MPTP n=8) and Aged (VH n=9; MPTP n=10) mice were sacrificed and the VTA was microdissected and UCH-L1 was measured via western blotting. Data is plotted as mean + SEM. No statistically significant difference was detected via two-way ANOVA ($p > 0.05$).

Discussion

In this chapter, the effects of aging and MPTP exposure were determined in NSDA axon terminals between young and aged mice. UPS function was estimated by measuring total Ub proteins. When the UPS is impaired, a buildup of poly-Ub substrates occurs (Canu et al., 2000) and we can compare the extent of accumulation between brain regions, ages, and treatment groups. In ST synaptosomes in aged and young mice, MPTP caused impairment of the UPS. This effect was not observed in ST microdissected tissue, however. The discrepancy in these results points out an important caveat for comparison between the ST and NAc in these studies, mainly because we are unable to assay endpoints specifically in axon terminals in the NAc due to the small size of the NAc in mice. In ST whole tissue, perhaps glial UPS function is intact, which masks the impairment we see in ST synaptosomes.

Although both synaptosome preps and tissue microdissection approaches are useful and provide insight into age and neurotoxicant exposure related impairments of UPS function, we must use some caution in interpreting the response, because a lack of impairment in the UPS in the NAc could also logically be due to glial cells. Similar to UPS function, UCH-L1 was also not altered in ST synaptosomes from young and aged mice exposed to MPTP. These results in young mice exposed to MPTP are congruent with UCH-L1 expression in ST synaptosomes demonstrated in **Chapter 4**.

Because there was no increased susceptibility to MPTP in aged NSDA and MLDA neurons in **Chapter 6**, we sought to determine if UPS function was altered with aging in the SN and VTA. We found that the UPS is impaired with aging in both brain regions,

which is an unexpected finding based on the lack of UPS impairment with age in the ST and NAc. Clearly, there are differences in UPS dynamics between the cell body regions and axon terminal regions, especially with respect to UCH-L1 which is only differentially regulated in the SN and VTA and maintained in axon terminal regions after MPTP exposure. Whether this difference between cell body regions and axon terminals is due to transport of UCH-L1 is unknown, since no mechanism for how UCH-L1 is transported from cell body regions to axon terminals has been reported. The fact that the UPS was impaired in both the SN and VTA with age demonstrates that aging impairs UPS activity to a similar degree in both regions.

We predicted that the VTA would be resistant to age-dependent UPS impairment based on the resistance of MLDA neurons to MPTP, but this was not the case. Understandably, the effect of acute MPTP on UPS is predicted to be much milder compared to the effects a large age difference between mice could produce. When we measured UCH-L1, we found no age-related decrease in UCH-L1 in either the SN or VTA. These results indicate that although UCH-L1 expression was maintained in each region with aging, total Ub proteins were increased with aging. To understand whether UCH-L1 function is decreased in aged SN or VTA, we measured mono-Ub levels and did not detect a difference in aged mice. Therefore, although UCH-L1 expression and function remain intact in aged SN and VTA, UPS function is impaired and there is an accumulation of Ub substrates. These results demonstrate an apparent disconnect between UCH-L1 expression and function with regard to UPS function and suggest that there are likely other factors that mediate UPS activity in aging. Another question addressed in these experiments is changes in UCH-L1 expression after MPTP in the cell body regions of

NSDA and MLDA neurons in aged mice. We wanted to know whether the decrease in UCH-L1 protein in the SN would be exacerbated in aged mice or if the VTA is rendered susceptible to loss of UCH-L1 expression with advanced age. The results showed that UCH-L1 is decreased to a similar extent in the SN in young and aged mice 24 h after MPTP exposure. Similarly, NSDA axon terminals also do not appear to be more susceptible to acute MPTP exposure with advanced age. UCH-L1 expression is not decreased in the VTA of aged mice 24 h after MPTP, suggesting that the resistance of MLDA neurons to MPTP is not affected by advanced age. Although maintenance of UCH-L1 expression is associated with decreased susceptibility to MPTP in MLDA neurons (**Chapter 3**) aging still caused impairment of the UPS in the VTA, which appears to be independent of UCH-L1 expression and function. Whether function of UCH-L1 truly serves to promote UPS activity is not fully understood, especially in the context of differential susceptibility and aging.

Summary and conclusions

This is the first study that has examined UCH-L1 expression and function and UPS function in regions containing NSDA and MLDA neurons in aged mice exposed to MPTP. Our data suggest that although UCH-L1 expression and function are maintained in regions containing MLDA neurons, aging caused UPS impairment in both susceptible and non-susceptible populations. Since mono-Ub pool levels may not directly influence UPS activity (if the impairment is in the 26S proteasome, for example), the contribution of UCH-L1 to promoting UPS function in aging and neurotoxicant treatment in the brain regions studied is not yet clear. Further studies to elucidate if the 26S proteasome itself

is impaired should be conducted in aged animals and animals exposed to acute MPTP toxicity.

REFERENCES

REFERENCES

- Benskey, M., Behrouz, B., Sunryd, J., Pappas, S.S., Baek, S.-H.H., Huebner, M., Lookingland, K.J., Goudreau, J.L., 2012. Recovery of hypothalamic tuberoinfundibular dopamine neurons from acute toxicant exposure is dependent upon protein synthesis and associated with an increase in parkin and ubiquitin carboxy-terminal hydrolase-L1 expression. *Neurotoxicology* 33, 321–31. doi:10.1016/j.neuro.2012.02.001
- Calne, D., William Langston, J., 1983. AETIOLOGY OF PARKINSON'S DISEASE. *Lancet* 322, 1457–1459. doi:10.1016/S0140-6736(83)90802-4
- Canu, N., Barbato, C., Ciotti, M.T., Serafino, A., Dus, L., Calissano, P., 2000. Proteasome involvement and accumulation of ubiquitinated proteins in cerebellar granule neurons undergoing apoptosis. *J. Neurosci.* 20, 589–99.
- Chen, D., Wilkinson, C.R.M., Watt, S., Penkett, C.J., Toone, W.M., Jones, N., Bähler, J., 2008. Multiple pathways differentially regulate global oxidative stress responses in fission yeast. *Mol. Biol. Cell* 19, 308–317. doi:10.1091/mbc.E07
- Floyd, R.A., Hensley, K., Takeda, A., Nunomura, A., Atwood, C., Perry, G., al., et, 2001. Oxidative stress in brain aging. Implications for therapeutics of neurodegenerative diseases. *Neurobiol. Aging* 23, 795–807. doi:10.1016/S0197-4580(02)00019-2
- Kitada, T., Asakawa, S., Hattori, N., Matsumine, H., Yamamura, Y., Minoshima, S., Yokochi, M., Mizuno, Y., Shimizu, N., 1998. Mutations in the parkin gene cause autosomal recessive juvenile parkinsonism. *Nature* 392, 605–8. doi:10.1038/33416
- Leroy, E., Boyer, R., Auburger, G., Leube, B., Ulm, G., Mezey, E., Harta, G., Brownstein, M.J., Jonnalagada, S., Chernova, T., Dehejia, A., Lavedan, C., Gasser, T., Steinbach, P.J., Wilkinson, K.D., Polymeropoulos, M.H., 1998. The ubiquitin pathway in Parkinson's disease. *Nature*. doi:10.1038/26652
- Ross, C. a., Pickart, C.M., 2004. The ubiquitin-proteasome pathway in Parkinson's disease and other neurodegenerative diseases. *Trends Cell Biol.* 14, 703–711. doi:10.1016/j.tcb.2004.10.006
- Setsuie, R., Wada, K., 2007. The functions of UCH-L1 and its relation to neurodegenerative diseases. *Neurochem. Int.* 51, 105–11. doi:10.1016/j.neuint.2007.05.007
- Stark, A.K., Pakkenberg, B., 2004. Histological changes of the dopaminergic nigrostriatal system in aging. *Cell Tissue Res.* 318, 81–92. doi:10.1007/s00441-004-0972-9

Sun, A., Chen, Y., 1998. Oxidative stress and neurodegenerative disorders. *J. Biomed. Sci.* 65212, 401–414.

Chapter 8: General Discussion

Differential regulation of UCH-L1 in regions containing NSDA and MLDA neurons

PD is a debilitating neurodegenerative disease that has no known cure. No disease modifying therapies are currently available to halt the degeneration of NSDA neurons and spread of pathology throughout the brain. Current therapies for PD only address the motor dysfunction and generally revolve around replacing DA. TIDA and MLDA neurons, however, are invulnerable and less vulnerable to degeneration in PD, respectively (Braak and Braak, 2000) and understanding how non-susceptible neurons evade destruction is a major avenue of investigation. To study the differential susceptibility between DA neuronal populations using a rodent model of oxidative stress that targets DA neurons, we use the acute MPTP paradigm which recapitulates vulnerability of NSDA neurons and resistance of TIDA and MLDA neurons (Behrouz et al., 2007; Benskey et al., 2012, 2015; Hung and Lee, 1998).

Since resistant TIDA neurons lack high expression of DAT, have drastically different axon lengths compared to NSDA neurons, are functionally dissimilar to NSDA neurons and are regulated differently (Lookingland and Moore, 2005), comparisons between NSDA and TIDA neurons are useful but may be limited. On the other hand, MLDA neurons are very similar to NSDA neurons and more work has been done to characterize the differential susceptibility between NSDA and MLDA neurons (Surmeier et al., 2017).

In previous studies involving comparisons between NSDA and MLDA neurons, the relevance of maintaining calcium homeostasis has been emphasized. Increased

cytosolic calcium can lead to apoptosis (Nagley et al., 2010). NSDA neurons are highly metabolically active and experience an influx of high concentrations of cytosolic calcium due to their abundance of L-type Ca^{2+} channels. MLDA neurons are also active, but express lower levels of L-type Ca^{2+} channels (Philippart et al., 2016) and also express a calcium binding protein called calbindin not expressed in the SN (Foehring et al., 2009) that is thought to protect MLDA neurons from the effects of high cytosolic calcium. A promising study for the calcium channel blocker isradipine to treat PD is currently in clinical trial (Surmeier et al., 2017).

A pathological hallmark of PD is the presence of Lewy bodies in the SN containing high amounts of α -syn (Spillantini et al., 1997). These cytosolic inclusions of misfolded proteins also contain Ub and Ub-proteins (Kuzuhara et al., 1988), which suggests that deficits in protein degradation could play a role in pathology of PD. Indeed, evidence of UPS impairment has been demonstrated in post mortem brain tissue from PD patients (McNaught and Jenner, 2001). Since UCH-L1 is a DUB mutated in familial PD (Leroy et al., 1998), demonstrated to influence availability of mono-Ub pools (Nagamine et al., 2010; Osaka et al., 2003), and by logical extension modulate UPS function, we have sought to investigate the contribution of UCH-L1 to susceptibility of NSDA neurons and non-susceptibility of MLDA neurons to acute MPTP exposure.

As demonstrated in **Chapter 3** UCH-L1 protein is decreased in the SN 24 h after MPTP exposure, a finding consistent with a previous report from our laboratory (Benskey et al., 2012). In TIDA neurons, however, UCH-L1 was upregulated (Benskey et al., 2012), leading to the hypothesis that UCH-L1 could contribute to resistance of TIDA neurons to MPTP-induced toxicity manifested by a decrease in intracellular DA and TH expression.

The expression of UCH-L1 in MLDA neurons had not been previously investigated, so we sought to characterize expression and function of UCH-L1 after MPTP exposure. As predicted, UCH-L1 expression was maintained in the VTA 24 h after MPTP. This maintenance of UCH-L1 protein was accompanied by maintenance of UCH-L1 function, as measured by levels of mono-Ub protein. Therefore, we hypothesized that UCH-L1 expression and function contributed to the differential susceptibility of NSDA and MLDA neurons to acute MPTP exposure.

The endpoints examined for determining differential susceptibility in the context of the acute MPTP model are intracellular DA and TH expression, since a single injection of 20 mg/kg MPTP does not result in cell death. One of the mechanisms of MPTP toxicity is displacement of DA in synaptic vesicles (Dauer and Przedborski, 2003), which results in increased cytosolic DA where it can become deprotonated and metabolized to toxic metabolites, resulting in oxidative stress and subsequent neuronal damage (Hastings et al., 1996). After MPTP exposure, the extent of DA loss in the ST was greater than in the NAc (**Chapter 3**)(Behrouz et al., 2007). This differential susceptibility is likely not due to tissue penetration of MPTP, since cell body and axon terminal regions of NSDA and MLDA neurons are in similar locations in the brain and MPTP easily crosses the blood-brain barrier.

DAT expression, however, is predicted to play a role in susceptibility to MPP⁺ toxicity because it is the avenue through which MPP⁺ gains access to the cytosol of DA neuron axon terminals (Dauer and Przedborski, 2003). One study determined that DA uptake is higher in the ST than the NAc (Marshall et al., 1990). Therefore, it was hypothesized that differential susceptibility of DA neuronal populations to toxicant models of DA

selective neurodegeneration (i.e., 6-OHDA and MPTP) is related to expression of DAT (Uhl, 1998). However, in a study that measured uptake of MPP⁺ specifically in the ST and NAc after chronic direct infusion of MPP⁺, no differences in uptake were detected (Hung et al., 1995), leading the authors to conclude that differential susceptibility between NSDA and MLDA neurons is not due to reduced uptake of MPP⁺ in the NAc. In addition, other models have demonstrated that MLDA neurons are less susceptible to neurodegeneration than NSDA neurons, including an rAAV overexpressing α -syn model (Maingay et al., 2006). Although intracellular DA depletion may not be a perfect endpoint to attempt to rescue using manipulations in pathways known to be affected in PD, it is one way in which MPP⁺ differentially affects NSDA and MLDA neurons that is not affected by uptake of MPP⁺.

The rate limiting enzyme of DA synthesis, TH, is also decreased in the ST to a greater extent than the NAc after MPTP (**Chapter 3**). A decrease in TH in the NSDA could logically result in decreased synthesis of DA, but with the effects of MPP⁺ on decreasing intracellular DA by itself, any decreases in synthesis of DA could be masked by these effects. Since MPP⁺ causes oxidative stress in mouse brain tissue (Johannessen et al., 1986), reactive oxygen species within the cell could cause oxidation of TH. Oxidatively damaged TH could become toxic to the cell, so therefore, oxidatively modified TH must be degraded. The main degradation pathway involved in regulating turnover of TH is the UPS (Congo Carbajosa et al., 2015). TH must be phosphorylated prior to UPS-mediated degradation (Nakashima et al., 2011). However, if TH is primarily degraded by the proteasome and UPS function becomes impaired, we would actually expect to see more TH protein in regions where the UPS is inhibited, such as in ST synaptosomes

(**Chapter 7**). It is possible that the total amount of TH does not actually decrease in the ST and NAc after MPP⁺ but is oxidatively modified, which could prevent the antibody from binding to the protein. In any case, our second DA neuron specific endpoint for comparing susceptibility between NSDA and MLDA neurons, TH expression, is decreased to a greater extent than in the NAc 24 h after MPTP exposure.

Although DA and TH are used as DA specific endpoints measured after MPTP exposure, a direct link between UCH-L1 and regulation of specific DA phenotype is not apparent. Rather, since UCH-L1 functions within the scope of the UPS, we predict that a decrease in UCH-L1 expression or function would result in UPS impairment. Indeed, UPS function (as estimated by the accumulation of total Ub proteins) is impaired in ST synaptosomes 24 h after MPTP (**Chapter 7**), while in whole NAc tissue UPS function is maintained. UPS dysfunction has been demonstrated in regions containing NSDA neurons (Lansdell, 2017). Unexpectedly, UCH-L1 function is not decreased in axon terminal regions of NSDA neurons 24 h after MPTP (**Chapter 3**), however, and actually recovers in ST synaptosomes after being decreased at 6 h (**Chapter 4**). An important caveat for examining UPS function in the ST and NAc is that any changes in mono-Ub or total Ub are likely masked by glial UPS function and do not reflect UPS function in DA neuron terminals. These results demonstrate that UCH-L1 expression and function may not directly influence UPS function and calls into question whether it would be logical to attempt to rescue NSDA neurons by overexpressing UCH-L1 in the SN. If the SN attempted to compensate for MPP⁺ induced toxicity by transporting UCH-L1 to the ST and that compensation did not have any effect on susceptibility to loss of TH or

impairment of UPS function, then it appears that restoring UCH-L1 to the ST would be no use.

Although we had predicted that levels of available mono-Ub likely influence proper function of the UPS since substrates must be tagged with Ub to be degraded by the 26S proteasome, dysfunction in the structure of the 26S proteasome itself could lead to accumulation of poly-Ub substrates, which would not necessarily be affected by UCH-L1 function. Oxidative modification of the proteasome has been demonstrated (Wang et al., 2010). Therefore, even though UCH-L1 (and not other related DUBs, as shown in **Chapter 4**) influences levels of mono-Ub in NSDA and MLDA neurons, impairment of the UPS could occur at a different part of the pathway, which renders availability of the mono-Ub pool potentially less relevant for promoting UPS function. Again, however, we are unable to separate the effects on UPS and mono-Ub in glial cells versus axon terminals. Mono-Ub is not only relevant for the UPS, however: K63-linked poly-Ub chains are found on substrates destined for autophagic degradation (Tan et al., 2007).

Possible contribution of UCH-L1 function in autophagy

In **Chapter 4**, we examined the potential role of UCH-L1 in promoting autophagy in parkin deficient mice. In the absence of parkin the UPS is impaired (Lansdell, 2017). In addition, mitochondrial quality is also decreased in parkin deficient mice (Palacino et al., 2004), which is predicted due to parkin's role in regulating mitophagy (Damiano et al., 2014). Despite these deficits, parkin deficient mice do not have an obvious parkinsonian phenotype (Perez and Palmiter, 2005). Lifetime compensation for the loss of parkin are

expected to play a role in the apparent disconnect between the importance of parkin function and relatively normal phenotype of the knock out mouse.

One obvious mechanism that could compensate for decreased UPS function in the absence of parkin is upregulation of the ALP, which was demonstrated in **Chapter 4**. Macroautophagy, rather than CMA, was found to be increased in parkin deficient mice due to the observed increase in LC3B-II protein (signifying an increase in abundance of autophagosomes) and no accumulation of p62 (signifying normal function of the ALP). How UCH-L1 function could contribute to upregulation of autophagy is not directly known, but one piece of the puzzle is how UCH-L1 is regulated directly by parkin: UCH-L1 is ubiquitinated by parkin via a K63-linked poly-Ub chain to signal degradation of UCH-L1 via autophagy (McKeon et al., 2014). It is thought that parkin downregulates UCH-L1 in conditions of stress in order to prevent UCH-L1-mediated removal of Ub, a function of UCH-L1 that could potentially interfere with UPS degradation of substrates. Since parkin is an E3 ligase (Shimura et al., 2000), its activity is considered to oppose the DUB function of UCH-L1. In absence of parkin, however, UCH-L1 expression is elevated in the SN (**Chapter 4**), which coincides with upregulation of autophagy in parkin deficient mice. In the face of UPS impairment, it may be beneficial to remove Ub from substrates to allow them to be degraded by autophagy.

One paper demonstrated that UCH-L1 in its dimeric form *in vitro* can act as a ligase and ubiquitinate α -syn via K63-linked poly-Ub chains, which would target the protein for degradation by autophagy (Liu et al., 2002). The presence of dimeric UCH-L1 and its ligase activity, however, has not been demonstrated *in vivo*. Also not clear is how maintenance of mono-Ub pools by UCH-L1 function could contribute to protein

degradation by autophagy. Little is known about the feasibility of how UCH-L1 function could contribute to autophagy and whether this influence involves regulation of mono-Ub pools. In a study using the UCH-L1 inhibitor LDN-57444, inhibition of UCH-L1 in transgenic mice overexpressing α -syn resulted in protective effects mediated by upregulation of autophagy (Cartier et al., 2012), essentially suggesting that UCH-L1 function under those particular conditions is detrimental rather than helpful in promoting autophagy. Clearly, more work is needed to understand how UCH-L1 function could relate to the ALP, but it is reasonable to think that UCH-L1 function could affect autophagic degradation of protein substrates and that this mechanism is important for compensation of loss of UPS activity.

Use of the UCH-L1 inhibitor LDN-57444 *in vivo*

Previous studies showed effects of LDN-57444 on synaptic structure and function in mice (Cartier et al., 2012, 2009; Gong et al., 2006; Zhang et al., 2014). These previous studies examined regions of the brain involved in memory and cognition with special relevance to AD. We sought to determine if loss of UCH-L1 function would render MLDA neurons more vulnerable to MPTP-induced toxicity and exacerbate susceptibility of NSDA neurons. Although LDN-57444 administration had no effect on DA homeostasis by itself, it exerted a protective effect against MPTP-induced loss of DA in both NSDA and MLDA neurons (**Chapter 5**). A protective role for UCH-L1 inhibition has already been demonstrated in pathological conditions (Cartier et al., 2012) with respect to α -syn clearance via autophagy, but the relevance of such mechanisms relating to susceptibility of DA neurons to neurotoxicant exposure is unknown in our acute MPTP

model, and we do not expect to induce α -syn pathology with an acute paradigm (Gibrat et al., 2009).

The apparent effect of LDN-57444 administration on susceptibility to loss of DA after MPTP could not be directly attributed to a decrease in UCH-L1 function because attempts to measure target engagement were inconclusive, since the ability of UCH-L1 to bind and sequester mono-Ub may not be affected by LDN-57444 or obscured by mono-Ub in other cells in tissue samples. Also currently unknown is how much LDN-57444 distributes in mouse brain tissue after i.p. administration, and a potential time course of events that affect its efficacy to reduce mono-Ub levels. One possibility, if UCH-L1 inhibition did occur, is that UCH-L1 plays a different role in DA neurons compared to previously studied hippocampal neurons. Synaptic structure and function is regulated in part by UPS mediated protein turnover (Yi and Ehlers, 2005), and therefore UCH-L1 can be hypothesized to play a role in UPS-mediated regulation at the level of the synapse. However, a specific role for UCH-L1 in DA neuron synaptic activity has not yet been established.

More research is needed to determine if there is a specific function of UCH-L1 with special relevance to DA neuronal homeostasis. The original model of UCH-L1 deficiency, the *gad* mouse (Nagamine et al., 2010), while afflicted with neurodegeneration in the gracile tract, has no parkinsonian phenotype and homozygous animals for the mutation die prematurely after only 6 months of life. Interestingly, the gracile tract contains the longest axons in the body, suggesting that UCH-L1 function is important for maintenance of axonal structure. Indeed, UCH-L1 is critical for maintenance of the neuromuscular junction (Chen et al., 2010). It is hypothesized that

perhaps if *gad* mice lived long enough, DA neurons would be affected by lack of UCH-L1 function. In one German family, a mutation in UCH-L1 that resulted in a 50% decrease in hydrolase activity (I93M) caused PD (Leroy et al., 1998). However, in children with a different mutation in UCH-L1 (Glu7Ala), a completely different phenotypic consequence of loss of UCH-L1 function is manifested, which the authors termed “neurodegeneration with optical atrophy” (Bilguvar et al., 2013).

From these mouse models lacking UCH-L1 and from human patients with UCH-L1 mutations, it is clear that UCH-L1 expression is necessary for proper function of the nervous system. It is possible that UCH-L1 fulfills a necessary function specifically in DA neurons that is yet to be uncovered, or that mutated UCH-L1 has an increased propensity to aggregate (Setsuie et al., 2007) in brain regions sensitive to perturbations in the UPS and autophagy, which could explain why patients with I93M mutation in UCH-L1 developed PD as opposed to a different neurodegenerative phenotype.

Effects of aging on susceptibility of NSDA and MLDA neurons

PD is a disease most commonly diagnosed in elderly patients, yet the majority of preclinical models to test new therapies do not take aging into account. Increased oxidative stress has been shown to occur with aging (Finkel and Holbrook, 2000), and with the pathology of PD closely linked to oxidative stress, it is reasonable to surmise that aged brains are more susceptible to development of PD due in part to age-related accumulation of oxidative damage. In the studies presented in this Dissertation no losses of DA, TH, DAT, or VMAT2 were observed in the ST of aged mice versus young mice (**Chapter 6**). In the NAc, however, we did observe an age-related decrease in DA

(without effects on TH, DAT, or VMAT2) in the aged mice. This decrease in DA in the aged NAc has been demonstrated before in rats (Huang et al., 1995).

In addition to potential effects of aging on DA neurons, aging could differentially affect glia in the ST and NAc, particularly astrocytes. Astrocytes are expected to play a role in DA metabolic homeostasis because they express MAO-B and COMT, which can uptake and metabolize DOPAC and DA, respectively (Levitt et al., 1982). An excess in synaptic DA is predicted to be harmful, since the incidence of DA adducts could increase and cause toxicity (Hastings et al., 1996). Therefore, astrocyte role in metabolism of extracellular DA is considered protective. We demonstrated in **Chapter 6** that astrocytes from the NAc, not the ST, retain the ability to metabolize DA into 3-MT (with no changes in either region to COMT). The idea that astrocytes maintain their protective function to prevent excess DA accumulation in the synapse is especially relevant when we examine the susceptibility of aged MLDA neurons to acute MPTP.

The susceptibility of aged mice to chronic MPTP has been previously reported and chronic MPTP exposure causes degeneration in both the SN and VTA in aged mice (to a lesser extent in the VTA than the SN) (Gupta et al., 1986). However, no information is available about the effects of a single dose of MPTP on differentially susceptible DA neuron populations. To determine whether MLDA neurons are rendered more susceptible to MPTP-induced damage, aged mice were acutely exposed to MPTP. As seen in young mice, depletion of DA is more extensive in both young and aged ST exposed to MPTP. However, aged MLDA neurons are still less susceptible to MPTP exposure compared to ST neurons (**Chapter 6**) and are not made more vulnerable to MPTP-induced injury.

One possibility as to why aged MLDA neurons retain their resistance to acute MPTP exposure is that NAc astrocytes retain their ability to metabolize synaptic DA and prevent DA-induced oxidative damage. Although the distribution of astrocytes between the ST and NAc in young animals is equivalent (Emsley and Macklis, 2006), age-related declines in astrocytes and their function have not been comprehensively examined in the ST and NAc. These data reveal that, although most of the focus of attempting to characterize and study mechanisms in NSDA and MLDA neurons that contribute to differential susceptibility focus on the DA neurons, we must not forget about the contributions of non-neuronal cells that could influence susceptibility.

Effects of aging on UPS and UCH-L1 function

No previous studies have been published reporting UCH-L1 expression in aged mice, so we sought to determine if there are age-related decreases in UPS and UCH-L1 function. In axon terminals of NSDA neurons, the UPS is impaired in both young and aged mice in the absence of alterations in UCH-L1 expression (**Chapter 7**). As discussed above, maintenance of UCH-L1 function does not seem to always result in maintenance of UPS function in ST synaptosomes. In microdissected ST and NAc tissue, however, UPS function was intact. The most interesting age-related effects occurred in the SN and VTA, where both regions experienced impairment of the UPS with advanced age (**Chapter 7**). There was no age-related decline in UCH-L1 protein or activity (as measured by mono-Ub levels) in the SN or VTA. The UPS has been shown to be compromised with advanced age (Saez and Vilchez, 2014), but until now, UCH-L1 expression in aging neurons had not yet been examined. We conclude that UCH-L1 expression is not lost in brain regions containing NSDA or MLDA neurons.

By 24 h after MPTP exposure, UCH-L1 was decreased in both young and aged mice in the SN (**Chapter 7**). In the VTA, however, MPTP exposure did not cause a decrease in UCH-L1 in either age group. If our hypothesis was correct and UCH-L1 was a major contributor to differences in NSDA and MLDA neuronal responses to toxicant exposure, we would predict that increased susceptibility of MLDA neurons to MPTP would be correlated with a decrease in UCH-L1 protein. The UCH-L1 expression in aged MLDA neurons matches the decreased susceptibility to MPTP compared to the NSDA neurons, but maintenance of UCH-L1 expression does not appear to protect aged NSDA or MLDA neurons from age-related UPS impairment. Since UCH-L1 was postulated above to have a potential role in promoting autophagy, perhaps maintenance of UCH-L1 contributes to autophagic degradation of substrates rather than UPS-mediated degradation. Autophagy is also decreased in aging (Cuervo, 2008), but has not been examined in NSDA and MLDA neurons in the context of acute MPTP administration. Further study is needed to understand how UCH-L1 may contribute to UPS function with age, neurotoxicant treatment, and a potential compensation for UPS impairment by promoting autophagy.

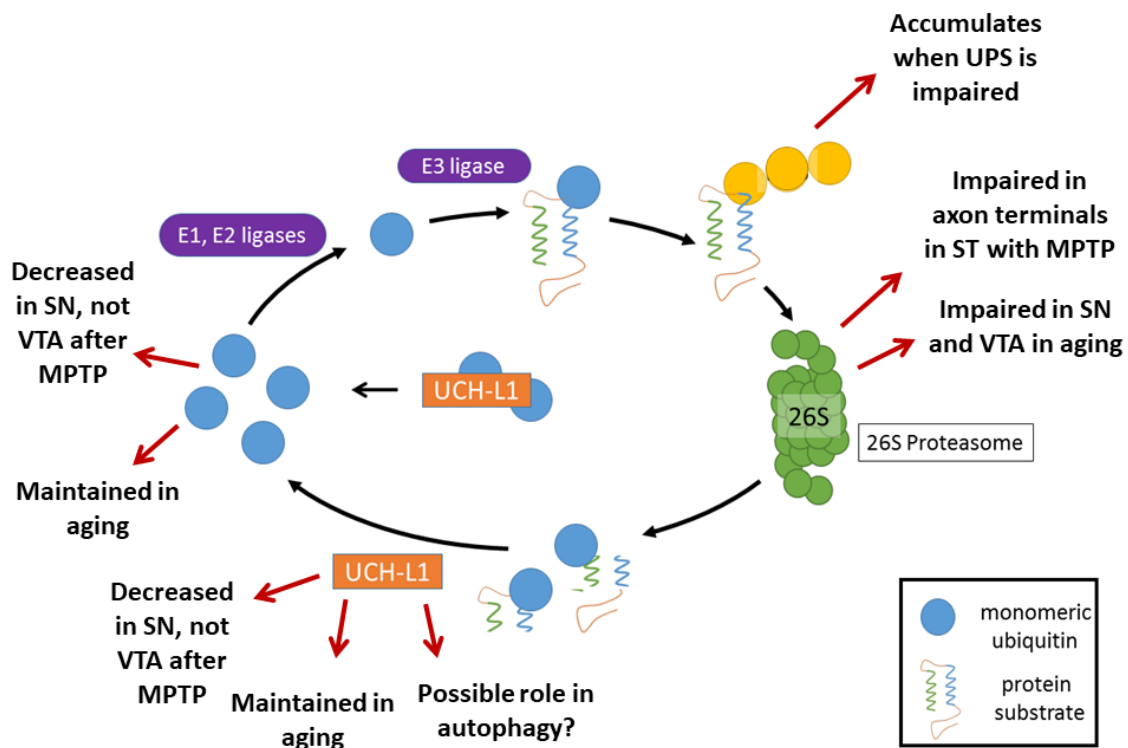


Figure 8.1. Summary of major findings in this Dissertation. This diagram summarizes new information demonstrated regarding UPS and UCH-L1 function after MPTP exposure and aging in regions containing NSDA and MLDA neurons.

Future directions

To directly test whether UCH-L1 protects MLDA neurons, an rAAV vector expressing an siRNA to knock down UCH-L1 could be delivered to the VTA to determine if MLDA neurons are made more susceptible to MPTP exposure. In addition, direct effects of UCH-L1 modulation on mono-Ub levels could be examined. To assess the effects of UCH-L1 knock out specifically in DA neurons, a DAT-Cre mouse could be used and the loxP system employed to knock out UCH-L1. To determine if increasing autophagy could protect DA neurons, administration of an autophagy inducer (such as rapamycin) could be performed *in vitro* and *in vivo* to assess if reduced susceptibility of DA neurons could be achieved. Finally, pharmacological enhancer of UCH-L1 could be used to determine if enhancing UCH-L1 function would protect or reverse oxidative damage to neurons in culture and *in vivo*.

Conclusions

In this Dissertation, a role for UCH-L1 in determining susceptibility of NSDA and MLDA neurons was investigated. We demonstrated that UCH-L1 is differentially regulated in NSDA and MLDA neurons exposed to MPTP. While maintenance of UCH-L1 expression and function were associated with reduced susceptibility to MPTP-induced injury, UPS function did not appear to be affected by changes in UCH-L1 or its hydrolase activity. A potential role for UCH-L1 in autophagy was also revealed, but more evidence is needed regarding the mechanisms underlying this oxidative stress-induced shift in proteostasis and how this changes with age. The effects of MPTP treatment and aging on UPS and UCH-L1 function are summarized in **Fig. 8.1**.

The contribution of age-related effects in regions containing cell bodies and axon terminals of NSDA and MLDA neurons was investigated and a potentially protective role for NAc astrocytes in synaptic DA homeostasis was revealed. Although it is currently not clear if UCH-L1 expression and function contribute to susceptibility between NSDA and MLDA neurons, what is clear from studies on mice and humans lacking functional UCH-L1 is that UCH-L1 is absolutely necessary for maintenance of normal function of the central nervous system. Potential future therapeutic strategies to target UCH-L1 and perhaps enhance its catalytic activity could be developed and tested for efficacy in modulating protein degradation pathways such as the UPS and autophagy. One such enhancer of UCH-L1 activity has been discovered but its effects on UCH-L1 were modest (increased by 111%) (Mitsui et al., 2010). More potent pharmacological modulators of UCH-L1 function should be investigated.

REFERENCES

REFERENCES

- Behrouz, B., Drolet, R.E., Sayed, Z.A., Lookingland, K.J., Goudreau, J.L., 2007. Unique responses to mitochondrial complex I inhibition in tuberoinfundibular dopamine neurons may impart resistance to toxic insult. *Neuroscience* 147, 592–8. doi:10.1016/j.neuroscience.2007.05.007
- Benskey, M., Behrouz, B., Sunryd, J., Pappas, S.S., Baek, S.-H.H., Huebner, M., Lookingland, K.J., Goudreau, J.L., 2012. Recovery of hypothalamic tuberoinfundibular dopamine neurons from acute toxicant exposure is dependent upon protein synthesis and associated with an increase in parkin and ubiquitin carboxy-terminal hydrolase-L1 expression. *Neurotoxicology* 33, 321–31. doi:10.1016/j.neuro.2012.02.001
- Benskey, M.J., Manfredsson, F.P., Lookingland, K.J., Goudreau, J.L., 2015. The role of parkin in the differential susceptibility of tuberoinfundibular and nigrostriatal dopamine neurons to acute toxicant exposure. *Neurotoxicology* 46, 1–11. doi:10.1016/j.neuro.2014.11.004
- Bilguvar, K., Tyagi, N.K., Ozkara, C., Tuysuz, B., Bakircioglu, M., Choi, M., Delil, S., Caglayan, A.O., Baranoski, J.F., Erturk, O., Yalcinkaya, C., Karacorlu, M., Dincer, A., Johnson, M.H., Mane, S., Chandra, S.S., Louvi, A., Boggon, T.J., Lifton, R.P., Horwich, A.L., Gunel, M., 2013. Recessive loss of function of the neuronal ubiquitin hydrolase UCHL1 leads to early-onset progressive neurodegeneration. *Proc. Natl. Acad. Sci. U. S. A.* 110, 3489–94. doi:10.1073/pnas.1222732110
- Braak, H., Braak, E., 2000. Pathoanatomy of Parkinson's disease. *J. Neurol.* 247 Suppl, I13-10. doi:10.1007/PL00007758
- Cartier, A.E., Djakovic, S.N., Salehi, A., Wilson, S.M., Masliah, E., Patrick, G.N., 2009. Regulation of synaptic structure by ubiquitin C-terminal hydrolase L1. *J. Neurosci.* 29, 7857–68. doi:10.1523/JNEUROSCI.1817-09.2009
- Cartier, A.E., Ubhi, K., Spencer, B., Vazquez-Roque, R. a., Kosberg, K.A., Fourgeaud, L., Kanayson, P., Patrick, C., Rockenstein, E., Patrick, G.N., Masliah, E., 2012. Differential effects of UCHL1 modulation on alpha-synuclein in PD-like models of alpha-synucleinopathy. *PLoS One* 7. doi:10.1371/journal.pone.0034713
- Chen, F., Sugiura, Y., Myers, K.G., Liu, Y., Lin, W., 2010. Ubiquitin carboxyl-terminal hydrolase L1 is required for maintaining the structure and function of the neuromuscular junction. *Proc. Natl. Acad. Sci.* 107, 1636–1641. doi:10.1073/pnas.0911516107
- Congo Carbajosa, N.A., Carbajosa, N.A.L., Corradi, G., Verrilli, M.A.L., Guil, M.J., Vatta, M.S., Gironacci, M.M., 2015. Tyrosine hydroxylase is short-term regulated by the

ubiquitin-proteasome system in PC12 cells and hypothalamic and brainstem neurons from spontaneously hypertensive rats: possible implications in hypertension. *PLoS One* 10, e0116597. doi:10.1371/journal.pone.0116597

- Cuervo, A.M., 2008. Autophagy and aging: keeping that old broom working. *Trends Genet.* 24, 604–12. doi:10.1016/j.tig.2008.10.002
- Damiano, M., Gautier, C. a., Bulteau, A.L., Ferrando-Miguel, R., Gouarne, C., Paoli, M.G., Pruss, R., Auchère, F., L’Hermitte-Stead, C., Bouillaud, F., Brice, A., Corti, O., Lombès, A., 2014. Tissue- and cell-specific mitochondrial defect in Parkinson-deficient mice. *PLoS One* 9. doi:10.1371/journal.pone.0099898
- Dauer, W., Przedborski, S., 2003. Parkinson ’ s Disease : Mechanisms and Models 39, 889–909.
- Emsley, J.G., Macklis, J.D., 2006. Astroglial heterogeneity closely reflects the neuronal-defined anatomy of the adult murine CNS. *Neuron Glia Biol.* 2, 175–86. doi:10.1017/S1740925X06000202
- Finkel, T., Holbrook, N.J., 2000. Oxidants, oxidative stress and the biology of ageing. *Nature* 408, 239–47. doi:10.1038/35041687
- Foehring, R.C., Zhang, X.F., Lee, J.C.F., Callaway, J.C., 2009. Endogenous Calcium Buffering Capacity of Substantia Nigral Dopamine Neurons. *J. Neurophysiol.* 102, 2326–2333. doi:10.1152/jn.00038.2009
- Gibrat, C., Saint-Pierre, M., Bousquet, M., Lévesque, D., Rouillard, C., Cicchetti, F., 2009. Differences between subacute and chronic MPTP mice models: investigation of dopaminergic neuronal degeneration and α -synuclein inclusions. *J. Neurochem.* 109, 1469–1482. doi:10.1111/j.1471-4159.2009.06072.x
- Gong, B., Cao, Z., Zheng, P., Vitolo, O. V, Liu, S., Staniszewski, A., Moolman, D., Zhang, H., Shelanski, M., Arancio, O., 2006. Ubiquitin hydrolase Uch-L1 rescues beta-amyloid-induced decreases in synaptic function and contextual memory. *Cell* 126, 775–88. doi:10.1016/j.cell.2006.06.046
- Gupta, M., Gupta, B.K., Thomas, R., Bruemmer, V., Sladek, J.R., Felten, D.L., 1986. Aged mice are more sensitive to 1-methyl-4-phenyl-1,2,3,6-tetrahydropyridine treatment than young adults. *Neurosci. Lett.* 70, 326–331. doi:10.1016/0304-3940(86)90573-2
- Hastings, T.G., Lewis, D.A., Zigmond, M.J., 1996. Role of oxidation in the neurotoxic effects of intrastriatal dopamine injections. *Proc. Natl. Acad. Sci.* 93, 1956–1961.
- Huang, R., Wang, C., Tai, M., Tsai, Y., Peng, M., 1995. Effects of age on dopamine nrelease in the nucleus accumbens and amphetamine-induced locomotor activity in rats. *Neurosci. Lett.* 200, 61–64.
- Hung, H.-C., Lee, E.H., 1998. MPTP Produces Differential Oxidative Stress and Antioxidative Responses in the Nigrostriatal and Mesolimbic Dopaminergic

- Pathways. *Free Radic. Biol. Med.* 24, 76–84. doi:10.1016/S0891-5849(97)00206-2
- Hung, H.C., Tao, P.L., Lee, E.H., 1995. 1-Methyl-4-phenyl-pyridinium (MPP+) uptake does not explain the differential toxicity of MPP+ in the nigrostriatal and mesolimbic dopaminergic pathways. *Neurosci. Lett.* 196, 93–6.
- Johannessen, J.N., Adams, J.D., Schuller, H.M., Bacon, J.P., Markey, S.P., 1986. 1-methyl-4-phenylpyridine (MPP+) induces oxidative stress in the rodent. *Life Sci.* 38, 743–749. doi:10.1016/0024-3205(86)90589-8
- Kuzuhara, S., Mori, H., Izumiyama, N., Yoshimura, M., Ihara, Y., 1988. Lewy bodies are ubiquitinated. *Acta Neuropathol.* 75, 345–353. doi:10.1007/BF00687787
- Lansdell, T., 2017. THE ROLE OF PARKIN IN MAINTAINING PROTEASOME ACTIVITY FOLLOWING.
- Leroy, E., Boyer, R., Auburger, G., Leube, B., Ulm, G., Mezey, E., Harta, G., Brownstein, M.J., Jonnalagada, S., Chernova, T., Dehejia, A., Lavedan, C., Gasser, T., Steinbach, P.J., Wilkinson, K.D., Polymeropoulos, M.H., 1998. The ubiquitin pathway in Parkinson's disease. *Nature.* doi:10.1038/26652
- Levitt, P., Pintart, J.E., Breakefieldt, X. O, 1982. Immunocytochemical demonstration of monoamine oxidase B in brain astrocytes and serotonergic neurons (central nervous system/rat/monoamine) 79, 6385–6389.
- Liu, Y., Fallon, L., Lashuel, H.A., Liu, Z., Lansbury, P.T., 2002. The UCH-L1 Gene Encodes Two Opposing Enzymatic Activities that Affect α -Synuclein Degradation and Parkinson ' s Disease Susceptibility 111, 209–218.
- Lookingland, K.J., Moore, K.E., 2005. Chapter VIII Functional neuroanatomy of hypothalamic dopaminergic neuroendocrine systems. *Handb. Chem. Neuroanat.* 21, 435–523. doi:10.1016/S0924-8196(05)80012-0
- Maingay, M., Romero-Ramos, M., Carta, M., Kirik, D., 2006. Ventral tegmental area dopamine neurons are resistant to human mutant alpha-synuclein overexpression. *Neurobiol. Dis.* 23, 522–32. doi:10.1016/j.nbd.2006.04.007
- Marshall, J.F., O'Dell, S.J., Navarrete, R., Rosenstein, A.J., 1990. Dopamine high-affinity transport site topography in rat brain: major differences between dorsal and ventral striatum. *Neuroscience* 37, 11–21.
- McKeon, J.E., Sha, D., Li, L., Chin, L.-S., 2014. Parkin-mediated K63-polyubiquitination targets ubiquitin C-terminal hydrolase L1 for degradation by the autophagy-lysosome system. *Cell. Mol. Life Sci.* doi:10.1007/s00018-014-1781-2
- McNaught, K.S.P., Jenner, P., 2001. Proteasomal function is impaired in substantia nigra in Parkinson's disease. *Neurosci. Lett.* 297, 191–194. doi:10.1016/S0304-3940(00)01701-8
- Mitsui, T., Hirayama, K., Aoki, S., Nishikawa, K., Uchida, K., Matsumoto, T., Kabuta, T.,

- Wada, K., 2010. Identification of a novel chemical potentiator and inhibitors of UCH-L1 by in silico drug screening. *Neurochem. Int.* 56, 679–686. doi:10.1016/j.neuint.2010.01.016
- Nagamine, S., Kabuta, T., Furuta, A., Yamamoto, K., Takahashi, A., Wada, K., 2010. Deficiency of ubiquitin carboxy-terminal hydrolase-L1 (UCH-L1) leads to vulnerability to lipid peroxidation. *Neurochem. Int.* 57, 102–110. doi:10.1016/j.neuint.2010.04.015
- Nagley, P., Higgins, G.C., Atkin, J.D., Beart, P.M., 2010. Multifaceted deaths orchestrated by mitochondria in neurones. *Biochim. Biophys. Acta - Mol. Basis Dis.* 1802, 167–185. doi:http://dx.doi.org/10.1016/j.bbadis.2009.09.004
- Nakashima, A., Mori, K., Kaneko, Y.S., Hayashi, N., Nagatsu, T., Ota, A., 2011. Phosphorylation of the N-terminal portion of tyrosine hydroxylase triggers proteasomal digestion of the enzyme. *Biochem. Biophys. Res. Commun.* 407, 343–347. doi:10.1016/j.bbrc.2011.03.020
- Osaka, H., Wang, Y.L., Takada, K., Takizawa, S., Setsuie, R., Li, H., Sato, Y., Nishikawa, K., Sun, Y.J., Sakurai, M., Harada, T., Hara, Y., Kimura, I., Chiba, S., Namikawa, K., Kiyama, H., Noda, M., Aoki, S., Wada, K., 2003. Ubiquitin carboxy-terminal hydrolase L1 binds to and stabilizes monoubiquitin in neuron. *Hum. Mol. Genet.* 12, 1945–1958. doi:10.1093/hmg/ddg211
- Palacino, J.J., Sagi, D., Goldberg, M.S., Krauss, S., Motz, C., Wacker, M., Klose, J., Shen, J., 2004. Mitochondrial dysfunction and oxidative damage in parkin-deficient mice. *J. Biol. Chem.* 279, 18614–18622. doi:10.1074/jbc.M401135200
- Perez, F.A., Palmiter, R.D., 2005. Parkin-deficient mice are not a robust model of parkinsonism. *Proc. Natl. Acad. Sci. U. S. A.* 102, 2174–9. doi:10.1073/pnas.0409598102
- Philippart, F., Destreel, G., Merino-Sepúlveda, P., Henny, P., Engel, D., Seutin, V., 2016. Differential Somatic Ca²⁺ Channel Profile in Midbrain Dopaminergic Neurons. *J. Neurosci.* 36, 7234 LP-7245.
- Saez, I., Vilchez, D., 2014. The Mechanistic Links Between Proteasome Activity, Aging and Age-related Diseases. *Curr. Genomics* 15, 38–51. doi:10.2174/138920291501140306113344
- Setsuie, R., Wang, Y.-L., Mochizuki, H., Osaka, H., Hayakawa, H., Ichihara, N., Li, H., Furuta, A., Sano, Y., Sun, Y.-J., Kwon, J., Kabuta, T., Yoshimi, K., Aoki, S., Mizuno, Y., Noda, M., Wada, K., 2007. Dopaminergic neuronal loss in transgenic mice expressing the Parkinson's disease-associated UCH-L1 I93M mutant. *Neurochem. Int.* 50, 119–29. doi:10.1016/j.neuint.2006.07.015
- Shimura, H., Hattori, N., Kubo, S. i, Mizuno, Y., Asakawa, S., Minoshima, S., Shimizu, N., Iwai, K., Chiba, T., Tanaka, K., Suzuki, T., 2000. Familial Parkinson disease gene product, parkin, is a ubiquitin-protein ligase. *Nat. Genet.* 25, 302–5.

doi:10.1038/77060

- Spillantini, M.G., Schmidt, M.L., Lee, V.M.-Y., Trojanowski, J.Q., Jakes, R., Goedert, M., 1997. [alpha]-Synuclein in Lewy bodies 388, 839–840.
- Surmeier, D.J., Obeso, J.A., Halliday, G.M., 2017. Selective neuronal vulnerability in Parkinson disease. *Nat. Rev. Neurosci.* 18, 101–113. doi:10.1038/nrn.2016.178
- Tan, J.M.M., Wong, E.S.P., Kirkpatrick, D.S., Pletnikova, O., Ko, H.S., Tay, S.-P., Ho, M.W.L., Troncoso, J., Gygi, S.P., Lee, M.K., Dawson, V.L., Dawson, T.M., Lim, K.-L., 2007. Lysine 63-linked ubiquitination promotes the formation and autophagic clearance of protein inclusions associated with neurodegenerative diseases. *Hum. Mol. Genet.* 17, 431–439. doi:10.1093/hmg/ddm320
- Uhl, G.R., 1998. Hypothesis: The role of dopaminergic transporters in selective vulnerability of cells in Parkinson's disease. *Ann. Neurol.* doi:10.1002/ana.410430503
- Wang, X., Yen, J., Kaiser, P., Huang, L., 2010. Regulation of the 26S Proteasome Complex During Oxidative Stress. *Sci. Signal.* 3.
- Yi, J.J., Ehlers, M.D., 2005. Ubiquitin and Protein Turnover in Synapse Function. *Neuron* 47, 629–632. doi:10.1016/j.neuron.2005.07.008
- Zhang, M., Cai, F., Zhang, S., Zhang, S., Song, W., 2014. Overexpression of ubiquitin carboxyl-terminal hydrolase L1 (UCHL1) delays Alzheimer's progression in vivo. *Sci. Rep.* 4, 7298. doi:10.1038/srep07298